SYNTHESIS OF ACTIVE R FILTERS, OSCILLATORS AND DELAY NETWORKS

A Thesis Submitted
in Partial Fulfilment of the Requirements
for the Degree of
DOCTOR OF PHILOSOPHY

By

Y. VENKATARAMANI

to the

DEPARTMENT OF ELECTRICAL ENGINEERING
INDIAN INSTITUTE OF TECHNOLOGY, KANPUR

OCTOBER, 1981

EE-1981-D-VEN-SYN

TO

MY

PARENTS

CERTIFICATE

Certified that this work, 'Synthesis of Active R Filters, Oscillators and Delay Networks' by Mr. Y. Venkataramani has been carried out under my supervision and that this work has not been submitted elsewhere for a degree.

(S. Venkateswaran)
Senior Professor
Department of Electrical Engineering
Indian Institute of Technology, Kanpur

ACKNOWLEDGEMENTS

The author records his deep sense of gratitude to Dr. S. Venkateswaran, Senior Professor, Dept of Electrical Engg. for suggesting the thesis topic and meticulously supervising this work to completion. The author is also indebted to him for his constant encouragement and for teaching the qualities that are necessary in a research worker. The author is grateful to Dr. R. Sharan, Head, Dept of Elec.Engg. for the facilities provided.

The author is thankful to the faculty of Electrical Engg. Dept. for their encouragement. Thanks are also due to the Staff of E.E. Dept. in particular S/Shri S.N. Sikdar, S.P. Chakravarti and S.S. Bhatnagar for their kind co-operation.

The author expresses his sincere thanks to his friends Anirudhan, Ashok Nedungadi, George Paul, Jose, Prem Malhotra, Ganesh, Rakesh Lal and Sunil Garg for their valuable help during the preparation of this thesis.

Shri C.M. Abraham deserves special thanks for careful and efficient typing and for his help in the thesis preparation. The tracing work by Shri A.K. Ganguly, Ammonia Printing by Shri Kalyan Das and the cyclostyling work by S/Shri T. Tiwari and Gangaram are gratefully acknowledged.

The author is deeply indebted to his wife Uma for her patience and understanding during the course of this work and to his son Jayaram for cheering him up at all times.

Y. Venkataramani

TABLE OF CONTENTS

LIST OF FIGURES

LIST OF TABLES

LIST OF SYMBOLS

A	Open loop gain of operational amplifier
A_i	Open loop gain of ith operational amplifier
A_o	DC open loop gain of operational amplifier
A_{oi}	DC open loop gain of ith operational amplifier
$B/2\pi$	Gain bandwidth product of operational amplifier
$B_i/2\pi$	Gain bandwidth product of ith operational amplifier
B_α	$\omega_{11}+\alpha B_1$
B_β	$\omega_{12}+\beta B_2$
B_γ	$\omega_{13}+\gamma B_3$
$D(\omega)$	Envelope delay
G	Amplifier gain; all pass filter magnitude
G_o	Resonant gain of band pass filter
$G_{2\text{ pole}}$	Magnitude of all pass filter based on two pole model for operational amplifiers
Q	Selectivity
R, R_x	Equivalent resistances
S_x^m	Sensitivity of m with respect to x
T	Delay
$T(s)$	Voltage transfer function
$T(s)_{2\text{ pole}}$	Voltage transfer function based on two pole model for operational amplifiers
$T_{BP}(s)$	Band pass filter transfer function
$T_{LP}(s)$	Low pass filter transfer function
V_{cc}	Bias voltage for operational amplifier

V_{GS}	Gate-source dc voltage of FET
V_i, V_o	Input and output voltages of network
Y_i	Input admittance
Z_i	Input impedance
f	Operating frequency
f_1	Operational amplifier first pole frequency
f_o	Centre frequency for BPF; frequency of oscillations
r_{DS}	Drain-source resistance of FET
α	$R_a/(R_a+R_b)$
β	$R_c/(R_c+R_d)$
$\beta_1(s)$	Frequency dependent feedback factor
β_2	Frequency independent feedback factor
γ	$R_e/(R_e+R_f)$
δ	$R_g/(R_g+R_h)$
ω	Operating angular frequency
ω_1	Operational amplifier first pole angular frequency
ω_2	Operational amplifier second pole angular frequency
ω_o	BPF angular centre frequency; angular frequency of oscillation
φ	Phase angle
$\varphi_{1\ pole}$	Phase angle based on single pole model for operational amplifier
$\varphi_{2\ pole}$	Phase angle based on two pole model for operational amplifier
τ_i	Delay in ith operational amplifier
τ_1	Operational amplifier first pole time constant = $1/\omega_1$

SYNOPSIS

SYNTHESIS OF ACTIVE R FILTERS,
OSCILLATORS AND DELAY NETWORKS
A Thesis Submitted
In Partial Fulfilment of the Requirements
for the Degree of
DOCTOR OF PHILOSOPHY
by
Y. VENKATARAMANI
to the
Department of Electrical Engineering
Indian Institute of Technology, Kanpur
October, 1981

Active filters have widespread application in present day electronic systems. They enable realisation of a variety of network functions for different applications. A large number of papers are available on active filters using operational amplifiers (OA), resistors and capacitors. These filters have two main limitations. First is the high frequency limitation due to the finite gain-bandwidth products of the OAs used. Second limitation is due to difficulties in incorporating capacitors during IC fabrication. To overcome these limitations a new class of active networks using only OAs and resistors, termed active R networks, have been developed. In recent years a number of active R circuits that realise different network functions have been reported. However,

synthesis techniques are not available for many of these circuits. This thesis presents systematic synthesis techniques for active R filters [band pass (BP), low pass (LP), high pass (HP), all pass (AP) and notch (BE)], oscillators and delay networks. A number of new circuits have been realised. The first chapter of the thesis introduces the concept of active R networks. The works reported in literature and this thesis are discussed.

The second chapter deals with OA modelling and parameter measurement relevant to active R networks. Characteristics of existing OA models are discussed. A new OA model is proposed that takes into account OA second pole effects without complicated analysis. This new pole-zero model enables easy design of active R networks for wide frequency range application. Available methods of OA parameter measurement are also described in this chapter.

Band pass and low pass filters form part of practically every electronic system. BPFs with high ω_o and Q values are particularly useful. Though a number of active R BP and LP filters have been reported in literature synthesis techniques for most of them have not been developed. In the third chapter synthesis techniques for inverting and non-inverting BP and LP filters are given. A circuit with multifunction capability [1] has been realised. It provides inverting BP, non-inverting LP, AP, BE and oscillator functions. It can

also provide non-inverting BP response if the polarities of both the OAs in the circuit are reversed. The circuit has been designed, based on pole-zero model for the OAs, and tested. Experimental results show the validity of this pole-zero model. Modifications of the synthesis technique lead to other reported BPF circuits. The synthesis techniques for LPFs realise nth order inverting and non-inverting LPFs.

All pass filters find application in phase shifters, delay equalisers and delay networks. Only few first and second order active R APFs have been reported in literature. Synthesis techniques for active R APFs and higher order active R APFs have not been realised till now. In the fourth and fifth chapters two new synthesis techniques to realise active R APF of any given order, both with real poles and zeros and with complex poles and zeros are proposed [2]. All circuits are realised with an attenuation constant due to resistive summation. This is because, an ideal active R summer circuit is not known. The effect of OA second pole on APF performance has been analysed and experimentally verified. The synthesis technique proposed in the fifth chapter leads to circuits with larger signal handling capacity.

The sixth chapter presents synthesis techniques for first and second order high pass filters and second order

notch filters. These circuits are also realised with an attenuation constant due to resistive summation. A symmetrical notch filter has been designed based on pole-zero model for high ω_o and Q values and experimentally tested.

Sinusoidal oscillators with wide tuning range, constant amplitude and low distortion with independent frequency control either by resistance variation or by voltage variation are required in many applications. A few active R oscillators have been reported in literature. Only some of them have independent frequency control facility. In the seventh chapter a synthesis technique for active R oscillators is proposed to realise a two OA six resistor oscillator circuit [3]. In this circuit condition for oscillations is maintained by one grounded resistor while its frequency is controlled by another grounded resistor. Replacement of the frequency controlling resistor by a JFET leads to a voltage controlled oscillator. Both resistance and voltage controlled oscillators give constant amplitude, low distortion oscillations over a wide frequency range.

Delay networks are required to provide improved transient response in pulse communication systems. Till now no active R delay network has been realised. In the eighth chapter an active R circuit to realise the fourth order Pade all pass approximation for e^{-sT}, has been synthesised [4]. The realised circuit has been designed and tested for a delay of 30 μs.

The synthesis techniques presented in this thesis are general. Hence, they can also realise active RC filters, oscillators and delay networks.

References

1. Venkataramani, Y. and Venkateswaran, S., 'Active R multifunction circuit synthesis', submitted for publication.
2. Venkataramani, Y. and Venkateswaran, S., 'Synthesis of active R all pass filters', submitted for publication.
3. Venkateswaran, S. and Venkataramani, Y., 'Continuously tunable active R oscillator with two operational amplifiers', J.IETE, Vol. 26, no.10, pp 523-525, October, 1980.
4. Venkataramani, Y. and Venkateswaran, S., 'Active R delay network synthesis', submitted for publication.

CHAPTER I

INTRODUCTION

The field of Electronics has undergone tremendous changes in the past two decades. A vast range of new devices and processes have been developed. Circuit designers have used these to realise a wide variety of system functions. In the field of linear networks, the advent of the monolithic integrated circuit operational amplifier (OA) has enabled realisation of practically all network functions. A number of synthesis techniques have been evolved for the realisation of active filters, oscillators and delay networks. The circuits realised by these techniques use OAs, resistors and capacitors. These circuits can realise the same functions that passive networks can provide, but without using inductors. The active RC networks have the further capability to realise non-positive real functions also.

These active RC networks are analysed assuming the OAs to have an infinite gain-bandwidth product. Practical OAs have a finite gain-bandwidth product. As a result of this active RC networks can be used only upto about 10 KHz. for satisfactory performance. Further, in monolithic IC technology, capacitors occupy a very large area compared to resistors and transistors. Hence, it is necessary to avoid capacitors in active networks

to be integrated.

The two considerations, viz., extending the frequency range of active networks and eliminating capacitors in them has led to the development of a new class of active networks, termed active R networks. In these, the low pass behaviour (due to finite gain-bandwidth product) of the OA is incorporated in the circuit design so that the network can function over a wider frequency range. Further, the low pass behaviour of the OA resulting in 6 dB/octave roll-off of the open loop gain, after the first pole frequency, simulates a capacitive effect so that the active R circuits do not require any external capacitors. Of course, the OAs which are internally compensated, have a small compensation capacitor inside the chip. Thus, capacitor is not fully eliminated. Apart from this internal capacitor, active R networks are capacitorless. It is also possible to incorporate the OA pole in active RC network design. In this case, a second order function can be realised by a circuit using one OA and only one external capacitor . These circuits are referred to as active RC networks using the OA pole.

A large number of active R networks (filters and oscillators) and active RC networks using OA pole have been reported in the literature in the recent past. However, clearcut synthesis techniques have not yet been reported for most active

R circuit realisations. This thesis introduces general synthesis techniques for active R filters (band pass, low pass, all pass, high pass and notch), oscillators and delay networks. A number of new circuits have been realised using these techniques. The next section of this chapter introduces the concept of active 'R' networks. Subsequent sections discuss the available literature on active R networks and the work reported in Chapters III to VIII. Chapter IX of the thesis indicates the conclusions drawn from the theoretical and experimental investigations and gives suggestions for further work.

1.1 Concept of active R network:

Traditional active network design has been based on the use of passive RC networks in conjunction with one or more active devices. These active devices are assumed to have infinite gain-bandwidth product. However, the commonly used active devices, viz., transistors and OAs have complex gains which exhibit low pass behaviour, i.e., the magnitude of gain decreases with frequency and the phase increases with frequency. This non-ideal behaviour of the active devices limits the useful frequency range of the active networks.

The concept of incorporating the low pass behaviour of the active device in the design to overcome the high frequency limitations was first proposed by Capparelli and Liberatore [1].

They have used the low pass behaviour of a transistor to realise a band pass network using only resistors and transistors. Radhakrishna Rao and Srinivasan [2] were the first to exploit the low pass behaviour of an internally compensated integrated circuit OA to realise high frequency networks. A band pass filter using one OA, resistors and a single external capacitor has been realised by them. Soderstrand [3] gave the name 'active R filters' to filters using only OAs and resistors. Subsequently, a large number of active R circuits have been reported in literature. The highest usable frequency of active R networks is limited by two factors. One is the slew rate limitations of the OAs used. The other is the effect of the second pole of the OA. Though the OA is modelled, in active R networks, on the basis of a single pole at low frequency, actual OA response indicates the presence of a second pole located at high frequency. Computer simulation of μA 741 OA [4] have indicated the presence of a number of poles and zeros at high frequencies. These can be together considered in terms of an equivalent high frequency pole. This second pole alters the magnitude and phase response at high frequencies.

Active R networks have the feature that all network characteristics are decided by OA parameters and resistor ratios only. Hence, individual resistor values can be conveniently chosen, as long as the ratio is maintained. In

monolithic IC technology resistor tolerances cannot be made small but accurate resistor ratios (tracking) can be achieved. Thus, from this point of view active R networks have a definite advantage over active RC networks.

1.2 OA modelling and parameter measurement :

Incorporation of the OA low pass behaviour necessiates modelling of the OA in terms of its parameters. The commonly used model is the one which takes into account a single low frequency pole, followed by a 6 dB/octave roll-off. This is the single pole model which is satisfactory for frequencies well below the gain-bandwidth products of the OAs. Simplification of this model, by neglecting the first pole frequency, for frequencies well above it, leads to the integrator model. If the high frequency effects of the OA are to be taken into account then the OA response must be more correctly represented by a two pole model consisting of a low frequency first pole and a high frequency second pole. Though results obtained using this model will be more accurate than those with single pole model, the circuit analysis, with this model, is very tedious unless a number of approximations are made. The effect of OA second pole can also be modelled as excess phase or delay [5]. However, analysis is not simplified with this model since exponential functions appear in the various expressions.

In Chapter II of this thesis a new OA model, termed pole-zero model, has been proposed. This is obtained from the two pole model by converting the second pole into an equivalent right half plane [RHP] zero, for frequencies well below the OA second pole frequency. For this frequency range, the pole-zero model analysis leads to the same results as those with two pole model, but with an analysis which is as simple as that with single pole model. Thus, this new model is particularly suited for the analysis of higher order active R networks.

The modelling of the OA in terms of its low pass behaviour necessiates the measurement of the parameters of the OA, viz., dc open loop gain, first and second pole frequencies and gain-bandwidth product. A number of methods are available [2,6,7,8] for the measurement of these parameters. In Chapter II a description of these methods is given.

1.3 Band pass and low pass filters :

Band pass filters (BPF) and low pass filters (LPF) find a range of applications in instrumentation and communications. A number of active R band pass filters have been reported in literature. In general, these use two OAs and while BP response is available at the output of one OA, LP response is available at the output of the other OA. Srinivasan [9] and Soderstrand [3] have reported two OA BPFs using six and three resistors

respectively. Soderstrand's circuit is a modification of the pseudo band pass circuit of Schaumann [10]. Venkateswaran and Sowrirajan [11] have synthesised a BPF using the concept of driving point functions. Venkateswaran and Pujari [12] have obtained an OA version of the transistor-resistor bandpass network of Gapparelli and Liberatore [1]. Soderstrand has also realised [13] a CMOS version of his active R BPF [3]. Schaumann and Brand [5], Li and Li [14] and Mitra and Aatre [15] have also proposed second order BPF circuits. Higher order BP and LP ladder networks have been synthesised by Soderstrand [16].

In Chapter III (Section 3.1) synthesis techniques for BPFs are given. A BPF circuit with multifunction capability has been realised. This circuit can realise inverting BP, non-inverting LP and oscillator functions. With the addition of three resistors it can realise all pass and notch functions. To take into account the effect of OA second pole on the filter performance, this circuit has been designed and tested on the basis of the new OA model.

Acar [17] has given a general method for realising nth order non-inverting low pass voltage transfer functions. The circuit realised by Acar uses a number of matched resistors. In Chapter III (Section 3.2) general synthesis techniques for nth order non-inverting and inverting LPFs are given. The

non-inverting LPFs realised are the same as those proposed by Venkateswaran [18]. The realised nth order non-inverting LPF circuit has a lower resistor count compared to Acar's circuit.

1.4 All pass filters:

All pass filters (APF) have the characteristic of frequency independent magnitude response and a prescribed, frequency dependent, phase response. Higher order active RC all pass filters can be obtained by cascading first and/or second order APFs. However, active R APFs can be realised at resistive summation point or at the input of an OA. Hence, cascading is not possible to realise higher order active R APFs. A number of second order APFs [15,19,20,21] and a first order APF [9] have been reported in literature. However, no higher order APF has been proposed till now.

In Chapter IV of this thesis a new synthesis technique, termed series realisation, has been proposed to realise active R APF of any given order, both with real poles and zeros and with complex poles and zeros. The technique is general and hence can realise active RC APF of any order. The realised first order circuit is the same as the circuit proposed by Srinivasan [9]. All the higher order circuits are new. Effects of OA second pole on these filters have been studied. The increase of magnitude response with frequency, indicated

by analysis based on two pole model, is borne out by the experimental results.

Higher order APFs realised by series realisation technique have low signal handling capacity due to cascading of first and second order basic sections. To overcome this problem an alternate synthesis technique, parallel realisation has been proposed in Chapter V. Here, the same signal gets applied to all basic sections. Hence, even for higher order filters the signal handling capacity is large. This technique also can realise APF of any order, both with real poles and zeros and with complex poles and zeros. Here also techniques are general and hence can realise active RC APFs of any order.

1.5 High pass and notch filters :

Second order high pass and notch transfer functions are derivable from a biquadratic transfer function as is the case with all pass transfer function. Soderstrand [3], Srinivasan [9], Kim and Ra [19] and Soliman and Fawzy [21] have realised high pass and notch functions either at the input of an OA or at the output of an OA whose gain-bandwidth product is assumed to be infinity. Mitra and Aatre [15] have obtained second order notch response at a resistive summation point.

In Chapter VI synthesis techniques for first and second order high pass filters and second order notch filters have been proposed. A second order symmetric notch filter has been

designed on the basis of pole-zero model and tested. All circuits are realised with an attenuation constant, because of resistive summation.

1.6 Oscillators :

Sinusoidal oscillators with low distortion, constant amplitude and wide frequency range are required in almost all electronic systems. Bhattacharyya and Natarajan [22] have proposed the first active R oscillator circuit using three OAs and six resistors. The circuit has independent control for frequency as shown by integrator model analysis. In this circuit oscillations are caused by the effect of OA second pole [23]. Nandi [24] and Ahmed and Siddiqui [25] have reported two OA, four resistor oscillator circuits which do not have independent frequency control. Pyara and Jamuar [26] and Drake and Michell [27] have reported oscillator circuits with eight and six resistors respectively.

A synthesis technique for active R oscillators has been proposed in Chapter VII of this thesis. The circuit realised by this technique uses two OAs and six resistors. The condition for oscillations is fixed by a grounded resistor. The frequency of oscillations can be varied over a wide range by another grounded resistor. If the frequency controlling grounded resistor is replaced by the drain-source circuit of a JFET whose gate-source dc voltage is varied, then the circuit

becomes a voltage controlled oscillator. Both the oscillator circuits give constant amplitude, low distortion oscillations over a wide frequency range. Modifications in the synthesis technique lead to other reported two OA oscillator circuits [24,25,26,27].

1.7 Delay networks :

In pulse communication systems, the transient response is important since it gives an idea of the distortion in the output pulse. If a circuit can be designed such that the output pulse is an exact replica of the input pulse, except for a time delay, then it will have an ideal transient response. Delay networks are designed by approximating e^{-sT} (T = delay) by a ratio of polynomials. Pade approximations are commonly used for this purpose. Till now no active R delay network has been reported in literature. In Chapter VIII an active R circuit, to realise the fourth order Pade approximation of e^{-sT} has been synthesised, by the parallel realisation technique. The circuit thus has a large signal handling capacity. Due to resistive summation the circuit is realised with an attenuation constant.

References

1. Capparelli, F. and Liberatore, A., 'Active band pass network with only resistors as passive elements', Electron. Lett., Vol. 8, no.2, pp 43-44, January, 1972.

2. Radhakrishna Rao, K. and Srinivasan, S., 'A band pass filter using the OA pole', IEEE Trans. JSSC, Vol. SC-8, no.6, pp 245-246, June, 1973.

3. Soderstrand, M.A., 'Design of active R filters using only resistors and operational amplifiers', Int. J. Electron., Vol. 40, no.6, pp 417-432, June, 1976.

4. Wooley, B.A., Wong, S.J. and Pederson, D.O., 'A computer aided evaluation of the 741 amplifier', IEEE JSSC., Vol. SC-6, no.6, pp 357-366, December, 1971.

5. Schaumann, R. and Brand, J.R., 'Active R filters: review of theory and practice', IEE J. Eln. Ckts. and Sys., Vol. 2, no.4, pp 89-101, July, 1978.

6. Gray, P.R. and Meyer, R.G., 'Recent advances in monolithic operational amplifier design', IEEE Trans. Ckts. and Sys., Vol. CAS-21, no.5, pp 317-327, May, 1974.

7. Graeme, J.G., Huelsman, H.P. and Tobey, G.E., 'Operational amplifiers - Design and applications', pp 445-447, McGraw-Hill - Koghakusha, Tokyo, 1971.

8. Kapustian, V., Bhattacharyya, B.B. and Swamy, M.N.S., 'Frequency limitations of active R filters using operational amplifiers', J. Franklin Institute, Vol. 308, no.2, pp 141-151, August, 1979.

9. Srinivasan, S., 'Synthesis of transfer functions using the OA pole', Int. J. Electron, Vol. 40, no.1, pp 5-13, January, 1976.

10. Schaumann, R., 'Low-sensitivity, high frequency, tunable active filter without external capacitors', IEEE Trans. Ckts. and Sys., Vol. CAS-22, no.1, pp 39-44, January, 1975.

11. Venkateswaran, S. and Sowrirajan, S., 'Novel active R band pass filter', J.IETE, Vol. 25, no.7, pp 275-278, July, 1979.

12. Venkateswaran, S. and Pujari, S.S., 'Active R band pass filter', J.IETE, Vol. 25, no.12, pp 479-481, December, 1979.

13. Soderstrand, M.A., 'An improved CMOS active R filter', Proc. IEEE, Vol. 65, no.8, pp 1204-1206, August, 1977.

14. Li, M.K. and Li, C.W., 'Active R filter using operational amplifier pole', Eln. Engg., Vol. 50, no.602, p 34, Frequency, 1978.

15. Mitra, A.K. and Aatre, V.K., 'Low sensitivity high frequency active R filters', IEEE Trans. Ckts. and Sys., Vol. CAS-23, no.11, pp 670-676, November, 1976.

16. Soderstrand, M.A., 'High frequency high order low sensitivity active R filters without external capacitors', IEEE Trans. Ckts. and Sys., Vol. CAS-25, no.12, pp 1032-1038, December, 1978.

17. Acar, C., 'Realisation of nth order low pass voltage transfer function by active R circuit: signal flow graph approach', Eln. Lett., Vol. 14, no.23, pp 729-730, November, 1978.

18. Venkateswaran, S., 'An active R chain network, Lecture notes, I.I.T. Kanpur, India, October, 1978.

19. Kim, H.K. and Ra, J.B., 'An active biquadratic building block without external capacitors', IEEE Trans. Ckts. and Sys., Vol. CAS-24, no.12, pp 689-694, December, 1977.

20. Soliman, A.M., 'A universal active R filter', Eln. Engg., Vol. 49, no.594, pp 49-50, July, 1977.

21. Soliman, A.M. and Fawzy, M., 'A universal active R biquad', Int. J. Ckt. Th. and Appn., Vol. 6, no.4, pp 153-157, April, 1978.

22. Bhattacharyya, B.B. and Natarajan, S., 'A new continuously tunable sinusoidal oscillator without external capacitors', Proc. IEEE, Vol. 65, no.12, pp 1726-1727, December, 1977.

23. Venkateswaran, S. and Venkataramani, Y., 'Comments on a new continuously tunable sinusoidal oscillator without external capacitors', Proc. IEEE, Vol. 67, no. 10, pp 1452-1453, October, 1979.

24. Nandi, R., 'Active R realisation of bilinear RL impedances and their application in high Q parallel resonator and external capacitorless oscillator', Proc. IEEE, Vol. 66, no.12, pp 1666-1668, December 1978.

25. Ahmed, M.T. and Siddiqui, M.A., 'A low component oscillator with operational amplifiers and resistors', Proc. 12th Asilomar Conf. Ckts., Sys. and Comp. (Calif.),(U.S.A.), November, 1978.

26. Pyara, V.P. and Jamuar, S.S., 'Single element controlled oscillator without external capacitors', Eln. Lett., Vol. 16, no.15, pp 607-608, July, 1980.

27. Drake, J.M. and Michell, J.A., 'Continuously tunable sinusoidal R oscillators with a minimum number of elements', Int. J. Electron., Vol. 50, no.2, pp 141-147, February, 1981.

CHAPTER II

OA MODELLING AND PARAMETER MEASUREMENT FOR ACTIVE R NETWORKS

The emergence of active R circuits as an important class of active circuits is due to two main reasons. First is the high frequency limitations of conventional active RC circuits due to the finite gain-bandwidth products of the OAs used. Second is the desirability of avoiding capacitors in any circuit from the point of view of monolithic integrated circuit fabrication, since they occupy a large portion of the chip area.

Conventional active RC filters use passive RC networks and one or more OAs whose gain is assumed to be large and independent of frequency. Practical OAs have complex gains which exhibit low pass behaviour, i.e. their magnitudes decrease with increasing frequency and they have a non-zero phase. This non-ideal behaviour of the OAs limits application of these filters to relatively low frequencies.

In active R networks the OA low pass behaviour is incorporated in the circuit design by considering a one pole model for the OA gain. Hence, active R networks can be operated over a wider frequency range compared to active RC filters. Incorporation of the frequency dependent OA gain in the circuit design however necessiates modelling of the OA in

terms of its parameters and measurement of these parameters for each of the OAs used in the circuit.

In this chapter modelling of the internally compensated OAs is considered first. Characteristics of single pole, two pole, delay and new pole-zero model are considered. Next, commonly used methods for the measurement of OA parameters relevant to active R networks are described.

2.1 OA modelling for active R networks :

For the analysis and synthesis of active R networks it is necessary to model the OA in terms of its parameters. The OA parameters of interest are (i) gain-bandwidth product $(B/2\pi)$, (ii) OA first pole frequency $(\omega_1/2\pi)$ and OA second pole frequency $(\omega_2/2\pi)$. The simplest OA model which is commonly used is the single pole model which incorporates only the first pole frequency. This model is valid only at low frequencies, where effect of OA second pole is negligible. A two pole model must be employed for analysing the high frequency behaviour of active R networks. However, two pole model analysis is very involved as compared to single pole model analysis. It is also possible to consider the effect of second pole in terms of a delay term added to the single pole model. In sub-section 2.1.4 a new pole-zero model has been proposed. This model takes into account the effect of OA second pole and at the same time enables analysis of the circuit in as simple a manner as with single pole model. Each

of the above models is suitable for a particular frequency range.

2.1.1 Single pole model :

Single pole model is based on the single pole, 6 dB/octave roll-off of the OA gain. This model is most commonly used for active R circuit analysis.

The single pole model for the ith OA is given by

$$A_i = \frac{A_{oi}\ \omega_{1i}}{s+\ \omega_{1i}} = \frac{B_i}{s+\ \omega_{1i}} \qquad (2.1)$$

where

A_o = DC open loop gain

$\omega_1/2\pi = f_1$ = first pole frequency

and

$B/2\pi$ = gain-bandwidth product.

For internally compensated OAs the typical values of f_1, $B./2\pi$ and A_o are 5 to 50 Hz, 1 to 2 MHz and 100 dB respectively. The magnitude and phase response of an internally compensated OA are shown in Figure 2.1. From the frequency response plot it is clear that the single pole model is valid for frequencies well below the unity gain frequency.

If the circuit operating frequency is much greater than the OA first pole frequency then equation (2.1) simplifies to

$$A_i \simeq \frac{B_i}{s} \quad \text{for} \quad \omega >> \omega_{1i} \qquad (2.2)$$

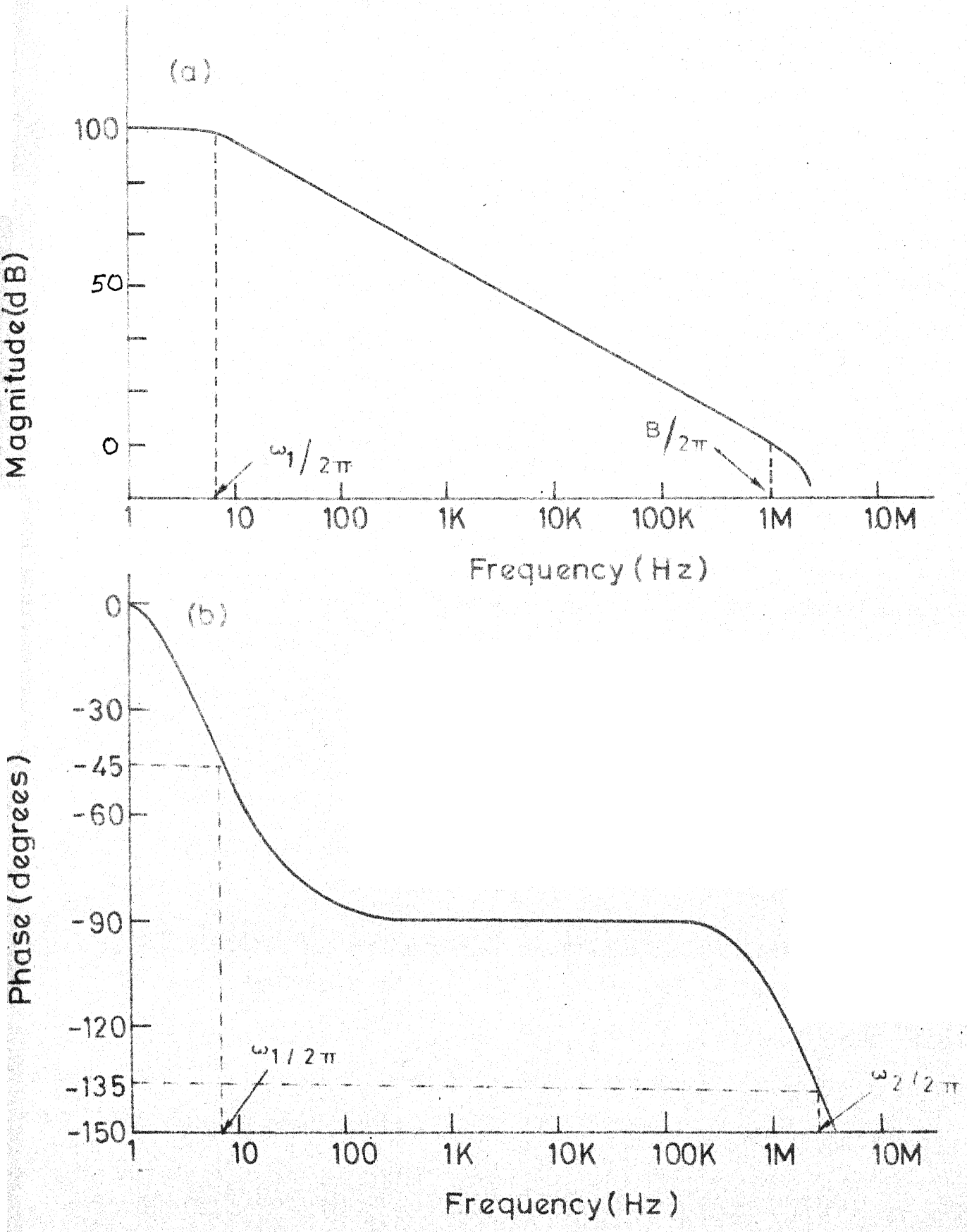

FIG. 2.1 OA FREQUENCY RESPONSE (a) MAGNITUDE (b) PHASE RESPONSE

This is termed as the integrator model for the OAs. It is valid for the frequency range $\omega_{1i} << \omega << B_i$. For most of the active R circuits single pole and integrator model analyses lead to identical results. However, in some cases, results are drastically different. For example, in the case of the oscillator circuit of Bhattacharyya and Natarajan [1], analysis with integrator model shows the circuit to be oscillatory while single pole model analysis [2] shows the circuit to be non-oscillatory. Hence, it is preferable to analyse any circuit with single pole model and then neglect ω_{1i} at appropriate places in the final expression.

2.1.2 Two pole model :

Single pole model adequately represents OA characteristics at low frequencies. But, at high frequencies, the second pole of the OA causes deviations in the magnitude and phase response. One effect of this, for example, is the oscillatory behaviour of an active R band pass filter designed for high centre frequency and selectivity values. To incorporate the effect of OA second pole in the design equations, a two pole model for the OA must be considered. The conventional two pole model for OAs is given by

$$A_i = \frac{B_i \omega_{2i}}{(s+ \omega_{1i})(s+ \omega_{2i})} \qquad (2.3)$$

where

$\frac{\omega_2}{2\pi}$ = second pole frequency of OA.

It can be seen from a comparison of equations (2.1) and (2.3) that with the two pole model, the order of the denominator polynomial of circuit transfer function will be doubled. Thus, even for a simple circuit with two OAs the characteristic equation will be of fourth order. In the case of second order active R band pass filter circuits this leads to difficulty in specifying centre frequency ($\omega_o/2\pi$) and selectivity (Q). However, with some approximations, two pole model analysis can be carried out to obtain the expressions for various parameters. One of the approximations usually made is that the OAs are all identical. This approximation enables easy evaluation of poles of the transfer function, with two pole model [2]. A second approximation usually made, is that the operating frequency, $\omega/2\pi$ is much lower than the OA second pole frequency, $\omega_2/2\pi$. With this approximation a higher order characteristic equation can be reduced to a lower order one and then analysis can be carried out with this lower order equation.

2.1.3 Delay model :

The magnitude contribution of OA second pole, as seen from equation (2.3) is $\omega_2/(\omega_2^2 + \omega^2)^{\frac{1}{2}}$ while the phase contribution is $-\tan^{-1}(\omega/\omega_2)$. For frequencies well below the OA second pole frequency

$$\frac{\omega_2}{(\omega_2^2 + \omega^2)^{\frac{1}{2}}} \simeq 1 \qquad (2.4)$$

However the phase contribution is non-zero.

Thus from equations (2.3) and (2.4), for $\omega << \omega_2$, magnitude of OA gain, with two pole model is nearly same as that with single pole model while the phase is different from that with single pole model. Schaumann and Brand [3] have proposed, on this basis, a model in which only the excess phase contribution of the OA second pole is taken into account, by means of a delay term. Their model is

$$A_i = \frac{B_i}{s + \omega_{1i}} e^{-s\tau_i} \simeq \frac{B_i}{s} e^{-s\tau_i} \qquad (2.5)$$

for $\omega >> \omega_{1i}$

where τ_i = delay of i^{th} OA

The analysis with this model is almost as tedious as with two pole model since the expressions will now be in terms of hyperbolic functions.

2.1.4 Pole-zero model :

Analysis with the two pole and the delay models is cumbersome even for simple two OA active R circuits. Further, clearcut expressions for the circuit parameters cannot be obtained without further approximations. This difficulty can be overcome by the simplified model, proposed here. This

model enables study of the effect of OA second pole without tedious analysis.

This model, termed as pole-zero model is obtained as shown here. Equation (2.3) can be rewritten as

$$A_i = \frac{B_i}{(s+ \omega_{1i})(1+ \frac{s}{\omega_{2i}})} \tag{2.6}$$

For $\omega << \omega_{2i}$

$$\frac{1}{1 + \frac{s}{\omega_{2i}}} \simeq 1 - \frac{s}{\omega_{2i}} \tag{2.7}$$

Therefore

$$A_i \simeq \frac{- B_i(s - \omega_{2i})}{\omega_{2i}(s + \omega_{1i})} \tag{2.8}$$

for $\omega << \omega_{2i}$

Comparison of equations (2.1) and (2.8) shows that analysis with the pole-zero model will be as simple as that with the single pole model since the order of the characteristic equation is unchanged. Since the normal operating frequency range of active R networks is much below the OA second pole frequency, the pole-zero model is as accurate as the two pole model for $\omega << \omega_{2i}$. Further, in the case of band pass filters, for example, design equations can be obtained in terms of this model and expressions for centre frequency and selectivity can be explicitly obtained.

2.2 OA parameter measurement :

In active RC filters, the OA is assumed to have infinit gain over the operating frequency range. Hence, the parameter of the OAs do not figure in the analysis. On the other hand, in active R networks the OA is modelled as per its actual frequency response. Hence, the OA parameters form are essential part of the analysis. Consequently, it is necessary to measure those parameters of the OA which are relevant for active R networks, before any circuit can be designed. The OA parameters of interest are : 1) DC open loop gain, A_o, 2) first pole frequency, $\omega_1/2\pi$, 3) gain bandwidth product, $B/2\pi$ and 4) second pole frequency, $\omega_2/2\pi$. A number of methods are available for the measurement of these parameters. Out of these the method proposed by Graeme et al [5] enables measurement of the above parameters, quite accurately.

2.2.1 Measurement of dc open loop gain :

A simple set up for the measurement of OA open loop gain [4] is shown in Figure 2.2. In this method a second OA (A_2) is used in a feedback configuration to force the output voltage of the OA under test (A_1) to be equal to the voltage V_a. The output of the second OA is applied to the OA under test, through a 1000:1 voltage divider. Hence the voltage at the output of A_2 is 1000 times the voltage at the input of A_1 required to produce V_a at its output. The gain

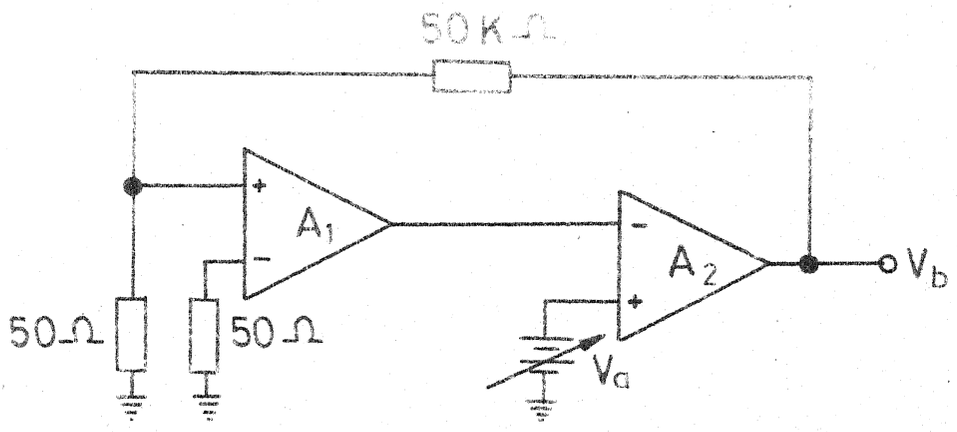

FIG. 2.2 DC OPEN LOOP GAIN MEASUREMENT CIRCUIT

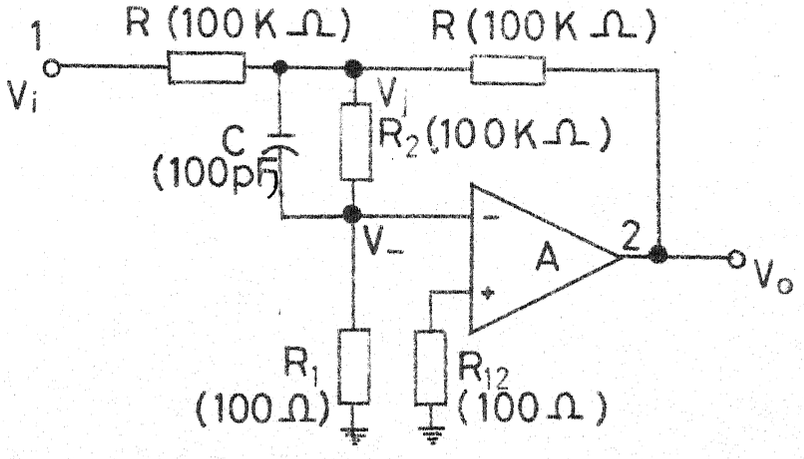

FIG. 2.3 OA FREQUENCY RESPONSE TEST SET UP.

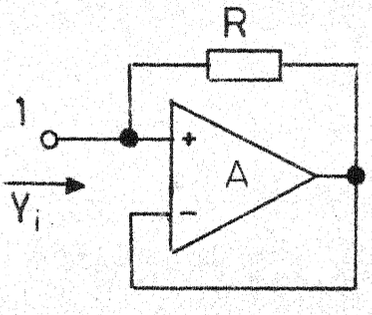

G. 2.4 IMPEDANCE MEASUREMENT SET UP.

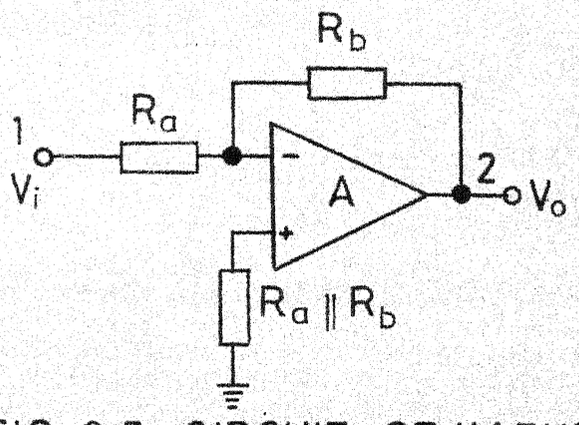

FIG. 2.5 CIRCUIT OF KAPUSTIAN et al.

is measured as an average by setting V_a equal to alternately +10 volts and -10 volts and measuring the difference between the two values of V_b that result. The average dc open loop gain then is

$$A_o = 1000 \left(\frac{V_a}{V_b}\right) \qquad (2.9)$$

where

V_a = 20 volts in this case.

2.2.2 OA frequency response measurement :

Graeme et al [5] have proposed a circuit arrangement for obtaining the frequency response (magnitude and phase) of an OA. This circuit is shown in Figure 2.3. Here, open loop parameters of OA are measured under closed loop conditions. In this method, for a specified output level (output of OA), the corresponding small differential input signal to the OA (at the inverting terminal of OA) is measured. To improve the accuracy of measurement of the differential input voltage to the OA, V_-, the voltage divider consisting of R_1 and R_2 is inserted between the summing junction J and the inverting input terminal of OA. Due to feedback V_j is an amplified replica of V_-. Hence, it can be measured more accurately. The frequencies at which the phase shift between output and input of the OA are 45° and 135° respectively, correspond to $\omega_1/2\pi$ and $\omega_2/2\pi$. A_o can be determined by measuring the gain at a frequency $\omega << \omega_1$. The gain is given by

$$A = -\frac{V_o}{V_-} = -\left(\frac{R_1+R_2}{R_1}\right)\left(\frac{V_o}{V_j}\right) \qquad (2.10)$$

At high frequencies, where the gain is very low, V_- can be directly measured instead of V_j.

2.2.3 Method of Rao et al

Rao et al [6] have proposed an admittance measurement method for determining the open loop gain and first pole frequency. Their circuit arrangement is shown in Figure 2.4. Here the OA is connected in noninverting unity gain mode with a resistance R between the noninverting input and output terminals. The input impedance (at terminal 1) is

$$Z_i = \frac{R}{1 - \frac{A}{1+A}} = R(1+A) \simeq RA \qquad (2.11)$$

for $A >> 1$

Hence, input admittance is

$$Y_i \simeq \frac{1}{RA} = \frac{1}{R}\left[\frac{s+\omega_1}{A_o \omega_1}\right] = \frac{1}{R}\left[\frac{1}{A_o} + \frac{s\tau_1}{A_o}\right] \qquad (2.12)$$

where $\tau_1 = \frac{1}{\omega_1}$ and A_o = open loop gain of OA.

The resistive and reactive parts of the input admittance are measured at reasonably low and high frequencies. From these measurements A_o and τ_1 and hence B and ω_1 are determined. R is chosen small enough for convenient admittance measurement.

2.2.4 Method of Kapustian et al. :

Kapustian et al [7] have proposed a new method for the measurement of OA parameters relevant to active R networks. The circuit arrangement is shown in Figure 2.5. For this circuit, with the two pole model of equation (2.3) the transfer function is

$$\frac{V_o}{V_i} = \frac{-(1-\alpha)B\ \omega_2}{s^2+(\omega_1+\omega_2)s + (\omega_1+\alpha B)\omega_2} \qquad (2.13)$$

$$\simeq \frac{-(1-\alpha)B\omega_2}{s^2+ \omega_2 s+\alpha B\omega_2} \qquad (2.14)$$

for $\omega_1 << \omega_2$ and $\omega_1 << \alpha B$

where

$$\alpha = \frac{R_a}{R_a+R_b}$$

Therefore,

$$\left| \frac{V_o}{V_i} \right|_{DC} = \frac{(1-\alpha)B}{\omega_1+\alpha B} \qquad (2.15)$$

From equation (2.13) the phase of gain is equal to $\pi/2$ radians at an angular frequency

$$\omega_a = [\omega_2(\omega_1+\alpha B)]^{\frac{1}{2}} \qquad (2.16)$$

At this frequency the magnitude of gain is

$$\left| \frac{V_o}{V_i} \right|_{\omega_a} = \frac{(1-\alpha)B}{\omega_a} \qquad (2.17)$$

Hence from equations (2.14) to (2.16) ω_1, B and ω_2 can be determined. The procedure is to first obtain the dc gain of the circuit of Figure 2.5. Next, determine the frequency ($\omega_a/2\pi$) at which the phase shift is exactly 90° and obtain the gain at this frequency. From these measurements, (at dc and at ω_a) all the parameters can be determined. The drawback of this method is the difficulty in precisely determining the frequency, ω_a at which the phase shift is 90°. This is because, over a fairly large frequency range the phase angle is close to 90°. Thus this method can be used only for approximate measurements.

2.3 Conclusions :

In this chapter the different OA models suitable for active R circuit analysis have been described. The single pole and integrator models are suitable for low frequency analysis. For higher frequencies, the two pole model is essential to account for the effects of OA second pole. A new simplified two pole model (pole-zero model) has been proposed to incorporate OA second pole effects in the design equations. This model

considerably simplifies circuit analysis. A few methods for the measurement of OA parameters, relevant to active R networks, have been given. Out of these the method proposed by Graeme et al [5] seems best suited from the point of view of active R circuits.

References

1 Bhattacharyya, B.B. and Natarajan, S., 'A new continuously tunable sinusoidal oscillator without external capacitors', Proc. IEEE, Vol. 65, no.12, pp 1726-1727, December, 1977.

2 Venkateswaran, S. and Venkataramani, Y., 'Comments on a new continuously tunable sinusoidal oscillator without external capacitors', Proc. IEEE, Vol. 67, no.10, pp 1452-1453, October, 1979.

3 Schaumann, R. and Brand, J.R., 'Active R filters: Review of theory and practice', IEE J. on Eln. Ckts. and Sys., Vol. 2, no.4, pp 89-101, July, 1978.

4 Gray, P.R. and Meyer, R.G., 'Recent advances in monolithic operational amplifier design', IEEE Trans. Ckts and Sys., Vol. CAS-21, no.5, pp 317-327, May, 1974.

5 Graeme, J.G., Huelsman, H.P. and Tobey, G.E., 'Operational amplifiers - design and applications', pp 445-447, McGraw-Hill, Koghakusha, Tokyo, 1971.

6 Radhakrishna Rao, K. and Srinivasan, S., 'A band pass filter using the OA pole', IEEE JSSC, Vol. SC-8, no.3, pp 245-246, June, 1973.

7 Kapustian, V., Bhattacharyya, B.B. and Swamy, M.N.S., 'Frequency limitations of active R filters using operational amplifiers', J. of Franklin Institute, Vol.308, no.2, pp 141-151, August, 1979.

CHAPTER III

SYNTHESIS OF BANDPASS AND LOWPASS FILTERS

Band pass (BPF) and low pass (LPF) filters find a wide range of applications in instrumentation and communication. Similar to the case of active RC filters, a large number of active R band pass and low pass filters have been reported in literature. All the second order active R BPF circuits have the characteristic that while BPF response is available at the output of one OA, simultaneously LPF response is available at the output of the other OA in the circuit. This feature is usually not obtainable in active RC BPFs.

In this chapter new synthesis techniques for inverting and non-inverting BPF and LPF are proposed. The BPF synthesis technique also realises the circuits of Laker et al. [1], Li and Li [2], Srinivasan [3], Soderstrand [4], Mitra and Aatre [5] and Ho and Chiu [6]. A new BPF circuit with multifunction capability has been synthesised. To take into account the effects of OA second pole, this circuit has been analysed and design equations developed, based on the newly proposed pole-zero model for the OAs. The circuit has low sensitivity of centre frequency and selectivity to all active and passive parameters.

The synthesis technique for non-inverting LPFs leads to the active R chain networks proposed by Venkateswaran [7]. New

inverting LPF of nth order has been synthesised. Experimental results for the BPF and an LPF circuit are included.

3.1 Band pass filter

The ideal second order BPF transfer function is

$$T_{BP}(s) = \frac{\pm G_o(\frac{\omega_o}{Q})s}{s^2 + (\frac{\omega_o}{Q})s + \omega_o^2} \qquad (3.1)$$

where

$\frac{\omega_o}{2\pi}$ = BPF centre frequency in Hz

Q = selectivity

G_o = resonant gain (gain at ω_o)

and

$\pm$ signs correspond to non-inverting and inverting BPF functions respectively.

Thus ω_o, Q and G_o are the three main parameters for a band pass filter. The requirement for any BPF circuit is that with ω_o, Q and G_o independently specified all the component values must be determined. In some circuits, once ω_o and Q are specified, G_o is automatically fixed. This is a disadvantage since there is no control over gain in this case.

3.1.1 Non-inverting BPF synthesis :

The non-inverting BPF transfer function can be written as

$$T_{BP}(s) = \frac{Ks}{s^2+(a-b)s+c} \tag{3.2}$$

$$= \frac{K_1 \cdot \frac{K_2}{(s+d)}}{[s^2+(a-b)s+c]/[s(s+d)]}$$

$$= \frac{K_1 \cdot (\frac{K_2}{s+d})}{1 + (\frac{K_2}{s+d})\left[\frac{(a-d)s+c}{K_2 s} - \frac{b}{K_2}\right]} \tag{3.3}$$

where $K_1K_2 = K$ and d = arbitrary parameter.

This transfer function is of the form

$$T(s) = \frac{K_1 G}{1+G[\beta_1(s) - \beta_2]} \tag{3.4}$$

where

G represents an amplifier with gain $= \frac{K_2}{s+d}$

$\beta_1(s)$ represents frequency dependent feedback factor $= [(a-d)s+c]/[K_2 s]$

and

β_2 represents frequency independent feedback factor $= \frac{b}{K_2}$

The block schematic and signal flow graph corresponding to this transfer function are shown in Figure 3.1. The amplifier, with gain G, can be realised by an internally compensate OA,

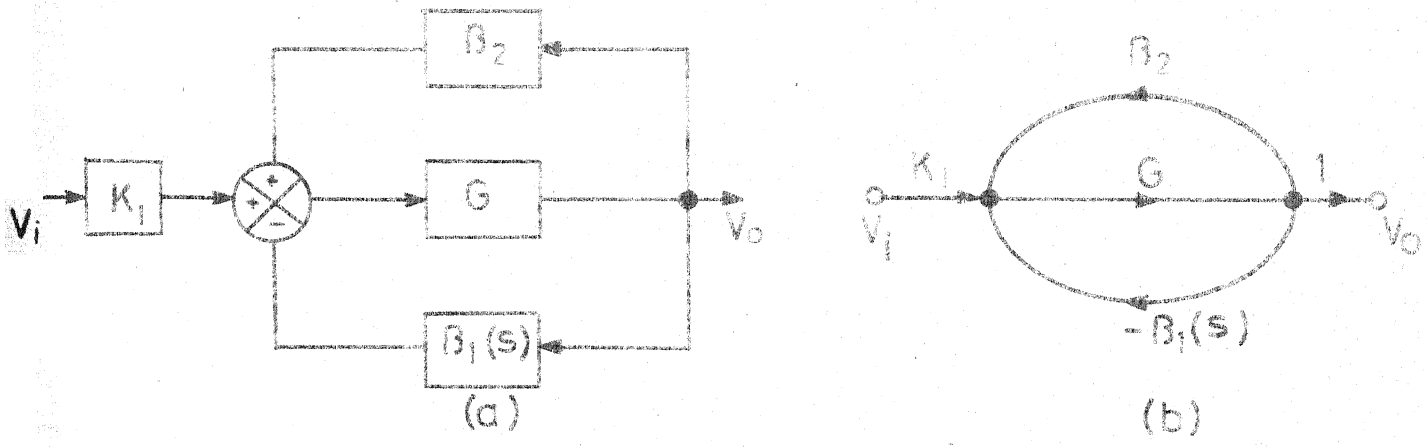

FIG. 3·1 BPF CONFIGURATION (a) BLOCK SCHEMATIC (b) SIGNAL FLOW GRAPH

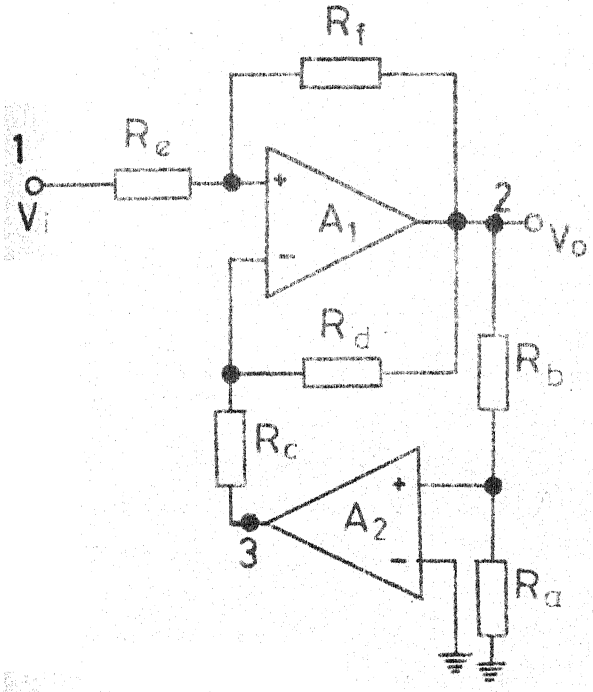

FIG 3·2 NON INVERTING BPF CIRCUIT

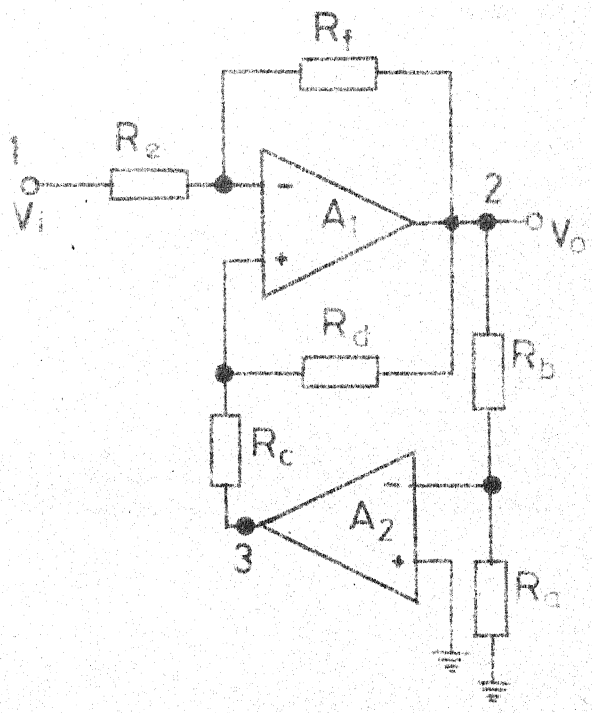

FIG. 3·3 INVERTING BPF CIRCUIT

whose gain, based on single pole model is $B_1/(s+\omega_{11})$. The frequency dependent feedback factor $\beta_1(s)$ can be rewritten as

$$\beta_1(s) = \frac{a-d}{K_2} + \frac{c}{K_2 s} \tag{3.5}$$

The first term in $\beta_1(s)$ can be realised by a resistive divider while the second term can be realised by an OA with an attenuat at its non-inverting input terminal. Then $\beta_1(s)$ is obtained by resistive summation of the two. β_2 is realised by a resistive divider. The obtained circuit is shown in Figure 3.2. In this circuit

$$\left.\begin{aligned} G = \frac{B_1}{s+\omega_{11}}, \quad \beta_1(s) = \beta + \frac{\alpha(1-\beta)B_2}{(s+\omega_{12})} \simeq \beta + \frac{\alpha(1-\beta)B_2}{s} \\ \text{for } \omega >> \omega_{12} \\ \beta_2 = \gamma, \quad K_1 = 1-\gamma \quad \text{and} \quad K_2 = B_1 \end{aligned}\right\} \tag{3.6}$$

where

$$\alpha = \frac{R_a}{R_a+R_b}, \quad \beta = \frac{R_c}{R_c+R_d} \quad \text{and} \quad \gamma = \frac{R_e}{R_e+R_f}$$

The transfer function of the circuit is

$$\left.\begin{aligned} T(s) = \frac{V_o}{V_i} = \frac{(1-\gamma)B_1(s+\omega_{12})}{D} \\ \simeq \frac{(1-\gamma)B_1 s}{D} \\ \text{for} \quad \omega >> \omega_{12} \end{aligned}\right\} \tag{3.7}$$

where

$$D = s^2 + [\omega_{11}+\omega_{12}+(\beta-\gamma)B_1]s+\omega_{11}\omega_{12}+(\beta-\gamma)B_1\omega_{12}+\alpha(1-\beta)B_1B_2$$

Comparison of equations (3.1) (for the non-inverting case) and (3.7) yields the following design equations :

$$(1-\gamma)B_1 = G_o \frac{\omega_o}{Q} \tag{3.8}$$

$$(\beta-\gamma)B_1 = \frac{\omega_o}{Q} - \omega_{11} - \omega_{12} \tag{3.9}$$

and

$$\alpha(1-\beta)B_1B_2 = \omega_o^2+\omega_{12}^2-\omega_{12}\frac{\omega_o}{Q} \tag{3.10}$$

Thus, from equation (3.8), γ can be obtained in terms of ω_o,Q, G_o and OA parameters. Then β can be determined from equation (3.9) and finally α can be obtained from equation (3.10). Thus, it can be seen that with ω_o,Q and G_o independently specified. α,β and γ values can be determined from equations (3.8) to (3.10). The expressions for ω_o,Q and G_o are :

$$\omega_o = [\omega_{11}\omega_{12} + (\beta-\gamma)B_1\omega_{12} + \alpha(1-\beta)B_1B_2]^{\frac{1}{2}} \tag{3.11}$$

$$Q = \frac{[\omega_{11}\omega_{12} + (\beta-\gamma)B_1\omega_{12} + \alpha(1-\beta)B_1B_2]^{\frac{1}{2}}}{\omega_{11} + \omega_{12} + (\beta-\gamma)B_1} \tag{3.12}$$

$$G_o = \frac{(1-\gamma)B_1}{\omega_{11} + \omega_{12} + (\beta-\gamma)B_1} \tag{3.13}$$

As is typical of all active R circuits, here also the filter characteristics are dependent on resistor ratios and not on

individual resistor values. From equations (3.11) to (3.13) it is observed that approximately

$$\omega_o \alpha (B_1 B_2)^{\frac{1}{2}}$$

$$Q \alpha (\frac{B_2}{B_1})^{\frac{1}{2}}$$

and G_o is independent of B_1 and B_2.

Hence, variations in B_1 and B_2 alter ω_o considerably while the effect on Q_o is negligible if the B variations are identical for both OAs (true if the two OAs are on a single chip). The gain-bandwidth product variations are mainly due to temperature variations. If OAs with temperature stabilised gain-band width products are used in the circuit then variations in ω_o with temperature can be very much reduced. An OA of this type is the National Semiconductor quad OA LM324.

3.1.2 Inverting BPF synthesis :

The inverting band pass transfer function can be written as :

$$T_{BP}(s) = \frac{-Ks}{s^2 + (a-b)s + c}$$

$$= \frac{-K_1 (K_2/s+d)}{[s^2 + (a-b)s + c]/[s(s+d)]}$$

$$= \frac{K_1(-K_2/s+d)}{1 + (\frac{-K_2}{s+d})[\frac{b}{K_2} - \frac{(a-d)s+c}{K_2 s}]} \qquad (3.14)$$

where $K_1K_2 = K$ and d = arbitrary parameter.

This transfer function is of the form

$$T(s) = \frac{K_1 G}{1+G[\beta_2-\beta_1(s)]} \qquad (3.15)$$

where

G represents an amplifier with gain $= \frac{-K_2}{s+d}$

$\beta_1(s)$ represents frequency dependent feedback factor $= [(a-d)s+c]/[K_2 s]$

β_2 represents frequency independent feedback factor $= \frac{b}{K_2}$.

Equation (3.15) is of the same form as equation (3.4) except for the reversal in signs of $G, \beta_1(s)$ and β_2. Hence, the inverting BPF circuit can be realised from the circuit of Figure 3.2 by simply reversing the polarities of both the OAs. The circuit realisation is shown in Figure 3.3. The transfer function for this circuit, based on single pole model, is

$$T(s) = \frac{V_o}{V_i} = \frac{-(1-\gamma)B_1(s+\omega_{12})}{D}$$

$$\simeq \frac{-(1-\gamma)B_1 s}{D} \qquad (3.16)$$

for $\omega >> \omega_{12}$

where

$$D = s^2+[\omega_{11}+\omega_{12}+(\gamma-\beta)B_1]s+\omega_{11}\omega_{12}+(\gamma-\beta)B_1\omega_{12}+\alpha(1-\beta)B_1B_2$$

$$\alpha = \frac{R_a}{R_a+R_b}, \quad \beta = \frac{R_c}{R_c+R_d}, \quad \gamma = \frac{R_e}{R_e+R_f}$$

Comparing equations (3.1) (for the inverting case) and (3.16) the design equations for the inverting BPF circuit are obtained as :

$$(1-\gamma)B_1 = G_o \frac{\omega_o}{Q} \tag{3.17}$$

$$(\gamma-\beta)\ B_1 = \frac{\omega_o}{Q} - \omega_{11} - \omega_{12} \tag{3.18}$$

$$\alpha(1-\beta)B_1B_2 = \omega_o^2 + \omega_{12}^2 - \omega_{12}\frac{\omega_o}{Q} \tag{3.19}$$

Thus, for the inverting BPF circuit, with ω_o, Q and G_o independently specified, values of α, β and γ and hence the resistor values can be determined from equations (3.17) to (3.19). The expressions for ω_o, Q and G_o for the inverting BPF are the same as equations (3.11), (3.12) and (3.13) respectively, except for the replacement of $(\beta-\gamma)$ by $(\gamma-\beta)$.

3.1.3 Multifunction capability :

Circuits with multifunction capability are useful since a variety of filter functions can be realised from a single circuit with a small number of components and minimum component changes. The circuit of Figure 3.3 has this capability. For

this circuit, the transfer function at the output of the second OA is

$$\frac{V_3}{V_i} = \frac{\alpha(1-\gamma)B_1B_2}{D} \qquad (3.20)$$

where D is as defined in equation (3.16).

The corresponding transfer function for the non-inverting BPF circuit of Figure 3.2 is obtained by replacing $(\gamma-\beta)$ by $(\beta-\gamma)$ in equation (3.20). Thus, the inverting and non-inverting BPF circuits realise non-inverting low pass functions in addition to the band pass functions. Further, as is shown subsequently, in Chapter IV on all pass filters and in Chapter VI on notch filters, from the inverting BPF circuit, all pass and notch functions can also be realised by including three additional resistors. In equation (3.16), which gives the transfer function of the inverting BPF circuit, if

$$\beta = \frac{\omega_{11} + \omega_{12} + \gamma B_1}{B_1} \qquad (3.21)$$

then the denominator 's' coefficient becomes zero. Thus, under this condition the circuit behaves as a sinusoidal oscillator with its angular frequency of oscillations given by

$$\omega_o = [\omega_{11}\omega_{12} + (\gamma-\beta)B_1\omega_{12} + \alpha(1-\beta)B_1B_2]^{\frac{1}{2}} \qquad (3.22)$$

The corresponding condition for oscillations for the non-inverting BPF circuit is

$$\gamma = \frac{\omega_{11} + \omega_{12} + \beta B_1}{B_1} \qquad (3.23)$$

The angular frequency of oscillations is given by equation (3.11) under the above condition.

Thus the circuit of Figure 3.3 realises inverting BP, non-inverting LP, AP, Notch and oscillator functions. The circuit of Figure 3.2 realises non-inverting BP and LP and oscillator functions.

3.1.4 Alternate non-inverting BPF realisations :

Equation (3.3), for non-inverting BPF, can be rewritten in a different way to realise some of the reported non-inverting BPF circuits. One way to write equation (3.3) is

$$T_{BP}(s) = \frac{K_1 \cdot \frac{K_2}{s+d}}{1 + \left(\frac{K_2}{s+d}\right)\left[\frac{a-b-d}{K_2} + \frac{c}{K_2 s}\right]} \qquad (3.24)$$

This is of the form

$$T(s) = \frac{K_1 G}{1 + G[\beta_1(s) + \beta_2]} \qquad (3.25)$$

i.e., both the feedbacks are negative. The corresponding circuit realisation, shown in Figure 3.4 is by Laker et al. [1]. The transfer function for this circuit is

$$T(s) = \frac{V_o}{V_i} \simeq \frac{\gamma \frac{B_1}{s+\omega_{11}}}{1 + \left(\frac{B_1}{s+\omega_{11}}\right)\left[(1-\beta) + \frac{\alpha\beta B_2}{s}\right]} \qquad (3.26)$$

for $\omega >> \omega_{12}$

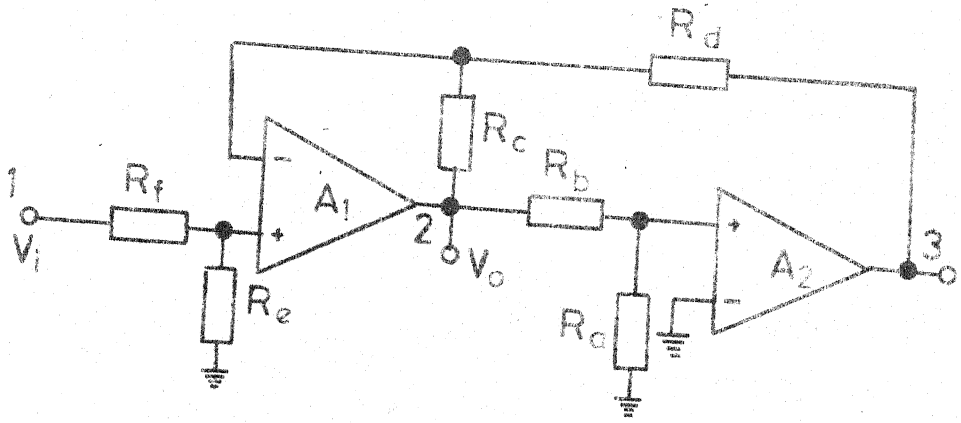

FIG. 3.4 BPF CIRCUIT OF LAKER et al.

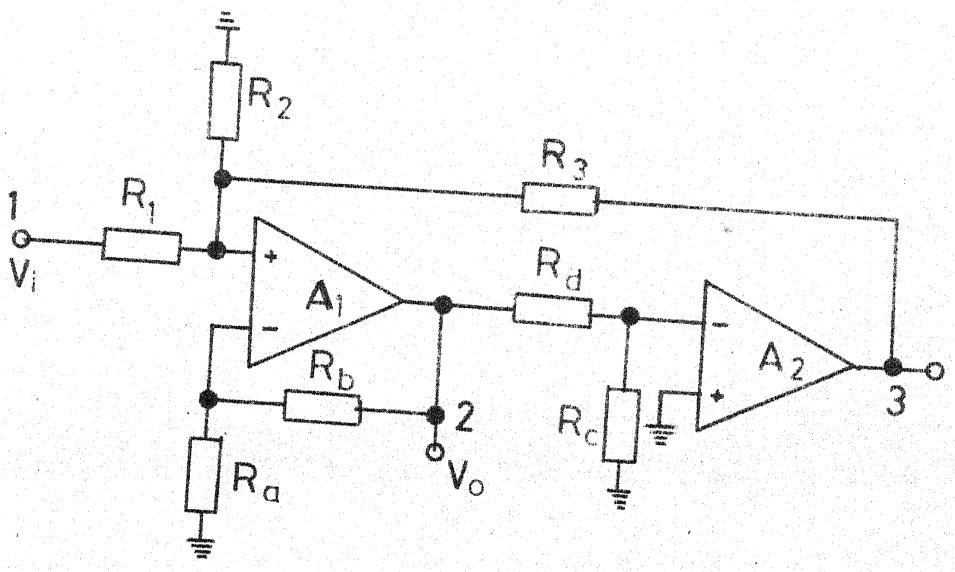

FIG. 3.5 BPF CIRCUIT OF LI AND LI

where

$$\alpha = \frac{R_a}{R_a+R_b}, \quad \beta = \frac{R_c}{R_c+R_d} \quad \text{and} \quad \gamma = \frac{R_e}{R_e+R_f}$$

At the output of the other OA, a non-inverting LP transfer function is realised. Thus, this circuit, with two OAs and six resistors realises only non-inverting BP and LP functions. The circuit of Li and Li [2] also follows from equation (3.24). This circuit, shown in Figure 3.5, uses two OAs and seven resistors. Its transfer function is

$$T(s) = \frac{V_o}{V_i} \simeq \frac{\frac{R}{R_1}\left(\frac{B_1}{s+\omega_{11}}\right)}{1 + \left(\frac{B_1}{s+\omega_{11}}\right)\left[\alpha + \frac{R}{R_3}\frac{\beta B_2}{s}\right]} \qquad (3.27)$$

$$\text{for } \omega >> \omega_{12}$$

where

$$R = R_1 || R_2 || R_3, \quad \alpha = \frac{R_a}{R_a+R_b}, \quad \beta = \frac{R_c}{R_c+R_d}$$

At the output of the other OA in this circuit, an inverting LP transfer function is obtained. Srinivasan [3] has proposed a non-inverting BPF circuit, using two OAs and six resistors. This circuit, shown in Figure 3.6 has the transfer function

$$T(s) = \frac{V_o}{V_i} \simeq \frac{B_1/(s+\omega_{11})}{1 + \left(\frac{B_1}{s+\omega_{11}}\right)\left[\alpha + \frac{(1-\alpha)^2 B_2}{s}\right]} \qquad (3.28)$$

$$\text{for } \omega >> \omega_{12}$$

where

$$\alpha = \frac{R_a}{R_a+R_b}$$

At the output of the other OA in this circuit, a non-inverting LP response is obtained. From equation (3.28) it can be seen that this circuit is of the same form as that of Laker et al [1]. This circuit of Srinivasan, has the advantage of high input impedance. But it has a major limitation that only one of the three parameters, ω_o, Q and G_o, can be independently specified.

3.1.5 Alternate inverting BPF realisations :

Equation (3.14) could be rewritten as

$$T(s) = \frac{K_1(\frac{-K_2}{s+d})}{1 + (\frac{-K_2}{s+d})\,[-\frac{a-b-d}{K_2} - \frac{c}{K_2 s}]} \qquad (3.29)$$

The corresponding inverting BPF realisation, proposed by Soderstrand [4] is given in Figure 3.7. The transfer function for this circuit is

$$T(s) = \frac{V_o}{V_i} \simeq \frac{(\frac{R}{R_3})(\frac{-B_1}{s+\omega_{11}})}{1 + (\frac{-B_1}{s+\omega_{11}})[-\frac{R}{R_2} - \frac{RB_2}{R_1 s}]} \qquad (3.30)$$

$$\text{for } \omega >> \omega_{12}$$

where $R = R_1 || R_2 || R_3$.

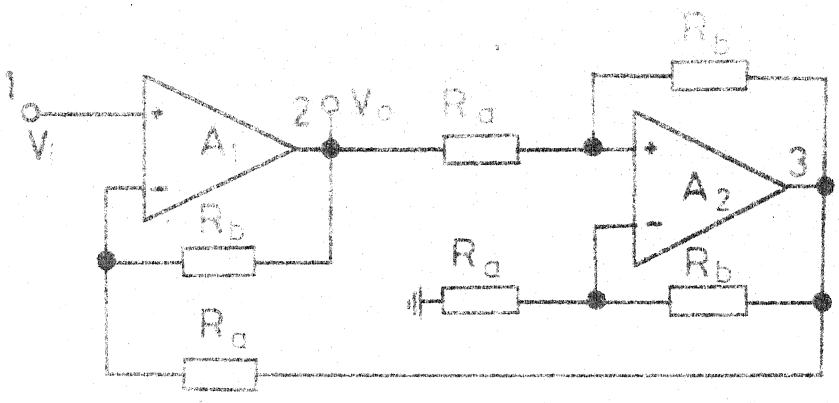

FIG. 3.6 BPF CIRCUIT OF SRINIVASAN

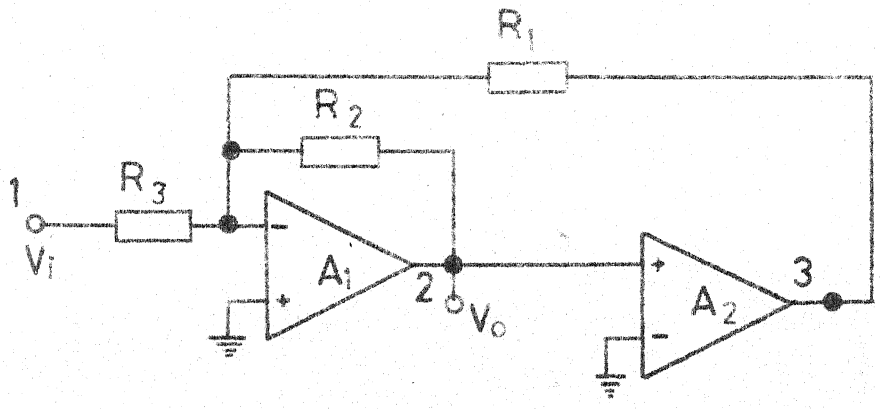

FIG. 3.7 BPF CIRCUIT OF SODERSTRAND

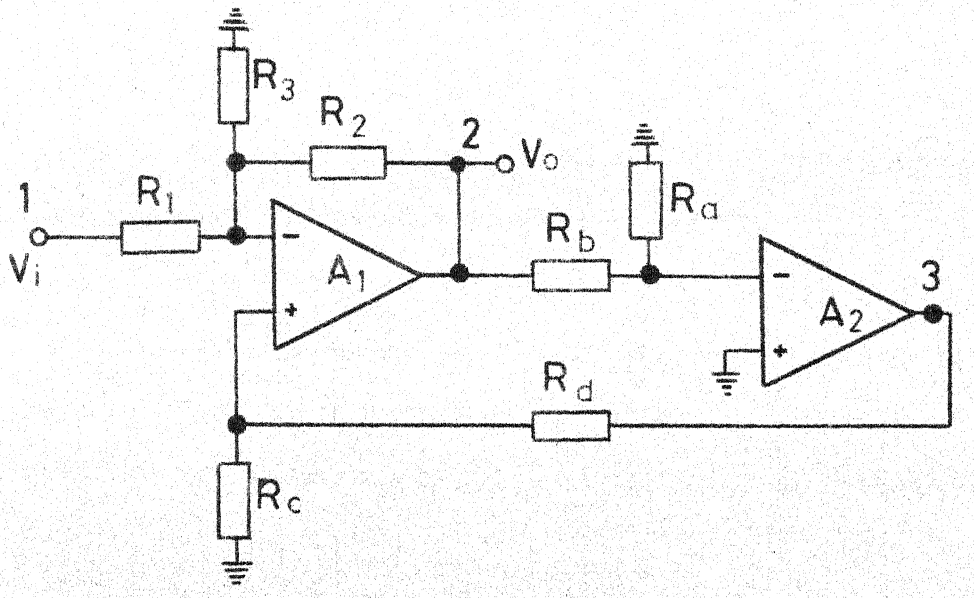

FIG. 3.8 BPF CIRCUIT OF MITRA AND AATRE

This circuit of Soderstrand has only three resistors and two OAs. But it has the disadvantage that only two of the three parameters, ω_o,Q and G_o can be independently specified. Soderstrand's circuit has an inverting LP response at the output of the other OA. With the addition of three more resistors this circuit can realise all pass and notch functions It cannot realise non-inverting BPF and oscillator functions.

The inverting BPF circuit of Mitra and Aatre [5] also follows from equation (3.29). This circuit, shown in Figure 3.8 has the transfer function

$$T(s) = \frac{V_o}{V_i} \approx \frac{\frac{R}{R_1}\left(\frac{-B_1}{s+\omega_{11}}\right)}{1 + \left(\frac{-B_1}{s+\omega_{11}}\right)\left[-\frac{R}{R_2} - \frac{\alpha\beta B_2}{s}\right]} \qquad (3.31)$$

for $\omega >> \omega_{12}$

where $R = R_1 || R_2 || R_3$, $\alpha = \frac{R_a}{R_a+R_b}$ and $\beta = \frac{R_c}{R_c+R_d}$

In Mitra and Aatre's circuit, ω_o,Q and G_o can be independently specified. With the addition of three resistors the circuit can realise all pass and notch functions. A non-inverting LP response is obtained at the output of the other OA. However, this circuit uses seven resistors as compared to six in the newly proposed BPF circuit of Figure 3.3. Also, it cannot realise non-inverting BPF and oscillator functions.

The circuit of Ho and Chiu [6] also follows from equation (3.29). This circuit can be obtained from the BPF circuit of Figure 3.3 by making $R_c = 0$ and $R_d = \infty$. The transfer function for $\omega >> \omega_{12}$ is

$$T(s) = \frac{(1-\gamma)\left(\frac{-B_1}{s+\omega_{11}}\right)}{1 + \left(\frac{-B_1}{s+\omega_{11}}\right)\left[-\gamma - \frac{\alpha B_2}{s}\right]} \qquad (3.32)$$

where

$$\alpha = \frac{R_a}{R_a+R_b} \quad \text{and} \quad \gamma = \frac{R_e}{R_e+R_f}$$

This circuit also realises a non-inverting LP function at the other OA output. It can realise AP and notch functions with the addition of three more resistors. Further as shown by Venkateswaran [8] it realises a notch response at the inverting input terminal of OA, A_1. However, it cannot realise non-inverting BPF and oscillator functions.

3.1.6 Sensitivity analysis :

Sensitivity of a circuit is a measure of the degree of variation of its performance from nominal, due to changes in the components of the circuit. It is desirable to have circuits with low sensitivity to parameter changes. In band pass filters, the sensitivity figures of interest are the sensitivities of ω_o, Q and G_o to all active and passive parameters of the filter.

Sensitivity is defined as

$$S_x^m = \left(\frac{\partial m}{m}\right)/\left(\frac{\partial x}{x}\right) = \frac{\partial m}{\partial x} \cdot \frac{x}{m} \qquad (3.33)$$

where S_x^m = sensitivity of 'm' with respect to 'x'.

For the non-inverting BPF circuit of Figure 3.2 ω_o, Q and G_o sensitivities, with respect to all active and passive parameters have been obtained. These are given in Table 3.1. From the tabulation, the following features can be noted.

$$\left.\begin{aligned} S_{\omega_{11}}^{\omega_o} + S_{\omega_{12}}^{\omega_o} + S_{B_1}^{\omega_o} + S_{B_2}^{\omega_o} &= 1 \\ S_{\omega_{11}}^{Q} + S_{\omega_{12}}^{Q} + S_{B_1}^{Q} + S_{B_2}^{Q} &= 0 \\ S_{\omega_{11}}^{G_o} + S_{\omega_{12}}^{G_o} + S_{B_1}^{G_o} + S_{B_2}^{G_o} &= 0 \\ \sum_{R=R_a}^{R_f} S_R^{\omega_o} = \sum_{R=R_a}^{R_f} S_R^{Q} = \sum_{R=R_a}^{R_f} S_R^{G_o} &= 0 \end{aligned}\right\} \qquad (3.34)$$

All passive and active sensitivities are less than 1. Only resistor ratios figure in the expressions for ω_o, Q, G_o [equations (3.11) to (3.13)]. Hence, the algebraic sum sensitivity of, each of ω_o, Q and G_o with respect to the six resistors is zero. While the algebraic sum sensitivities of Q and

TABLE 3.1

ω_o, Q and G_o sensitivities for non-inverting BPF

Parameter	$S_x^{\omega_o}$	S_x^{Q}	$S_x^{G_o}$
R_a	$\frac{\alpha(1-\alpha)(1-\beta)B_1B_2}{2\omega_o^2}$	$\frac{\alpha(1-\alpha)(1-\beta)B_1B_2}{2\omega_o^2}$	0
R_b	$-S_{R_a}^{\omega_o}$	$-S_{R_a}^{Q}$	$-S_{R_a}^{G_o}$
R_c	$\frac{\beta(1-\beta)B_1(\omega_{12}-\alpha B_2)}{2\omega_o^2}$	$\frac{\beta(1-\beta)B_1[\omega_a(\omega_{12}-\alpha B_2)-2\omega_o^2]}{2\omega_o^2\omega_a}$	$-\frac{\beta(1-\beta)B_1}{\omega_a}$
R_d	$-S_{R_c}^{\omega_o}$	$-S_{R_c}^{Q}$	$-S_{R_c}^{G_o}$
R_e	$-\frac{\gamma(1-\gamma)B_1\omega_{12}}{2\omega_o^2}$	$\frac{\gamma(1-\gamma)B_1(2\omega_o^2-\omega_a\omega_{12})}{2\omega_o^2\omega_a}$	$\frac{\gamma[(1-\beta)B_1-\omega_{11}-\omega_{12}]}{\omega_a}$

Contd...

Parameter	$S_x^{\omega_o}$	S_x^Q	$S_x^{G_o}$
R_f	$-S_{R_e}^{\omega_o}$	$-S_{R_e}^{Q}$	$-S_{R_e}^{G_o}$
ω_{11}	$\dfrac{\omega_{11}\omega_{12}}{2\omega_o^2}$	$-\dfrac{\omega_{11}[\omega_{12}(\omega_a-2\omega_{12})+2\alpha(1-\beta)B_1B_2]}{2\omega_o^2\omega_a}$	$-\dfrac{\omega_{11}}{\omega_a}$
ω_{12}	$\dfrac{\omega_{12}(\omega_a-\omega_{12})}{2\omega_o^2}$	$\dfrac{\omega_{12}[\omega_a(\omega_a-\omega_{12})-2\omega_o^2]}{2\omega_o^2\omega_a}$	$-\dfrac{\omega_{12}}{\omega_a}$
B_1	$\dfrac{\omega_o^2-\omega_{11}\omega_{12}}{2\omega_o^2}$	$\dfrac{\omega_a(\omega_o^2-\omega_{11}\omega_{12})-2(\beta-\gamma)B_1\omega_o^2}{2\omega_o^2\omega_a}$	$\dfrac{\omega_{11}+\omega_{12}}{\omega_a}$
B_2	$\dfrac{\alpha(1-\beta)B_1B_2}{2\omega_o^2}$	$\dfrac{\alpha(1-\beta)B_1B_2}{2\omega_o^2}$	0

Note : $\omega_o^2 = \omega_{11}\omega_{12} + (\beta-\gamma)B_1\omega_{12}+\alpha(1-\beta)B_1B_2$; $\omega_a = \omega_{11}+\omega_{12}+(\beta-\gamma)B_1$

(2.6). This is reproduced below

$$A_i = \frac{-B_i(s - \omega_{2i})}{\omega_{2i}(s + \omega_{1i})} \tag{3.35}$$

With this model, the transfer function for the non-inverting BPF circuit is

$$T_{BP}(s) = \frac{V_o}{V_i} = \frac{(1-\gamma)B_1\omega_{22}(s+\omega_{12})(\omega_{21}-s)}{D}$$

$$\simeq \frac{(1-\gamma)B_1\omega_{21}\omega_{22}s}{D} \tag{3.36}$$

$$\text{for } \omega_{21} >> \omega \text{ and } \omega >> \omega_{12}$$

where

$$D = [\omega_{21}\omega_{22} - (\beta-\gamma)B_1\omega_{22}+\alpha(1-\beta)B_1B_2]s^2$$

$$+ [\omega_{21}\omega_{22}\{\omega_{11}+\omega_{12}+(\beta-\gamma)B_1\} -(\beta-\gamma)B_1\omega_{12}\omega_{22}$$

$$- \alpha(1-\beta)B_1B_2(\omega_{21}+\omega_{22})]s+\omega_{21}\omega_{22}[\omega_{11}\omega_{12}+(\beta-\gamma)B_1\omega_{12}$$

$$+ \alpha(1-\beta)B_1B_2]$$

From equation (3.36) expressions for centre frequency (ω_o') selectivity (Q') and resonant gain (G_o') based on pole-zero model can be obtained as

$$\omega_o' = \left[\frac{\omega_{21}\omega_{22}\,[\omega_{11}\omega_{12}+(\beta-\gamma)B_1\omega_{12}+\alpha(1-\beta)B_1B_2]}{\omega_{21}\omega_{22}-(\beta-\gamma)B_1\omega_{22}+\alpha(1-\beta)B_1B_2}\right]^{\frac{1}{2}} \qquad (3.37)$$

$$Q' = \frac{\omega_o'\,[\omega_{21}\omega_{22}-(\beta-\gamma)B_1\omega_{22}+\alpha(1-\beta)B_1B_2]}{P} \qquad (3.38)$$

and

$$G_o' = \frac{(1-\gamma)B_1\omega_{21}\omega_{22}}{P} \qquad (3.39)$$

where

$$P = \omega_{21}\omega_{22}[\omega_{11}+\omega_{12}+(\beta-\gamma)B_1]-(\beta-\gamma)B_1\omega_{12}\omega_{22}-\alpha(1-\beta)B_1B_2(\omega_{21}+\omega_{22})$$

ω_o', Q' and G_o' can be expressed in terms of ω_o, Q and G_o the corresponding parameters based on single pole model, by substituting for $(1-\gamma)B_1$, $(\beta-\gamma)B_1$ and $\alpha(1-\beta)B_1B_2$ from equations (3.8) to (3.10) in equations (3.37) to (3.39). This leads to the following expressions for ω_o', Q' and G_o'.

$$\omega_o' = \left[\frac{\omega_{21}\omega_{22}\,\omega_o^2}{\omega_{21}\omega_{22}-\frac{\omega_o}{Q}(\omega_{22}+\omega_{12})+\omega_o^2+\omega_{22}(\omega_{11}+\omega_{12})+\omega_{12}^2}\right]^{\frac{1}{2}} \qquad (3.40)$$

$$\simeq \omega_o$$

since $\omega_o \ll \omega_{21}$ and ω_{22}

$$Q' = \frac{\omega_o\omega_{21}\omega_{22}}{\omega_{21}\omega_{22}\frac{\omega_o}{Q}-(\frac{\omega_o}{Q}-\omega_{11}-\omega_{12})\omega_{12}\omega_{22}-[\omega_o^2-(\frac{\omega_o}{Q}-\omega_{12})\omega_{12}](\omega_{21}+\omega_{22})}$$

$$Q' \simeq \frac{\omega_o \omega_{21} \omega_{22}}{\omega_{21}\omega_{22}\frac{\omega_o}{Q} - \omega_o^2(\omega_{21}+\omega_{22})} \qquad (3.41)$$

for ω_{11} and $\omega_{12} << \omega_o$

and

$$G_o' \simeq \frac{G_o \frac{\omega_o}{Q} \omega_{21}\omega_{22}}{\omega_{21}\omega_{22}\frac{\omega_o}{Q} - \omega_o^2(\omega_{21}+\omega_{22})} \qquad (3.42)$$

From equation (3.40) it is seen that the centre frequency is practically unaffected by the effect of OA second pole. Equations (3.41) and (3.42) show that both selectivity and resonant gain are enhanced due to the effect of second pole. If ω_o and Q are so chosen that

$$\frac{\omega_o}{Q} = \frac{\omega_o^2(\omega_{21}+\omega_{22})}{\omega_{21}\omega_{22}} \qquad (3.43)$$

then both Q' and G_o' become infinity, i.e., the circuit becomes oscillatory. Thus equation (3.43) gives the lower limit for the ratio $\frac{\omega_o}{Q}$. Kapustian et al [9] have arrived at a similar result as equation (3.43) by a lengthy analysis with the conventional two pole model, assuming the two OAs to be identical. They have suggested introduction of a small capacitor - across R_d in the BPF circuit of Mitra and Aatre [5], shown in Figure 3.8 to compensate for the excess phase contributed by the OA second pole.

3.1.8 Design equations based on pole-zero model :

An alternate procedure to eliminate the effect of OA second pole on BPF performance is to obtain the design equations for the circuit from equations (3.37) to (3.39) instead of from equations (3.8) to (3.10). From equations (3.37) to (3.39) with ω_o', Q' and G_o' replaced by ω_o, Q and G_o the design equations are obtained as

$$(1-\gamma)B_1 = \frac{G_o\left[\frac{\omega_o}{Q}\ \omega_{21}^2\omega_{22} + \omega_o^2(\omega_{21}^2-\omega_{22}^2+\omega_{22}\omega_{11}+\omega_{22}\omega_{12})\right]}{\omega_{22}\left(\omega_o^2 + \omega_{21}\frac{\omega_o}{Q} + \omega_{21}^2\right)} \qquad (3.44)$$

$$(\beta-\gamma)B_1 = \frac{\omega_{21}\left[\omega_o^2(\omega_{21}+\omega_{22})+\omega_{21}\omega_{22}\left(\frac{\omega_o}{Q}-\omega_{11}-\omega_{12}\right)\right]}{\omega_{22}\left(\omega_o^2 + \omega_{21}\frac{\omega_o}{Q} + \omega_{21}^2\right)} \qquad (3.45)$$

and

$$\alpha(1-\beta)B_1B_2 = \frac{\omega_{21}\ \omega_{22}\ \omega_o^2}{\omega_o^2 + \omega_{21}\frac{\omega_o}{Q} + \omega_{21}^2} \qquad (3.46)$$

Since ω_{11} and $\omega_{12} << \omega_{21}$ and ω_{22}

Hence, from equation (3.44) γ can be obtained in terms of ω_o, Q, G_o and OA parameters (including OA second pole frequency). Then β can be determined from equation (3.45) and finally α can be obtained from equation (3.46). Thus the effects of OA second pole are incorporated in the design equations obtained using the pole-zero model. BPF circuits designed on the basis of equations (3.44) to (3.46) can operate at higher

centre frequencies and Q values as compared to the circuits designed based on single pole model for OAs. At the same time, the design procedure is as simple as that with single pole model analysis.

3.1.9 Experimental results :

The non-inverting band pass filter circuit of Figure 3.2 was tested using two NE 536 OAs, 0.5 percent metal film resistors and miniature multiturn potentiometers. The relevant parameters of the two OAs were measured using the method of Graeme et al [10]. All voltage and resistance measurements were carried out using Philips model PM 2522 digital voltmeter. Phase measurements were done with HP 1742A, 100 MHz dual trace oscilloscope. Frequency measurements were made with ECIL frequency counter, model EC 730. HP 651A test oscillator was the signal source. The measured parameters of the OAs are given in Table 3.2.

TABLE 3.2

OA Parameters (NE 536)

Parameter	OA 1	OA 2
$\frac{\omega_{1i}}{2\pi}$ (Hz)	12.0	11.0
$\frac{\omega_{2i}}{2\pi}$ (MHz)	4.0	4.0
$\frac{B_i}{2\pi}$ (MHz)	2.63	2.59
V_{cc}	± 12V	± 12V
Temp.	$27^{o}C$	

The BPF circuit was tested for three different sets of specifications. The experimental and theoretical values are shown in Table 3.3.

TABLE 3.3

Band pass filter performance

BPF	$\omega_o/2\pi$ (KHz)		Q		G_o	
	Theo.	Expt.	Theo.	Expt.	Theo.	Expt.
(a)	250	250	10.0	9.98	105	105
(b)	250	251	25.0	25.3	260	262
(c)	500	500	25.0	24.9	133	132

The resistor values (in Kilo ohms) for the three sets of specifications are given in Table 3.4.

TABLE 3.4

Resistor values for band pass filters

BPF	R_a (KΩ)	R_b (KΩ)	R_c (KΩ)	R_d (KΩ)	R_e (KΩ)	R_f (KΩ)
(a)	1.00	105	1.00	38.0	1.00	100
(b)	1.00	109	1.00	38.7	1.00	100
(c)	1.00	25.0	1.00	14.6	1.00	100

The BPF frequency responses are shown in Figures 3.9 to 3.11. From the obtained responses, the validity of the pole-zero model and its usefulness in designing BPFs with large ω_o and Q values is seen.

3.1.10 Comparison of BPF circuits :

The newly synthesised BPF circuit has multifunction capability. It provides inverting BP, non-inverting BP (with polarities of both OAs reversed), non-inverting LP and oscillator functions. With the addition of three more resistors, as suggested by Mitra and Aatre [5], it can realise AP and notch functions. A comparison of the new circuit, with reported BPF circuits in terms of number of resistors and functions realised is given in Table 3.5.

All the inverting BPF circuits can realise AP and notch functions with the addition of three more resistor . From Table 3.5 it is seen that only the newly proposed circuit realise, three separate functions, viz., inverting or non-inverting BP, non-inverting LP and oscillators. The circuit have the desirable characteristic that they can be designed, based on single pole or pole-zero model for OAs, with ω_o, Q and G_o independently specified. Soderstrand's circuit uses only three resistors to realise inverting BP and LP functions. But it has the disadvantage that, once ω_o and Q are specified. G_o is automatically fixed. The circuit of Mitra

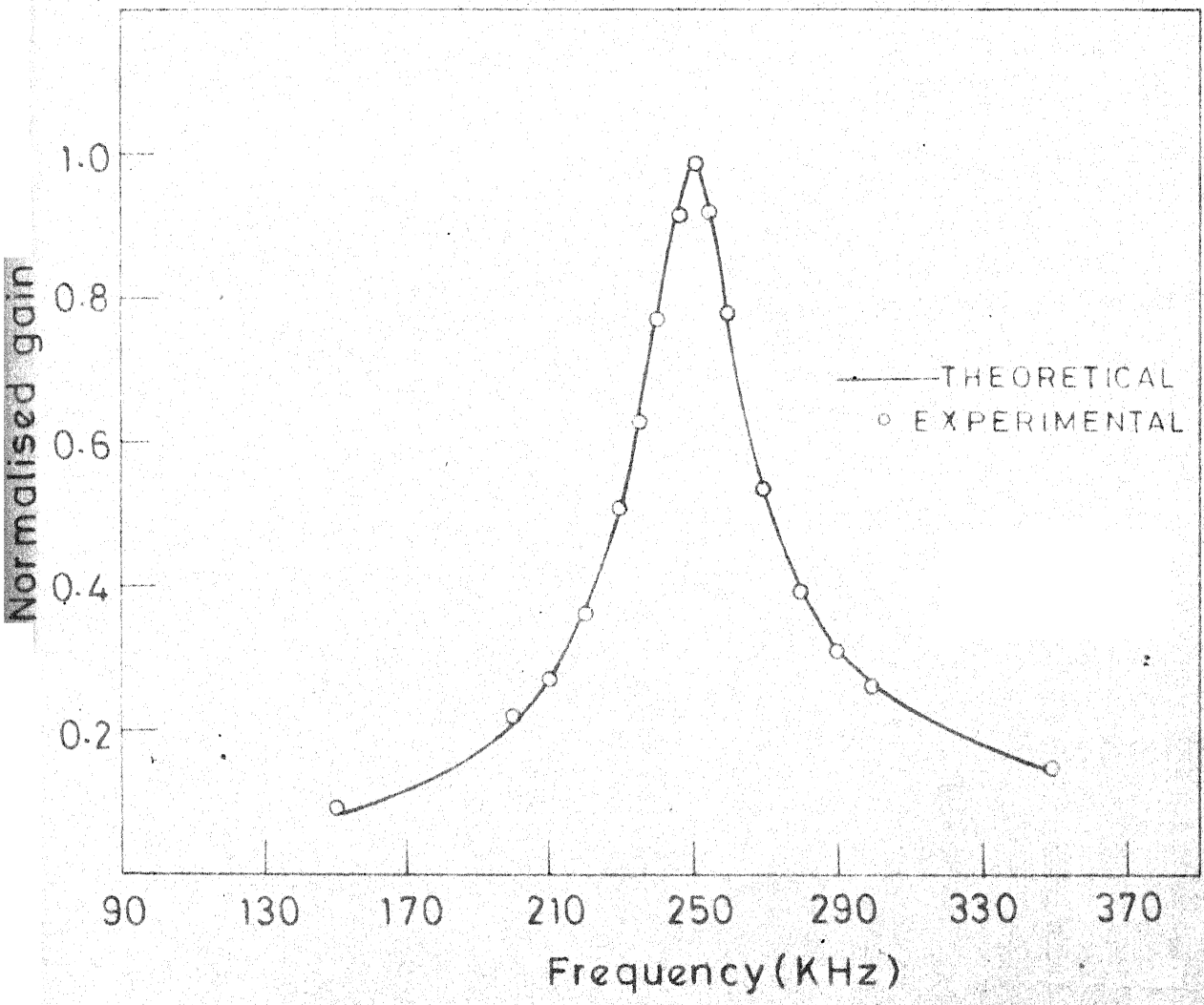

FIG. 3.9 NON INVERTING BPF FREQUENCY RESPONSE
(f_o = 250 KHz , Q = 10)

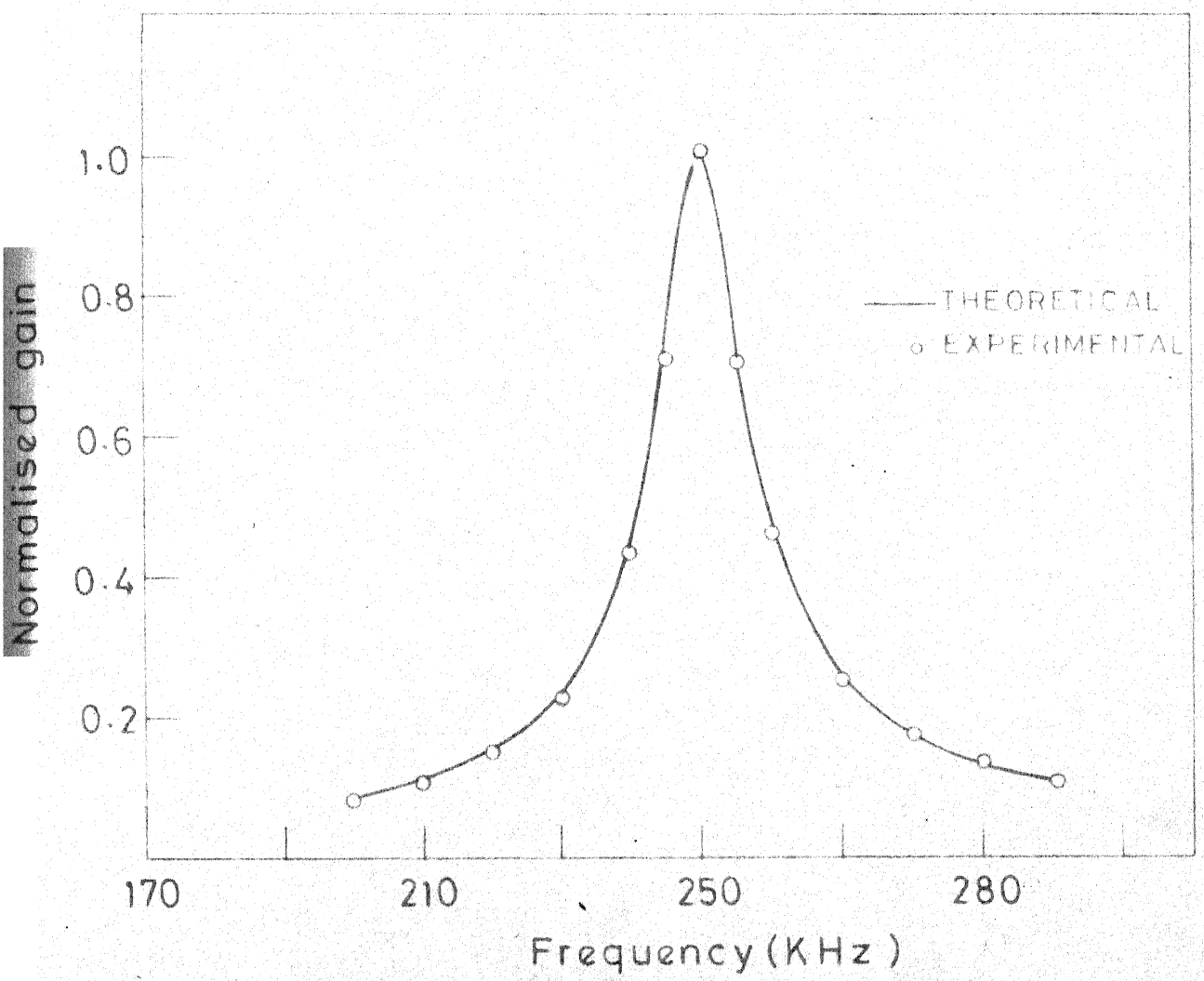

FIG. 3.10 NON INVERTING BPF FREQUENCY RESPONSE (f_o = 250 KHz , Q = 25)

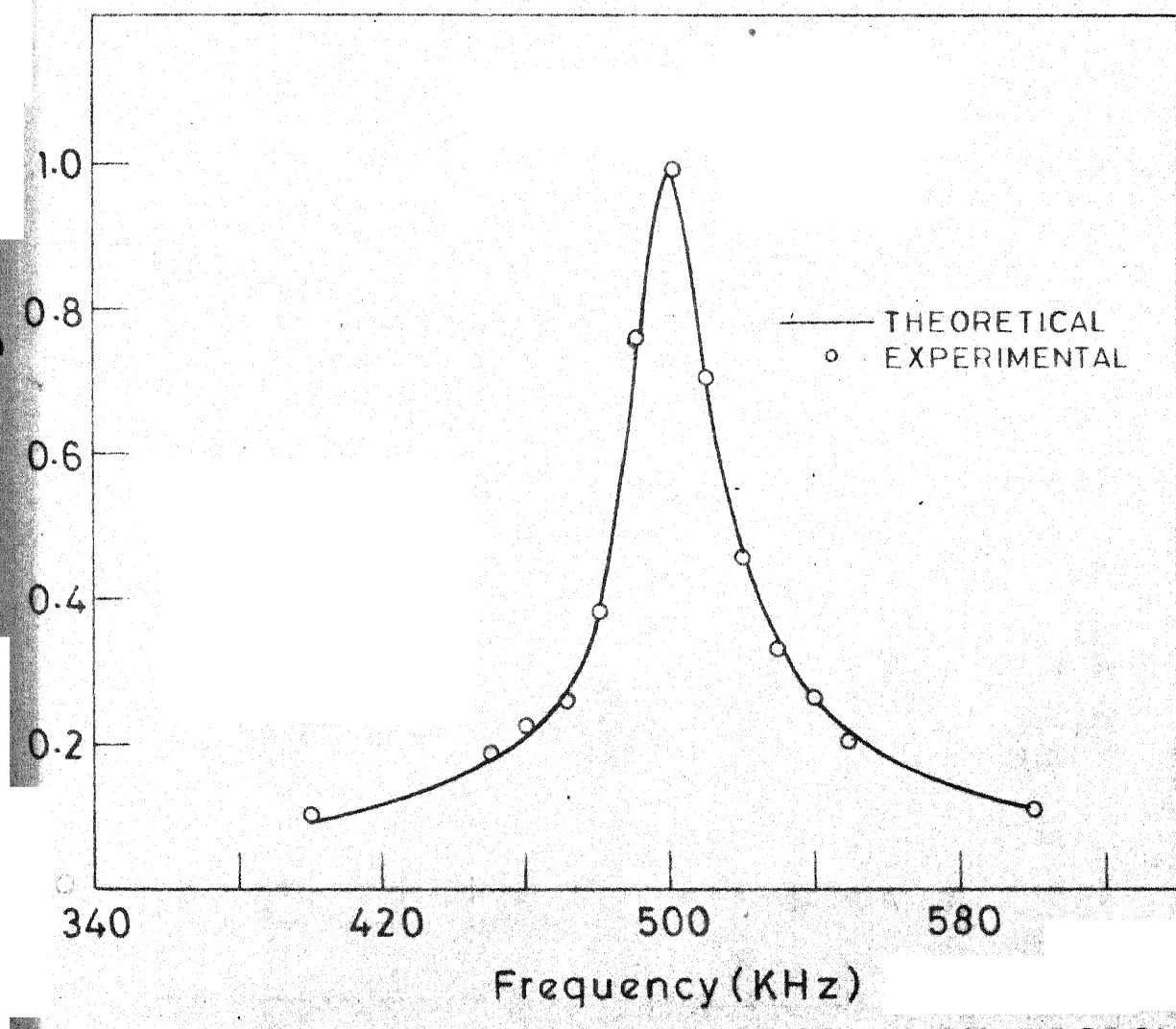

FIG. 3.11 NON INVERTING BPF FREQUENCY RESPONSE
(f_o = 500 KHz , Q = 25)

TABLE 3.5

Comparison of band pass filters

Circuit	Figure No.	Number of resistors	Functions realised
Proposed	3.2	6	NINV BP and LP,OSC
	3.3	6	INV BP,NINV LP,OSC
Laker et al.	3.4	6	NINV BP, NINV LP
Li and Li	3.5	7	NINV BP, INV LP,
Srinivasan	3.6	6	NINV BP, NINV LP
Soderstrand	3.7	3	INV BP, INV LP
Mitra and Aatre	3.8	7	INV BP, NINV LP
Ho and Chiu	3.3 (with R_c=0, $R_d = \infty$)	4	INV BP NINV LP

Note : INV = inverting, NINV = non-inverting, OSC = oscillator.

and Aatre uses seven resistors to realise inverting BP and non-inverting LP. However, it does not realise oscillator function. Ho and Chiu's circuit realises the same two functions with only four resistors. But in this circuit only ω_o and Q can be independently specified. The non-inverting BPF circuits of

Laker et al., Li and Li and Srinivasan realise just two functions with , six, seven and six resistors respectively. Of these the circuit of Laker et al. has minimum number of resistors and at the same time has facility for specifying ω_o, Q and G_o independently.

If both non-inverting and inverting BP and LP transfer functions are required from a single circuit then more number of resistors are required. The two circuits of Schaumann and Brand [11], with seven and eight resistors respectively, realise these. These circuits, shown in Figures 3.12(a) and 3.12(b), however, do not realise oscillator function.

3.2 Low pass filter :

3.2.1 Non-inverting LPF synthesis :

The typical nth order non-inverting low pass transfer function is

$$T_{LP}(s) = \frac{a_n}{s^n + a_1 s^{n-1} + a_2 s^{n-2} + \ldots + a_{n-1} s + a_n} \qquad (3.47)$$

This could be written in the form

$$T_{LP}(s) = \frac{b_1 b_2 \ldots b_n}{s^n + b_1 s^{n-1} + b_1 b_2 s^{n-2} + \ldots + b_1 b_2 \ldots b_n} \qquad (3.48)$$

Let us consider the first order non-inverting low pass transfer function

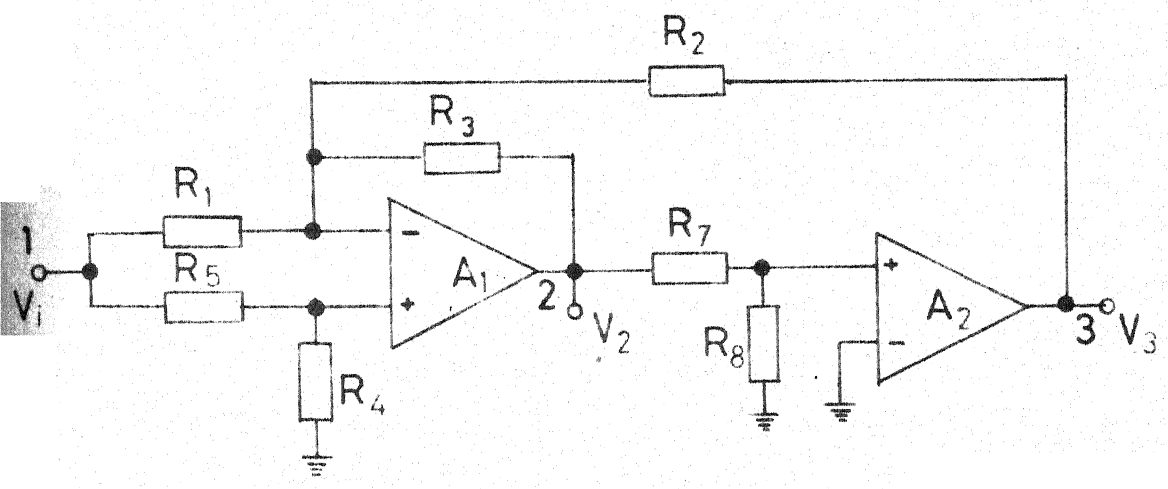

(a)

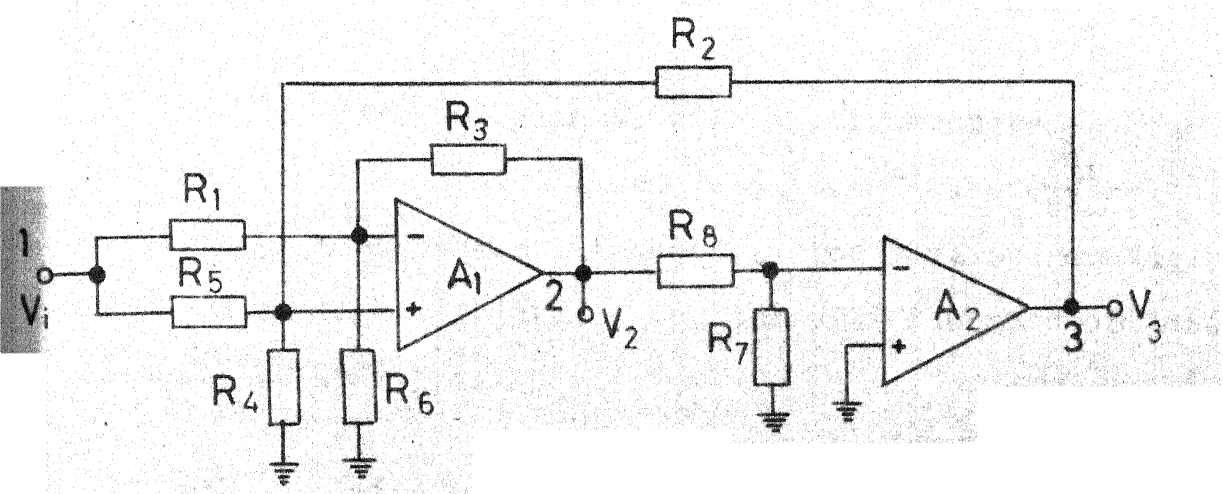

(b)

G. 3.12 (a) & (b) BPF CIRCUITS OF SCHAUMANN AND BRANI

$$T_{LP1}(s) = \frac{b_1}{s+b_1} \tag{3.49}$$

Equation (3.49) can be rewritten as

$$T_{LP1}(s) = \frac{b_1/(s+c_1)}{1 + (\frac{b_1}{s+c_1})(\frac{b_1-c_1}{b_1})}$$

$$\simeq \frac{b_1/(s+c_1)}{1 + \frac{b_1}{s+c_1}} \tag{3.50}$$

for $c_1 << b_1$

where c_1 = arbitrary parameter.

This transfer function is of the form

$$T(s) = \frac{G}{1 + G} \tag{3.51}$$

i.e., an amplifier of gain G, with unity negative feedback. This amplifier can be realised by an OA of gain $(\frac{B_1}{s+\omega_{11}})$ followed by a resistive attenuator. The realised configuration is shown in Figure 3.13(a). The transfer function of this circuit, at node 2 is,

$$T(s) = \frac{V_{o1}}{V_i} = \frac{\alpha B_1}{s+\omega_{11}+\alpha B_1} \tag{3.52}$$

$$\simeq \frac{\alpha B_1}{s+\alpha B_1}, \quad \text{for } \alpha B_1 >> \omega_{11}$$

where $\alpha = \frac{R_a}{R_a+R_b}$

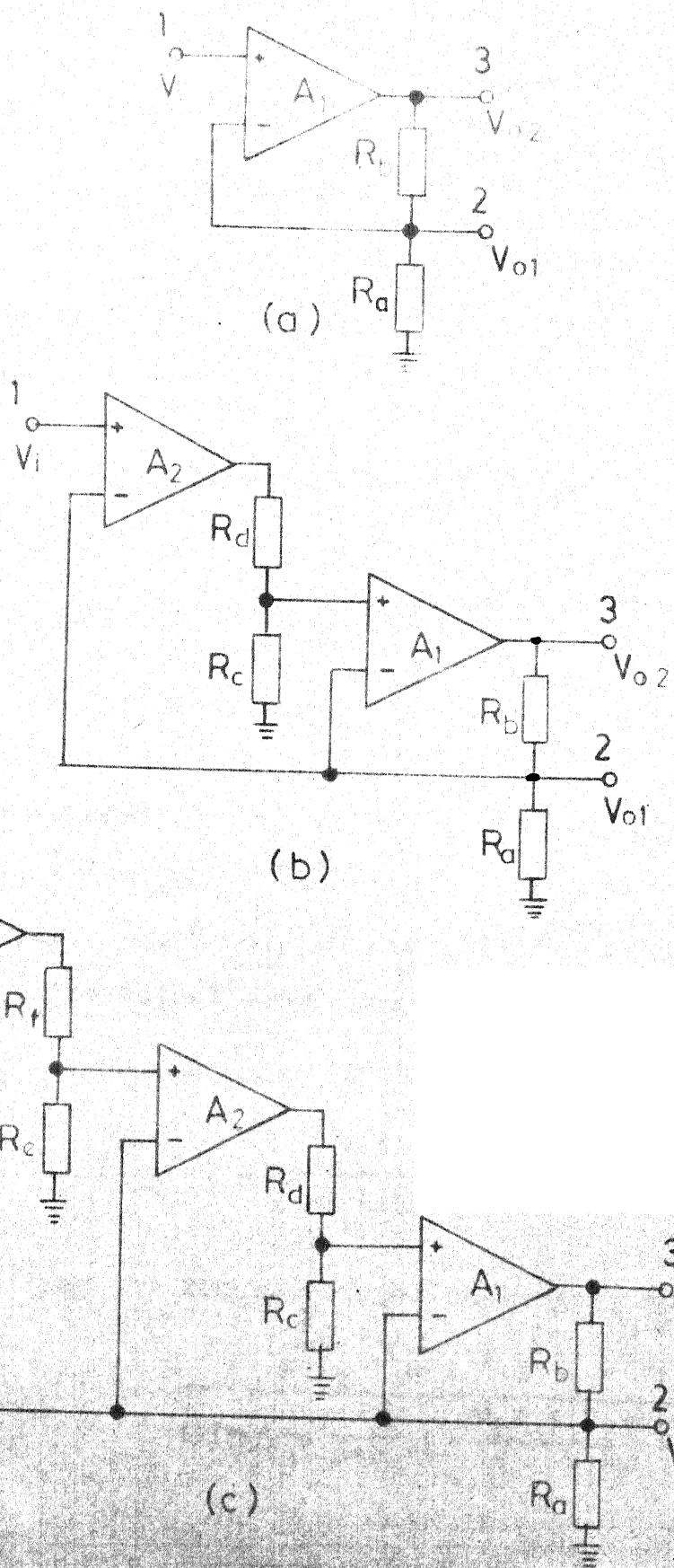

3.13 NON-INVERTING LPF CIRCUITS (a) FIRST ORDER (b) SECOND ORDER (c) THIRD ORDER

By comparing equations (3.49) and (3.52) the design equation for the first order non-inverting LPF can be obtained as

$$\alpha = \frac{b_1}{B_1} \tag{3.53}$$

Thus, as in the case of all active R filters, only resistor ratios and not individual resistor values matter. Since $\alpha < 1$, the maximum realisable value of b_1 is B_1, the gain-bandwidth product of the OA. At node 3, the transfer function is

$$\frac{V_{o2}}{V_i} = \frac{B_1}{s+\omega_{11}+\alpha B_1} \simeq \frac{B_1}{s+\alpha B_1} \quad \text{for} \quad \alpha B_1 >> \omega_{11} \tag{3.54}$$

Thus, while a LP transfer function with unity pass band gain is realised at node 2, a non-unity gain LP transfer function is realised at node 3. Taking output from node 3 is preferable since the output impedance is lower at this node.

The second order non-inverting LP transfer function is

$$T_{LP2}(s) = \frac{b_1 b_2}{s^2+b_1 s+b_1 b_2} \tag{3.55}$$

Rewriting the transfer function we get

$$T_{LP2}(s) = \frac{\left(\frac{b_2}{s+c_2}\right)\left(\frac{b_1}{s+b_1}\right)}{1+\left(\frac{b_2}{s+c_2}\right)\left(\frac{b_1}{s+b_1}\right)\left(-\frac{c_2 s+b_1 b_2-b_1 c_2}{b_1 b_2}\right)}$$

$$\simeq \frac{\left(\frac{b_2}{s+c_2}\right)\left(\frac{b_1}{s+b_1}\right)}{1+\left(\frac{b_2}{s+c_2}\right)\left(\frac{b_1}{s+b_1}\right)} \tag{3.56}$$

for $c_2 << b_1$ and $c_2 << b_2$

where c_2 = arbitrary parameter

This transfer function is of the form

$$T(s) = \frac{G\, T_{LP_1}(s)}{1+GT_{LP_1}(s)} \qquad (3.57)$$

where G represents amplifier with gain $(\frac{b_2}{s+c_2})$

and $T_{LP_1}(s)$ = first order non-inverting LP transfer function.

G can be realised by an OA followed by a resistive attenuator. Then the second order non-inverting LPF can be realised by cascading this amplifier with the first order noninverting LPF circuit of Figure 3.13(a) and applying unity negative feedback across the combination. The circuit, shown in Figure 3.13(b) has the transfer function

$$T(s) = \frac{V_{o1}}{V_i} = \frac{\alpha\beta B_1 B_2}{s^2+(\omega_{11}+\omega_{12}+\alpha B_1)s+\omega_{11}\omega_{12}+\alpha B_1\omega_{12}+\alpha\beta B_1 B_2}$$

$$\simeq \frac{\alpha\beta B_1 B_2}{s^2+\alpha B_1 s+\alpha\beta B_1 B_2} \qquad (3.58)$$

for $\alpha B_1 >> (\omega_{11}+\omega_{12})$ and $\beta B_2 >> \omega_{12}$

where $\alpha = \frac{R_a}{R_a+R_b}$ and $\beta = \frac{R_c}{R_c+R_d}$

Comparison of equations (3.55) and (3.58) gives the following design equations for the second order non-inverting LPF circuit.

$$\alpha = \frac{b_1}{B_1} \quad , \qquad \beta = \frac{b_2}{B_2} \tag{3.59}$$

Since α and β are ≤ 1, the maximum realisable values of b_1 and b_2 are equal to B_1 and B_2 respectively. At node 3, a nonunity gain non-inverting LP response is obtained.

The third order non-inverting LP transfer function is

$$T_{LP3}(s) = \frac{b_1 b_2 b_3}{s^3+b_1 s^2+b_1 b_2 s+b_1 b_2 b_3} \tag{3.60}$$

This can be rewritten as

$$T_{LP3}(s) = \frac{(\frac{b_3}{s+c_3})(\frac{b_1 b_2}{s^2+b_1 s+b_1 b_2})}{1+(\frac{b_3}{s+c_3})(\frac{b_1 b_2}{s^2+b_1 s+b_1 b_2})(\frac{-c_3 s^2-b_1 c_3 s+b_1 b_2 b_3-b_1 b_2 c_3}{b_1 b_2 b_3})}$$

$$\simeq \frac{(\frac{b_3}{s+c_3})(\frac{b_1 b_2}{s^2+b_1 s+b_1 b_2})}{1+(\frac{b_3}{s+c_3})(\frac{b_1 b_2}{s^2+b_1 s+b_1 b_2})} \tag{3.61}$$

for $c_3 \ll b_1$, b_2 and b_3.

Hence,

$$T_{LP3}(s) = \frac{(\frac{b_3}{s+c_3})\, T_{LP2}(s)}{1+(\frac{b_3}{s+c_3})T_{Lp2}(s)}$$

The circuit configuration is shown in Figure 3.13(c). The transfer function for this circuit is

$$T(s) = \frac{V_{o1}}{V_i} \quad \frac{\alpha\beta\gamma B_1 B_2 B_3}{s^3+\alpha B_1 s^2+\alpha\beta B_1 B_2 s+\alpha\beta\gamma B_1 B_2 B_3} \qquad (3.62)$$

for $\alpha B_1 >> \omega_{11}+\omega_{12}+\omega_{13}$

$\beta B_2 >> \omega_{12}+\omega_{13}$

and $\gamma B_3 >> \omega_{13}$

where

$$\alpha = \frac{R_a}{R_a+R_b}, \quad \beta = \frac{R_c}{R_c+R_d} \quad \text{and} \quad \gamma = \frac{R_e}{R_e+R_f}$$

Comparing equations (3.60) and (3.62), the design equations are

$$\alpha = \frac{b_1}{B_1}, \quad \beta = \frac{b_2}{B_2} \quad \text{and} \quad \gamma = \frac{b_3}{B_3}$$

At node 3 the transfer function is

$$T(s) = \frac{V_{o2}}{V_i} = \frac{\beta\gamma B_1 B_2 B_3}{s^3+\alpha B_1 s^2+\alpha\beta B_1 B_2 s+\alpha\beta\gamma B_1 B_2 B_3} \qquad (3.63)$$

i.e., a non-unity gain non-inverting LP response is obtained at this node. Here the output impedance is low. The first, second and third order filters realised are the same as the circuits proposed by Venkateswaran [7].

From the previous analysis for first, second and third order low pass filters, a general method for the synthesis of nth order non-inverting LP transfer function can be obtained.

The nth order transfer function, given by equation (3.48) can be rewritten as

$$T_{LPn}(s) = \frac{\frac{bn}{s} T_{LP(n-1)}(s)}{1 + \frac{bn}{s} T_{LP(n-1)} s} \qquad (3.64)$$

where

$$T_{LP(n-1)}(s) = \frac{b_1 b_2 \cdots b_{n-1}}{s^{n-1} + b_1 s^{n-2} + b_1 b_2 s^{n-3} + \ldots + b_1 b_2 \ldots b_{n-1}}$$

Thus, the nth order non-inverting low pass filter can be obtained by cascading an amplifier of gain $\frac{bn}{s}$ with the $(n-1)^{th}$ order non-inverting low pass filter and applying unity negative feedback across the combination. The amplifier of gain $\frac{bn}{s}$ can be realised by an OA with a gain $\frac{B_1}{s}$ (for $\omega >> \omega_{11}$) followed by a resistive divider. The nth order LPF has n OAs and 2n resistors. The realised LPF circuits have high input impedance (ideally infinity).

Acar [12] has arrived at a general nth order non-inverting low pass configuration using the signal flow graph approach. Acar's circuit shown in Figure 3.14 has n OAs and 4n resistors. Thus the circuits of Figure 3.13 have a lesser resistor count as compared to the corresponding circuits of Acar [12]. Further Acar's circuits have low input impedance while the newly synthesised circuits have, ideally, infinite input impedance. Acar's circuits require a number of matched resistors. Hence,

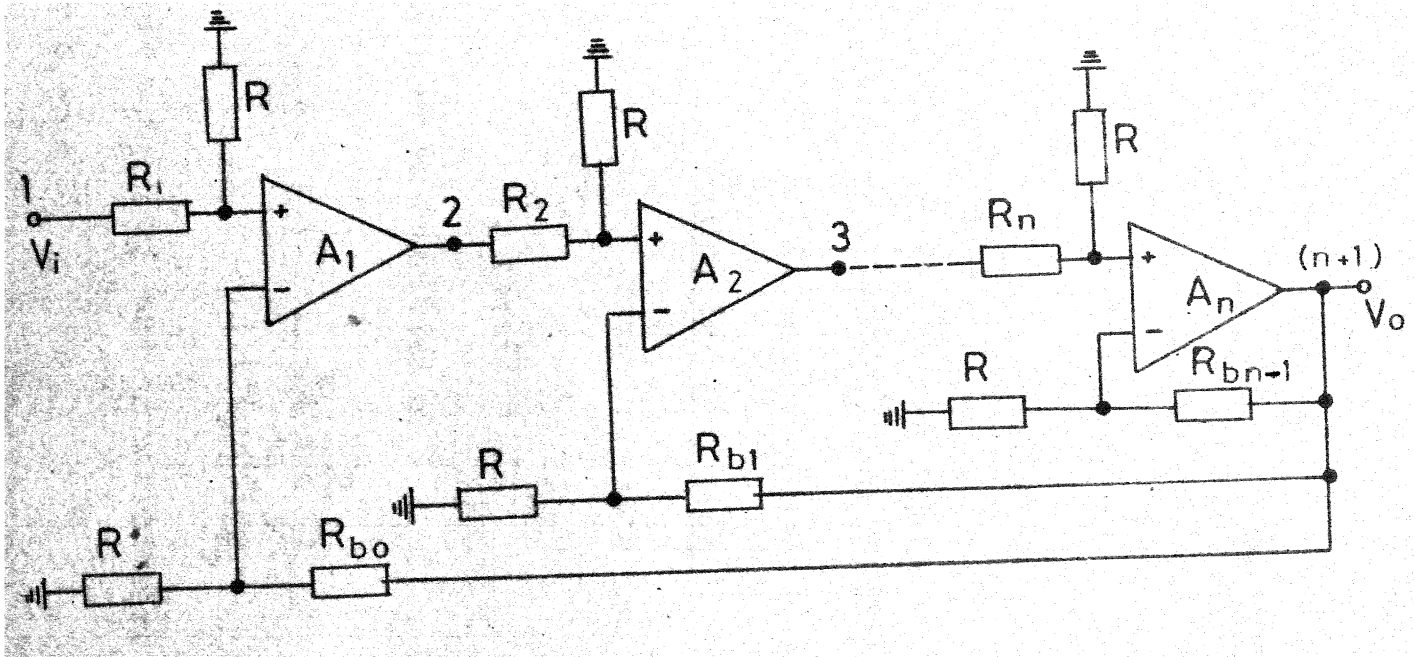

FIG. 3.14 n^{th} ORDER LPF CIRCUIT OF ACAR

the synthesised circuits are superior to those of Acar.

The synthesised third order circuit, shown in Figure 3.13(c) is identical to the circuit of Bhattacharyya and Natarajan [13]. In equation (3.63) which gives the transfer function of this circuit, if

$$\alpha B_1 \leq \gamma B_3$$

then the circuit becomes oscillatory. This is true of any third order system. If αB_1 is always kept greater than γB_3, then the circuit remains absolutely stable.

3.2.2 Inverting LPF synthesis :

The first order inverting LPF transfer function is

$$T_{LP1}(s) = \frac{-a_o}{s+b_1} \tag{3.65}$$

This can be rewritten as

$$T_{LP1}(s) = \frac{a_1\left(\frac{-a_2}{s+d}\right)}{1 + \left(\frac{-a_2}{s+d}\right)\left(\frac{b_1-d}{-a_2}\right)} \tag{3.66}$$

where $a_1 a_2 = a_o$ and d = arbitrary parameters.

For $b_1 >> d$

$$T_{LP1}(s) = \frac{a_1\left(\frac{-a_2}{s+d}\right)}{1+\left(\frac{-a_2}{s+d}\right)\left(-\frac{b_1}{a_2}\right)} \tag{3.67}$$

The corresponding circuit realisation, shown in Figure 3.15(a), has the transfer function

$$T(s) = \frac{V_o}{V_i} = \frac{-(1-\alpha)B_1}{s+\omega_{11}+(\alpha-\beta)B_1}$$

$$\simeq \frac{-(1-\alpha)B_1}{s+(\alpha-\beta)B_1} \qquad (3.68)$$

for $(\alpha-\beta)B_1 >> \omega_{11}$

where

$$\alpha = \frac{R_a}{R_a+R_b}, \qquad \beta = \frac{R_c}{R_c+R_d}$$

Comparison of equations (3.65) and (3.68) gives the design equations as

$$\alpha = \frac{B_1-a_o}{B_1} \quad \text{and} \quad \beta = \frac{B_1-a_o-b_1}{B_1} \qquad (3.69)$$

The limitation on maximum realisable a_o and b_1 values is

$$a_o+b_1 \leq B_1$$

The transfer function of a second order inverting LPF can be written as

$$T_{LP2}(s) = \frac{-a_o}{s^2+b_1 s+b_2} \qquad (3.70)$$

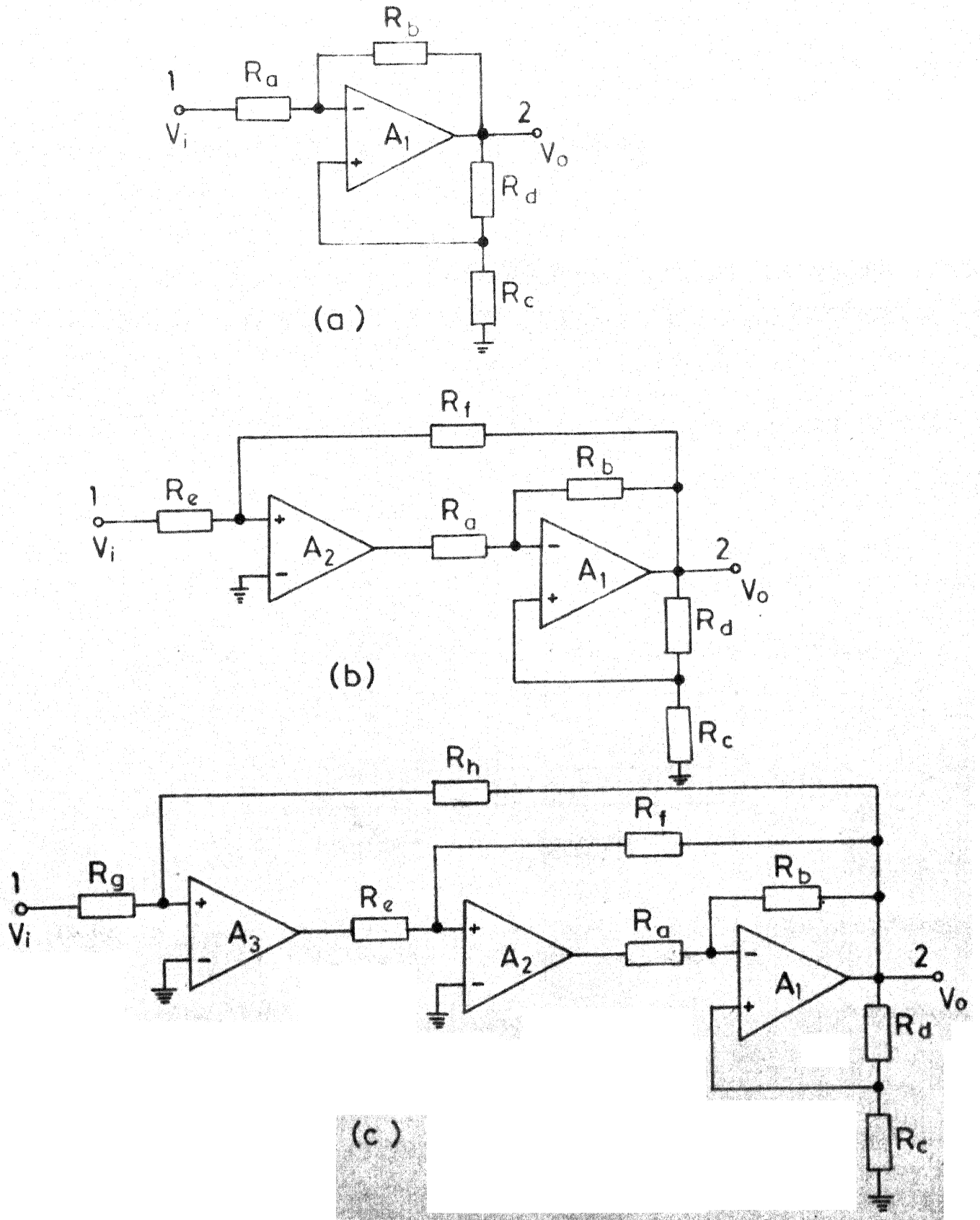

FIG 3.15 INVERTING LPF CIRCUITS (a) FIRST (b) SECOND (c) THIRD ORDER

This can be modified as

$$T_{LP2}(s) = \frac{a_1\left(\frac{a_2}{s}\right)\left(\frac{-a_3}{s+b_1}\right)}{1+\left(\frac{a_2}{s}\right)\left(\frac{-a_3}{s+b_1}\right)\left(\frac{b_2}{-a_2a_3}\right)} \qquad (3.71)$$

where $a_1a_2a_3 = a_o$

This transfer function is of the form

$$T(s) = \frac{a_1G_1G_2}{1+G_1G_2\beta_1} \qquad (3.72)$$

Here G_2 corresponds to first order inverting LP transfer function. G_1 represents amplifier of gain $(\frac{a_2}{s})$. It can be realised by a resistive divider. The circuit realisation is shown in Figure 3.15(b). Its transfer function

$$T(s) = \frac{V_o}{V_i} = \frac{(1-\gamma)\left(\frac{B_2}{s+\omega_{12}}\right)\left[\frac{-(1-\alpha)B_1}{s+\omega_{11}+(\alpha-\beta)B_1}\right]}{1+\left(\frac{B_2}{s+\omega_{12}}\right)\left[\frac{-(1-\alpha)B_1}{s+\omega_{11}+(\alpha-\beta)B_1}\right](-\gamma)} \qquad (3.73)$$

for $\omega >> \omega_{12}$

where

$$\alpha = \frac{R_a}{R_a+R_b}, \quad \beta = \frac{R_c}{R_c+R_d} \text{ and } \quad \gamma = \frac{R_e}{R_e+R_f}$$

Comparing equations (3.70) and (3.73) the design equations are obtained as

$$(\alpha-\beta)B_1 = b_1-\omega_{11}-\omega_{12} \tag{3.74}$$

$$\gamma(1-\alpha)B_1B_2 = b_2+\omega_{12}^2-\omega_{12}b_1 \tag{3.75}$$

$$(1-\gamma)(1-\alpha)B_1B_2 = a_o \tag{3.76}$$

Solving for α,β and γ we get

$$\alpha = \frac{B_1B_2-a_o-b_2-\omega_{12}^2+b_1\omega_{12}}{B_1B_2} \tag{3.77}$$

$$\beta = \frac{B_1B_2-a_o-b_2-\omega_{12}^2+b_1\omega_{12}-b_1B_2+B_2+\omega_{11}+B_2\omega_{12}}{B_1B_2} \tag{3.78}$$

$$\gamma = \frac{b_2 + \omega_{12}^2 - \omega_{12}b_1}{a_o+b_2 + \omega_{12}^2-\omega_{12}b_1} \tag{3.79}$$

Thus with a_o, b_1 and b_2 specified, α,β and γ values can be obtained from equations (3.77) to (3.79).

The third order inverting LP transfer function is

$$T_{LP3}(s) = \frac{-a_o}{s^3+b_1s^2+b_2s+b_3} \tag{3.80}$$

This can be rewritten as

$$T_{LP3}(s) = \frac{a_1(\frac{a_2}{s})(\frac{-a_3}{s^2+b_1s+b_2})}{1+(\frac{a_2}{s})(\frac{-a_3}{s^2+b_1s+b_2})(\frac{b_3}{-a_2a_3})} \tag{3.81}$$

where $a_1a_2a_3 = a_o$.

The circuit realisation is shown in Figure 3.15(c). The transfer function of the circuit is

$$T(s) = \frac{V_o}{V_i} = \frac{-(1-\delta)(1-\gamma)(1-\alpha)B_1B_2B_3}{D} \qquad (3.82)$$

where

$$D = s^3+[\omega_{11}+\omega_{12}+\omega_{13}+(\alpha-\beta)B_1]s^2+[\omega_{11}(\omega_{12}+\omega_{13})+\omega_{12}\omega_{13} + (\alpha-\beta)B_1(\omega_{12}+\omega_{13})+\gamma(1-\alpha)B_1B_2]s+[\omega_{11}\omega_{12}\omega_{13} + (\alpha-\beta)B_1\omega_{12}\omega_{13}+\gamma(1-\alpha)B_1B_2\omega_{13}+\delta(1-\gamma)(1-\alpha)B_1B_2B_3]$$

$$\alpha = \frac{R_a}{R_a+R_b}\ ,\ \beta = \frac{R_c}{R_c+R_d}\ ,\ \gamma = \frac{R_e}{R_e+R_f}\ ,\quad \delta = \frac{R_g}{R_g+R_h}$$

By comparing equations (3.80) and (3.82), the values of α,β,γ and δ, in terms of a_o,b_1,b_2,b_3 and the OA parameters, can be obtained.

In general the nth order inverting LP transfer function can be written as

$$T_{LPn}(s) = \frac{-a_o}{s^n+b_1s^{n-1}+b_2s^{n-2}+\ \ldots\ +b_n}$$

$$= \frac{a_1(\frac{a_2}{s})[T_{LP(n-1)}(s)]}{1+(\frac{a_2}{s})\ T_{LP(n-1)}(s)(\frac{b_n}{-a_2a_3})} \qquad (3.83)$$

where

$$T_{LP(n-1)}(s) = \frac{-a_3}{s^{n-1} + b_1 s^{n-2} + \ldots + b_{n-1}}$$

$$a_1 a_2 a_3 = a_o$$

Hence the nth order inverting LPF can be obtained by cascading an amplifier of gain $(\frac{a_2}{s})$ with the (n-1)th order inverting LPF and applying negative feedback across the combination.

3.2.3 Sensitivity analysis :

For low pass filters, the sensitivity figures of interest are i) transfer function sensitivity (S_x^T) and ii) polynomial sensitivity (S_x^D). These sensitivities can be determined using the general sensitivity definition given by equation (3.33). Transfer function and polynomial sensitivities with respect to all passive and active parameters have been determined for the first to third order non-inverting and inverting LPF circuits. The sensitivity figures, for the three non-inverting LPF circuits, provided by Anjali Joshi [14] are given in Table 3.6. The sensitivity figures for the first to third order inverting LPF circuits are given in Table 3.7. From Tables 3.6 and 3.7 it is seen that the algebraic sum sensitivity with respect to all passive parameters, i.e., resistor values, is zero for first, second and third order non-inverting and inverting LPFs. Thus, for non-inverting LPFs

$$\sum_{i=a}^{b} S_{R_i}^{T_1} = 0, \quad \sum_{i=a}^{d} S_{R_i}^{T_2} = 0, \quad \sum_{i=a}^{f} S_{R_i}^{T_3} = 0$$

$$\sum_{i=a}^{b} S_{R_i}^{D_1} = 0, \quad \sum_{i=a}^{d} S_{R_i}^{D_2} = 0, \quad \sum_{i=a}^{f} S_{R_i}^{D_3} = 0$$

and for inverting LPFs

$$\sum_{i=a}^{d} S_{R_i}^{T_1} = 0, \quad \sum_{i=a}^{f} S_{R_i}^{T_2} = 0, \quad \sum_{i=a}^{h} S_{R_i}^{T_3} = 0$$

$$\sum_{i=a}^{d} S_{R_i}^{D_1} = 0, \quad \sum_{i=a}^{f} S_{R_i}^{D_2} = 0, \quad \sum_{i=a}^{h} S_{R_i}^{D_3} = 0$$

If the filters are fabricated with monolithic IC technology then resistor ratios track and so passive algebraic sum sensitivities will be zero. Thus the transfer function and denominator polynomial are unchanged due to changes in the passive elements. The algebraic sum sensitivities with respect to the OA gain-bandwidth products are not zero. These could be greater than one. Gain-bandwidth product is highly sensitive to temperature and bias voltage variations. Hence, for satisfactory operation of these filters either temperature stabilised OAs (such as the National LM 324) must be used or external stabilisation arrangements must be provided. Radhakrishna Rao and

TABLE 3.6

Transfer function and polynomial sensitivities for non-inverting LPF

S.No.	Parameter (x)	S_x^T	S_x^D
(a) First order			
1	B_1	$\frac{s}{(s+\alpha B_1)}$	$\frac{B_1}{(s+\alpha B_1)}$
2	R_a	$\frac{s(1-\alpha)}{(s+\alpha B_1)}$	$-\frac{s(1-\alpha)}{(s+\alpha B_1)}$
3	R_b	$-S^T_{R_a}$	$-S^D_{R_a}$
(b) Second order			
1	B_1	$\frac{s^2}{D_2}$	$\frac{\alpha B_1(s+\beta B_2)}{D_2}$
2	B_2	$\frac{s(s+\alpha B_1)}{D_2}$	$\frac{\alpha\beta B_1 B_2}{D_2}$
3	R_a	$\frac{s^2(1-\alpha)}{D_2}$	$-\frac{s^2(1-\alpha)}{D_2}$
4	R_b	$-S^T_{R_a}$	$-S^D_{R_a}$
5	R_c	$\frac{(1-\beta)s(s+\alpha B_1)}{D_2}$	$-\frac{(1-\beta)s(s+\alpha B_1)}{D_2}$
6	R_d	$-S^T_{R_c}$	$-S^D_{R_c}$

contd ...

S.No.	Parameter (x)	S_x^T	S_x^D
(c)	Third order		
1	B_1	$\frac{s^3}{D_3}$	$\frac{\alpha B_1(s^2+\beta B_2 s+\beta\gamma B_2 B_3)}{D_3}$
2	B_2	$\frac{s^2(s+\alpha B_1)}{D_3}$	$\frac{\alpha\beta B_1 B_2(s+\gamma B_3)}{D_3}$
3	B_3	$\frac{s(s^2+\alpha B_1 s+\alpha\beta B_1 B_2)}{D_3}$	$\frac{\alpha\beta\gamma B_1 B_2 B_3}{D_3}$
4	R_a	$\frac{(1-\alpha)s^3}{D_3}$	$-\frac{(1-\alpha)s^3}{D_3}$
5	R_b	$-S_{R_a}^T$	$-S_{R_a}^D$
6	R_c	$\frac{(1-\beta)s^2(s+\alpha B_1)}{D_3}$	$-\frac{(1-\beta)s^2(s+\alpha B_1)}{D_3}$
7	R_d	$-S_{R_c}^T$	$-S_{R_c}^D$
8	R_e	$\frac{(1-\gamma)s(s^2+\alpha B_1 s+\alpha\beta B_1 B_2)}{D_3}$	$\frac{(1-\beta)s^2(s+\alpha B_1)}{D_3}$
9	R_f	$-S_{R_e}^T$	$-S_{R_e}^D$

Note : $D_2 = s^2+\alpha B_1 s+\alpha\beta B_1 B_2$

$D_3 = s^3+\alpha B_1 s^2+\alpha\beta B_1 B_2 s+\alpha\beta\gamma B_1 B_2 B_3$

TABLE 3.7

Transfer function and polynomial sensitivities for inverting LPF

S.No.	Parameter (x)	S_x^T	S_x^D
(a)	First order		
1	B_1	$\frac{s}{D_1}$	$\frac{(\alpha-\beta)B_1}{D_1}$
2	R_a	$-\frac{\alpha[s+(1-\beta)B_1]}{D_1}$	$\frac{\alpha(1-\alpha)B_1}{D_1}$
3	R_b	$-S_{R_a}^T$	$-S_{R_a}^D$
4	R_c	$\frac{\beta(1-\beta)B_1}{D_1}$	$-\frac{\beta(1-\beta)B_1}{D_1}$
5	R_d	$-S_{R_c}^T$	$-S_{R_c}^D$
(b)	Second order		
1	B_1	$\frac{s^2}{D_2}$	$\frac{B_1[(\alpha-\beta)s+\gamma(1-\alpha)B_2]}{D_2}$
2	B_2	$\frac{s[s+(\alpha-\beta)B_1]}{D_2}$	$\frac{\gamma(1-\alpha)B_1B_2}{D_2}$
3	R_a	$-\frac{\alpha s[s+(1-\beta)B_1]}{D_2}$	$\frac{\alpha(1-\alpha)B_1(s-\gamma B_2)}{D_2}$

contd ...

S.No.	Parameter	S_x^T	S_x^D
4	R_b	$-S_{R_a}^T$	$-S_{R_a}^D$
5	R_c	$\frac{\beta(1-\beta)B_1 s}{D_2}$	$-\frac{\beta(1-\beta)B_1 s}{D_2}$
6	R_d	$-S_{R_c}^T$	$-S_{R_c}^D$
7	R_e	$-\frac{\gamma[D_2+(1-\gamma)(1-\alpha)B_1B_2]}{D_2}$	$\frac{\gamma(1-\gamma)(1-\alpha)B_1B_2}{D_2}$
8	R_f	$-S_{R_e}^T$	$-S_{R_e}^D$
(c)	Third order		
1	B_1	$\frac{s^3}{D_3}$	$B_1[(\alpha-\beta)s^2+\gamma(1-\alpha)B_2 s + \delta(1-\gamma)(1-\alpha)B_2B_3]/D_3$
2	B_2	$\frac{s^2[s+(\alpha-\beta)B_1]}{D_3}$	$\frac{B_1B_2[\gamma(1-\alpha)s+\delta(1-\gamma)(1-\alpha)B_3]}{D_3}$
3	B_3	$\frac{sD_2}{D_3}$	$\frac{\delta(1-\gamma)(1-\alpha)B_1B_2B_3}{D_3}$
4	R_a	$-\frac{\alpha s^2[s+(1-\beta)B_1]}{D_3}$	$\frac{\alpha(1-\alpha)B_1[s^2-\gamma B_2 s-\delta(1-\gamma)B_2B_3]}{D_3}$
5	R_b	$-S_{R_a}^T$	$-S_{R_a}^D$

contd ...

S.No.	Parameter	S_x^T	S_x^D
6	R_c	$\frac{\beta(1-\beta)B_1 s^2}{D_3}$	$-\frac{\beta(1-\beta)B_1 s^2}{D_3}$
7	R_d	$-S_{R_c}^T$	$-S_{R_c}^D$
8	R_e	$-\frac{\gamma s[s^2+(\alpha-\beta)B_1 s+(1-\alpha)B_1B_2]}{D_3}$	$\frac{\gamma(1-\gamma)(1-\alpha)B_1B_2(s-\delta B_3)}{D_3}$
9	R_f	$-S_{R_e}^T$	$-S_{R_e}^D$
10	R_g	$-\frac{\delta[D_3+(1-\delta)(1-\gamma)(1-\alpha)B_1B_2B_3]}{D_3}$	
11			$\frac{\delta(1-\delta)(1-\gamma)(1-\alpha)B_1B_2B_3}{D_3}$
11	R_h	$-S_{R_g}^T$	$-S_{R_g}^D$

Note : $D_1 = s+(\alpha-\beta)B_1$, $D_2 = s^2+(\alpha-\beta)B_1 s+\gamma(1-\alpha)B_1B_2$

$D_3 = s^3+(\alpha-\beta)B_1 s^2+\gamma(1-\alpha)B_1B_2+\delta(1-\gamma)(1-\alpha)B_1B_2B_3$

Srinivasan [15] have proposed a simple arrangement to compensate for variations in gain bandwidth product.

3.2.4 Effect of OA second pole on LPF performance :

The effect of OA second pole on LPF performance can be studied by using the pole-zero model to analyse the LPF circuits. The transfer function of the first order non-inverting LPF (Figure 3.12(a)), based on pole-zero model is

$$T(s) = \frac{V_o}{V_i} = \frac{\alpha B_1 \omega_{21}/(\omega_{21}-\alpha B_1)}{s + \frac{\omega_{21}}{\omega_{21}-\alpha B_1}(\alpha B_1)} \qquad (3.84)$$

for $\omega << \omega_{21}$ and $\alpha B_1 >> \omega_{11}$

From a comparison of equations (3.52) and (3,84) it is seen that the constant terms in the numerator and denominator are multiplied by the same factors. Hence, due to OA second pole, there is no effect on low frequency gain. The cut-off frequency is, however, increased due to second pole.

Hence, the phase response slightly deviates from the single pole model response, at high frequencies. If the effect of OA second pole is to be eliminated then the design equations must be obtained in terms of pole-zero model parameters. For example, the design equation for the non-inverting first order LPF, based on pole-zero model, would be

$$\alpha = \frac{\omega_{21} b_1}{(\omega_{21}+b_1)B_1} \qquad (3.85)$$

Comparison of equations (3.53) and (3.85) shows that, the α value required is reduced for same LPF specifications when the OA second pole frequency is incorporated in the design equations.

3.2.5 Experimental results :

The design steps and the experimental results obtained by Anjali Joshi [14] for the third order non-inverting LPF circuit of Figure 3.12(c) are given here. The circuit was designed to obtain a third order Butterworth response with a cut-off frequency ($\frac{\omega_o}{2\pi}$) of 10 KHz. Normalising all frequencies with respect to ω_o, in equation (3.60), we get

$$s_n = \frac{s}{\omega_o}, \quad b_{1n} = \frac{b_1}{\omega_o}, \quad b_{2n} = \frac{b_2}{\omega_o} \text{ and } \quad b_{3n} = \frac{b_3}{\omega_o}$$

The normalised transfer function is

$$T_{LP3}(s_n) = \frac{b_{1n}b_{2n}b_{3n}}{s_n^3+b_{1n}s_n^2+b_{1n}b_{2n}s_n+b_{1n}b_{2n}b_{3n}} \qquad (3.86)$$

The standard third order Butterworth transfer function is

$$T(s_n) = \frac{H_n}{s_n^3+2s_n^2+2s_n+1} \qquad (3.87)$$

Hence, comparison of equations (3.86) and (3.87) yields

$$b_{1n} = 2, \quad b_{2n} = 1 \quad \text{and} \quad b_{3n} = 0.5$$

Therefore,

$$\alpha B_1 = b_1 = b_{1n}\omega_o = 2\omega_o$$

$$\beta B_2 = b_2 = b_{2n}\omega_o = \omega_o \qquad (3.88)$$

and

$$\gamma B_3 = b_3 = b_{3n}\omega_o = 0.5\ \omega_o$$

The circuit has been tested using National Semiconductor LM 324 quad OA, 1 percent metal film resistors and multiturn potentiometers. The measured parameters of three of the OAs in the chip are given in Table 3.8.

TABLE 3.8

Parameters of OA (LM 324)

Parameter	OA1	OA2	OA3
$\omega_{1i}/2\pi$ (Hz)	5.6	5.7	5.7
$\omega_{2i}/2\pi$ (MHz)	1.5	1.5	1.5
$B_i/2\pi$ (KHz)	560	570	570
$V_{cc} = \pm$ 12V,	$T = 27^{o}C$		

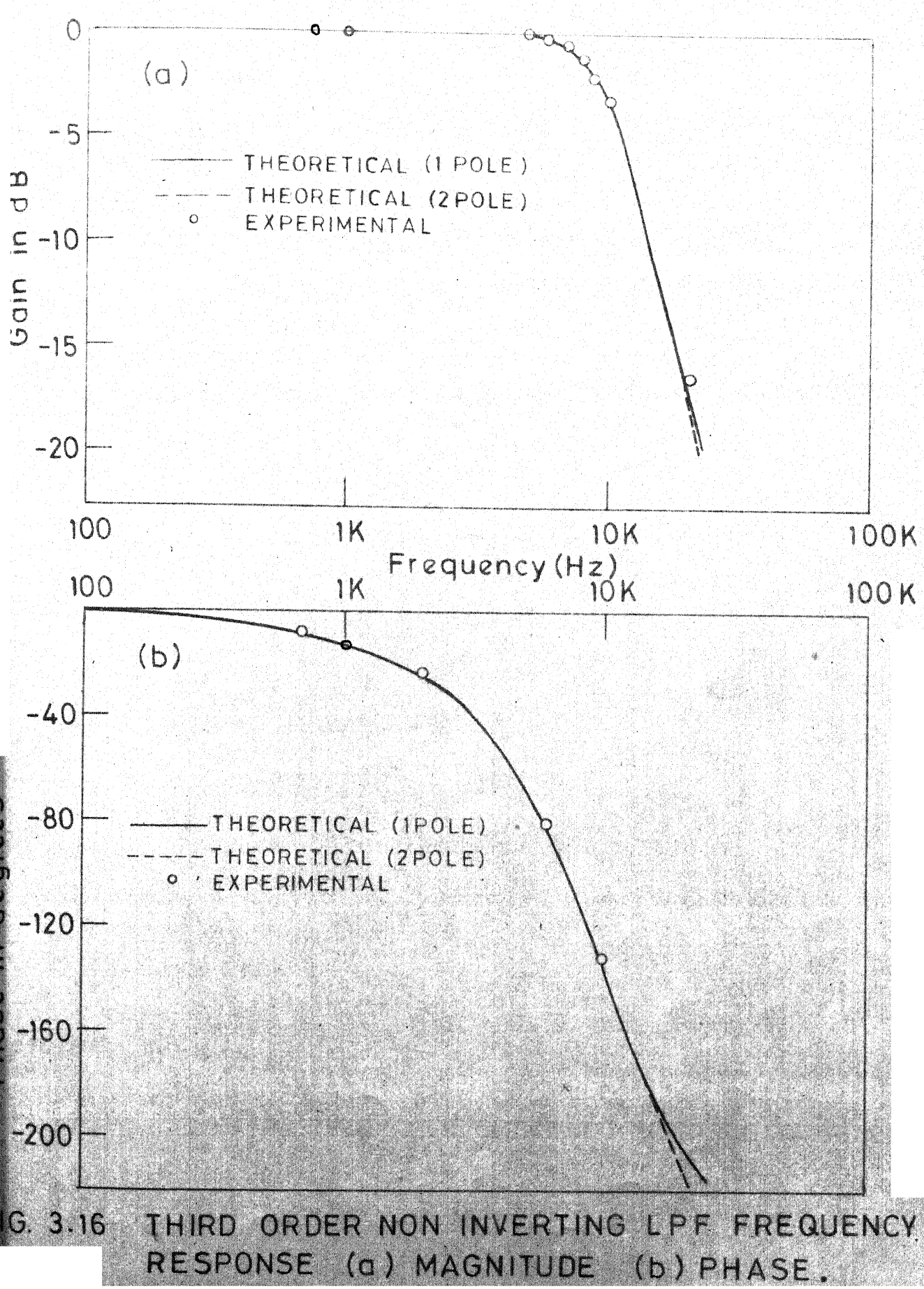

FIG. 3.16 THIRD ORDER NON INVERTING LPF FREQUENCY RESPONSE (a) MAGNITUDE (b) PHASE.

pole-zero model instead of the single pole model for the OAs. All the realised circuits have low sensitivities with respec to passive and active parameters. Further all the circuits have same or lesser component count as compared to reported circuits of similar performance.

References

1. Laker, K.R., Schaumann, R., and Brand, J.R., 'Multiple loop feedback active R filters', Proc. IEEE ISCAS/76, pp 279-282, April, 1976.

2. Li, M.K. and Li, C.W., 'Active R filter using operationa amplifier pole', Electron. Engg., Vol. 50, no.602, p 34, February, 1978.

3. Srinivasan, S., 'Synthesis of transfer functions using operational amplifier pole', Int. J. Electron., Vol. 40, no.1, pp 5-13, January, 1976.

4. Soderstrand, M.A., 'Design of active R filters using onl resistors and operational amplifiers', Int. J. Electron. Vol. 40, no.5, pp 417-432, May, 1976.

5. Mitra, A.K. and Aatre, V.K., 'Low sensitivity high frequency active R filters', IEEE Trans. Ckts., and Sys., Vol. CAS-23, no.11, pp 670-676, November, 1976.

6. Ho, C.F. and Chiu, P.L., 'Realisation of active R filters using operational amplifier pole', Proc. IEE, Vol. 123, no.5, pp 406-410, May, 1976.

7. Venkateswaran, S., 'An active R chain network', Lecture notes, I.I.T. Kanpur, India, October, 1978.

8. Venkateswaran, S., 'Multifunction active R filter with tw operational amplifiers', Electron. Lett., Vol. 14, no.23, pp 741-742, November, 1978.

9. Kapustian, V., Bhattacharyya, B.B. and Swamy, M.N.S., 'Frequency limitations of active R filters, using operational amplifiers', J. Franklin Inst., vol. 308, no.2, pp 141-151, August 1979.

10. Graeme, J.G., Huelsman, H.P. and Tobey, G.E., 'Operational Amplifiers - Design and applications', pp 445-447, McGraw-Hill - Koghakusha, Tokyo, 1971.

11. Schaumann, R. and Brand, J.R., 'Active R filters: review of theory and practice', IEE J Electron ckts and sys., Vol. 2, no.4, pp 89-101, July 1978.

12. Acar, C., 'Realisation of nth order low pass voltage transfer function by active R circuit: signal flow graph approach', Electron Lett., Vol. 14, no.23, pp 729-730, November 1978.

13. Bhattacharyya, B.B. and Natarajan, S., 'A new continuously tunable oscillator without external capacitors', Proc. IEEE Vol. 65, no.12, pp 1726-1727, December 1977.

14. Anjali Joshi, 'Low pass active R chain networks', B.Tech. Project Report, I.I.T. Kanpur, India, April 1981.

15. Radhakrishna Rao, K. and Srinivasan, S., 'A high Q temperature insensitive band pass filter using the operational amplifier pole', Proc. IEEE, Vol. 62, no.12, pp 1713-1714, December 1974.

CHAPTER IV

SYNTHESIS OF ALL PASS FILTERS - SERIES REALISATION

All pass filters (APF) are widely used as phase shifters, delay equalisers and delay networks. They are characterised by a flat magnitude response and a frequency dependent phase response. A large number of active RC APFs of different orders have been reported in the literature. However, only few active R APF circuits have been reported. The first active R APF circuit to be proposed was the first order APF circuit of Srinivasan [1]. Soliman [2], Soliman and Fawzy [3] and Kim and Ra [4] have proposed second order active R circuits in which APF response is obtained at the input of an OA. Hence, these circuits suffer from loading problems. Mitra and Aatre [5] have obtained second order all pass response by resistive summation of the input and output of a second order inverting BPF under particular conditions. However, to date synthesis techniques and circuit realisations for higher order APFs have not been reported.

In this chapter new synthesis techniques, to obtain active R APFs of any order both with real poles and zeros and with complex poles and zeros have been proposed. The techniques are general and hence can also be applied to synthesise active RC APF of any order.

4.1 Characteristics of all pass filter :

An all pass filter has two main characteristics. The magnitude response of an ideal APF is independent of frequency while the phase response is a definite function of frequency. Such characteristics arise because the zeros of an APF are mirror images of the poles around jω axis as is shown in Figure 4.1. Since the zeros are located in the right half plane while the poles are in the left half plane the AP transfer function is a non-minimum phase function. The poles and zeros can be either real or complex. Figure 4.2 shows the magnitude and phase response of a typical APF.

The general nth order APF transfer function is

$$T_n(s) = \frac{s^n - a_1 s^{n-1} + a_2 s^{n-2} - \ldots + (-1)^n a_n}{s^n + a_1 s^{n-1} + a_2 s^{n-2} + \ldots + (-1)^n a_n} \qquad (4.1)$$

If this transfer function is decomposed into a number of first or second order terms, then the circuit blocks corresponding to these low order terms can be identified and hence the circuit corresponding to the complete transfer function can be realised.

4.2 Synthesis :

4.2.1 APFs with real poles and zeros :

The first order AP transfer function is

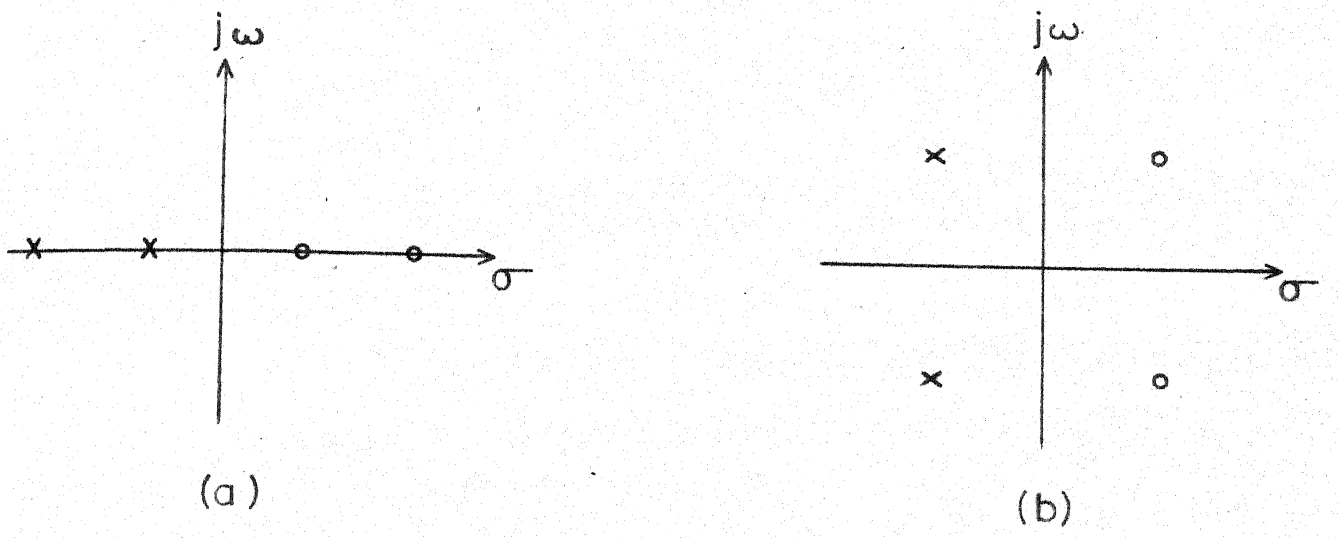

IG.4.1 SECOND ORDER APF POLE ZERO LOCATIONS (a) REAL POLES AND ZEROS (b) COMPLEX POLES AND ZEROS

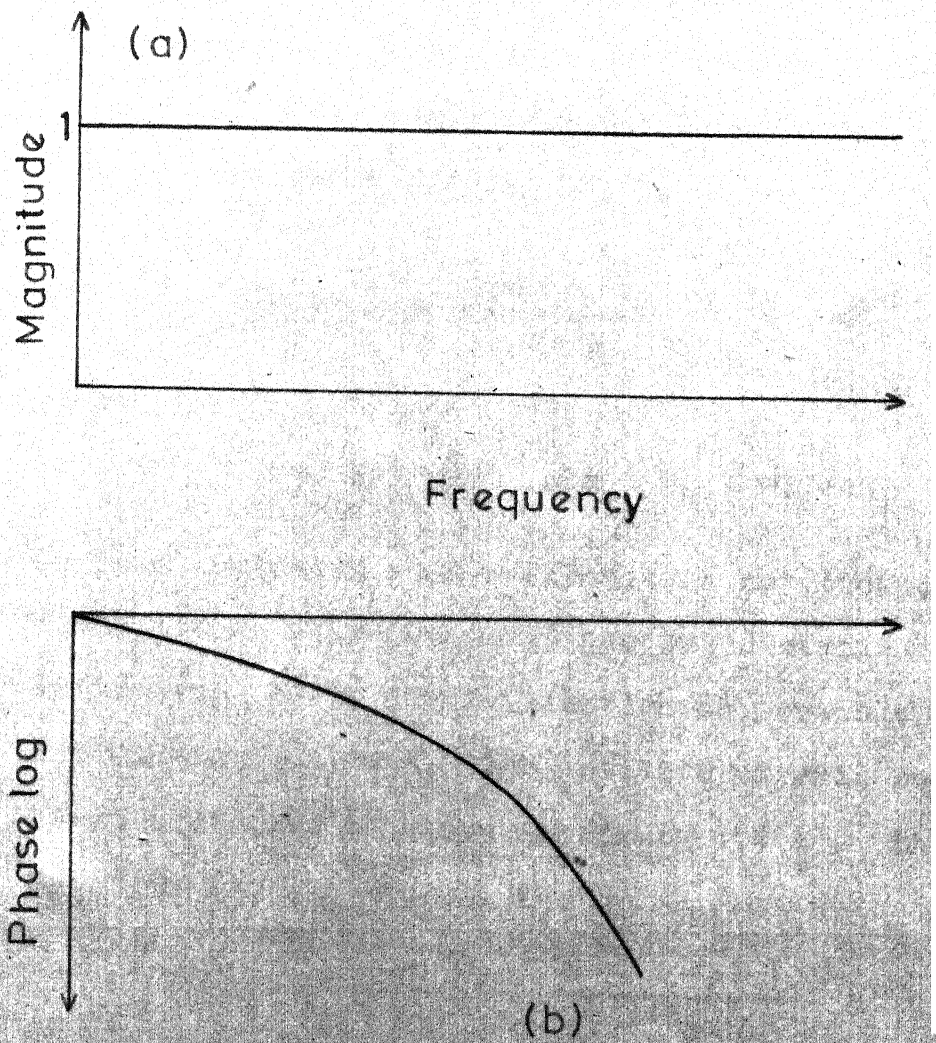

G.4.2 APF FREQUENCY RESPONSE (a) MAGNITUDE (b) PHASE RESPONSE

$$T_1(s) = \frac{s-a}{s+a} \qquad (4.2)$$

Equation (4.2) can be rewritten as

$$T_1(s) = 1 + \frac{-2a}{s+a} \qquad (4.3)$$

The second term in equation (4.3) represents a first order inverting LP transfer function. Hence, the first order APF can be realised by summing the input and output of a first order inverting LPF with a dc gain of two. The simplest first order active R inverting LPF circuit is shown in Figure 4.3. The transfer function of this circuit, based on single pole model for the OA, is

$$T(s) = \frac{V_o}{V_i} = \frac{-(1-\alpha)B_1}{s+B_\alpha} \qquad (4.4)$$

where

$$\alpha = \frac{R_a}{R_a+R_b} \quad \text{and} \quad B_\alpha = \omega_{11}+\alpha B_1$$

An ideal active R summer circuit is not known. Hence, the summation in equation (4.3) has to be carried out using resistors. Hence APF realisation is possible only with an attenuation constant. The active R circuit realisation for first order APF is shown in Figure 4.4(a). The transfer function of this circuit is

$$T(s) = \frac{V_o}{V_i} = \frac{R}{R_1}\left[1 + \frac{-(1-\alpha)\frac{R_1}{R_2}B_1}{s+B_\alpha}\right] \qquad (4.5)$$

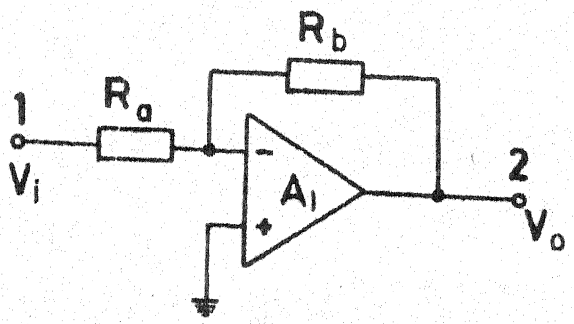

FIG. 4.3 FIRST ORDER INVERTING LPF

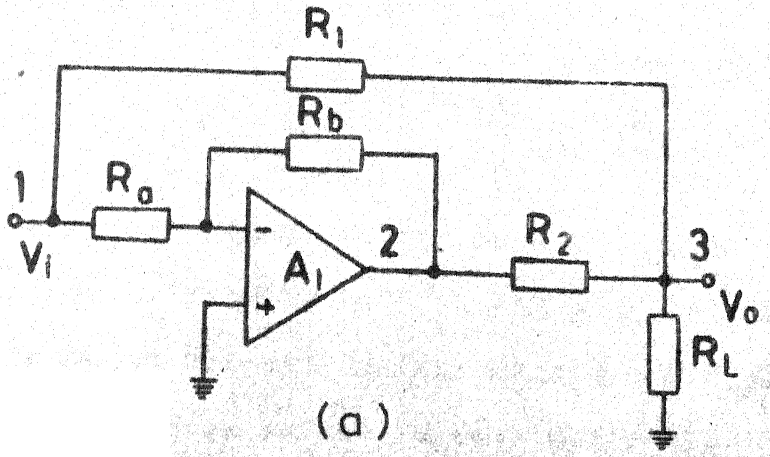

(a)

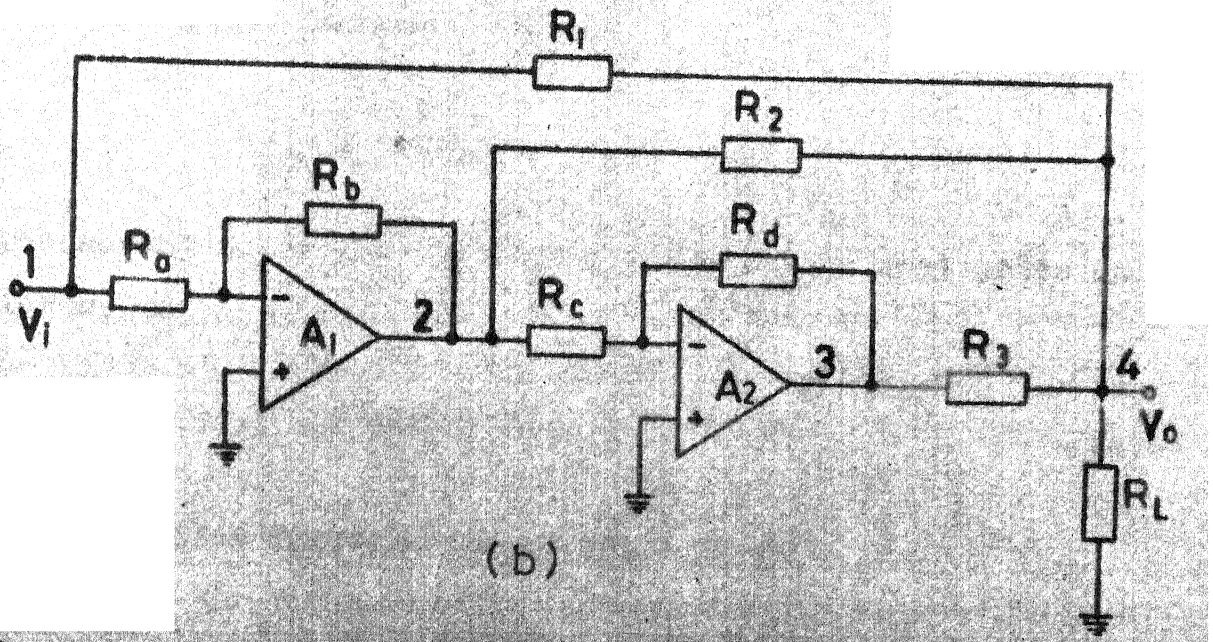

(b)

FIG. 4.4 APFS WITH REAL POLES AND ZEROS (a) FIRST ORDER (b) SECOND ORDER

where $R = R_1 || R_2 || R_L$, $\alpha = \frac{R_a}{R_a+R_b}$ and $B_\alpha = \omega_{11}+\alpha B_1$.

Here R_1 and R_2 represent the summation resistors. R_L is the load resistance. The circuit is realised with an attenuation constant of R/R_1. The APF circuit of Figure 4.4(a) is the same as the circuit proposed by Srinivasan [1]. Comparison of equations (4.3) (with attenuation constant K included) and (4.5) leads to the following design equations.

$$\frac{R}{R_1} = K, \quad \alpha = \frac{a-\omega_{11}}{B_1}, \quad \frac{R_1}{R_2} = \frac{2a}{B_1+\omega_{11}-a} \tag{4.6}$$

The design equations are in terms of resistor ratios. The load resistance R_L appears only in the attenuation constant. Hence, any change in circuit loading only changes the attenuation. The all pass response is unaltered. Under all pass condition equation (4.5) becomes

$$T(s) = \frac{R}{R_1}\left(\frac{s-B_\alpha}{s+B_\alpha}\right) \tag{4.7}$$

The second order APF transfer function, with real poles and zeros, is

$$T(s) = K\,\frac{(s-a)(s-b)}{(s+a)(s+b)} \tag{4.8}$$

This transfer function can be split up as

$$T(s) = K\left[1 + \frac{-2(a+b)}{s+a} + \frac{2b(a+b)}{(s+a)(s+b)}\right] \tag{4.9}$$

The second term in equation (4.9) is a first order inverting LP function while the third term can be considered as the cascade of two first order inverting LP transfer functions. Using the circuit of Figure 4.3 as the basic block the second and third terms can be realised. The realised circuit, shown in Figure 4.4(b), has the transfer function

$$T(s) = \frac{V_o}{V_i} = \frac{R}{R_1}\left[1 + \frac{-(1-\alpha)\frac{R_1}{R_2}B_1}{s+B_\alpha} + \frac{(1-\alpha)(1-\beta)\frac{R_1}{R_3}B_1B_2}{(s+B_\alpha)(s+B_\beta)}\right] \quad (4.10)$$

where

$$R = R_1 \| R_2 \| R_3 \| R_L, \quad \alpha = \frac{R_a}{R_a+R_b}, \quad \beta = \frac{R_c}{R_e+R_d},$$

$$B_\alpha = \omega_{11}+\alpha B_1, \quad B_\beta = \omega_{12}+\beta B_2.$$

Comparing equations (4.9) and (4.10) the following design equations are obtained.

$$\left.\begin{aligned} &\frac{R}{R_2} = K, \quad \alpha = \frac{a-\omega_{11}}{B_1}, \quad \beta = \frac{b-\omega_{12}}{B_2} \\ &\frac{R_1}{R_2} = \frac{2(a+b)}{B_1+\omega_{11}-a}, \quad \frac{R_1}{R_3} = \frac{2b(a+b)}{(B_1+\omega_{11}-a)(B_2+\omega_{12}-b)} \end{aligned}\right\} \quad (4.11)$$

The third order APF transfer function, with real poles and zeros, is

$$T_3(s) = K\frac{(s-a)(s-b)(s-c)}{(s+a)(s+b)(s+c)} \quad (4.12)$$

This transfer function can be decomposed as

$$T_3(s) = K\left[1+\frac{-2(a+b+c)}{s+a}+\frac{2(b+c)(a+b+c)}{(s+a)(s+b)}+\frac{-2c(b+c)(a+c)}{(s+a)(s+b)(s+c)}\right] \tag{4.13}$$

Here the second and third terms are similar to the second and third terms respectively, of equation (4.9). The fourth term represents a cascade of three first order inverting LP functions. Thus the third order APF, with real poles and zeros, can be realised by cascading three first order inverting LPFs and summing the outputs of the three LPFs with the input. The circuit realisation is shown in Figure 4.5. This circuit has the transfer function

$$T(s) = \frac{V_o}{V_i} = \frac{R}{R_1}\left[1+\frac{-(1-\alpha)\frac{R_1}{R_2}B_1}{s+B_\alpha}+\frac{(1-\alpha)(1-\beta)\frac{R_1}{R_3}B_1B_2}{(s+B_\alpha)(s+B_\beta)}+\frac{-(1-\alpha)(1-\beta)(1-\gamma)\frac{R_1}{R_4}B_1B_2B_3}{(s+B_\alpha)(s+B_\beta)(s+B_\gamma)}\right] \tag{4.14}$$

where

$$R = R_1||R_2||R_3||R_4||R_L,\ \alpha = \frac{R_a}{R_a+R_b},\ \beta = \frac{R_c}{R_c+R_d},\ \gamma = \frac{R_e}{R_e+R_f},$$

$$B_\alpha = \omega_{11}+\alpha B_1,\ B_\beta = \omega_{12}+\beta B_2 \quad \text{and} \quad B_\gamma = \omega_{13}+\gamma B_3.$$

The design equations for the circuit, obtained by comparing equations (4.13) and (4.14) are

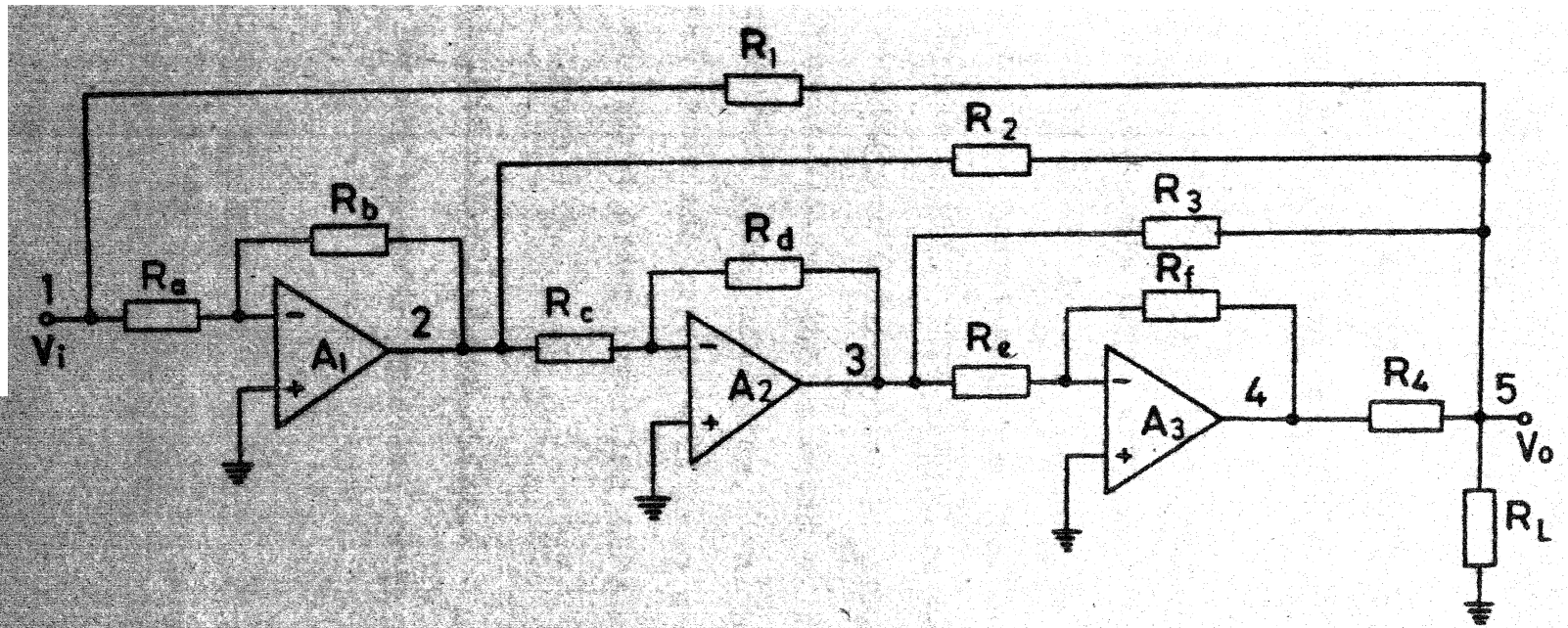

FIG. 4.5 THIRD ORDER APF WITH REAL POLES AND ZEROS

$$\left.\begin{aligned} &\frac{R}{R_1} = K,\ \alpha = \frac{a-\omega_{11}}{B_1},\ \beta = \frac{b-\omega_{12}}{B_2},\ \gamma = \frac{c-\omega_{13}}{B_3} \\ &\frac{R_1}{R_2} = \frac{2(a+b+c)}{B_1+\omega_{11}-a},\ \frac{R_1}{R_3} = \frac{2(b+c)(a+b+c)}{(B_1+\omega_{11}-a)(B_2+\omega_{12}-b)},\ \\ &\frac{R_1}{R_4} = \frac{2c(b+c)(a+c)}{(B_1+\omega_{11}-a)(B_2+\omega_{12}-b)(B_3+\omega_{13}-c)} \end{aligned}\right\} \quad (4.15)$$

Based on the first to third order APF realisations, the procedure for obtaining nth order APF, with real poles and zeros, can be stated as follows : (1) cascade n first order inverting LPFs and (2) resistively sum the outputs of all the n LPFs with the input. This procedure being general can be applied to realise nth order active RC APFs with real poles and zeros. Figure 4.6 shows the circuit of fourth order active R APF with real poles and zeros. The nth order active R APF, with real poles and zeros, will have n OAs and (3n+2) resistors, if the first order inverting LPFs are realised by the circuit of Figure 4.3.

4.2.2 APFs with complex poles and zeros :

Second order APF transfer function, with complex poles and zeros, is

$$T(s) = K\,\frac{s^2-as+b}{s^2+as+b} \quad (4.16)$$

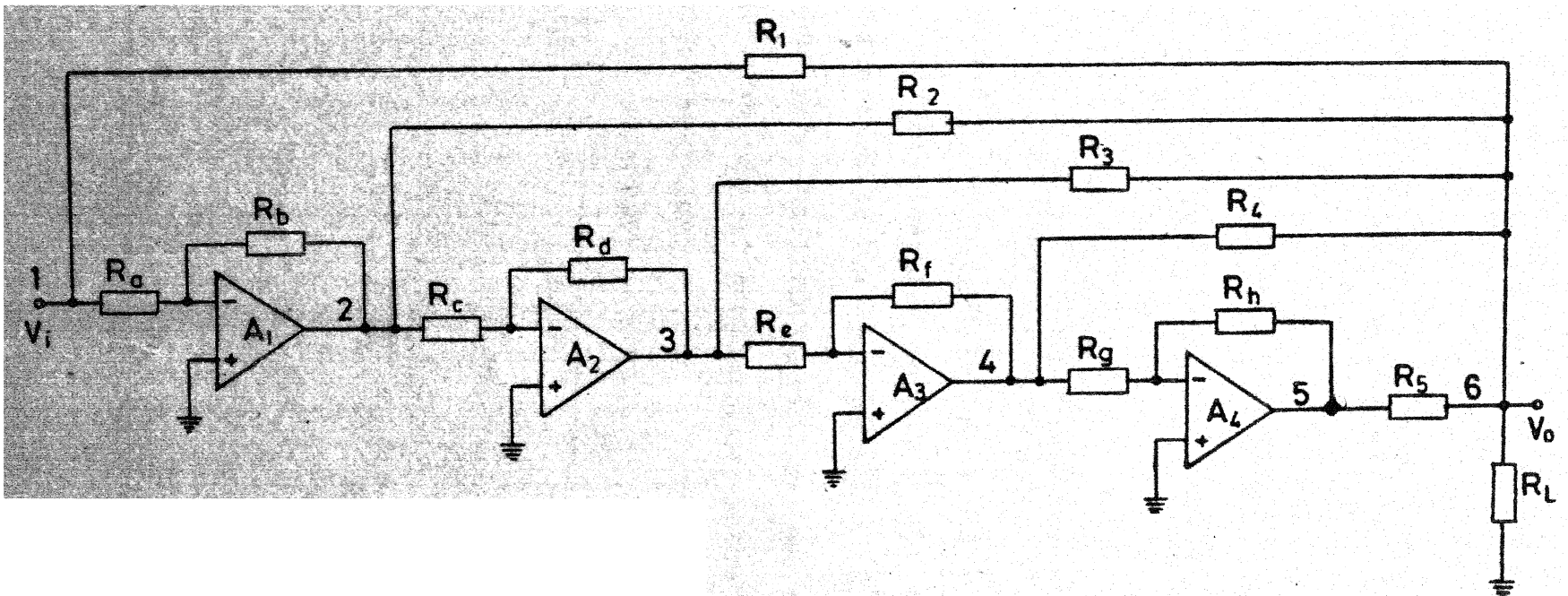

FIG. 4.6 FOURTH ORDER APF WITH REAL POLES AND ZEROS.

where K = attenuation constant and $a^2 < 4b$.

Rewriting the transfer function

$$T(s) = K\left[1 + \frac{-(2as+K_1)}{s^2+as+b} + \frac{K_1}{s^2+as+b}\right] \qquad (4.17)$$

Here the second and third terms represent inverting second order pseudo band pass and second order non-inverting low pass (for $K_1 > o$) functions respectively. The low pass function is realised by cascading two first order inverting LPFs and applying negative feedback across the combination. Then, while the LP function is realised at the output of one OA, the pseudo band pass function is realised at the output of the other OA. The circuit realisation, shown in Figure 4.7(a), has the transfer function

$$T(s) = \frac{V_o}{V_i} = \frac{R}{R_1}\left[1 + \frac{-(1-\alpha)\frac{R_1}{R_2}B_1(s+B_\beta)}{D} + \frac{(1-\alpha)(1-\beta)\frac{R_1}{R_3}B_1B_2}{D}\right] \qquad (4.18)$$

where

$$R = R_1||R_2||R_3||R_L,\ \alpha = \frac{R_a}{R_a+R_b},\quad \beta = \frac{R_c}{R_c+R_d},$$

$$D = s^2+(B_\alpha+B_\beta)s + B_\alpha B_\beta + \gamma(1-\beta)B_1B_2$$

$$\gamma = \frac{R_e}{R_e+R_f},\ B_\alpha = \omega_{11}+\alpha B_1,\ B_\beta = \omega_{12}+\beta B_2$$

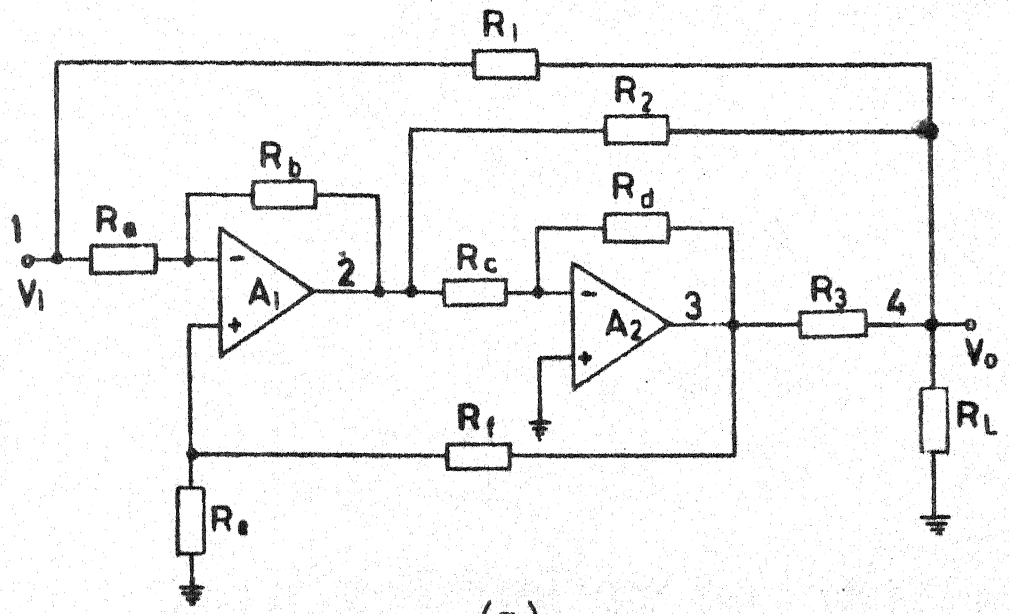

(a)

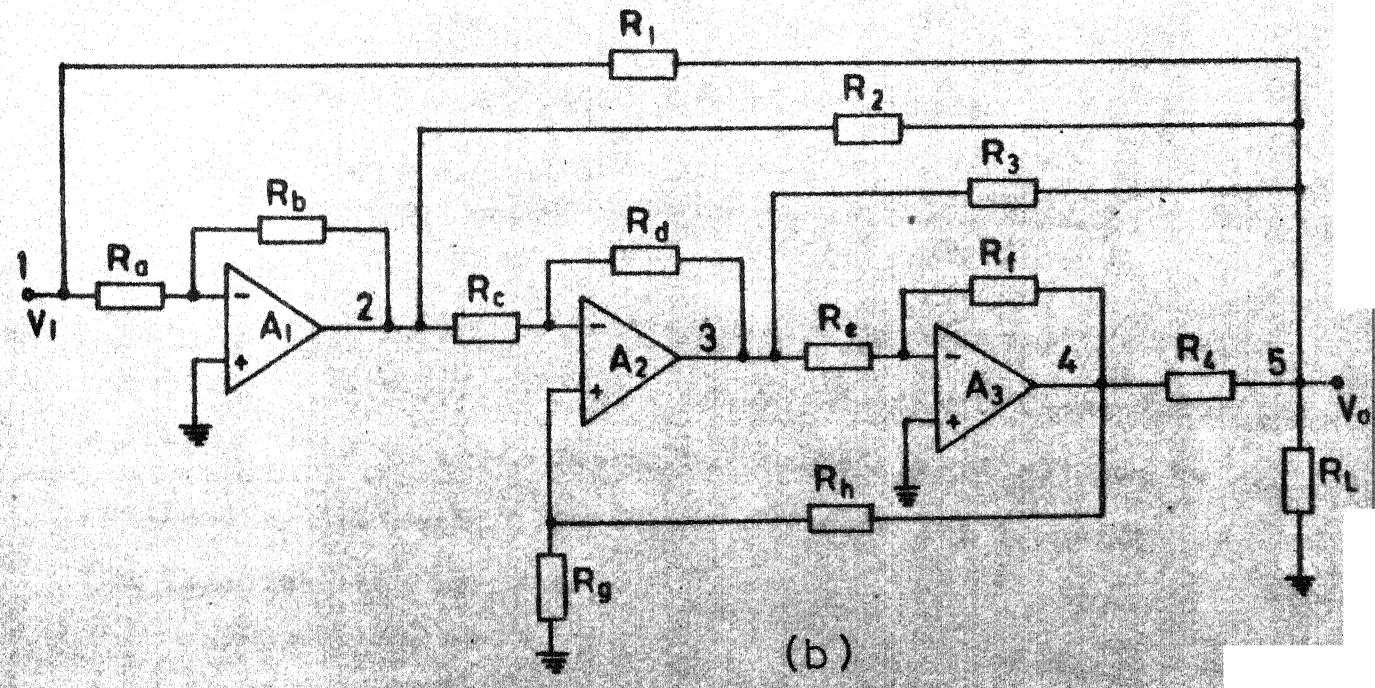

(b)

FIG.4.7 APF S WITH COMPLEX POLES AND ZEROS
(a) SECOND ORDER (b) THIRD ORDER

Comparison of equations (4.17) and (4.18) yields the following design equations (with α assumed) :

$$\left.\begin{aligned} \beta &= \frac{a-\omega_{12}-B_\alpha}{B_2}\ ,\ \gamma = \frac{b+B_\alpha^2-aB_\alpha}{B_1(B_2+\omega_{12}+B_\alpha-a)}\ ,\ \frac{R_1}{R_2} = \frac{2a}{(1-\alpha)B_1}\ , \\ \frac{R_1}{R_3} &= \frac{2a(a-B\alpha)}{(1-\alpha)B_1(B_2+\omega_{12}+B_\alpha-a)}\quad \frac{R}{R_1} = K \end{aligned}\right] \qquad (4.19)$$

Thus, with one parameter (α) assumed, all the other parameters can be determined from the design equations of equation (4.19).

The third order all pass transfer function with a pair of complex conjugate poles and zeros is

$$T(s) = K\,\frac{(s-a)(s^2-bs+c)}{(s+a)(s^2+bs+c)} \qquad (4.20)$$

where $K < 1$ and $b^2 < 4c$

Decomposition of this transfer function yields

$$T(s) = K\left[1 + \frac{-2(a+b)}{s+a} + \frac{2b(a+b)s+2bc}{(s^2+bs+c)(s+a)}\right] \qquad (4.21)$$

Here, the second term is a first order inverting LPF transfer function. The third term is a one by three order non-inverting function. The transfer function of equation (4.21) can be realised by the circuit of Figure 4.7(b). The transfer function for this circuit is

$$T(s) = \frac{V_o}{V_i} = \frac{R}{R_1}\left[1+\frac{-(1-\alpha)\frac{R_1}{R_2}B_1}{s+B_\alpha}+\frac{(1-\alpha)(1-\beta)\frac{R_1}{R_3}B_1B_2(s+B_\gamma)}{(s+B_\alpha)D}\right.$$

$$\left.+\frac{-(1-\alpha)(1-\beta)(1-\gamma)\frac{R_1}{R_4}B_1B_2B_3}{(s+B_\alpha)D}\right] \qquad (4.22)$$

where

$$R = R_1||R_2||R_3||R_4||R_L$$

$$D = s^2+(B_\beta+B_\gamma)s+B_\beta B_\gamma+\delta(1-\gamma)B_2B_3$$

$$\alpha = \frac{R_a}{R_a+R_b},\ \beta = \frac{R_c}{R_c+R_d},\ \gamma = \frac{R_e}{R_e+R_f},\ \delta = \frac{R_g}{R_g+R_h},$$

$$B_\alpha = \omega_{11}+\alpha B_1,\ B_\beta = \omega_{12}+\beta B_2,\ B_\gamma = \omega_{13}+\gamma B_3$$

Comparing equations (4.21) and (4.22), the design equations, with β assumed, are :

$$\left.\begin{aligned}
&\frac{R}{R_1} = K,\ \alpha = \frac{a-\omega_{11}}{B_1},\ \gamma = \frac{b-\omega_{13}-B_\beta}{B_3},\ \delta = \frac{c+B_\beta^2-bB_\beta}{(B_3+\omega_{13}+B_\beta-b)B_2},\\
&\frac{R_1}{R_2} = \frac{2(a+b)}{(B_1+\omega_{11}-a)},\ \frac{R_1}{R_3} = \frac{2b(a+b)}{(B_1+\omega_{11}-a)(1-\beta)B_2},\\
&\frac{R_1}{R_4} = \frac{2b[(a+b)(b-B_\beta)-c]}{(B_1+\omega_{11}-a)(1-\beta)(B_3+\omega_{13}+B_\beta-b)B_2}
\end{aligned}\right\} \qquad (4.23)$$

A fourth order APF with a pair of complex poles and zeros can be obtained if the circuit of Figure 4.6 is modified by

adding a resistive potential divider either from mode 3 to the non-inverting input of A_1 or from node 5 to the non-inverting input of A_3. In a similar manner, APFs of any order, with a pair of complex conjugate poles and zeros, can be realised. The nth order APF with a pair of complex conjugate poles and zeros will have n OAs and (3n+4) resistors.

4.2.3 Alternate APF realisations :

The second order AP transfer function, with a pair of complex conjugate poles and zeros can also be realised by the resistive summation of the input of a second order inverting BPF with a resonant gain of two. For the general inverting BP function, such a summation leads to

$$T(s) = K \left[1 + \frac{-K_1 \frac{\omega_o}{Q} G_o s}{s^2 + (\frac{\omega_o}{Q})s + \omega_o^2}\right] \qquad (4.24)$$

This becomes

$$T(s) = K \frac{s^2 - (\frac{\omega_o}{Q})s + \omega_o^2}{s^2 + (\frac{\omega_o}{Q})s + \omega_o^2} \qquad (4.25)$$

if $K_1 = \frac{2}{G_o}$

where K and K_1 represent the resistance ratios introduced by the resistive summation.

Such an APF can be realised from the inverting BPF circuit of Figure 3.3. The resulting APF circuit shown in Figure 4.8 has the transfer function

$$T(s) \simeq \frac{R}{R_1}\left[1 + \frac{-(1-\gamma)\frac{R_1}{R_2}B_1 s}{D}\right] \qquad (4.26)$$

for $\omega >> \omega_{12}$

where

$$R = R_1 || R_2 || R_L$$

$$\alpha = \frac{R_a}{R_a+R_b}\ ,\ \beta = \frac{R_c}{R_c+R_d}\ ,\ \gamma = \frac{R_e}{R_e+R_f}$$

and

$$D = s^2+[\omega_{11}+\omega_{12}+(\gamma-\beta)B_1]s+\omega_{11}\omega_{12}+(\gamma-\beta)B_1\omega_{12}$$

$$+ \alpha(1-\beta)B_1B_2$$

By comparing equations (4.17) (with $K_1 = 0$) and (4.26) the design equations can be obtained for this circuit. This circuit uses only two OAs and nine resistors as compared to two OAs and ten resistors used in the circuit of Figure 4.7(b).

Second order APFs with complex poles and zeros can also be obtained from the inverting BPF circuits of Mitra and Aatre [5], Soderstrand [6], Ho and Chiu [7] and Schaumann and Brand [8], by adding two summation resistors and a load resistor, in a similar manner. This possibility of realising

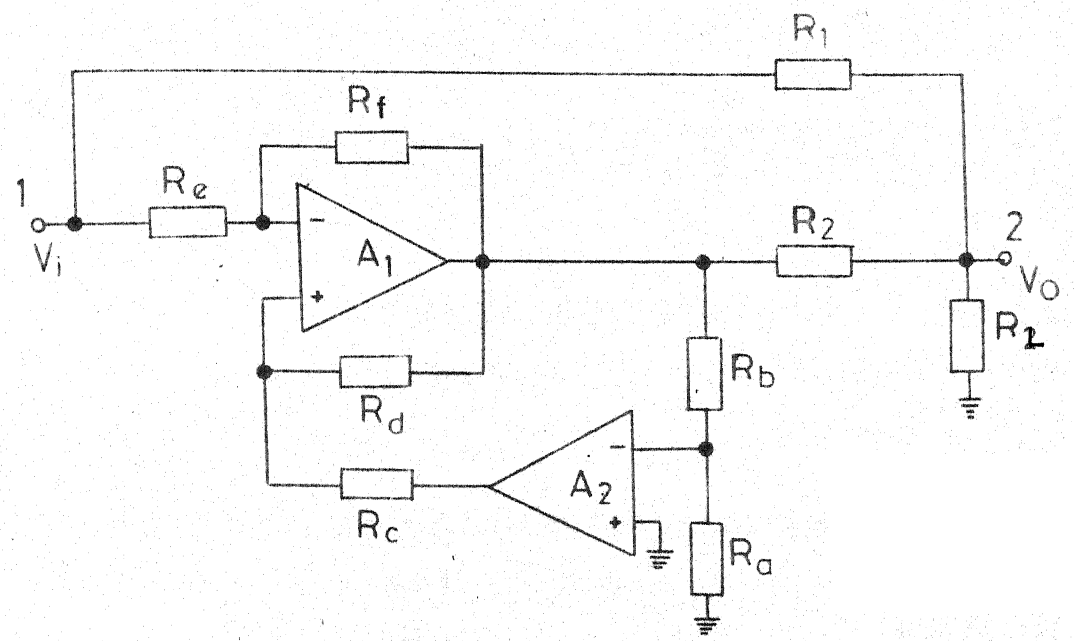

G.4.8 SECOND ORDER APF DERIVED FROM INVERTING BPF CIRCUIT

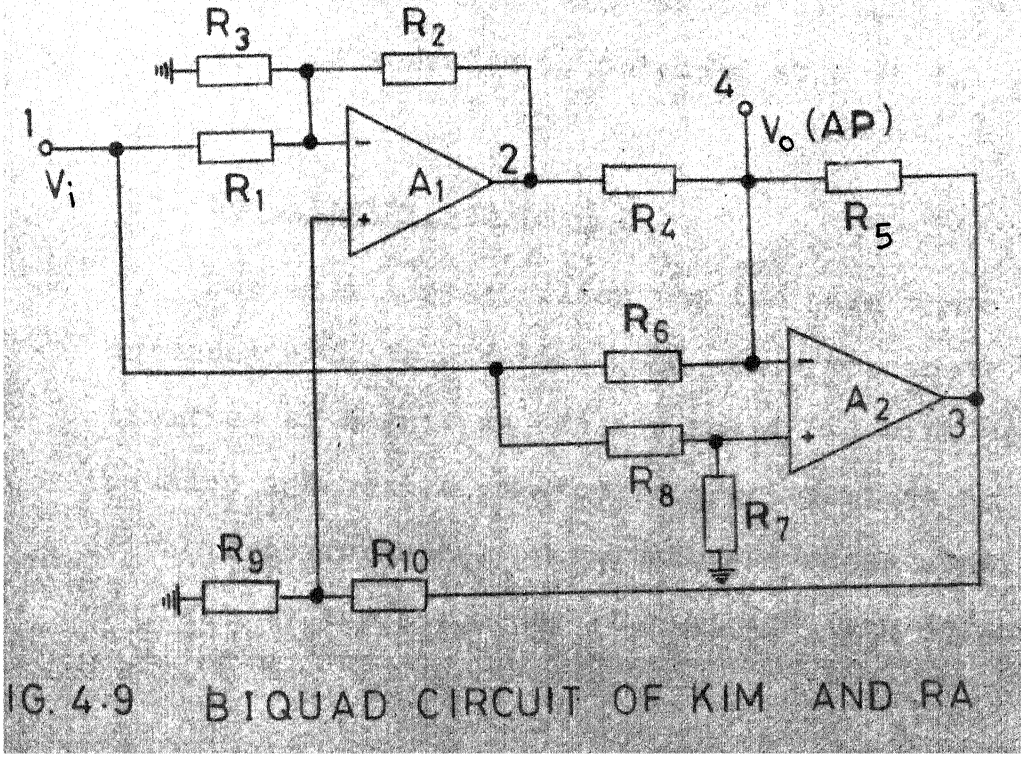

IG. 4.9 BIQUAD CIRCUIT OF KIM AND RA

an AP response by modifying an inverting BPF circuit has been first indicated by Mitra and Aatre [5].

The biquad circuit of Kim and Ra [4] realises second order AP response at the input terminal of an OA. This circuit, shown in Figure 4.9 realises AP response at node 4. Variations in load resistance affect the all pass conditions in this circuit. Hence, for every change in load resistance, other parameters in the circuit must be adjusted to maintain all pass conditions. Soliman [2] has proposed a three OA, nine resistor circuit which realises AP response at the input of an OA. This circuit is shown in Figure 4.10(a). Soliman and Fawzy [3] have proposed a modification of this circuit in which AP response is obtained using only two OAs and nine resistors. In Soliman and Fawzy's circuit, shown in Figure 4.10(b), AP response is obtained at node 2,i.e.at the input of an OA.

4.3 Sensitivity analysis :

For an all pass filter the two main characteristics of interest are its magnitude and phase responses. Hence sensitivities of magnitude (G) and phase (φ) with respect to all passive and active parameters are important in evaluating the circuit performance. Magnitude and phase sensitivities, with respect to any parameter, for an APF, are defined as

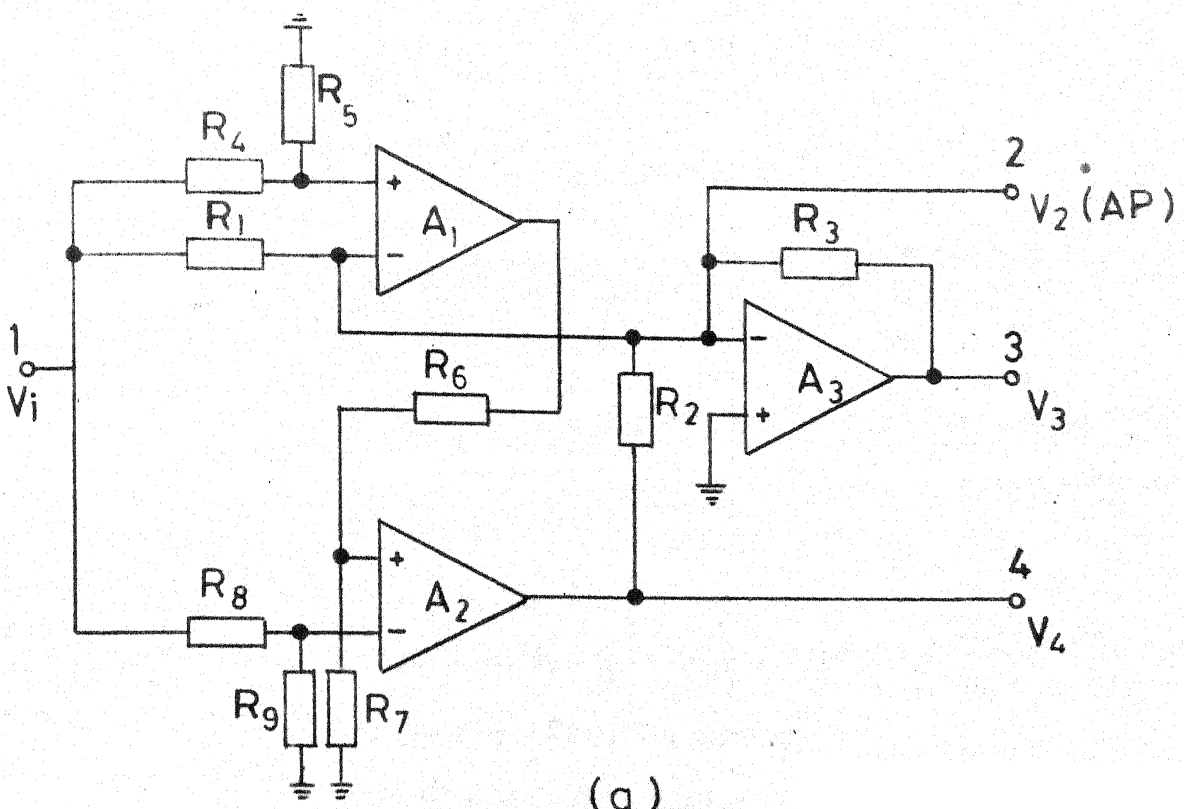

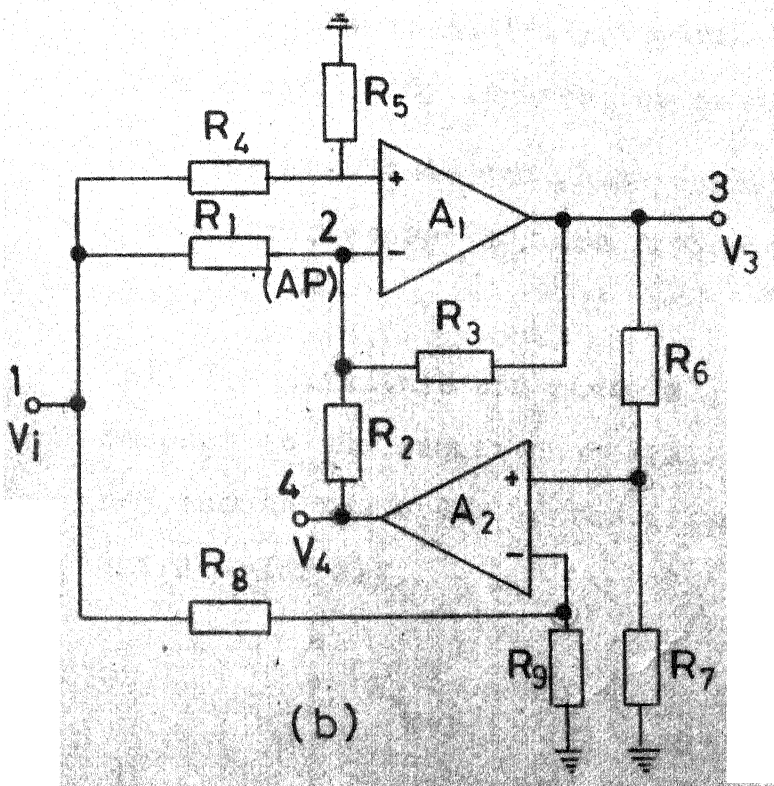

4.10 APF CIRCUITS (a) CIRCUIT OF SOLIMAN (b) CIRCUIT OF SOLIMAN AND FAWZY

$$S_x^G = \left(\frac{\partial G}{\partial x} \cdot \frac{x}{G}\right)_{\text{All pass}} \quad \text{and} \quad S_x^\varphi = \left(\frac{\partial \varphi}{\partial x} \cdot x\right)_{\text{All pass}} \qquad (4.27)$$

Magnitude and phase sensitivities must first be evaluated starting with expressions for G and φ without application of all pass conditions. Then appropriate all pass conditions must be imposed on these sensitivity figures to arrive at the APF magnitude and phase sensitivities. Magnitude and phase sensitivities with respect to all passive and active parameters have been calculated for (i) first to third order APFs with real poles and zeros (Figures 4.4(a), 4.4(b) and 4.5) and (ii) second order APF with complex poles and zeros (Figure 4.7(a)). The sensitivity figures are given in Table 4.1. From these sensitivity figures the following features are noted.

(a) The magnitude and phase sensitivities with respect to all parameters, except R_L, are frequency dependent for all the APFs.

(b) The magnitude and phase algebraic sum sensitivites with respect to the summation resistors R_1 to R_{n+1} (where n represents the order of the filter) and R_L are each zero. For third order APF,

$$\sum_{n=0}^{3} S_{R_{n+1}}^G + S_{R_L}^G = \sum_{n=0}^{3} S_{R_{n+1}}^\varphi + S_{R_L}^\varphi = 0 \qquad (4.28)$$

(c) Magnitude and phase algebraic sum sensitivities with respect to the resistors $R_a R_b, R_c$, etc. are each equal to zero.

TABLE 4.1

Magnitude and phase sensitivities of APFs

Variable	S_x^G	S_x^φ
(a) First order		
R_a	$-\frac{2\alpha B_\alpha (B_1+\omega_{11})}{D_1}$	$-\frac{2\omega\alpha B_\alpha}{D_1}$
R_b	$-S_{R_a}^G$	$-S_{R_a}^\varphi$
R_1	$-1+\frac{R}{R_1}+\frac{2B_\alpha^2}{D_1}$	$\frac{2B_\alpha}{D_1}$
R_2	$\frac{R}{R_2}-\frac{2B_\alpha^2}{D_1}$	$-\frac{2B_\alpha}{D_1}$
R_L	$\frac{R}{R_L}$	0
ω_{11}	$-\frac{2B_\alpha\omega_{11}}{D_1}$	0
B_1	$\frac{2B_\alpha\omega_{11}}{D_1}$	$\frac{2\omega B_\alpha}{D_1}$

Note : $D_1 = \omega^2 + B_\alpha^2$, $R = R_1 \,||\, R_2 \,||\, R_L$

contd ...

Variable	S_x^G	S_x^φ
(b) Second order (real poles and zeros)		
R_a	$-\frac{2\alpha(B_\alpha+B_\beta)(B_1+\omega_{11}+B_\beta)\omega^2}{D_2}$	$\frac{2\omega\alpha(B_\alpha+B_\beta)[B_\beta(\omega_{11}+B_1)-\omega^2]}{D_2}$
R_b	$-S^G_{R_a}$	$-S^\varphi_{R_a}$
R_c	$-\frac{2\beta B_\beta(B_\alpha+B_\beta)[B_\alpha(B_2+\omega_{12})-\omega^2]}{D_2}$	$-\frac{2\omega\beta B_\beta(B_\alpha+B_\beta)(B_2+\omega_{12}+B_\alpha)}{D_2}$
R_d	$-S^G_{R_c}$	$-S^\varphi_{R_c}$
R_1	$-1+\frac{R}{R_1}+\frac{2\omega^2(B_\alpha+B_\beta)^2}{D_2}$	$-\frac{2\omega(B_\alpha+B_\beta)(B_\alpha B_\beta-\omega^2)}{D_2}$
R_2	$\frac{R}{R_2}+\frac{2(B_\alpha+B_\beta)[B_\alpha B_\beta^2-\omega^2(B_\alpha+2B_\beta)]}{D_2}$	$\frac{2\omega(B_\alpha+B_\beta)(B_\beta^2+2B_\alpha B_\beta-\omega^2)}{D_2}$
R_3	$\frac{R}{R_3}-\frac{2B_\beta(B_\alpha+B_\beta)(B_\alpha B_\beta-\omega^2)}{D_2}$	$-\frac{2\omega B_\beta(B_\alpha+B_\beta)^2}{D_2}$
R_L	$\frac{R}{R_L}$	0
ω_{11}	$-\frac{2\omega_{11}\omega^2(B_\alpha+B_\beta)}{D_2}$	$\frac{2\omega\omega_{11}B_\beta(B_\alpha+B_\beta)}{D_2}$
ω_{12}	$-\frac{2\omega_{12}B_\alpha B_\beta(B_\alpha+B_\beta)}{D_2}$	$-\frac{2\omega\omega_{12}B_\beta(B_\alpha+B_\beta)}{D_2}$

contd ...

Variable	S_x^G	S_x^φ
B_1	$\frac{2(B_\alpha+B_\beta)\ \omega^2(\omega_{11}+B_\beta)}{D_2}$	$\frac{2\omega(B_\alpha+B_\beta)(\omega^2-\omega_{11}B_\beta)}{D_2}$
B_2	$\frac{2B_\beta(B_\alpha+B_\beta)(B_\alpha\omega_{12}-\omega^2)}{D_2}$	$\frac{2\,\omega\,B_\beta(B_\alpha+B_\beta)(B_\alpha+\omega_{12})}{D_2}$

Note : $D_2 = (B_\alpha B_\beta-\omega^2)^2 + \omega^2(B_\alpha+B_\beta)^2$; $R = R_1 || R_2 || R_3 || R_L$

(c) Third order (real poles and zeros)

Variable	S_x^G
R_a	$\frac{2\alpha P[(B_1+\omega_{11})(B_\beta B_\gamma-\omega^2)-\omega^2(B_\beta+B_\gamma)]}{D_3}$
R_b	$-S^G_{R_a}$
R_c	$-\frac{2\beta[P\{B_\gamma(B_\beta+B_\gamma)(\omega_{12}+B_2)+(1-\beta)B_2\omega^2\}+\omega^2Q(\omega_{12}+B_2+B_\gamma)(B_\alpha+B_\beta+B_\gamma}{D_3}$
R_d	$-S^G_{R_c}$
R_e	$\frac{2\gamma[P(B_\alpha+B_\gamma)(B_\beta+B_\gamma)(B_3+\omega_{13})-\omega^2Q(1-\gamma)B_3(B_\alpha+B_\beta+B_\gamma)]}{D_3}$
R_f	$-S^G_{R_e}$

contd ...

Variable	S_x^G
R_1	$-1 + \frac{R}{R_1} + \frac{2P^2}{D_3}$
R_2	$\frac{R}{R_2} - \frac{2(B_\alpha+B_\beta+B_\gamma)[P(\omega^2-B_\beta B_\gamma) - \omega^2 Q(B_\beta+B_\gamma)]}{D_3}$
R_3	$\frac{R}{R_3} - \frac{2(B_\beta+B_\gamma)(B_\beta+B_\gamma)[B_\gamma P+\omega^2 Q]}{D_3}$
R_4	$\frac{R}{R_4} + \frac{2B_\gamma(B_\alpha+B_\gamma)(B_\beta+B_\gamma)P}{D_3}$
R_L	$\frac{R}{R_L}$
ω_{11}	$\frac{2\ \omega_{11}P(B_\beta B_\gamma - \omega^2)}{D_3}$
ω_{12}	$-\frac{2\ \omega_{12}[\{B_\gamma(B_\beta+B_\gamma)+\omega^2\}P+\omega^2 Q]}{D_3}$
ω_{13}	$\frac{2\ \omega_{13}[\{(B_\alpha+B_\gamma)(B_\beta+B_\gamma)-\omega^2\}P-\omega^2 Q(B_\alpha+B_\beta+B_\gamma)]}{D_3}$
B_1	$\frac{2P[\omega^2(\omega_{11}+B_\beta+B_\gamma)-B_\beta B_\gamma\ \omega_{11}]}{D_3}$
B_2	$\frac{2[\{\omega_{12}B_\gamma(B_\beta+B_\gamma)-\beta B_2\omega^2\}P+\omega^2 Q(\omega_{12}+B_\gamma)(B_\alpha+B_\beta+B_\gamma)]}{D_3}$
B_3	$-\frac{2[\{\omega_{13}(B_\alpha+B_\gamma)(B_\beta+B_\gamma)+\gamma B_3\omega^2\}P+\omega^2 Q\gamma B_3(B_\alpha+B_\beta+B_\gamma)]}{D_3}$

contd ...

Variable	S_x^{φ}
R_a	$\dfrac{2\,\omega\,\alpha P[(B_1+\omega_{11})(B_\beta+B_\gamma)+B_\beta B_\gamma-\omega^2]}{D_3}$
R_b	$-S^{\varphi}_{R_a}$
R_c	$-\dfrac{2\omega\beta[\{B_\beta(B_\alpha+B_2+\omega_{12}+B_\gamma)+B_\gamma(B_\alpha+B_\beta+B_\gamma)\}P-QB_\gamma\{(B_\beta+B_\gamma)(\omega_{12}+B_2)+(1-\beta)B_2B_\alpha\}]}{D_3}$
R_d	$-S^{\varphi}_{R_c}$
R_e	$-\dfrac{2\omega\gamma[(1-\gamma)B_3B_\gamma P+QB_\gamma\{(B_\beta+B_\gamma)(B_\alpha+B_3+\omega_{13})+(1-\gamma)B_\alpha B_3\}]}{D_3}$
R_f	$-S^{\varphi}_{R_e}$
R_1	$-\dfrac{2\omega PQ}{D_3}$
R_2	$\dfrac{2\,\omega(B_\alpha+B_\beta+B_\gamma)[(B_\beta+B_\gamma)P-(B_\beta B_\gamma-\omega^2)Q]}{D_3}$
R_3	$-\dfrac{2\omega(B_\beta+B_\gamma)(B_\alpha+B_\beta+B_\gamma)[P-B_\gamma Q]}{D_3}$
R_4	$-\dfrac{2\omega B_\gamma Q(B_\alpha+B_\gamma)(B_\beta+B_\gamma)}{D_3}$
R_L	0

contd ...

Variable	S_x^{φ}
ω_{11}	$\dfrac{2\omega\omega_{11}P(B_\beta+B_\gamma)}{D_3}$
ω_{12}	$-\dfrac{2\omega\omega_{12}[B_\beta P - B_\gamma Q(B_\alpha+B_\beta+B_\gamma)]}{D_3}$
ω_{13}	$-\dfrac{2\omega\omega_{13}[B_\gamma P + B_\gamma Q(B_\alpha+B_\beta+B_\gamma)]}{D_3}$
B_1	$-\dfrac{2\omega P[\omega_{11}(B_\beta+B_\gamma) + B_\beta B_\gamma - \omega^2]}{D_3}$
B_2	$\dfrac{2\omega[\{B_\beta(B_\alpha+\omega_{12}+B_\gamma)+B_\gamma(B_\alpha+B_\beta+B_\gamma)\}P-\{\omega_{12}(B_\beta+B_\gamma)-\beta B_2 B_\alpha\}B_\gamma Q]}{D_3}$
B_3	$-\dfrac{2\omega[\gamma B_3 B_\gamma P-\{\gamma B_3 B_\alpha^2 - (B_\beta+B_\gamma)(B_\gamma^2+B_\alpha\omega_{13})\}Q]}{D_3}$

Note : $P = (B_\alpha+B_\beta+B_\gamma)\omega^2 - B_\alpha B_\beta B_\gamma$; $Q = B_\alpha(B_\beta+B_\gamma) + B_\beta B_\gamma - \omega^2$

$D_3 = P^2 + \omega^2 Q^2$; $R = R_1 || R_2 || R_3 || R_4 || R_L$

contd ...

Variable	S_x^G	S_x^φ
(d) Second order (complex poles and zeros)		
R_a	$-\frac{2\alpha M\omega^2(B_1+\omega_{11}+B_\beta)}{D_{2c}}$	$\frac{2\omega M\alpha[(\omega_{11}+B_1)B_\beta+\gamma(1-\beta)B_1B_2-\omega^2]}{D_{2c}}$
R_b	$-S^G_{R_a}$	$-S^\varphi_{R_a}$
R_c	$-\frac{2\beta M[(B_2+\omega_{12})N-B_\beta\omega^2]}{D_{2c}}$	$-\frac{2\omega M\beta[N+B_\beta(B_2+\omega_{12})]}{D_{2c}}$
R_d	$-S^G_{R_c}$	$-S^\varphi_{R_c}$
R_e	0	$\frac{2\omega M\gamma(1-\beta)(1-\gamma)B_1B_2}{D_{2c}}$
R_f	$-S^G_{R_e}$	$-S^\varphi_{R_e}$

contd ...

Variable	S_x^G	S_x^φ
R_1	$-1+\frac{R}{R_1}+\frac{2M\omega^2(B_\alpha+B_\beta)}{D_{2c}}$	$-\frac{2\omega M(N-\omega^2)}{D_{2c}}$
R_2	$\frac{R}{R_2}+\frac{2M[NB_\beta-(B_\alpha+2B_\beta)\omega^2]}{D_{2c}}$	$\frac{2\omega M[B_\beta(B_\alpha+B_\beta)+N-\omega^2]}{D_{2c}}$
R_3	$\frac{R}{R_3}-\frac{2MB_\beta[N-\omega^2]}{D_{2c}}$	$-\frac{2\omega MB_\beta(B_\alpha+B_\beta)}{D_{2c}}$
R_L	$\frac{R}{R_L}$	0
ω_{11}	$-\frac{2M\omega_{11}\omega^2}{D_{2c}}$	$\frac{2\omega M\omega_{11}B_\beta}{D_{2c}}$
ω_{12}	$-\frac{2M\omega_{12}N}{D_{2c}}$	$-\frac{2\omega M\omega_{12}B_\beta}{D_{2c}}$
B_1	$\frac{2M\omega^2(\omega_{11}+B_\beta)}{D_{2c}}$	$\frac{2\omega M(\omega^2-B_\beta\omega_{11})}{D_{2c}}$
B_2	$\frac{2M(N\omega_{12}-B_\beta\omega^2)}{D_{2c}}$	$\frac{2\omega M(N+B_\beta\omega_{12})}{D_{2c}}$

Note : $D_{2c} = (N-\omega^2)^2+M^2\omega^2$; $M = B_\alpha+B_\beta$; $N = B_\alpha B_\beta+\gamma(1-\beta)B_1B_2$

$R = R_1||R_2||R_3||R_L$

For third order APF

$$\sum_{i=a}^{f} S_{R_i}^{G} = \sum_{i=a}^{f} S_{R_i}^{\varphi} = 0 \qquad (4.29)$$

Thus, from equations (4.28) and (4.29) it is seen that the magnitude and phase algebraic sum sensitivities with respect to all passive parameters are zero.

(d) The algebraic sum sensitivity of magnitude with respect to all active parameters, i.e., OA first pole frequency and OA gain-bandwidth product is zero for each APF. But the algebraic sum sensitivity of phase with respect to all active parameters is not zero.

Variations of magnitude and phase sensitivities with frequency have been calculated on the basis of parameters indicated in Table 4.3 for first and second order APFs with real poles and zeros and second order APF with complex poles and zeros. These are shown in Figures 4.11 to 4.16. The figures are drawn for various dependent variables, viz., x values and these are indicated in the figures themselves.

4.4 Effect ofOA second pole on APF performance :

The effect of OA second pole on APF performance can be considered by analysing the APF circuit with two pole model for the OAs. The transfer function of the first order APF (Figure 4.4(a)), under all pass condition is

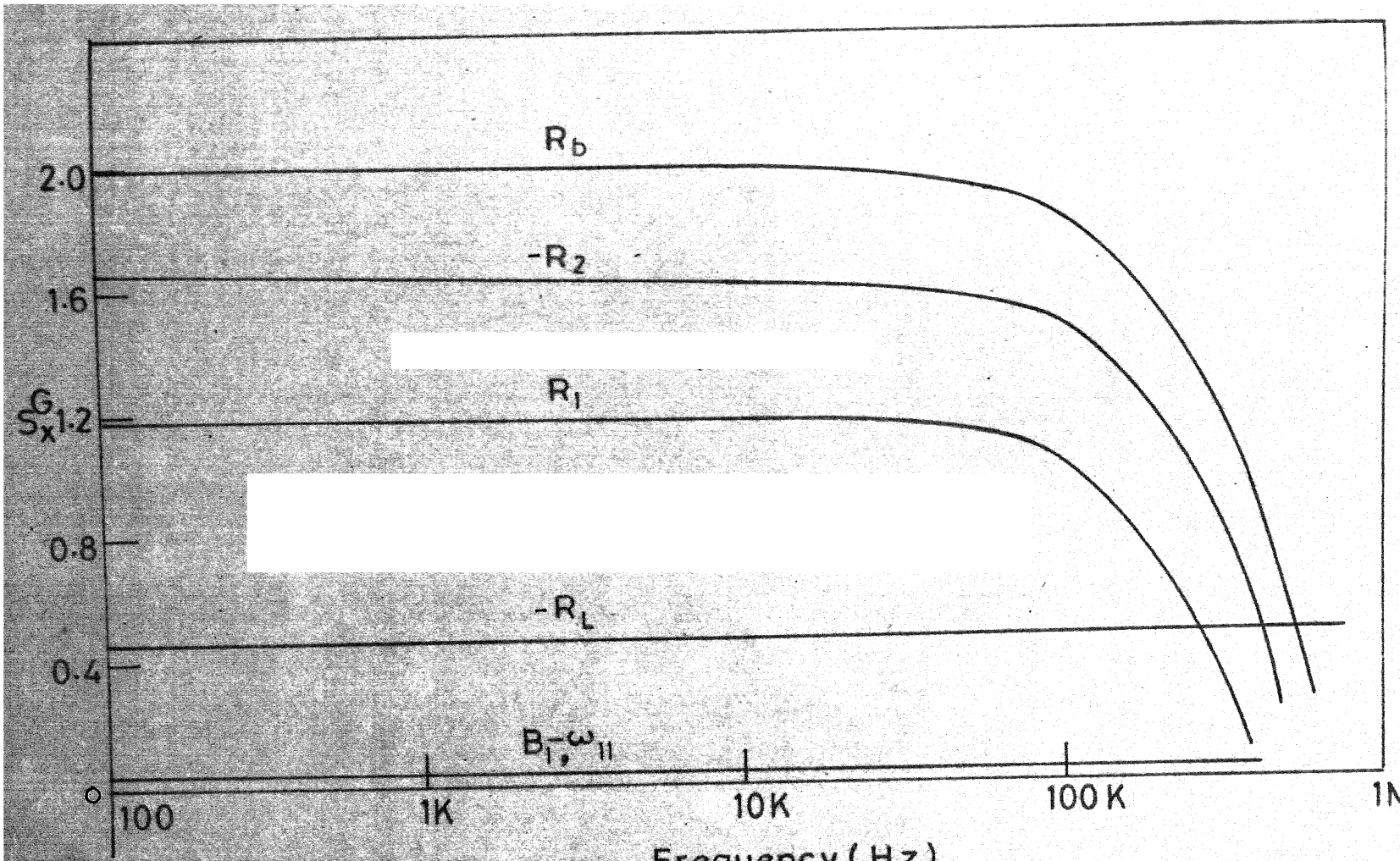

FIG. 4.11 FIRST ORDER APF – VARIATION OF MAGNITUDE SENSITIVITIES WITH FREQUENCY

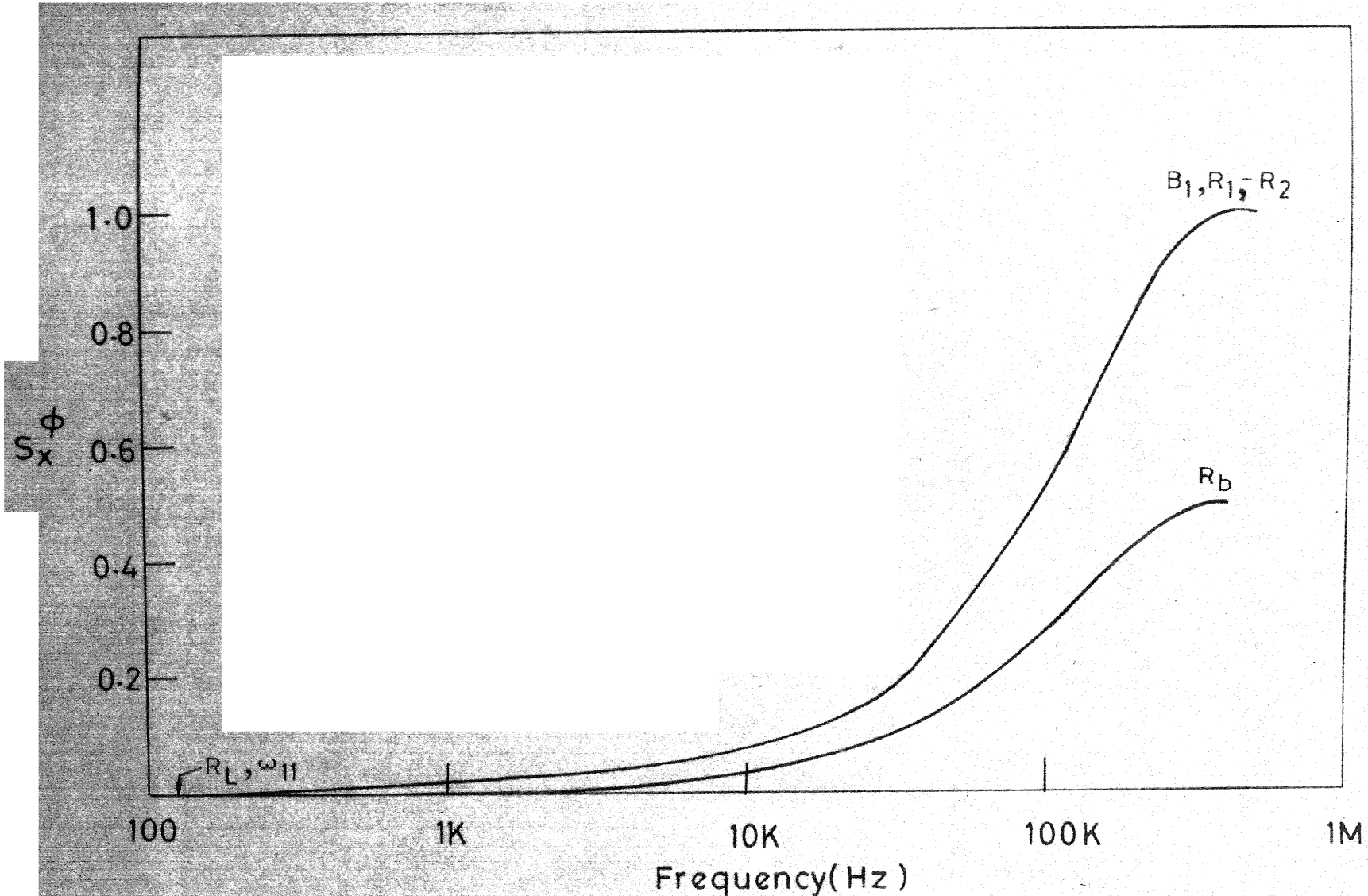

FIG. 4.12 FIRST ORDER APF : VARIATION OF PHASE SENSITIVITIES WITH FREQUENCY.

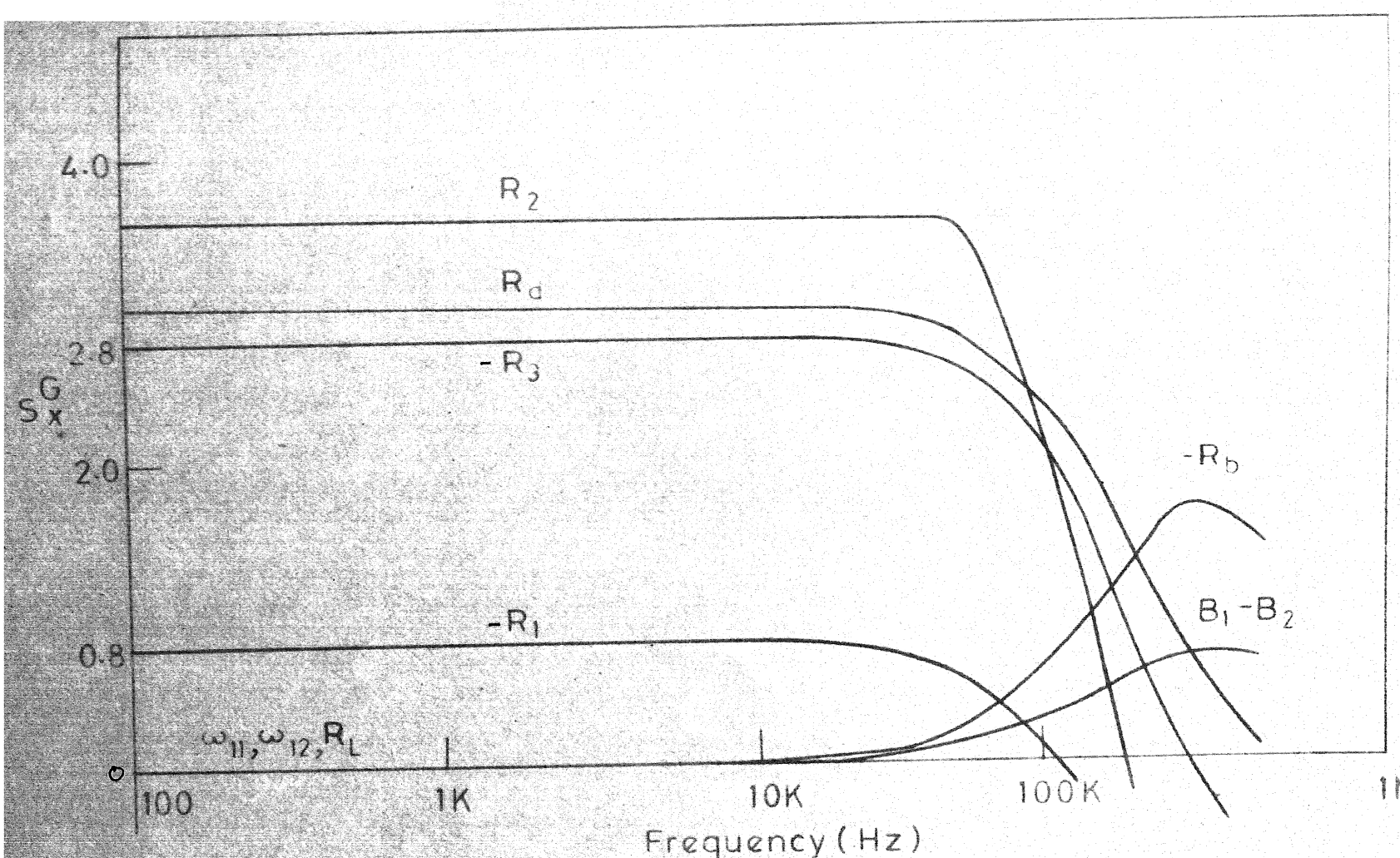

FIG. 4.13 SECOND ORDER APF (real poles & zeros) VARIATION OF MAGNITUDE SENSITIVITIES WITH FREQUENCY

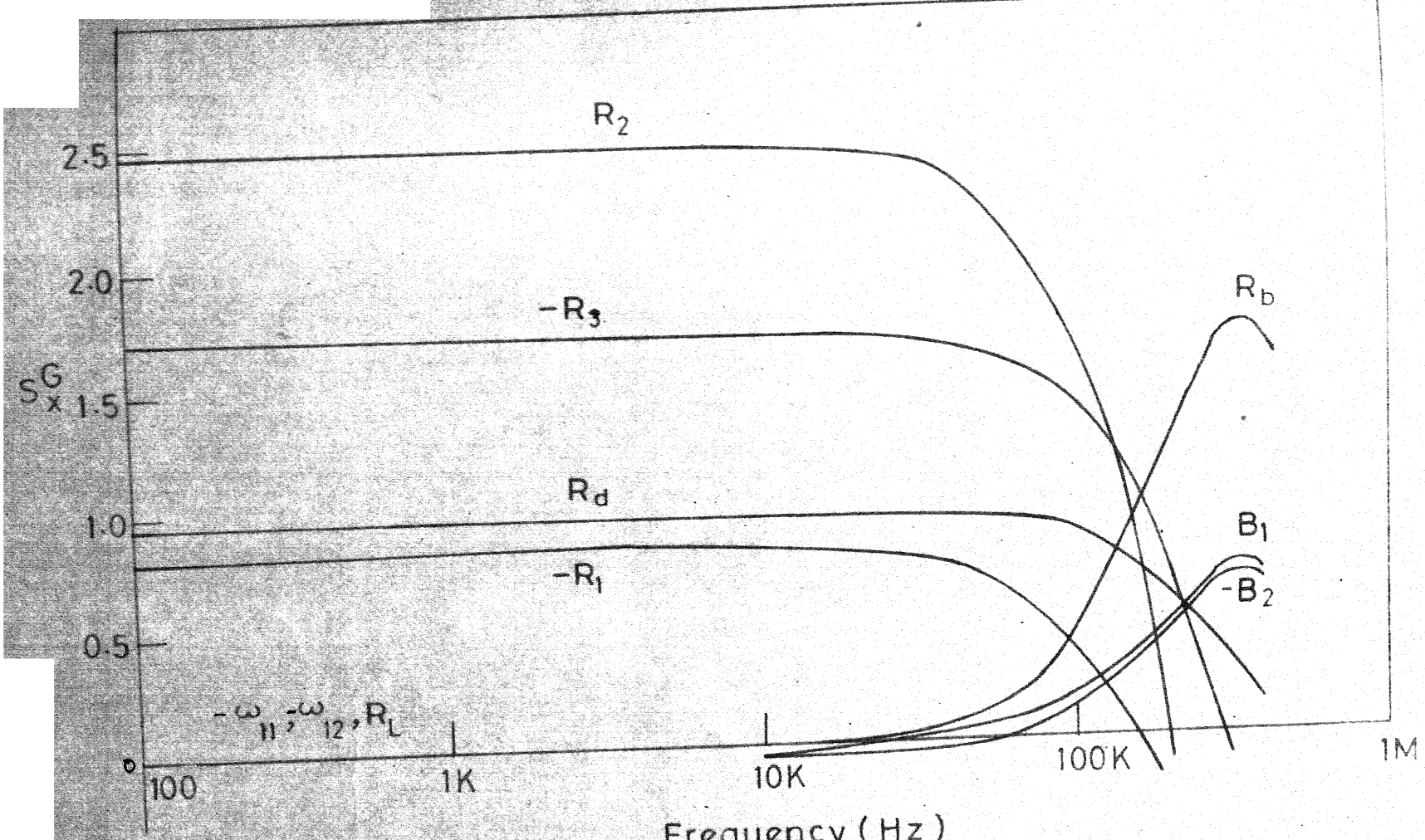

FIG. 4.15 SECOND ORDER APF (complex poles & zeros) VARIATION OF MAGNITUDE SENSITIVITIES WITH FREQUENCY

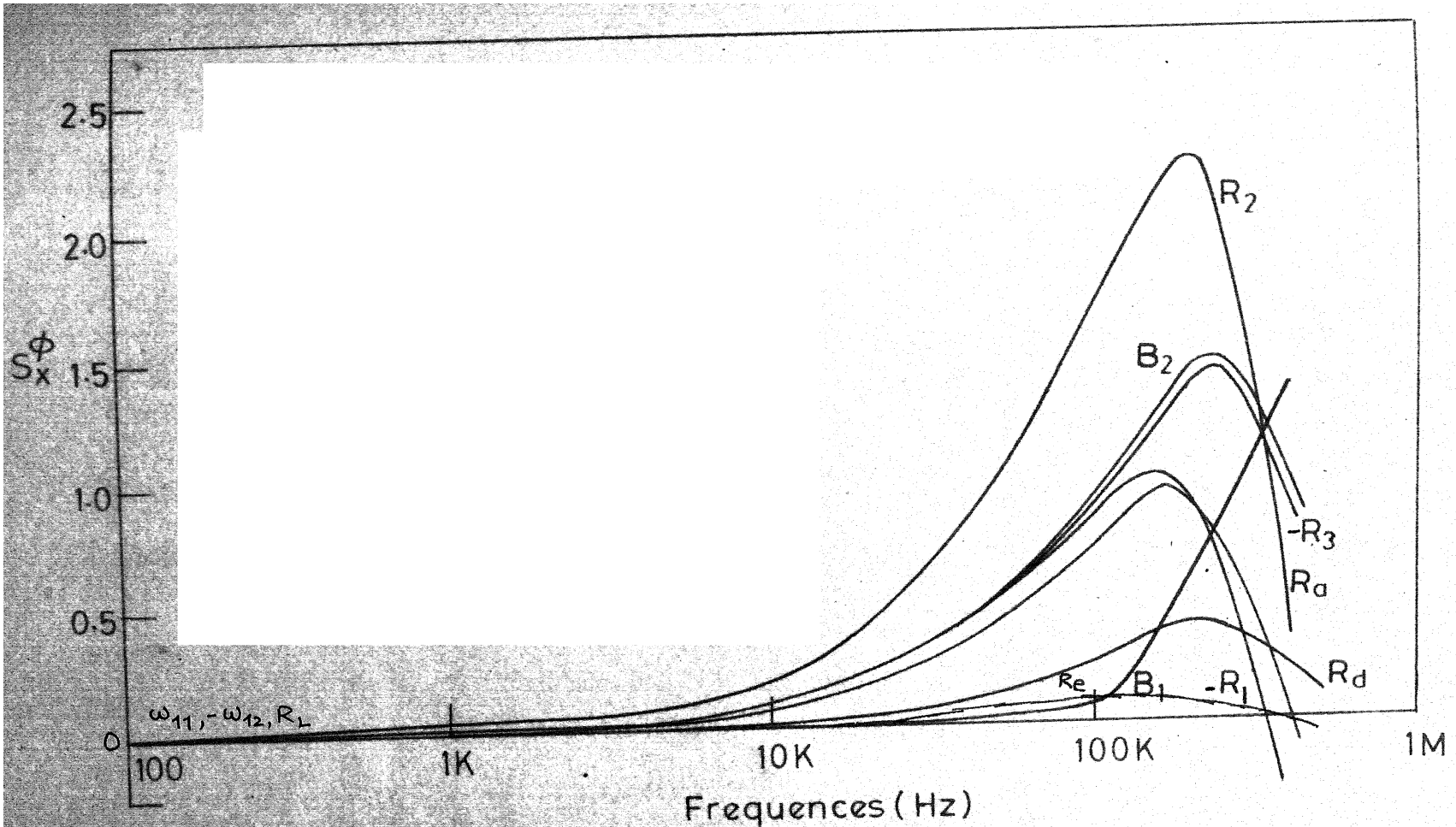

FIG. 4.16 SECOND ORDER APF (Complex poles & zeros) VARIATION OF PHASE SENSITIVITIES WITH FREQUENCY

$$R(s)\ T(s) = \frac{R}{R_1}\ \frac{s-\omega_{11}-\alpha B_1}{s+\omega_{11}+\alpha B_1} \qquad (4.30)$$

If the circuit is analysed, based on two pole model, the transfer function becomes

$$T(s)_{2\ pole} = \frac{R}{R_1}\left[\frac{s^2+(\omega_{21}-\omega_{11})s-\omega_{21}B_\alpha}{s^2+(\omega_{21}+\omega_{11})s+\omega_{21}B_\alpha}\right] \qquad (4.31)$$

under single pole model all pass condition. From equation (4.31) APF magnitude can be written as

$$G_{2\ pole} = \left|\frac{V_o}{V_i}\right|_{2\ pole} = \frac{R}{R_1}\left[\frac{(1-\frac{\omega_{11}}{\omega_{21}})^2\ \omega^2 + (B_\alpha + \frac{\omega^2}{\omega_{21}})^2}{(1+\frac{\omega_{11}}{\omega_{21}})^2\ \omega^2 + (B_\alpha - \frac{\omega^2}{\omega_{21}})^2}\right]$$

$$\simeq \frac{R}{R_1}\left[\frac{\omega^2 + (B_\alpha + \frac{\omega^2}{\omega_{21}})^2}{\omega^2 + (B_\alpha - \frac{\omega^2}{\omega_{21}})^2}\right] \qquad (4.32)$$

since $\omega_{11} << \omega_{21}$

From equation (4.32) it is seen that the magnitude of the first order APF transfer function becomes frequency dependent, due to the effect of OA second pole. The numerator of the magnitude expression increases with frequency at a faster rate than the denominator. Hence, there is a net increase of magnitude as frequency increases. Consequently the magnitude response deviates more and more from true all pass response, as the frequency increases.

The expression for phase, in terms of two pole model, can be written from equation (4.31) as

$$\varphi_{2\ pole} \simeq -\tan^{-1}\frac{\omega}{B_\alpha + \frac{\omega^2}{\omega_{21}}} - \tan^{-1}\frac{\omega}{B_\alpha - \frac{\omega^2}{\omega_{21}}} \qquad (4.33)$$

since $\omega_{11} << \omega_{21}$

The phase angle, based on single pole model, is

$$\varphi_{1\ pole} = -\tan^{-1}\frac{\omega}{B_\alpha} - \tan^{-1}\frac{\omega}{B_\alpha} \qquad (4.34)$$

Comparison of corresponding terms in equations (4.33) and (4.34) shows that the two terms in equation (4.33) contribute to decrease and increase of phase respectively, with increase of frequency. Hence, there is near cancellation of second pole effect on phase response at low frequencies. At high frequencies the second term in equation (4.33) predominates and there is a net increase of phase as compared to single pole model. Phase given by equation (4.34).

The effects of OA second pole on APF performance can be overcome by obtaining the design equations in terms of two pole or pole-zero model for OAs, instead of single pole model. For the circuit of Figure 4.8 the transfer function, based on pole-zero model is

$$T(s) = \frac{V_o}{V_i} = \frac{R}{R_1}\left[1+\frac{-(1-\gamma)\frac{R_1}{R_2}B_1\omega_{21}\omega_{22}s}{D}\right] \qquad (4.35)$$

where

$$D = [\omega_{21}\omega_{22}-(\gamma-\beta)B_1\omega_{22}+\alpha(1-\beta)B_1B_2\ ]s^2+[\omega_{21}\omega_{22}\{\omega_{11}+\omega_{12}$$
$$+\ (\gamma-\beta)B_1\}\ -(\gamma-\beta)B_1\omega_{12}\omega_{22}-\alpha(1-\beta)B_1B_2(\omega_{21}+\omega_{22})]s$$
$$+\ \omega_{21}\omega_{22}[\omega_{11}\omega_{12}+(\gamma-\beta)B_1\omega_{12}+\alpha(1-\beta)B_1B_2]$$

and α,β,γ and R are as defined in equation (4.26).

Comparing equations (4.17)(with $K_1 = 0$) and (4.35) the design equations, based on pole-zero model for the OAs, are :

$$(1-\gamma)\frac{R_1}{R_2}B_1 = \frac{2[a\ \omega_{21}^2\omega_{22}+b(\omega_{21}^2-\omega_{22}^2+\omega_{22}\omega_{11}+\omega_{22}\omega_{12})]}{\omega_{22}D} \qquad (4.36)$$

$$(\gamma-\beta)B_1 = \frac{\omega_{21}[b(\omega_{21}+\omega_{22})+\omega_{21}\omega_{22}(a-\omega_{11}-\omega_{12})]}{\omega_{22}D} \qquad (4.37)$$

$$\alpha(1-\beta)B_1B_2 = \frac{b\ \omega_{21}\omega_{22}}{D} \qquad (4.38)$$

where

$$D = b + \omega_{21}a + \omega_{21}^2$$

With γ assumed, R_1/R_2 and β can be determined from equations (4.36) and (4.37) respectively. Then α can be obtained from equation (4.38).

4.5 Experimental results :

The first to fourth order APFs with real poles and zeros (Figures 4.4 to 4.6), the third order APF with a pair of complex conjugate poles and zeros (Figure 4.7(b)) and the second order circuit of Figure 4.8 have been tested. The circuits of Figures 4.4 to 4.6 and 4.7(b)) were built using National Semiconductor, LM 324 quad OA, 0.1 percent metal film resistors and miniature multiturn potentiometers. The relevant measured parameters of the four OAs in the LM 324 chip used are given in Table 4.2.

TABLE 4.2

Parameters of LM 324 OA

Parameter	OA 1	OA 2	OA 3	OA 4
$\omega_{1i}/2\pi$ (Hz)	7.0	5.5	6.0	6.0
$\omega_{2i}/2\pi$ (MHz)	1.60	1.75	1.50	1.70
$B_i/2\pi$ (KHz)	728	746	738	742
V_{cc} (Volts)	$\pm$ 12	$\pm$ 12	$\pm$ 12	$\pm$ 12
Temp (^{o}C)		27		

The circuit of Figure 4.8 was built using two NE 536 OAs whose parameters are given in Table 3.2 (Chapter III). The resistor values for the six circuits are given in Table 4.3.

The all pass responses (magnitude and phase) of the six APF circuits are shown in Figures 4.17 to 4.22. The magnitude response plots clearly show the deviation in response, due to OA second pole, at high frequencies. The magnitude response is flat within 0.5 dB upto 133 KHz for first order, upto 79.4 KHz for second order, upto 60 KHz for third order and upto 56 KHz for fourth order APFs with real poles and zeros. Magnitude response is flat withnin 0.5 dB upto 60 KHz for the third order APF with complex poles and zeros and upto 500 KHz for the second order circuit of Figure 4.8. It is seen from Figure 4.22(a) that when the APF is designed, based on pole-zero model, the magnitude response remains flat over a very wide frequency range.

Figures 4.17(a) to 4.22(a) show that the phase response is practically unaffected by OA second pole effects except at very high frequencies. Higher the order of the APF, larger is the range of phase variation with frequency, i.e., for a given change in frequency the phase variation is much larger for higher order APFs as compared to lower order APFs.

4.6 Conclusions :

In this chapter a new technique for synthesising active

TABLE 4.3

Resistor values for APF circuits

S.No.	APF circuit and Figure No.	Resistor values (in Kilo ohms)
1.	First order (Fig. 4.4(a))	$R_a = R_b = 3.0$, $R_1 = 12$, $R_2 = 6$, $R_L = 4.7$
2.	Second order (real poles and zeros) [Fig.4.4(b)]	$R_a = R_b = R_d = 3.0$, $R_c = R_1 = 1.0$, $R_3 = 0.99$, $R_L = 4.7$, $R_2 = 0.33$
3.	Third order (real poles and zeros)[Fig.4.5]	$R_a = R_b = 3.0$, $R_c = R_e = R_1 = 1.0$, $R_d = 4.0$, $R_f = 9.0$, $R_2 = 0.31$, $R_3 = 0.83$, $R_4 = 10$, $R_L = 4.7$
4.	Fourth order (real poles and zeros)[Fig.4.6]	$R_a = R_b = R_d = 12$, $R_c = R_g = 3.0$, $R_e = 1.0$, $R_f = 1.5$, $R_h = 27$, $R_1 = 5.0$, $R_2 = 1.1$, $R_3 = 1.2$, $R_4 = 1.8$, $R_5 = 60$, $R_L = 4.7$
5.	Third order (complex poles and zeros)[Fig.4.7(b)]	$R_a = R_b = R_f = 6.0$, $R_c = R_1 = 1.0$, $R_d = 3.0$, $R_e = 1.5$, $R_g = 0.2$, $R_h = 1.8$, $R_2 = 0.26$, $R_3 = 0.44$, $R_4 = 5.7$, $R_L = 4.7$
6.	Second order (complex poles and zeros) [Fig. 4.8]	$R_a = R_d = R_f = 1.0$, $R_c = 4.9$, $R_e = 5.7$, $R_1 = 0.15$, $R_2 = 3.0$, $R_L = 4.7$, $R_b = 17$

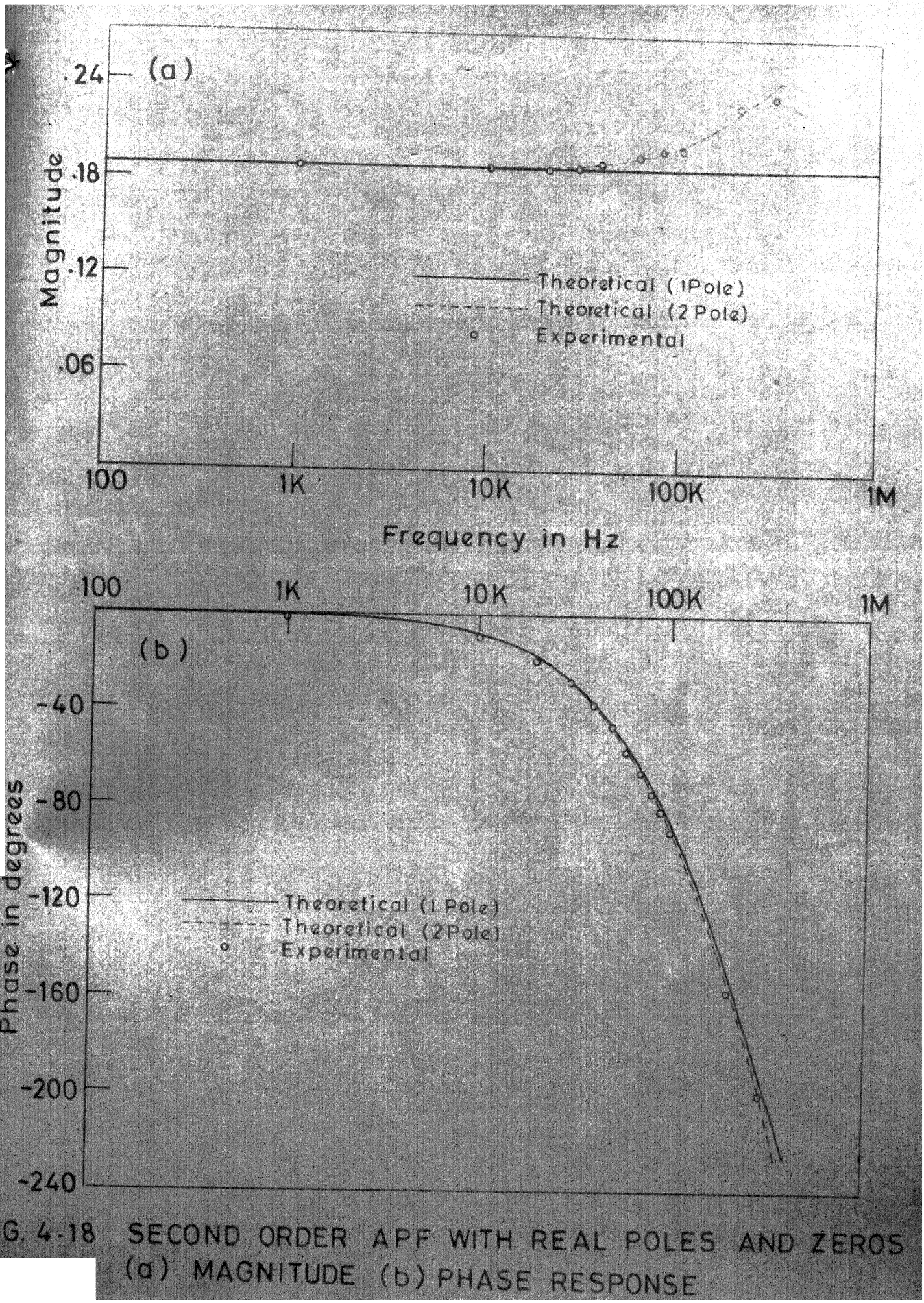

FIG. 4-18 SECOND ORDER APF WITH REAL POLES AND ZEROS (a) MAGNITUDE (b) PHASE RESPONSE

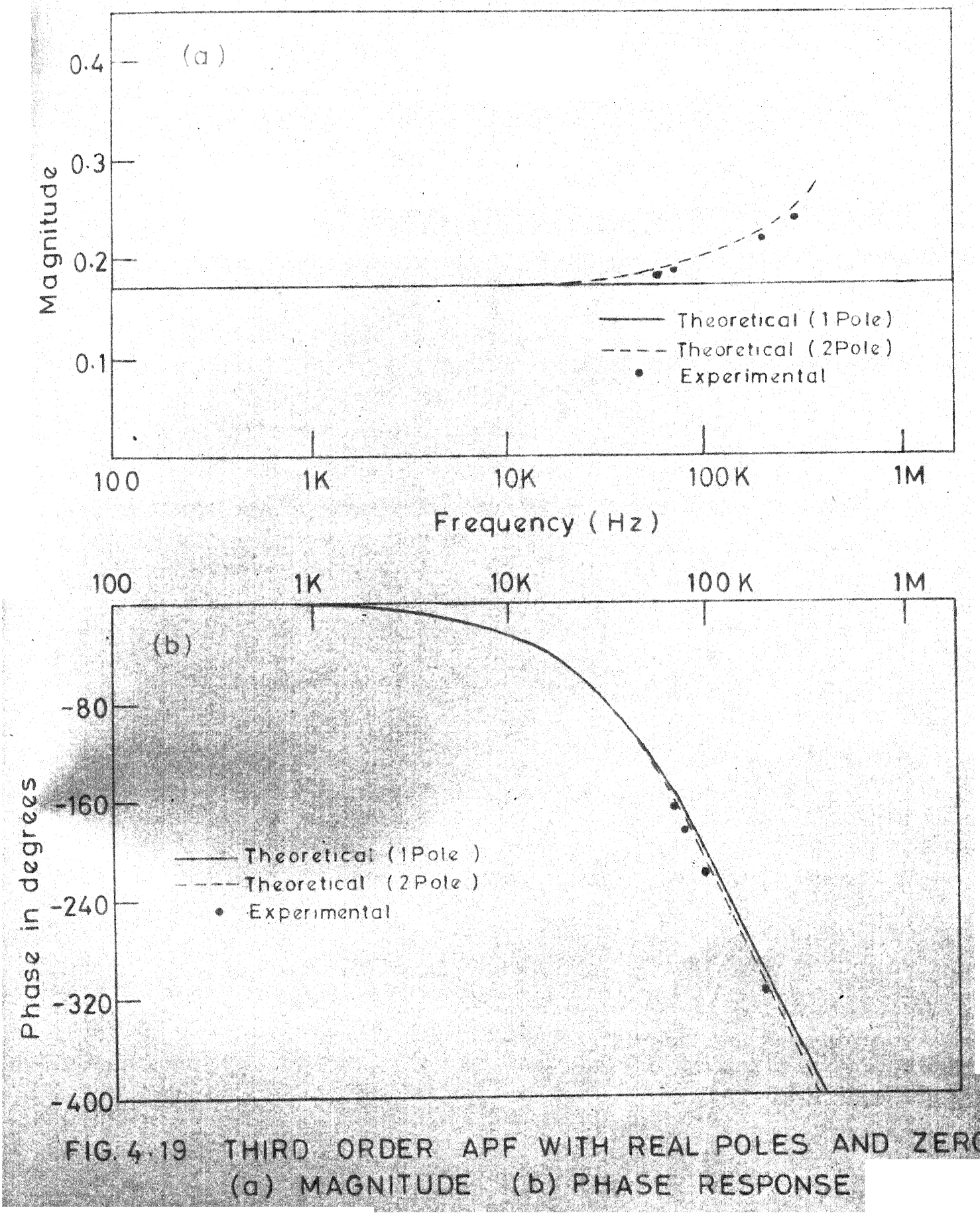

FIG. 4.19 THIRD ORDER APF WITH REAL POLES AND ZEROS
(a) MAGNITUDE (b) PHASE RESPONSE

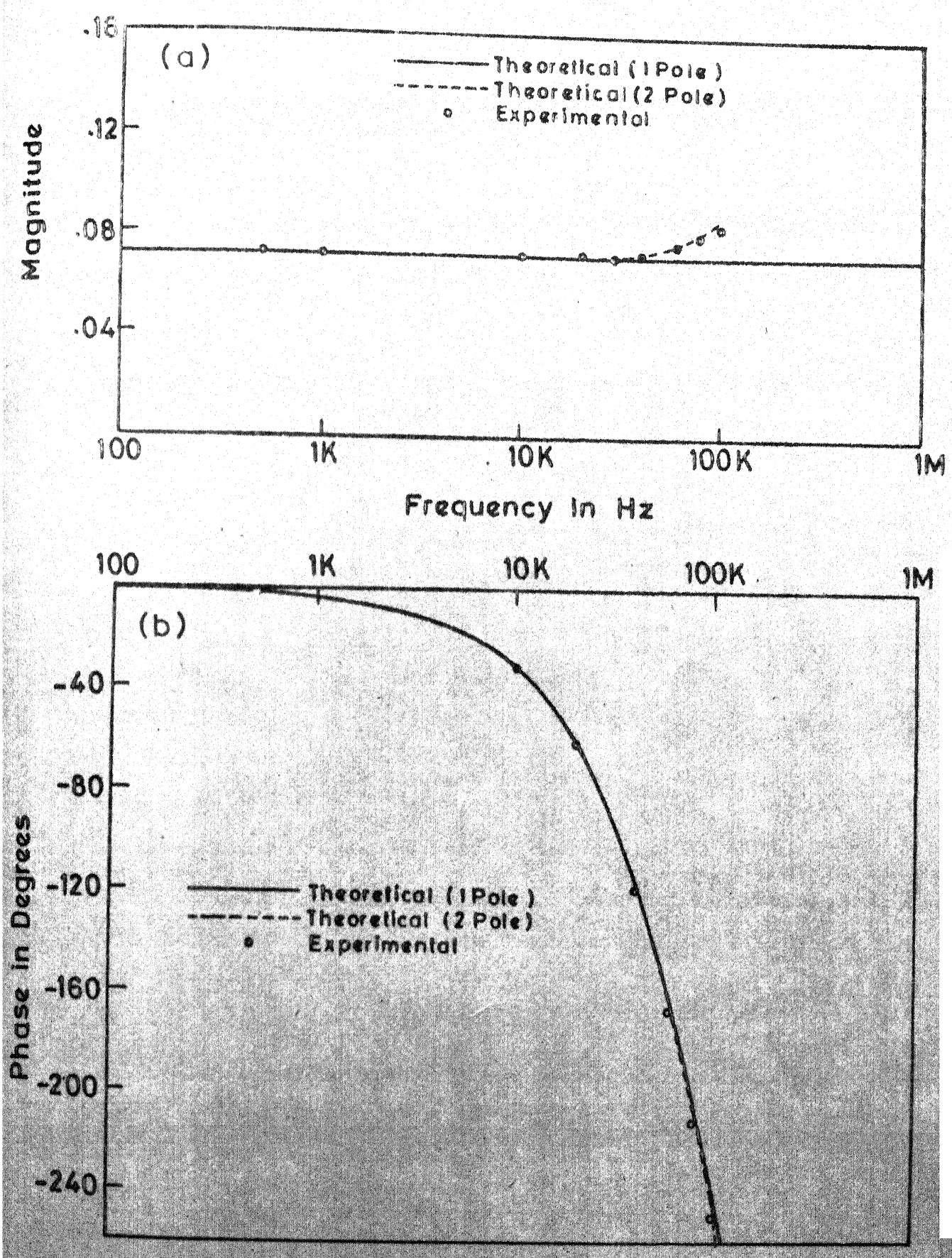

FIG. 4.20 FOURTH ORDER APF WITH REAL POLES AND ZEROS
(a) MAGNITUDE (b) PHASE RESPONSE

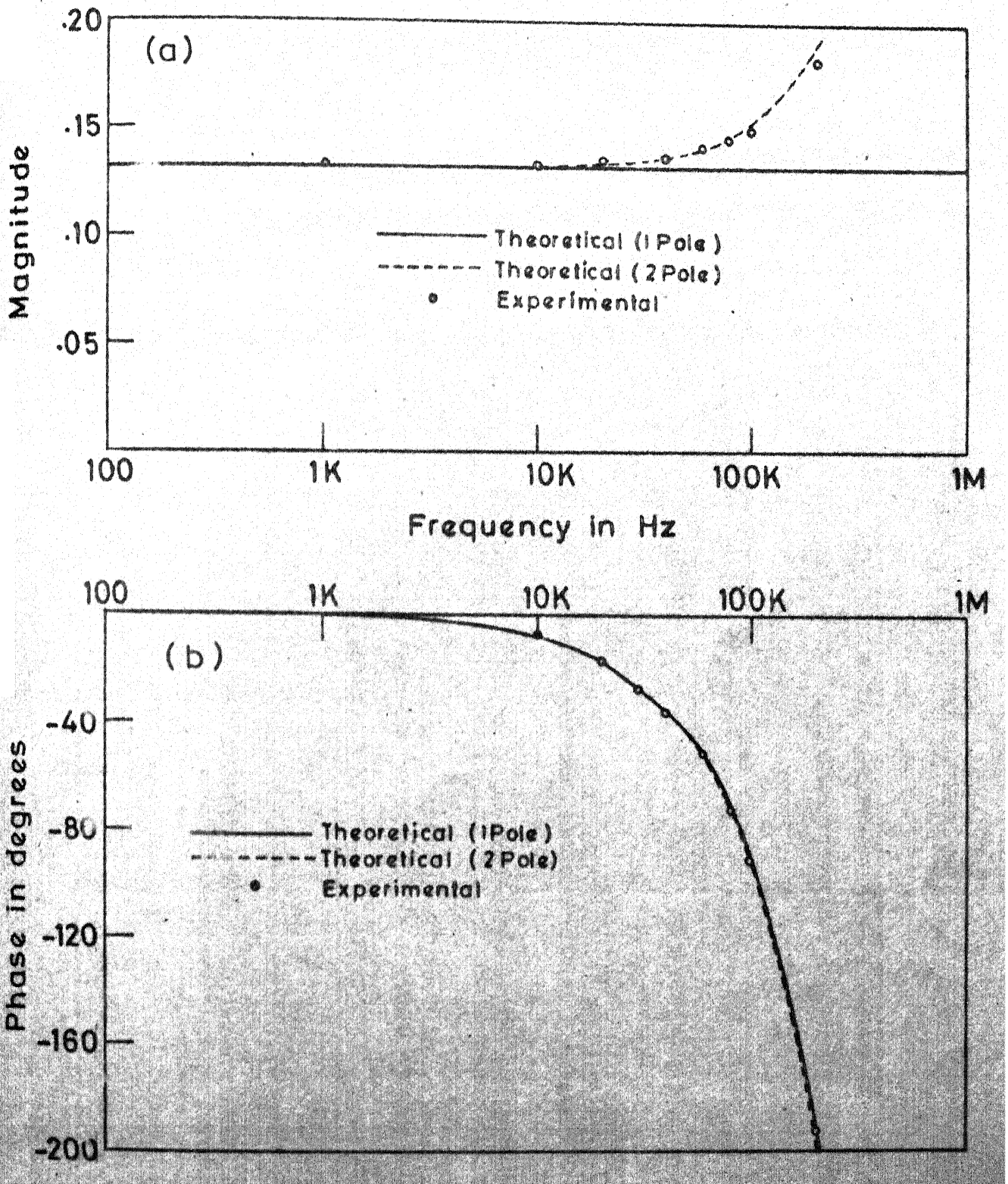

FIG. 4.21 THIRD ORDER APF WITH COMPLEX POLES AND ZEROS (a) MAGNITUDE (b) PHASE RESPONSE

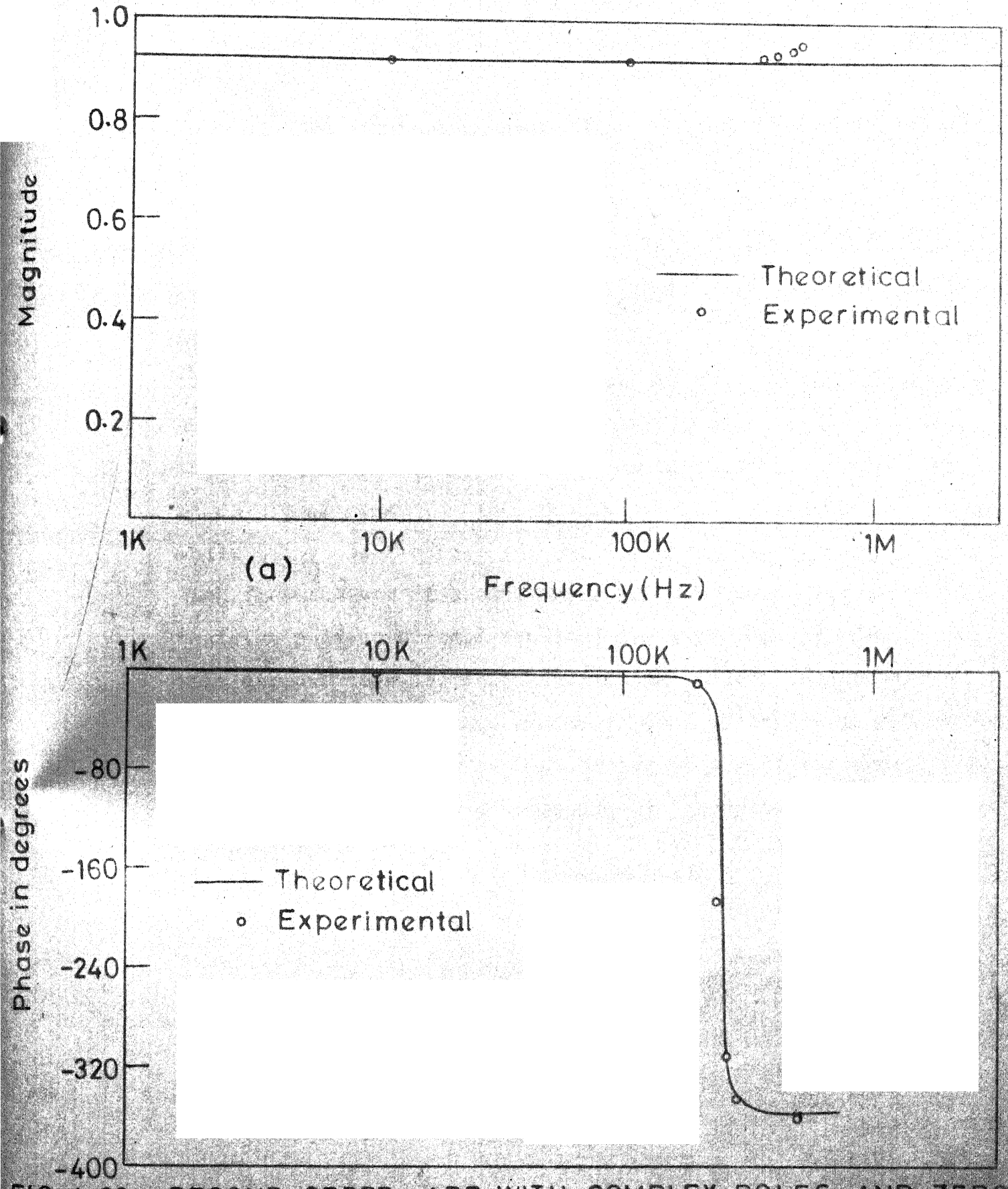

FIG. 4.22 SECOND ORDER APF WITH COMPLEX POLES AND ZEROS (pole-zero model) (a) Magnitude (b) Phase response

R APF of any order, both with real poles and zeros and with complex poles and zeros has been proposed. The first order circuit obtained by this technique is the same as the circuit of Srinivasan [1]. The second and higher order APFs synthesised are new circuits. The realised second order APFs have same or lesser resistor count as compared to reported second order APF circuits. Since resistive summation is used to achieve all pass response, realisations are possible only with an attenuation constant. Due to the effect of OA second pole, the magnitude response for the APF tends to increase with frequency while the phase response is practically unaffected upto fairly high frequencies. A second order APF has been designed on the basis of pole-zero model and tested. Experimental results for this circuit show the constancy of magnitude response over a very wide frequency range. The proposed synthesis technique being general can also realise active RC APF of any order, both with real poles and zeros and with complex poles and zeros.

References

1. Srinivasan, S., 'Synthesis of transfer functions using operational amplifier pole', Int.J.Electron., Vol. 40, no.1, pp 5-13, January, 1976.

2. Soliman, A.M., 'A universal active R filter', Electron. Engg., Vol. 49, no.594, pp 49-50, July, 1977.

3. Soliman, A.M. and Fawzy, M., 'A universal active R biquad', Int.J.Ckt.Th. and Appn., Vol. 6, no.4, pp 153-157, April, 1978.

4. Kim, H.K. and Ra, J.B., 'An active biquadratic building block without external capacitors', IEEE Trans. Ckts. and Sys., Vol. CAS-24, no.12, pp 689-694, December, 1977.

5. Mitra, A.K. and Aatre, V.K., 'Low sensitivity high frequency active R filters', IEEE Trans. Ckts. and Sys., Vol. CAS-23, no.11, pp 670-676, November, 1976.

6. Soderstrand, M.A., 'Design of active R filters using only resistors and operational amplifiers', Int.J.Electron. Vol. 40, no.5, pp 417-432, May, 1976.

7. Ho, C.F. and Chiu, P.L., 'Realisation of active R filters using operational amplifier pole', Proc. IEE, Vol. 123, no.5, pp 406-410, May, 1976.

8. Schaumann, R. and Brand, J.R., 'Active R filters: Review of theory and practice', IEE J. Electron. Ckts. and Sys., Vol. 2, no.4, pp 89-101, July, 1978.

CHAPTER V

SYNTHESIS OF ALL PASS FILTERS PARALLEL REALISATION

The series realisation technique, proposed in Chapter IV, has the drawback that for higher order filters, the signal handling capacity is very much reduced due to cascading of lower order LPF sections. This problem can be overcome by the alternate technique, proposed in this chapter. Here, the transfer function (with no multiple poles) is expanded in terms of partial fractions. The resulting low order sections are resistively summed to realise the transfer function. The realised circuits have the same OA and resistor count as the corresponding series realisation circuits. The effect of OA second pole on these circuits is identical to that for series realisation circuits.

5.1 Synthesis :

In this section, synthesis techniques for all pass filters of any order with real poles and zeros and with complex poles and zeros are proposed. The technique involves partial fraction expansion of the given transfer function into a number of first or second order terms. These individual terms are identified in terms of the transfer functions of known first and second order active R building blocks. Resistive summation of

these blocks enables realisation of the complete transfer function. The technique is valid for transfer functions with no multiple poles.

5.1.1 APFs with real poles and zeros :

The general nth order all pass transfer function with distinct real poles and zeros is

$$T(s) = \frac{(s-a_1)(s-a_2) \ldots (s-a_{n-1})(s-a_n)}{(s+a_1)(s+a_2) \ldots (s+a_{n-1})(s+a_n)} \qquad (5.1)$$

Let

$$a_{n-1} > a_n \qquad \text{for } n = 2,3,\ldots, n$$

Equation (5.1) can be expanded in terms of partial fractions.

$$T(s) = \left[1 + \frac{K_1}{s+a_1} + \frac{K_2}{s+a_2} + \ldots + \frac{K_n}{s+a_n}\right] \qquad (5.2)$$

where $K_1, K_2, \ldots, K_n$, represent the residues of the poles. The residue K_r is obtained as

$$K_r = T(s)(s+a_r)\Big|_{s=-a_r} \qquad (5.3)$$

$$= \frac{2(-1)^n a_r(a_1+a_r)(a_2+a_r) \ldots (a_n+a_r)}{(a_1-a_r)(a_2-a_r) \ldots (a_n-a_r)} \qquad (5.4)$$

where the term (a_r+a_r) in numerator is written as $2a_r$ and (a_r-a_r) is absent in denominator. For the assumption under

equation (5.1) the sign of K_r is negative for odd r values and positive for even r values. The transfer function of equation (5.2) represents the summation of n first order LP functions with their common input. The first order APF circuit obtainable by this technique is identical to the first order APF obtained by series realisation technique (Figure 4.4(a)).

The second order all pass transfer function with real poles and zeros is given by

$$T(s) = K\frac{(s-a)(s-b)}{(s+a)(s+b)} \qquad (5.5)$$

where K = attenuation constant.

For $a > b$, the transfer function can be expanded, in terms of partial fractions, as

$$T(s) = K\left[1 + \frac{-2a(a+b)}{(a-b)(s+a)} + \frac{2b(a+b)}{(a-b)(s+b)}\right] \qquad (5.6)$$

The second and third terms represent inverting and non-inverting first order LP transfer functions respectively. The inverting LPF can be realised by the circuit of Figure 4.3, whose transfer function is

$$T(s) = \frac{-(1-\alpha)B_1}{s+B_\alpha} \qquad (5.7)$$

where

$$\alpha = \frac{R_a}{R_a+R_b} \quad \text{and} \quad B_\alpha = \omega_{11} + \alpha B_1$$

The non-inverting first order LPF can be realised by the circuit shown in Figure 5.1. Its transfer function

$$T(s) = \frac{B_1}{s+B_\alpha} \tag{5.8}$$

where

$$\alpha = \frac{R_a}{R_a+R_b}, \qquad B_\alpha = \omega_{11} + \alpha B_1$$

Resistive summation of the outputs of these two LPFs with their common input gives rise to the second order APF with real poles and zeros. The complete circuit is shown in Figure 5.2. The transfer function of this circuit is

$$T(s) = \frac{V_o}{V_i} = \frac{R}{R_1}\left[1 + \frac{-(1-\alpha)\frac{R_1}{R_2}B_1}{s+B_\alpha} + \frac{\frac{R_1}{R_3}B_2}{s+B_\beta}\right] \tag{5.9}$$

where

$$R = R_1 || R_2 || R_3 || R_L, \quad \alpha = \frac{R_a}{R_a+R_b}, \quad \beta = \frac{R_c}{R_c+R_d}$$

$$B_\alpha = \omega_{11} + \alpha B_1 \qquad \text{and } B_\beta = \omega_{12} + \beta B_2$$

The design equations for this circuit, obtained by comparing equations (5.6) and (5.9) are :

$$\left.\begin{aligned} &\alpha = \frac{a-\omega_{11}}{B_1}, \quad \beta = \frac{b-\omega_{12}}{B_2}, \quad \frac{R}{R_1} = K, \\ &\frac{R_1}{R_2} = \frac{2a(a+b)}{(a-b)(B_1+\omega_{11}-a)}, \quad \frac{R_1}{R_3} = \frac{2b(a+b)}{(a-b)B_2} \end{aligned}\right\} \tag{5.10}$$

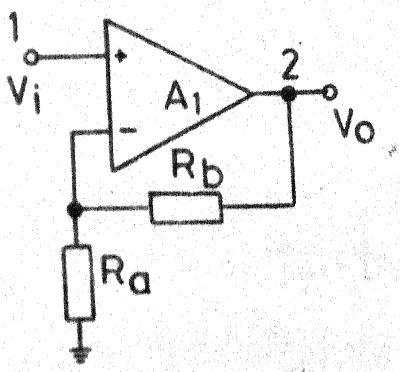

FIG.5.1 FIRST ORDER NON INVERTING LPF CIRCUIT

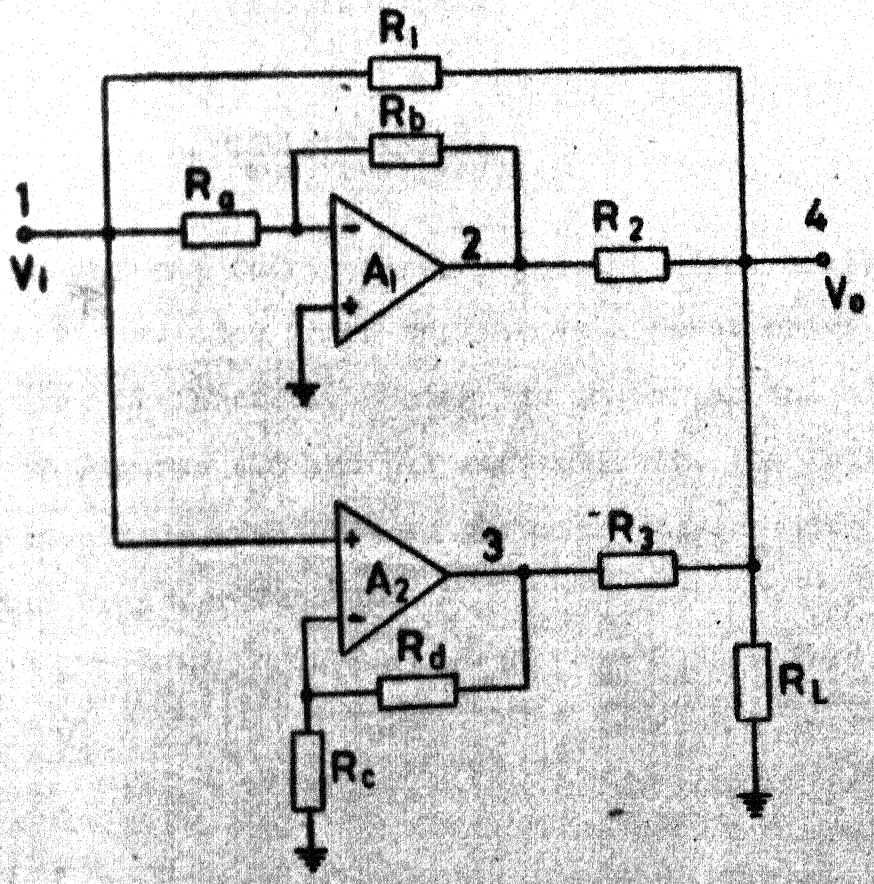

FIG. 5.2 SECOND ORDER APF WITH REAL POLES AND ZEROS

The third order all pass transfer function, with real poles and zeros, is given by

$$T(s) = K \frac{(s-a)(s-b)(s-c)}{(s+a)(s+b)(s+c)} \qquad (5.11)$$

For $a > b > c$ the transfer function becomes

$$T(s) = K \left[1 + \frac{-2a(a+b)(a+c)}{(a-b)(a-c)(s+a)} + \frac{2b(a+b)(b+c)}{(a-b)(b-c)(s+b)} + \frac{-2c(a+c)(b+c)}{(a-c)(b-c)(s+c)} \right] \qquad (5.12)$$

The second and fourth terms represent first order inverting LP functions. The third represents a first order non-inverting LP function. Using the inverting and non-inverting LPFs of Figures 4.3 and 5.1 respectively, the third order APF circuit is realised, as shown in Figure 5.3. This circuit has the transfer function

$$T(s) = \frac{V_o}{V_i} = \frac{R}{R_1} \left[1 + \frac{-(1-\alpha)\frac{R_1}{R_2} B_1}{s+B_\alpha} + \frac{\frac{R_1}{R_3} B_2}{s+B_\beta} + \frac{-(1-\gamma)\frac{R_1}{R_4} B_3}{s+B} \right] \qquad (5.13)$$

where

$$R = R_1 || R_2 || R_3 || R_4 || R_L, \quad \alpha = \frac{R_a}{R_a+R_b}, \quad \beta = \frac{R_c}{R_c+R_d},$$

$$\gamma = \frac{R_e}{R_e+R_f}, \quad B_\alpha = \omega_{11}+\alpha B_1, \quad B_\beta = \omega_{12}+\beta B_2, \quad B_\gamma = \omega_{13}+\gamma B_3$$

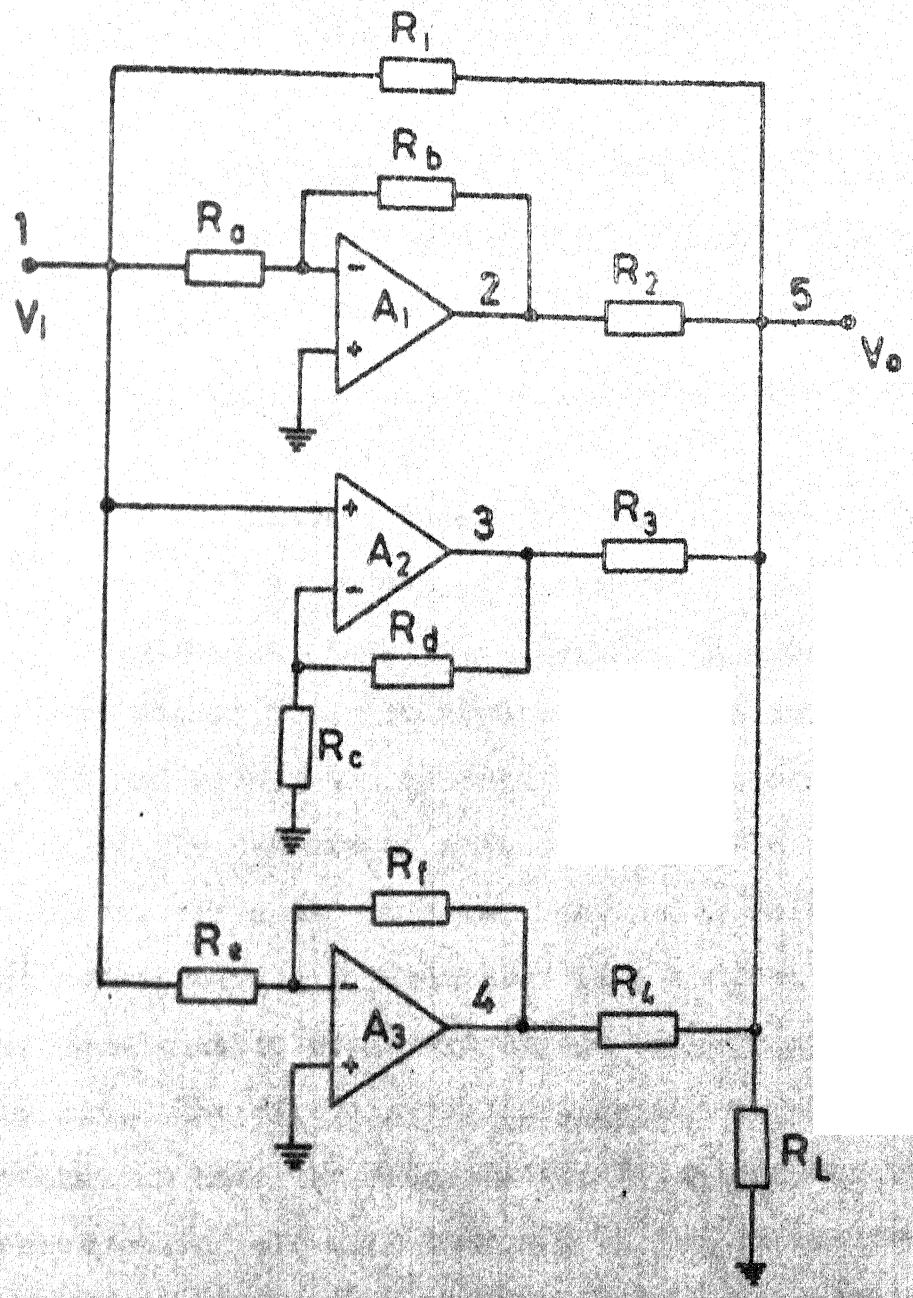

FIG. 5.3 THIRD ORDER APF WITH REAL POLES AND ZEROS

Comparison of equations (5.12) and (5.13) yields the following design equations

$$\left.\begin{aligned} &\alpha = \frac{a-\omega_{11}}{B_1}\ ,\ \beta = \frac{b-\omega_{12}}{B_2}\ ,\ \gamma = \frac{c-\omega_{13}}{B_3}\ ,\ \frac{R}{R_1} = K \\ &\frac{R_1}{R_2} = \frac{2a(a+b)(a+c)}{(a-b)(a-c)(B_1+\omega_{11}-a)},\ \frac{R_1}{R_3} = \frac{2b(a+b)(b+c)}{(a-b)(b-c)B_2}\ , \\ &\frac{R_1}{R_4} = \frac{2c(a+c)(b+c)}{(a-c)(b-c)(B_3+c-\omega_{13})} \end{aligned}\right\} \quad (5.14)$$

In a similar manner, fourth and higher order all pass filters, with real poles and zeros can be obtained by the parallel realisation technique. The fourth order circuit is shown in Figure 5.4. In general, the nth order APF, with real poles and zeros, can be realised by the resistive summation of the outputs of n first order LPFs with their common input. If n is odd then there will be $\frac{n+1}{2}$ inverting and $\frac{n-1}{2}$ non-inverting LPF blocks. If n is even then there will be equal number of inverting and non-inverting LPFs in the circuit. The circuits realised by the parallel realisation technique have the same number of OAs and resistors as the corresponding circuits obtained by series realisation technique. Thus, the nth order APF, with real poles and zeros, will have n OAs and (3n+2) resistors.

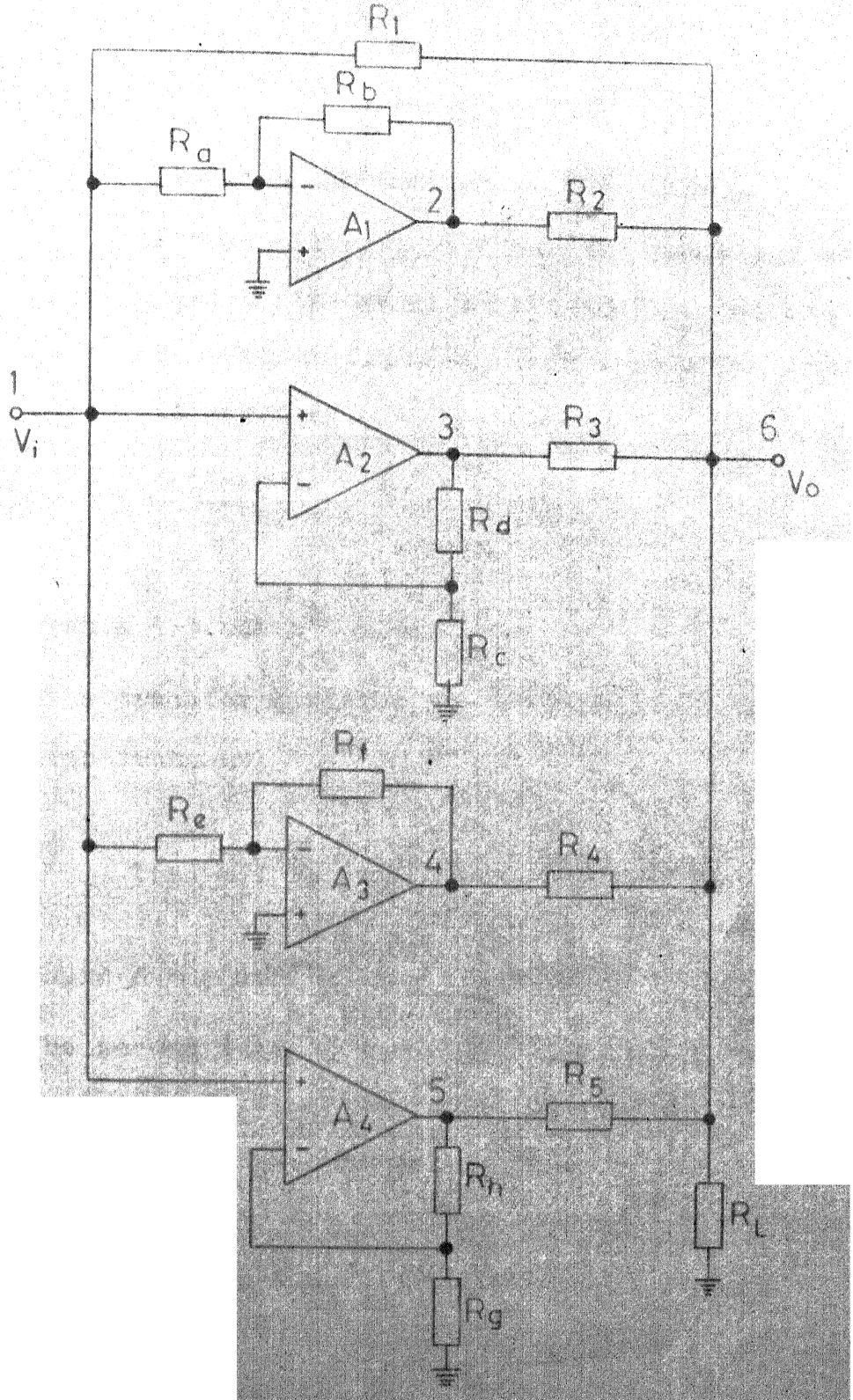

FIG. 5.4 FOURTH ORDER APF WITH REAL POLES AND ZEROS

5.1.2 APFs with complex poles and zeros :

All pass filters, with complex poles and zeros, can also be realised by the parallel realisation technique. The third order AP transfer function, with a pair of complex poles and zeros, is given by

$$T(s) = K \frac{(s-a)(s^2-bs+c)}{(s+a)(s^2+bs+c)} \qquad (5.15)$$

with $K < 1$ and $b^2 < 4c$.

This transfer function can be expressed, in terms of partial fractions, as

$$T(s) = K \left[1 + \frac{-2a\ M}{N(s+a)} + \frac{2b\ Ps + 4abc}{N(s^2+bs+c)}\right] \qquad (5.16)$$

where $M = a(a+b)+c$, $N = a(a-b)+c$, $P = a(a+b)-c$

The second term in equation (5.16) represents a first order inverting LP function, while the third term represents a second order non-inverting pseudo BP function for $-a^2 < (ab-c) < a^2$. The corresponding circuit realisation is shown in Figure 5.5. The transfer function of this circuit is

$$T(s) = \frac{R}{R_1}\left[1 + \frac{-(1-\alpha)\frac{R_1}{R_2}B_1}{s+B_\alpha} + \frac{\frac{R_1}{R_3}B_3(s+B_\beta)}{D}\right] \qquad (5.17)$$

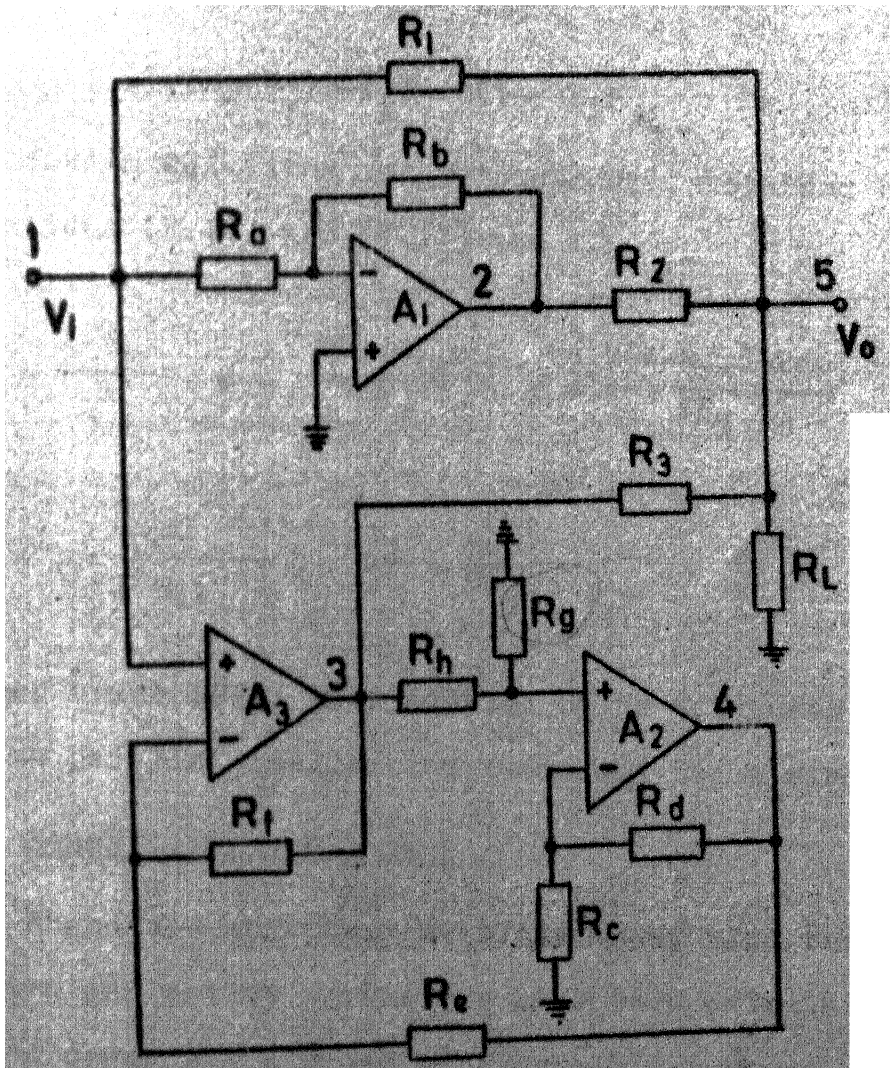

IG. 5.5 THIRD ORDER APF WITH COMPLEX POLES AND ZEROS

where

$$R = R_1 || R_2 || R_3 || R_L,\ \alpha = \frac{R_a}{R_a+R_b}\ ,\ \beta = \frac{R_c}{R_c+R_d}\ ,\ \gamma = \frac{R_e}{R_e+R_f}\ ,$$

$$\delta = \frac{R_g}{R_g+R_h}\ ,\ B_\alpha = \omega_{11}+\alpha B_1,\ B_\beta = \omega_{12}+\beta B_2,\ B_\gamma = \omega_{13}+\gamma B_3$$

and

$$D = s^2+(B_\beta+B_\gamma)s+B_\beta B_\gamma+\delta(1-\gamma)B_2B_3.$$

The design equations for this circuit, obtained by comparing equations (5.16) and (5.17), are :

$$\left.\begin{aligned} &\alpha = \frac{a-\omega_{11}}{B_1}\ ,\ \beta = \frac{2ac-\omega_{12}P}{PB_2}\ ,\ \gamma = \frac{P(b-\omega_{13})-2ac}{PB_3}\ ,\ \frac{R}{R_1} = K \\ &\frac{R_1}{R_2} = \frac{2aM}{N(B_1+\omega_{11}-a)}\ ,\quad \frac{R_1}{R_3} = \frac{2bP}{NB_3} \end{aligned}\right\} \quad (5.18)$$

Higher order APFs, with complex poles and zeros can be obtained, by the parallel realisation technique, in a similar way.

5.2 Sensitivity analysis :

Magnitude and phase sensitivities, with respect to all passive and active parameters have been calculated for the second order APF circuit of Figure 5.2. These are given in Table 5.1. From the sensitivity figures it can be noted that the algebraic sum sensitivity with respect to all passive parameters is zero. The algebraic sum sensitivity of APF magnitude, with respect to all active parameters is also zero.

where

$$R = R_1 || R_2 || R_3 || R_L,\quad \alpha = \frac{R_a}{R_a+R_b}\ ,\ \beta = \frac{R_c}{R_c+R_d}\ ,\ \gamma = \frac{R_e}{R_e+R_f}\ ,$$

$$\delta = \frac{R_g}{R_g+R_h}\ ,\ B_\alpha = \omega_{11}+\alpha B_1,\ B_\beta = \omega_{12}+\beta B_2,\ B_\gamma = \omega_{13}+\gamma B_3$$

and

$$D = s^2+(B_\beta+B_\gamma)s+B_\beta B_\gamma+\delta(1-\gamma)B_2B_3.$$

The design equations for this circuit, obtained by comparing equations (5.16) and (5.17), are :

$$\left.\begin{aligned} &\alpha = \frac{a-\omega_{11}}{B_1}\ ,\ \beta = \frac{2ac-\omega_{12}P}{PB_2}\ ,\ \gamma = \frac{P(b-\omega_{13})-2ac}{PB_3}\ ,\ \frac{R}{R_1} = K \\ &\frac{R_1}{R_2} = \frac{2aM}{N(B_1+\omega_{11}-a)}\ ,\quad \frac{R_1}{R_3} = \frac{2bP}{NB_3} \end{aligned}\right\} \quad (5.18)$$

Higher order APFs, with complex poles and zeros can be obtained, by the parallel realisation technique, in a similar way.

5.2 Sensitivity analysis :

Magnitude and phase sensitivities, with respect to all passive and active parameters have been calculated for the second order APF circuit of Figure 5.2. These are given in Table 5.1. From the sensitivity figures it can be noted that the algebraic sum sensitivity with respect to all passive parameters is zero. The algebraic sum sensitivity of APF magnitude, with respect to all active parameters is also zero.

But the algebraic sum sensitivity of APF phase with respect to all active parameters is not zero.

Variations of magnitude and phase sensitivities, with frequency, have been calculated on the basis of parameters indicated in Section 5.5 for the second order APF with real poles and zeros (Figure 5.2). These are shown in Figures 5.6 and 5.7 respectively. The figures are drawn for various dependent variables, viz., x and these are indicated in the figures themselves. Comparison of Figures 5.6 and 4.13 and Figures 5.7 and 4.14 shows that for same pole locations, the sensitivities for the parallel realisation circuit are higher than those for the series realisation circuit. From Figure 5.6 it is seen that the sensitivities with respect to the summation resistors R_2 and R_3 are quite large at low

TABLE 5.1

Magnitude and phase sensitivities - second order APF (real poles and zeros)

Variable	S_x^G	S_x^φ
R_a	$\frac{2\alpha B_\alpha M[B_\beta^2-\omega^2)N+2B_\beta\omega^2]}{D}$	$\frac{2\omega M\alpha B_\alpha[B_\beta(B_\beta+2B_1+2\omega_{11})-\omega^2]}{D}$
R_b	$-S_{R_a}^G$	$-S_{R_a}^\varphi$

contd...

Variable	S_x^G	S_x^φ
R_c	$-\frac{2\beta B_\beta M(1-\beta)B_2(B_\alpha^2-\omega^2)}{D}$	$-\frac{2\omega M\beta(1-\beta)B_2B_\alpha B_\beta}{D}$
R_d	$-S^G_{R_c}$	$-S^\varphi_{R_c}$
R_1	$-1+\frac{R.}{R_1}+\frac{2M\omega^2(B_\alpha^2-B_\beta^2)}{D}$	$-\frac{2\omega M(B_\alpha B_\beta-\omega^2)(B_\alpha-B_\beta)}{D}$
R_2	$\frac{R}{R_2}+\frac{2MB_\alpha[B_\alpha B_\beta^2-(B_\alpha+2B_\beta)\omega^2]}{D}$	$\frac{2\omega MB_\alpha(B_\beta^2+2B_\alpha B_\beta-\omega^2)}{D}$
R_3	$\frac{R}{R_3}-\frac{2MB_\beta[B_\alpha^2B_\beta-(2B_\alpha+B_\beta)\omega^2]}{D}$	$-\frac{2\omega MB_\beta(B_\alpha^2+2B_\alpha B_\beta-\omega^2)}{D}$
R_L	$\frac{R}{R_L}$	0
ω_{11}	$\frac{2M\omega_{11}B_\alpha(B_\beta^2-\omega^2)}{D}$	$\frac{2\omega M\omega_{11}B_\alpha B_\beta}{D}$
ω_{12}	$-\frac{2M\omega_{12}B_\beta(B_\alpha^2-\omega^2)}{D}$	$-\frac{2\omega M\omega_{12}B_\alpha B_\beta}{D}$
B_1	$-\frac{2MB_\alpha[B_\beta^2\omega_{11}-\omega^2(\omega_{11}+2B_\beta)]}{D}$	$\frac{2\omega MB_\alpha(2B_\alpha B_\beta-B_\beta^2-2\omega_{11}B_\beta-\omega^2)}{D}$
B_2	$\frac{2MB_\beta[B_\alpha^2\omega_{12}-\omega^2(\omega_{12}+2B_\alpha)]}{D}$	$\frac{2\omega MB_\beta(B_\alpha^2+2B_\alpha\omega_{12}-\omega^2)}{D}$

Note : $D = (B_\alpha-B_\beta)[(B_\alpha B_\beta-\omega^2)^2 + (B_\alpha+B_\beta)^2\omega^2]$, $M = (B_\alpha+B_\beta)$

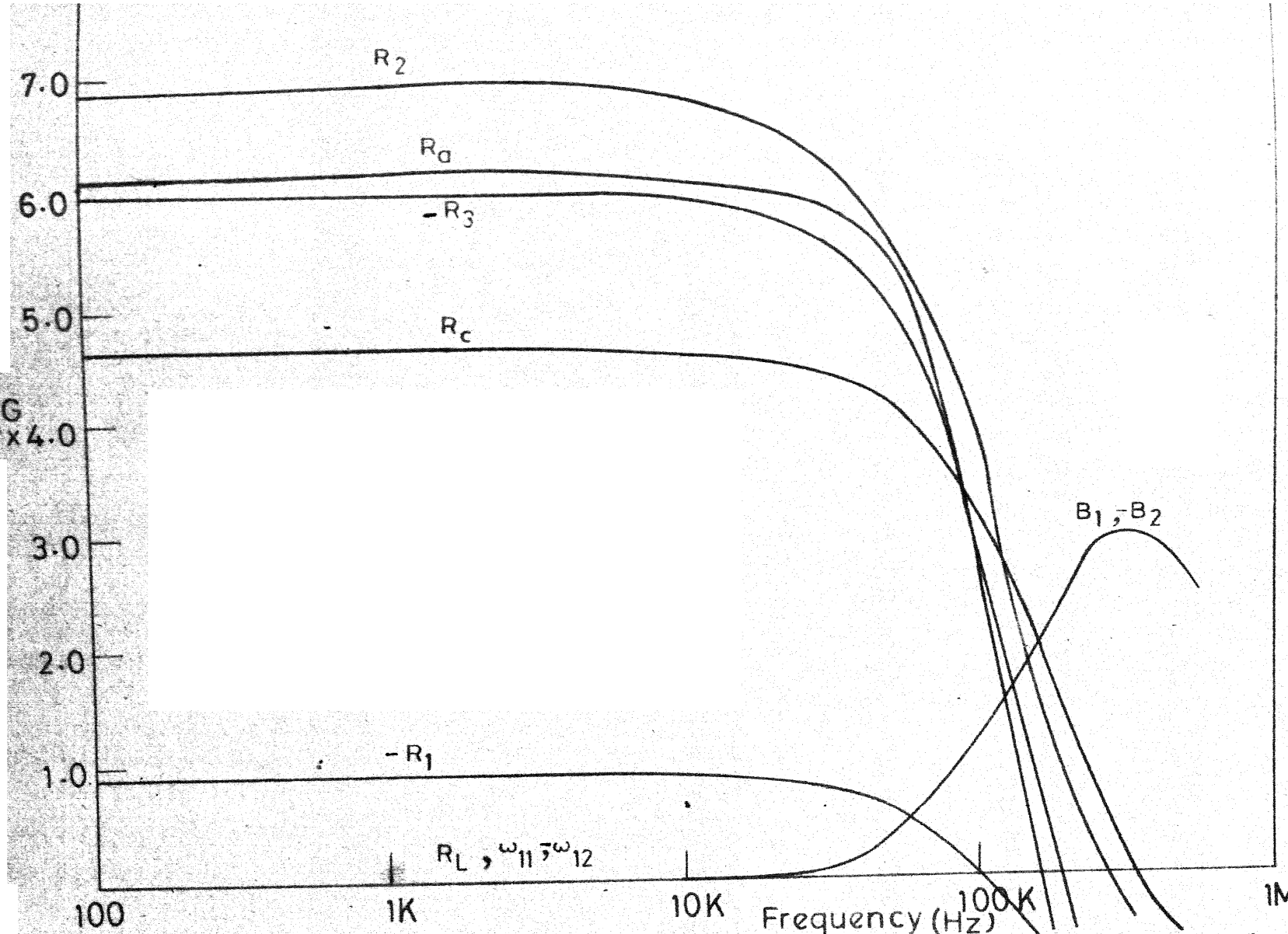

FIG. 5.6 SECOND ORDER APF PARALLEL REALISATION (real poles & zeros): VARIATION OF MAGNITUDE SENSITIVITIES WITH FREQUENCY

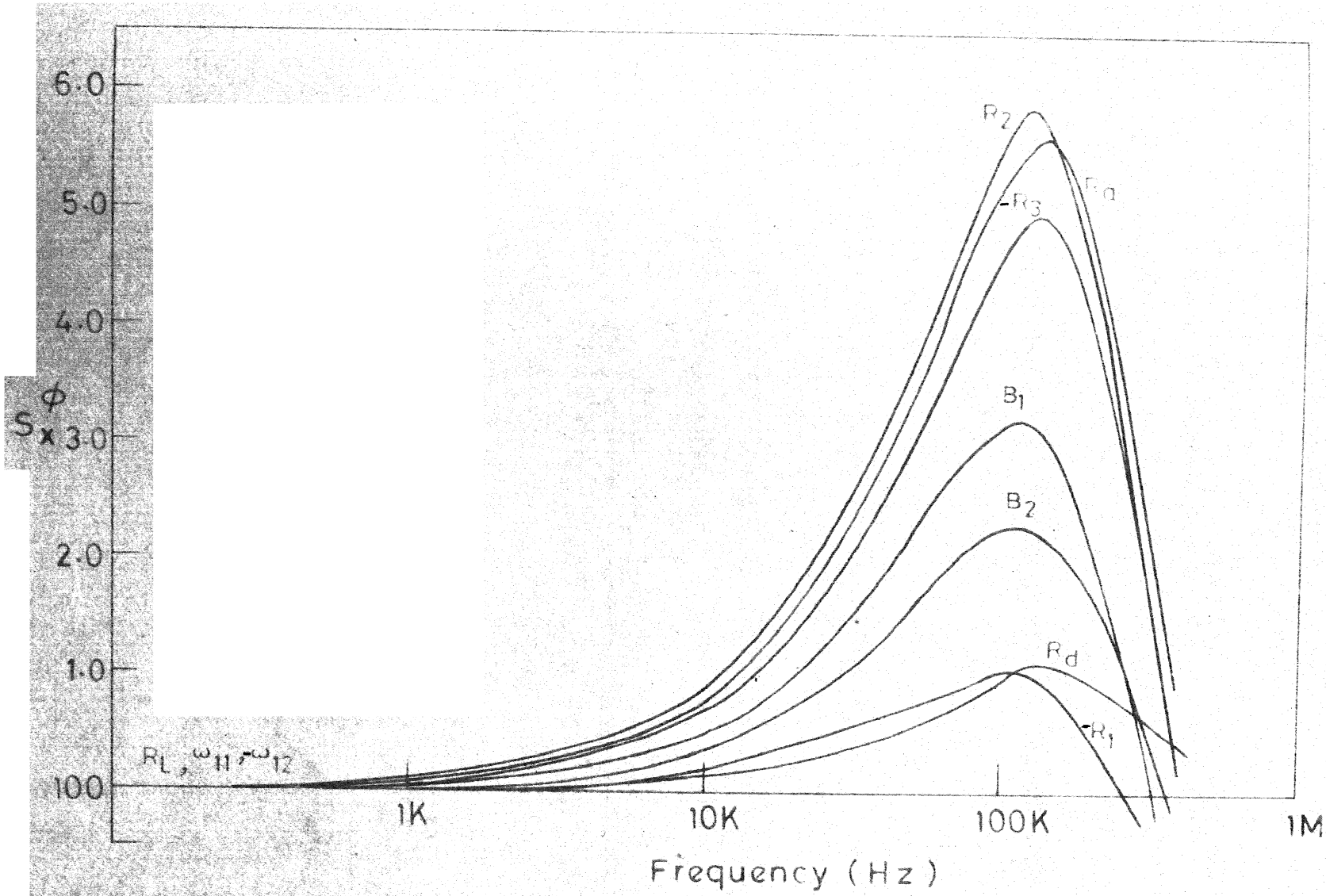

FIG. 5.7 SECOND ORDER APF (real poles and zeros): PARALLEL REALISATION - VARIATION OF PHASE SENSITIVITIES WITH FREQUENCY

frequencies. At high frequencies these values reduce rapidly. These high sensitivity values will not pose any problem if the ratios $\frac{R_1}{R_2}$, $\frac{R_1}{R_3}$, etc. are maintained constant. This is possible in monolithic IC technology where resistor ratios track.

5.3 Effect of OA second pole on APF performance :

The second order AP transfer function, with real poles and zeros, is

$$T(s) = \frac{R}{R_1}\left[\frac{(s-B_\alpha)(s-B_\beta)}{(s+B_\alpha)(s+B_\beta)}\right] \tag{5.19}$$

for the circuit of Figure 5.2. The transfer function, in terms of two pole model is,

$$T(s)_{2\ pole} = \frac{R}{R_1}\left[\frac{s^2+(\omega_{21}-\omega_{11})s-\omega_{21}B_\alpha}{s^2+(\omega_{21}+\omega_{11})s+\omega_{21}B_\alpha}\right]\left[\frac{s^2+(\omega_{22}-\omega_{12})s-\omega_{22}B_\beta}{s^2+(\omega_{22}+\omega_{12})s+\omega_{22}B_\beta}\right] \tag{5.20}$$

From equation (5.20) the APF magnitude is

$$G_{2\ pole} = \left|T(j\omega)\right|_{2\ pole} \simeq \frac{R}{R_1}\left[\frac{\omega^2+(B_\alpha+\frac{\omega^2}{\omega_{21}})^2}{\omega^2+(B_\alpha-\frac{\omega^2}{\omega_{21}})^2}\right]^{\frac{1}{2}}\left[\frac{\omega^2+(B_\beta+\frac{\omega^2}{\omega_{22}})^2}{\omega^2+(B_\beta-\frac{\omega^2}{\omega_{22}})^2}\right]^{\frac{1}{2}} \tag{5.21}$$

since $\omega_{1i} << \omega_{2i}$.

From equation (5.21) it can be seen that the APF magnitude becomes frequency dependent, due to the effect of OA second pole. The numerator increases at a faster rate with frequency as compared to the denominator. Hence, there is a net increase of magnitude with frequency. This effect is identical to that observed in APFs realised by the series realisation technique. The expression for phase, in terms of two pole model, is

$$\varphi_{2\ pole} \approx -\tan^{-1}\frac{\omega}{B_\alpha + \frac{\omega^2}{\omega_{21}}} - \tan^{-1}\frac{\omega}{B_\beta + \frac{\omega^2}{\omega_{21}}} - \tan^{-1}\frac{\omega}{B_\alpha - \frac{\omega^2}{\omega_{21}}} - \tan^{-1}\frac{\omega}{B_\beta - \frac{\omega^2}{\omega_{21}}} \qquad (5.22)$$

since $\omega_{1i} \ll \omega_{2i}$.

The phase, in terms of single pole model, is

$$\varphi_{1\ pole} = -2\tan^{-1}\frac{\omega}{B_\alpha} - 2\tan^{-1}\frac{\omega}{B_\beta} \qquad (5.23)$$

The first two terms in equation (5.22) contribute to decrease of phase with frequency, over the single pole model phase, given by equation (5.23). The last two terms contribute to an increase of phase with frequency. Consequently, there is near cancellation of the two effects and the phase is practically unaffected by the effect of OA second pole. At high frequencies

there is a slight increase of phase since the third and fourth terms in equation (5.22) predominate over the first two terms at these frequencies.

5.4 Comparison of series and parallel realisation techniques :

Series and parallel realisation techniques are general and hence both can realise active R and active RC APFs of any order. The active R APFs, with real poles and zeros obtained by the two techniques have same component count for corresponding order. In series realisation, basic circuit blocks are cascaded and then resistively summed to obtain higher order APFs. Hence, the signal handling capacity of higher order APFs, obtained by series realisation technique, is low due to slew rate limitations. In parallel realisation, there is no cascading and the same signal gets applied to the inputs of all the individual sections. Hence, the signal handling capacity is much larger for higher order circuits obtained by parallel realisation technique. The effect of OA second pole on APF magnitude and phase response is identical for both series and parallel realisation circuits. Comparison of sensitivity figures shows that for the same pole locations, the second order APF with real poles and zeros, obtained by parallel realisation technique has higher sensitivities compared to the corresponding circuit obtained by series realisation technique.

5.5 Experimental results :

The second order APF circuit of Figure 5.2 was built using two of the OAs (OA1 and OA2) in a LM 324 quad OA. The relevant parameters of the two OAs are given in Table 4.2 (Chapter IV). The resistance values in the circuit were : $R_a = R_b = R_d = 3.0\ K\Omega$, $R_c = 1.0\ K\Omega$, $R_1 = 1.5\ K\Omega$, $R_2 = 0.24\ K\Omega$, $R_3 = 0.97\ K\Omega$ and $R_L = 4.7\ K\Omega$. The magnitude and phase response of the APF are shown in Figure 5.8. From the plots the effect of OA second pole on magnitude response is seen. The magnitude response is flat within 0.5 dB upto 100 KHz. From Figure 5.8 it is seen that the phase response is practically unaffected by the OA second pole effects.

5.6 Conclusions :

In this chapter an alternate synthesis technique for realising APF of any order has been proposed. This technique, termed parallel realisation, can realise APFs with real poles and zeros and with complex poles and zeros. Circuits realised by this technique can handle larger signals without slew rate limitations as compared to circuits obtained by the series realisation technique. Experimental results for the second order APF, with real poles and zeros, have been obtained. These show the marked effect of OA second pole on magnitude response.

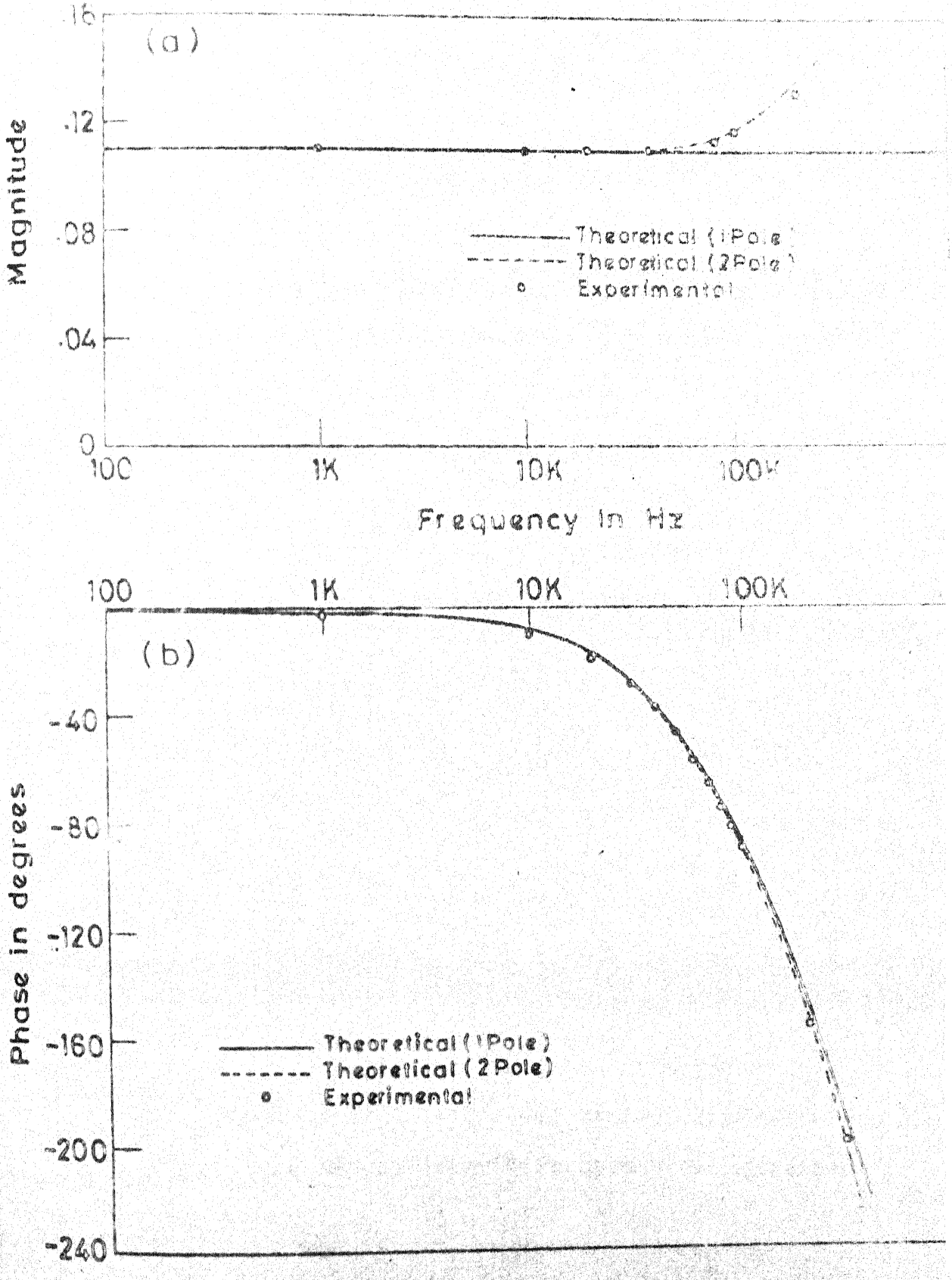

FIG. 5.8 SECOND ORDER APF WITH REAL POLES AND ZERO
(a) MAGNITUDE (b) PHASE RESPONSE.

6.1.1 Synthesis :

The first order HP transfer function, with unity high frequency gain is

$$T(s) = \frac{s}{s+a} \qquad (6.1)$$

This can be rewritten as

$$T(s) = 1 + \frac{-a}{s+a} \qquad (6.2)$$

Thus summation of the input and output of a first order, unity dc gain, inverting LPF a first order HP response can be obtained, Since ideal active R summers have not been realised in practice, only resistive summation is possible. Hence, realisations are possible only with an attenuation constant. The transfer function of equation (6.2) with an attenuation constant included, can be realised by the circuit of Figure 6.1. The transfer function of this circuit is

$$T(s) = \frac{V_o}{V_i} = \frac{R}{R_1}\left[1 + \frac{-(1-\alpha)\frac{R_1}{R_2}B_1}{s+B_\alpha}\right] \qquad (6.3)$$

where

$$R = R_1 || R_2 || R_L, \quad \alpha = \frac{R_a}{R_a+R_b}, \quad B_\alpha = \omega_{11}+\alpha B_1$$

It may be noted that the circuit configuration of Figure 6.1 is identical to that of first order APF given by Figure 4.4(a). However, the design equations, to realise HP response are

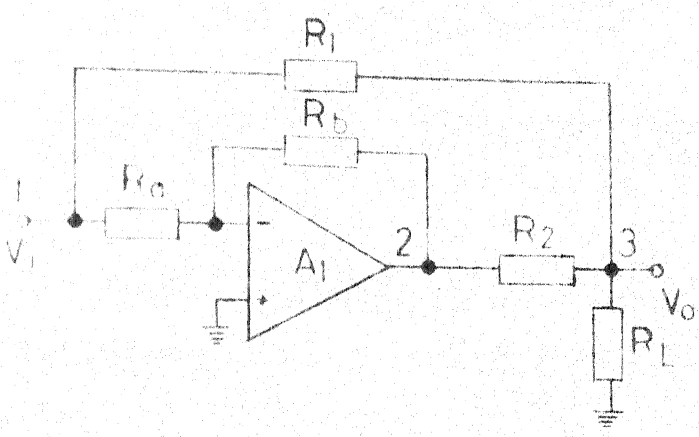

FIG. 6.1 FIRST ORDER HPF CIRCUIT

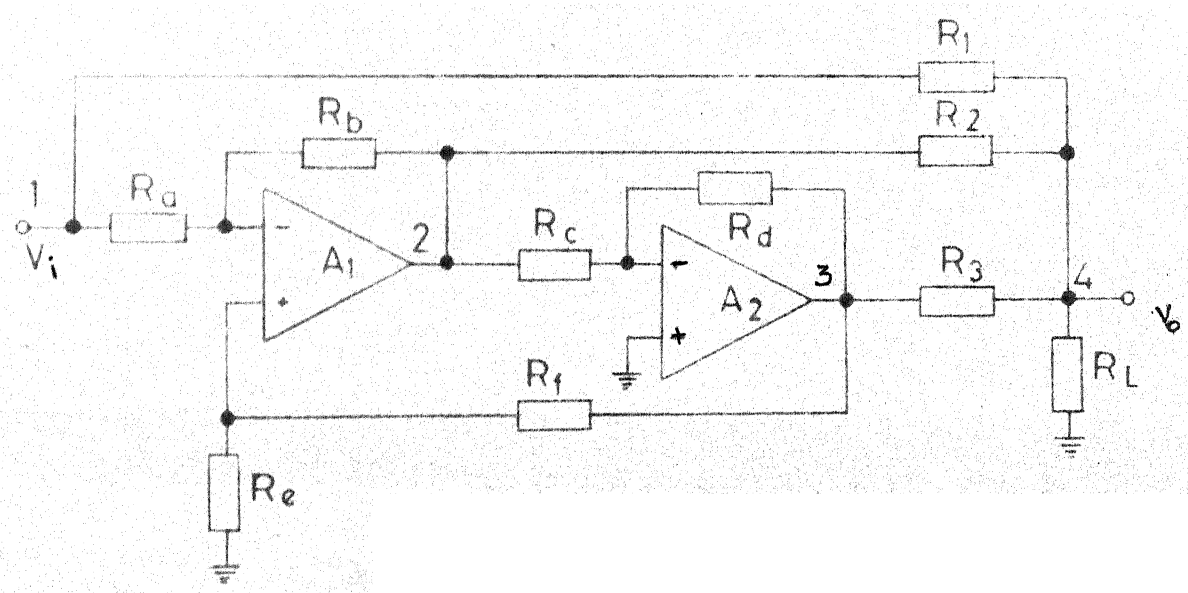

FIG. 6.2 SECOND ORDER HPF / NF CIRCUIT

different from those for the APF. Comparison of equation (6.2) (with attenuation constant K included) with equation (6.3) yields the following design equations.

$$\alpha = \frac{a-\omega_{11}}{B_1}\ ,\ \frac{R}{R_1} = K \quad \text{and} \quad \frac{R_1}{R_2} = \frac{a}{B_1+\omega_{11}-a} \tag{6.4}$$

The second order HP transfer function, with an attenuation constant K, is

$$T(s) = K\,\frac{s^2}{s^2+as+b} \tag{6.5}$$

This transfer function can be rewritten as

$$T(s) = K\left[1 + \frac{-(as+b)}{s^2+as+b}\right] \tag{6.6}$$

The second term in equation (6.6) represents a second order inverting pseudo BP function. This transfer function can be realised by the circuit of Figure 6.2. This circuit has the transfer function

$$T(s) = \frac{V_o}{V_i} = \frac{R}{R_1}\left[1 + \frac{-(1-\alpha)\,\frac{R_1}{R_2}\,B_1(s+B_\beta)}{D} + \frac{(1-\alpha)(1-\beta)\frac{R_1}{R_3}\,B_1B_2}{D}\right] \tag{6.7}$$

where

$$R = R_1 \,||\, R_2 \,||\, R_3 \,||\, R_L,\ \alpha = \frac{R_a}{R_a+R_b},\ \beta = \frac{R_c}{R_c+R_d},\ \gamma = \frac{R_e}{R_e+R_f}\ ,$$

$$B_\alpha = \omega_{11}+\alpha B_1, \qquad B_\beta = \omega_{12}+\beta B_2$$

$$D = s^2+(B_\alpha+B_\beta)s + B_\alpha B_\beta + \gamma(1-\beta)B_1B_2$$

Comparison of equations (6.6) and (6.7), with α assumed, yields the following design equations

$$\left.\begin{aligned} \beta &= \frac{a-B_\alpha-\omega_{12}}{B_2}\ ,\ \gamma = \frac{b-B_\alpha(a-B_\alpha)}{(B_2+B_\alpha+\omega_{12}-a)B_1},\ \frac{R}{R_1} = K \\ \frac{R_1}{R_2} &= \frac{a}{(1-\alpha)B_1}\ ,\ \frac{R_1}{R_3} = \frac{a(a-B_\alpha)-b}{(1-\alpha)B_1(B_2+\omega_{12}+B_\alpha-a)} \end{aligned}\right\} \quad (6.8)$$

For β,γ and $\frac{R_1}{R_3}$ to be positive the requirements are

$$B_\alpha < a-\omega_{12},\ B_\alpha > \frac{a\pm\sqrt{a^2-4b}}{2} \quad \text{and} \quad B_\alpha < \frac{a^2-b}{a}$$

For $\frac{b}{a} > \omega_{12}$ the requirements become

$$\frac{a\pm\sqrt{a^2-4b}}{2} < B_\alpha < \frac{a^2-b}{a} \quad (6.9)$$

In equation (6.7) the second term itself represents a second order inverting pseudo BP function. Hence, in the circuit of Figure 6.2 if R_3 is made infinity, a high pass response is still obtained. For this case ($R_3 = \infty$) the design equations are

$$\left.\begin{aligned} \alpha &= \frac{a^2-b-a\omega_{11}}{aB_1}\ ,\ \beta = \frac{b-a\omega_{12}}{aB_2}\ ,\ \frac{R}{R_1} = K \\ \gamma &= \frac{b^2}{aB_1[a(B_2+\omega_{12})-b]},\ \frac{R_1}{R_2} = \frac{a^2}{a(B_1+\omega_{11}-a)+b} \end{aligned}\right\} \quad (6.10)$$

In equation (6.10), for α and $\frac{R_1}{R_2}$ to be positive the requirements are

$$\frac{\omega_{11}+(\omega_{11}^2+4b)^{\frac{1}{2}}}{2} < a < \frac{B_1+\omega_{11}+[(B_1+\omega_{11})^2+4b]^{\frac{1}{2}}}{2} \qquad (6.11)$$

For $B_1 >> \omega_{11}$ and $4b >> \omega_{11}^2$ this simplifies to

$$b^{\frac{1}{2}} < a < \frac{B_1+(B_1^2+4b)^{\frac{1}{2}}}{2} \qquad (6.12)$$

Thus, for the case of $R_3 = \infty$, HP realisation is possible with nine resistors instead of ten. Further, α value does not have to be assumed. The realisation is possible for HPFs with real poles and zeros and with complex poles and zeros.

6.1.2 Sensitivity analysis :

Transfer function and denominator polynomial sensitivities S_x^T and S_x^D with respect to all active and passive parameters, for the first order HPF, under high pass condition, have been determined. These are given in Table 6.1. For obtaining transfer function sensitivities, differentiation was carried out on equation (6.3) and then the high pass condition, viz., $(1-\alpha)\frac{R_1}{R_2} B_1 = B_\alpha$ is applied. The sensitivities are very low at high frequencies.

6.1.3 Effect of OA second pole on HPF performance :

The effect of OA second pole on HPF performance can be studied by analysing the circuit of Figure 6.1 (under high pass condition) using the pole-zero model. The transfer

TABLE 6.1

First order HPF sensitivities

Variable	S_x^T	S_x^D
R_a	$\frac{\alpha B_\alpha (s+B_1+\omega_{11})}{sD}$	$\frac{\alpha(1-\alpha)B_1}{D}$
R_b	$-S_{R_a}^T$	$-S_{R_a}^D$
R_1	$-1+\frac{R}{R_1}-\frac{B_\alpha}{s}$	0
R_2	$\frac{R}{R_2}+\frac{B_\alpha}{s}$	0
R_L	$\frac{R}{R_L}$	0
ω_{11}	$\frac{B_\alpha \omega_{11}}{sD}$	$\frac{\omega_{11}}{D}$
B_1	$-\frac{B_\alpha(s+\omega_{11})}{sD}$	$\frac{\alpha B_1}{D}$

Note : $D = s+\omega_{11}+\alpha B_1$

function, based on single pole model under high pass condition is

$$T(s) = \frac{R}{R_1} \frac{s}{(s+B_\alpha)} \tag{6.13}$$

Using the pole-zero model for the OA, i.e.

$$A_i = \frac{-B_i(s-\omega_{2i})}{\omega_{2i}(s+\omega_{1i})} \tag{6.14}$$

equation (6.13) becomes

$$T(s)\Big|_{\text{pole-zero}} = \frac{R}{R_1} \frac{\omega_{21}s/(\omega_{21}-\alpha B_1)}{s+\frac{\omega_{21}B_\alpha}{\omega_{21}-\alpha B_1}} \tag{6.15}$$

Comparison of equations (6.13) and (6.15) shows that, due to the effect of OA second pole, the high frequency pass band gain and the 3 dB cut-off frequency are both increased by the factor $\omega_{21}/(\omega_{21}-\alpha B_1)$. The effect of OA second pole can be overcome by obtaining the design equations based on pole-zero model, instead of single pole model.

6.2 Notch filter :

Notch or band reject transfer functions have a pair of conjugate zeros on $j\omega$ axis and real and/or complex conjugate poles on LHP. Soderstrand[2] has proposed a three OA circuit (with one OA being treated as ideal)to realise a second order notch response. Srinivasan [1] has reported a second order

medium Q notch filter using three OAs. In the second order circuits of Soliman [3], Soliman and Fawzy [4] and Kim and Ra [6] notch response is available at the input of an OA. Mitra and Aatre [7] have obtained notch response, by resistive summation, in an inverting BPF circuit.

6.2.1 Synthesis :

Second order notch filter transfer function with an attenuation constant included, is

$$T(s) = K \frac{s^2+c}{s^2+as+b} \qquad (6.16)$$

where c = notch frequency.

From equation (6.16) three classes of notch response arise. These are :

i) $c = b$ symmetrical notch

ii) $c > b$ low pass notch

and

iii) $c < b$ high pass notch.

The transfer function can be written as

$$T(s) = K \left(1 + \frac{-as}{s^2+as+b}\right) \qquad (6.17)$$

for c = b.

The second term in equation (6.17) is a second order inverting BP function, with unity resonant gain. Thus, summation of the

input and output of a second order inverting BPF as above, leads to a second order symmetrical notch response. For the case of low pass and high pass notch response equation (6.16) can be written as

$$T(s) = K[1 + \frac{-as}{s^2+as+b} + \frac{c-b}{s^2+as+b}] \qquad (6.18)$$

The second term is a inverting second order BP function. The third term represents a second order LP transfer function, which is non-inverting for low pass notch ($c > b$) and inverting for high pass notch ($c < b$). Thus second order active R circuits realising inverting BP and inverting LP responses at the outputs of the two OAs respectively can realise a high pass notch function. Similarly, circuits realising inverting BP and non-inverting LP at the outputs of the two OAs can realise a low pass notch function.

The inverting BPF circuit, proposed in Chapter III (Figure 3.3) can realise a symmetric notch response by resistive summation of its BP output and its input. This circuit is shown in Figure 6.3. The transfer function for this circuit, based on single pole model, is

$$T(s) = \frac{V_o}{V_i} \simeq \frac{R}{R_1}\left[1 + \frac{-(1-\gamma)\frac{R_1}{R_2}B_1 s}{D}\right] \qquad (6.19)$$

$$\text{for } \omega >> \omega_{12}$$

where

$$D = s^2+[\omega_{11}+\omega_{12}+(\gamma-\beta)B_1]s+\omega_{11}\omega_{12}+(\gamma-\beta)B_1\omega_{12}+\alpha(1-\beta)B_1B_2$$

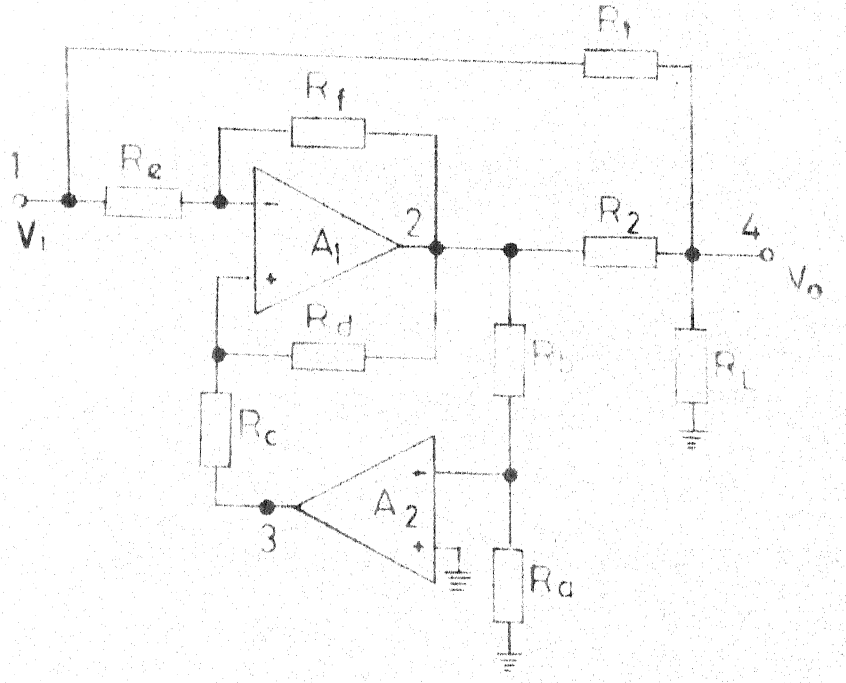

FIG. 6.3 SYMMETRIC NOTCH FILTER CIRCUIT

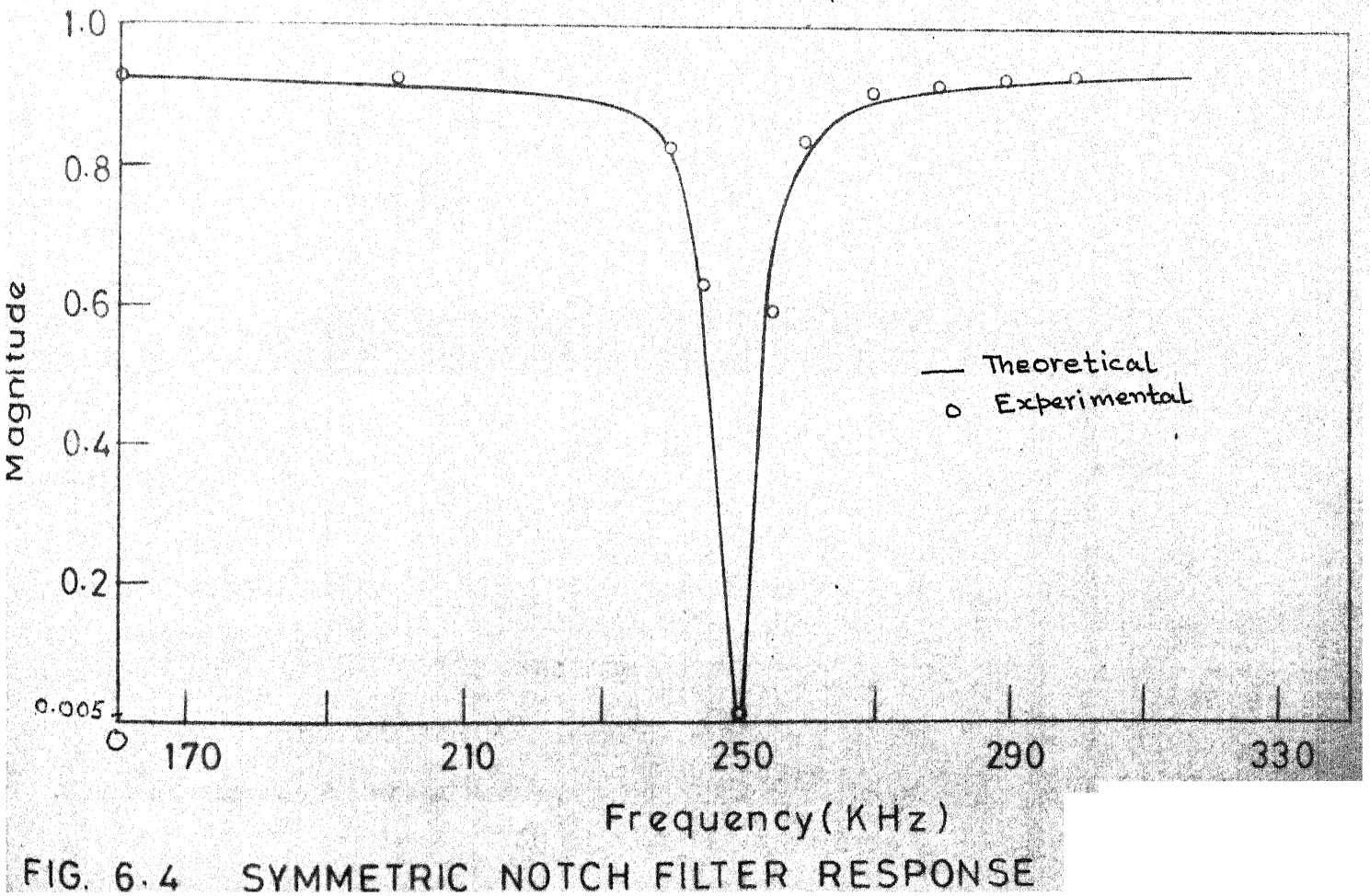

FIG. 6.4 SYMMETRIC NOTCH FILTER RESPONSE

$$\alpha = \frac{R_a}{R_a+R_b}\ ,\quad \beta = \frac{R_c}{R_c+R_d}\ ,\quad \gamma = \frac{R_e}{R_e+R_f} \quad \text{and} \quad R = R_1 \,||\, R_2 \,||\, R_L$$

Comparing equations (6.18) (with c = b) and (6.19) the design equations, with γ assumed, are

$$\left.\begin{aligned} &\frac{R}{R_1} = K,\ \alpha = \frac{b+\omega_{12}^2 - a\omega_{12}}{B_2[B_1+a-\omega_{11}-\omega_{12}-\gamma B_1]}\ ,\ \beta = \frac{\omega_{11}+\omega_{12}+\gamma B_1 - a}{B_1}\ , \\ &\frac{R_1}{R_2} = \frac{a}{(1-\gamma)B_1} \end{aligned}\right\} \quad (6.20)$$

The transfer function, with notch condition imposed, is

$$\frac{V_o}{V_i} = \frac{R}{R_1}\ \frac{s^2+\omega_o^2}{s^2+(\frac{\omega_o}{Q})s+\omega_o^2} \qquad (6.21)$$

where

$$\omega_o = [\omega_{11}\omega_{12}+(\gamma-\beta)B_1\omega_{12}+\alpha(1-\beta)B_1B_2]^{\frac{1}{2}}$$

and

$$\frac{\omega_o}{Q} = \omega_{11}+\omega_{12}+(\gamma-\beta)B_1$$

$\frac{\omega_o}{2\pi}$ is the notch frequency while Q is the pole selectivity.

For the case of symmetric notch filter (c=b) equation (6.18) can be rewritten as

$$T(s) = K[1 + \frac{-(as+K_1)}{s^2+as+b} + \frac{K_1}{s^2+as+b}\ ] \qquad (6.22)$$

This transfer function can be realised by the circuit of Figure 6.2, whose transfer function is given by equation (6.7).

Comparison of equations (6.7) and (6.22) leads to the following design equations (with α assumed) :

$$\left.\begin{aligned} \beta &= \frac{a - B_\alpha - \omega_{12}}{B_2}, \quad \gamma = \frac{c - B_\alpha(a - B_\alpha)}{B_1(B_2 + B_\alpha + \omega_{12} - a)}, \quad \frac{R}{R_1} = K \\ \frac{R_1}{R_2} &= \frac{a}{(1-\alpha)B_1}, \quad \frac{R_1}{R_3} = \frac{(a - B_\alpha)a}{(1-\alpha)B_1(B_2 + B_\alpha + \omega_{12} - a)} \end{aligned}\right\} \quad (6.23)$$

Thus, while the circuit of Figure 6.2 realises a symmetric notch response with two OAs and ten resistors, the circuit of Figure 6.3 gives symmetrical notch response with two OAs and only nine resistors.

6.2.2 Sensitivity analysis :

Notch frequency (ω_o) and pole selectivity (Q) sensitivities with respect to all passive and active parameters have been determined for the circuit of Figure 6.3. These are given in Table 6.2. All the sensitivities are less than unity.

6.2.3 Effect of OA second pole on NF performance :

To study the effect of OA second pole on NF performance, the circuit of Figure 6.3 can be analysed in terms of the pole-zero model. The resulting transfer function is

$$T(s)\Big|_{\text{pole-zero}} = \frac{R}{R_1}\left[1 + \frac{-(1-\gamma)\frac{R_1}{R_2} B_1 \omega_{21} \omega_{22} s}{D}\right] \quad (6.24)$$

for $\omega >> \omega_{12}$ and $\omega << \omega_{21}$ and ω_{22}.

TABLE 6.2

Notch filter sensitivities

Parameter	$S_x^{\omega_o}$	S_x^{Q}
R_a	$\frac{\alpha(1-\alpha)(1-\beta)B_1B_2}{2\omega_o^2}$	$\frac{\alpha(1-\alpha)(1-\beta)B_1B_2}{\omega_o^2}$
R_b	$-S_{R_a}^{\omega_o}$	$-S_{R_a}^{Q}$
R_c	$-\frac{(1-\beta)B_1(\omega_{12}+\alpha B_2)}{2\omega_o^2}$	$\frac{\beta(1-\beta)B_1[2\omega_o^2-\omega_a(\omega_{12}+\alpha B_2)]}{2\omega_o^2\omega_a}$
R_d	$-S_{R_c}^{\omega_o}$	$-S_{R_c}^{Q}$
R_e	$\frac{\gamma(1-\gamma)B_1\omega_{12}}{2\omega_o^2}$	$\frac{\gamma(1-\gamma)B_1[\omega_{12}\omega_a-2\omega_o^2]}{2\omega_o^2\omega_a}$
R_f	$-S_{R_e}^{\omega_o}$	$-S_{R_e}^{Q}$
ω_{11}	$\frac{\omega_{11}\omega_{12}}{2\omega_o^2}$	$\frac{\omega_{11}(\omega_{12}\omega_a-2\omega_o^2)}{2\omega_o^2\omega_a}$
ω_{12}	$\frac{\omega_{12}(\omega_a-\omega_{12})}{2\omega_o^2}$	$\frac{\omega_{12}[\omega_a(\omega_a-\omega_{12})-2\omega_o^2]}{2\omega_o^2\omega_a}$

contd...

Parameter	$S_x^{\omega_o}$	S_x^Q
B_1	$\frac{2\omega_o^2-\omega_{11}\omega_{12}}{2\omega_o^2}$	$\frac{\omega_a(\omega_o^2-\omega_{11}\omega_{12})-2\omega_o^2(\gamma-\beta)B_1}{2\omega_o^2\omega_a}$
B_2	$\frac{\alpha(1-\beta)B_1B_2}{2\omega_o^2}$	$\frac{\alpha(1-\beta)B_1B_2}{2\omega_o^2}$

Note : ω_o is as defined under equation (6.21).

$\omega_a = \omega_{11}+\omega_{12}+(\gamma-\beta)B_1$

where

$$D = [\omega_{21}\omega_{22}-(\gamma-\beta)B_1\omega_{22}+\alpha(1-\beta)B_1B_2]s^2$$

$$+ [\omega_{21}\omega_{22}\{\omega_{11}+\omega_{12}+(\gamma-\beta)B_1\}-(\gamma-\beta)B_1\omega_{12}\omega_{22}$$

$$- \alpha(1-\beta)B_1B_2(\omega_{21}+\omega_{22})]s+\omega_{21}\omega_{22}[\omega_{11}\omega_{12}+(\gamma-\beta)B_1\omega_{12}$$

$$+ \alpha(1-\beta)B_1B_2]$$

If the notch conditions of equation (6.20) are imposed in equation (6.24) then a transfer function of the form

$$T(s) = \frac{R}{R_1}\left[\frac{a_1s^2+a_2s+a_3}{a_1s^2+a_4s+a_3}\right] \qquad (6.25)$$

results. Thus, the transfer function becomes a biquadratic function and thus is no more a notch function. Further, for certain values of α,β and γ the 's' coefficient of the denominator in equation (6.24) could become zero, making the circuit oscillatory.

To overcome the effect of OA second pole, design equations can be obtained by comparing equations (6.18) (with c = b) and (6.24). Then, under the new conditions the circuit will provide a true symmetric notch response. The design equations obtained by this comparison are :

$$(1-\gamma)\frac{R_1}{R_2}B_1 = \frac{a\omega_{21}^2\omega_{22}+b(\omega_{21}^2-\omega_{22}^2+\omega_{22}\omega_{11}+\omega_{22}\omega_{12})}{\omega_{22}(b + a\omega_{21} + \omega_{21}^2)} \qquad (6.26)$$

$$(\gamma-\beta)B_1 = \frac{\omega_{21}[b(\omega_{21}+\omega_{22})+\omega_{21}\omega_{22}(a-\omega_{11}-\omega_{12})]}{\omega_{22}(b + a\omega_{21} + \omega_{21}^2)} \qquad (6.27)$$

$$\alpha(1-\beta)B_1B_2 = \frac{b\omega_{21}\omega_{22}}{b+a\omega_{21}+\omega_{21}^2} \qquad (6.28)$$

with γ assumed, $\frac{R_1}{R_2}$ and β can be obtained from equations (6.26) and (6.27) respectively. Then α can be obtained from equation (6.28).

6.2.4 Experimental results :

The symmetric notch filter circuit of Figure 6.3 was designed using the pole-zero model design equations. Two

NE 536 OAs, whose parameters are given in Table 3.2 (Chapter III 0.5 percent metal film resistors and miniature multiturn potentiometers were used to build the circuit. The resistor values for the circuit, in kilo ohms, were : $R_a = 1.0$, $R_b = 17$, $R_c = 5.0$, $R_d = 1.0$, $R_e = 10$, $R_f = 1.8$, $R_1 = 0.5$, $R_2 = 20$ and $R_L = 10$. The notch response for a notch frequency of 250 KHz and pole selectivity of 25 is shown in Figure 6.4. Comparison of theoretical and experimental results is given in Table 6.3.

TABLE 6.3

Symmetric notch filter response

Parameter	Theoretical	Experimental
$\omega_o/2\pi$ (KHz)	250	250
Q	25.0	24.5
Attenuation at ω_o	∞	46 dB

6.3 Conclusions :

In this chapter synthesis techniques for first and second order high pass filters and second order notch filters have been proposed. All the circuits are realised with an attenuation constant. The effects of OA second pole on HPF and NF

performances have been studied. For first order HPF, the high frequency gain and the 3 dB cut-off frequency are increased by the same amount due to OA second pole. For notch filter, the transfer function becomes a general biquadratic function. For high values of notch frequency the circuit may even become oscillatory. The effects of OA second pole can be overcome by designing the circuit on the basis of pole-zero model, instead of single pole model.

References

1. Srinivasan, S., 'Synthesis of transfer functions using operational amplifier pole', Int.J.Electron., Vol. 40, no.1, pp 5-13, January, 1976.

2. Soderstrand, M.A., 'Design of active R filters using only resistors and operational amplifiers', Int.J. Electron., Vol. 40, no.5, pp 417-432, May, 1976.

3. Soliman, A.M., 'A universal active R filter, Eln. Engg., Vol. 49, no.594, pp 49-50, July, 1977.

4. Soliman, A.M. and Fawzy, M., 'A universal active R biquad', Int. J. Ckt. Th. and Appn., Vol.6, no.4, pp 153-157, April, 1978.

5. Soliman, A.M. and Fawzy, M., 'A new active R band pass filter', J. Franklin Inst., Vol. 306, no.2, pp 159-163, August, 1978.

6. Kim, H.K. and Ra, J.B., 'An active biquadratic building block without external capacitors', IEEE Trans. Ckts. and Sys., Vol. CAS-24, no.12, pp 689-694, December, 1977.

7. Mitra, A.K. and Aatre, V.K., 'Low sensitivity high frequency active R filters', IEEE Trans. Ckts. and Sys., Vol. CAS-23, no.11, pp 670-676, November, 1976.

CHAPTER VII

SYNTHESIS OF OSCILLATORS

Sinusoidal oscillators with large tuning range and low harmonic distortion are desirable for a number of applications. Particularly desirable are those circuits in which the frequency of oscillations can be varied without upsetting the condition for oscillations. An additional useful feature is the facility for voltage control of the frequency of oscillations. Such voltage controlled oscillators are especially suited for phase locked loops. Bhattacharyya and Natarajan [1] have proposed a three OA, six resistor active R oscillator circuit . In this circuit expressions for oscillation condition and the frequency of oscillations have been obtained on the basis of integrator model for the OAs. Ahmed and Siddiqui [2] have obtained a two OA, four resistor circuit. Nandi [3] has proposed a modified version of this circuit. Pyara and Jamuar [4] have synthesised a two OA, eight resistor oscillator circuit. Two oscillator circuits, each with two OAs and six resistors have been proposed by Drake and Michell [5].

In this chapter a synthesis technique for active R oscillators is presented. An oscillator circuit with independent control of frequency has been synthesised. Replacement of the frequency controlling grounded resistor, in this circuit,

by a junction field effect transistor (JFET) leads to a voltage controlled oscillator, Modifications of the synthesis technique to realise other reported two OA active R oscillators, are indicated.

7.1 Synthesis :

The transfer function of a circuit, which can realise oscillatory response can be written as

$$T(s) = \frac{d(s+e)}{s^2+(a-b)s+c} \quad , \quad c > 0 \qquad (7.1)$$

For oscillations to take place, a pair of conjugate poles must exist on the $j\omega$ axis. This condition is obtained when the 's' coefficient of the denominator in equation (7.1) becomes zero. Under this condition (a=b), the circuit becomes an oscillator if the input node is grounded. The requirement for independent control of frequency is that the expression for the frequency of oscillations [$\omega_o = \sqrt{c}$ in equation (7.1)] should have at least one parameter which is not present in the condition for oscillations (a=b). Equation (7.1) can be rewritten as

$$T(s) = \frac{d/(s+f)}{1 + \frac{d}{s+f}\left[\frac{c-e(a-b-e)}{d(s+e)} - \frac{b+e+f-a}{d}\right]} \qquad (7.2)$$

where f = arbitrary parameter.

This transfer function is of the form

$$T(s) = \frac{G}{1+G[\beta_1(s)-\beta_2]} \tag{7.3}$$

where

G represents an amplifier of gain $= \frac{d}{s+f}$

$\beta_1(s)$ represents frequency dependent feedback factor

$$= \frac{c-e\ (a-b-e)}{d(s+e)}$$

and

β_2 represents frequency independent feedback factor

$$= \frac{b+e+f-a}{d}$$

The amplifier G can be realised by an operational amplifier, whose gain is $B_1/(s+\omega_{11})$. $\beta_1(s)$ represents a first order non-inverting LP function, under oscillation condition (a=b). It can be realised by an OA with negative feedback and with an attenuator at the non-inverting input terminal. The realised circuit is shown in Figure 7.1. The transfer function of this circuit is

$$T(s) = \frac{V_o}{V_i} = \frac{(1-\gamma)\ \frac{B_1}{s+\omega_{11}}}{1 + \frac{B_1}{s+\omega_{11}}\left[\frac{\alpha B_2}{s+B_\beta} - \gamma\right]}$$

$$= \frac{(1-\gamma)B_1(s+B_\beta)}{s^2+(\omega_{11}+B_\beta-\gamma B_1)s+\omega_{11}B_\beta-\gamma B_1\omega_{12}+(\alpha-\beta\gamma)B_1B_2} \tag{7.4}$$

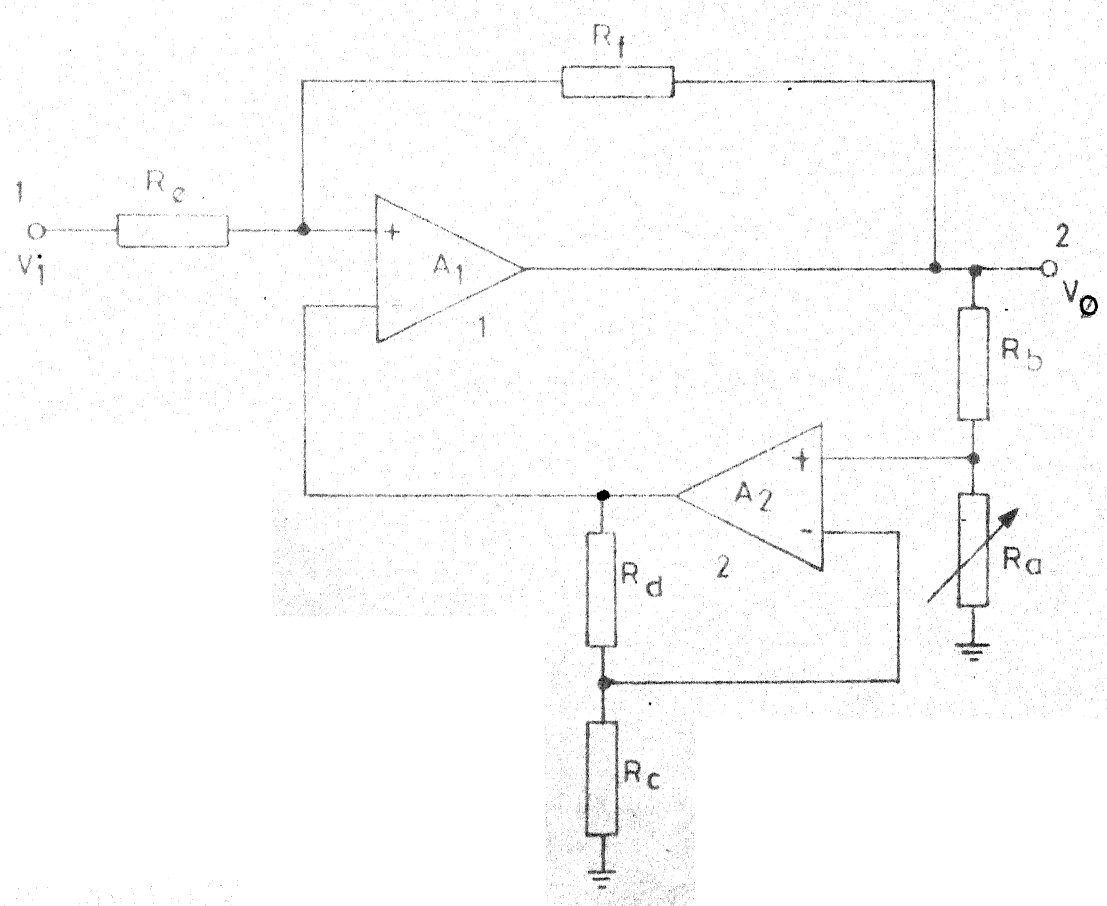

FIG. 7.1 RESISTANCE CONTROLLED OSCILLATOR CIRCUIT

From equations (7.8) and (7.9) it is seen that the condition for oscillations is determined by β,γ and the OA parameters while the frequency of oscillations is determined by α,β,γ and the OA parameters. Hence β or γ can establish the condition for oscillations and α can provide an independent control for frequency without upsetting the condition for oscillations. Specifically, grounded resistor R_a controls frequency while grounded resistors R_c or R_e maintain oscillations. Both condition for oscillations and frequency of oscillations are determined by resistor ratios only and not by individual resistor values.

7.2 Alternate oscillator realisations :

The reported active R oscillator circuits of Ahmed and Siddiqui [2], Nandi [3] and Drake and Michell [5] can be obtained by rewriting equation (7.2) in alternate ways.

One way of rewriting equation (7.2) is

$$T(s) = \frac{d/(s+f)}{1 + \frac{d}{s+f}\left[\frac{K_1}{s+e} - K_2\right]}$$

$$= \frac{d/(s+f)}{1 + \frac{d}{s+f}\left[\frac{K_4(s+e+(K_1/K_4))}{s+e} - K_3\right]} \qquad (7.10)$$

where $K_1 = \frac{c-e(a-b-e)}{d}$, $K_2 = \frac{b+e+f-a}{d}$ and $K_3-K_4 = K_2$.

The corresponding circuit realisation by Ahmed and Siddiqui [2] is shown in Figure 7.2. The transfer function of this circuit is

$$T(s) = \frac{V_o}{V_i} = \frac{(1-\alpha)B_1/(s+\omega_{11})}{1 + \frac{B_1}{s+\omega_{11}}\left[\frac{\beta(s+B_2+\omega_{12})}{s+B_\beta} - \alpha\right]}$$

$$= \frac{(1-\alpha)B_1(s+B_\beta)}{s^2+[\omega_{11}+B_\beta+(\beta-\alpha)B_1]s+\omega_{11}B_\beta+(\beta-\alpha)B_1\omega_{12} + \beta(1-\alpha)B_1B_2} \qquad (7.11)$$

where $\alpha = \frac{R_a}{R_a+R_b}$, $\beta = \frac{R_c}{R_c+R_d}$, $B_\beta = \omega_{12}+\beta B_2$

The condition for oscillation is

$$\alpha \geq \frac{\omega_{11}+B_\beta+\beta B_1}{B_1} \qquad (7.12)$$

and the frequency of oscillations is

$$f_o = \frac{1}{2\pi}\left[\omega_{11}B_\beta+(\beta-\alpha)B_1\omega_{12}+\beta(1-\alpha)B_1B_2\right]^{\frac{1}{2}} \qquad (7.13)$$

From equations (7.12) and (7.13) it is seen that both the condition for oscillations and the frequency of oscillations are functions of α, β and OA parameters. Hence, independent control of frequency is not possible. Nandi [3] has obtained a modified version of this circuit. Nandi's circuit, shown in Figure 7.3 has the transfer function

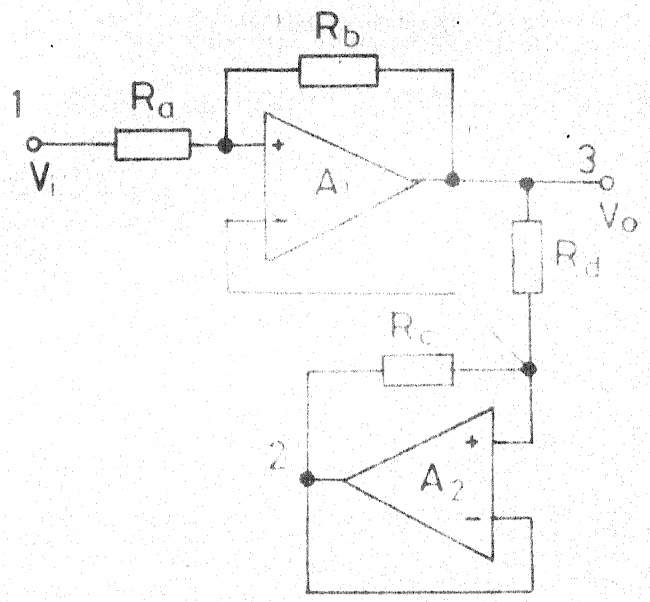

FIG. 7.2 OSCILLATOR CIRCUIT OF AHMED AND SIDDIQUI

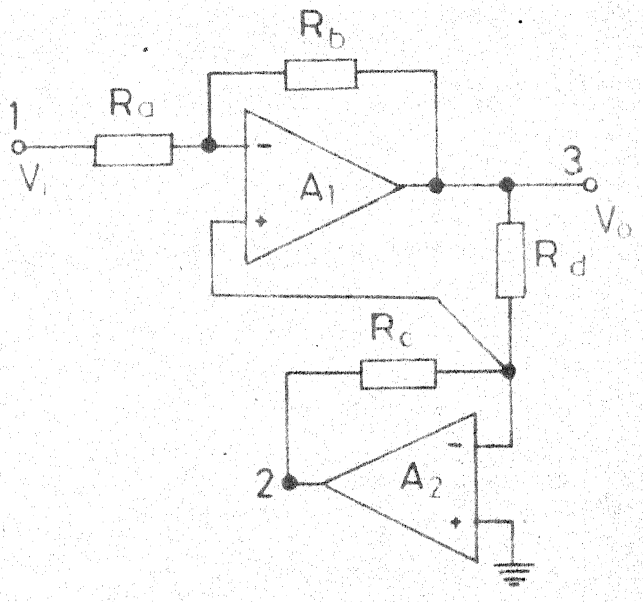

FIG. 7.3 OSCILLATOR CIRCUIT OF NANDI

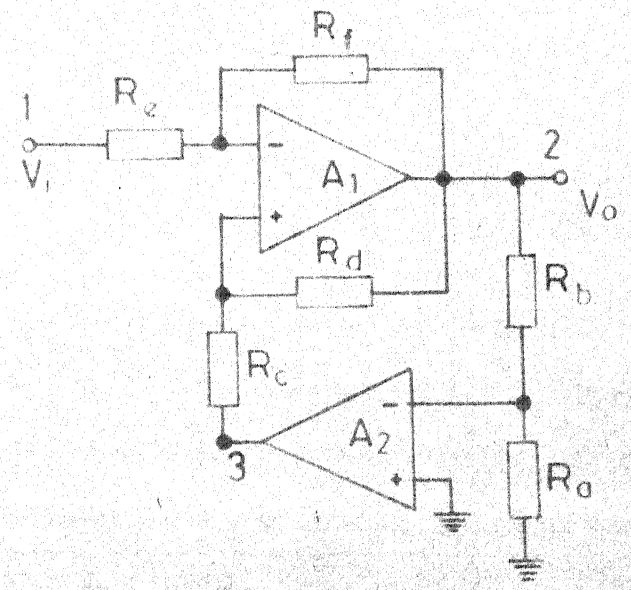

FIG. 7.4 OSCILLATOR CIRCUIT OF DRAKE AND MICHELL

$$T(s) = \frac{V_o}{V_i} = (1-\alpha)\,\frac{\dfrac{-B_1/(s+\omega_{11})}{}}{1 + \dfrac{-B_1}{s+\omega_{11}}\left[\dfrac{\beta(s+\omega_{12})}{s+\omega_{12}+(1-\beta)B_2} - \alpha\right]}$$

$$= \frac{-(1-\alpha)B_1[s+\omega_{12}+(1-\beta)B_2]}{D} \qquad (7.14)$$

where $\alpha = \dfrac{R_a}{R_a+R_b}$, $\beta = \dfrac{R_c}{R_c+R_d}$

and

$$D = s^2+[\omega_{11}+\omega_{12}+(1-\beta)B_2+(\alpha-\beta)B_1]s+\omega_{11}\omega_{12}+(1-\beta)B_2\omega_{11}$$

$$+ (\alpha-\beta)B_1\omega_{12}+\alpha(1-\beta)B_1B_2$$

The condition for oscillations is

$$\beta \geq \frac{\omega_{11}+\omega_{12}+\alpha B_1+B_2}{B_1+B_2} \qquad (7.15)$$

and the frequency of oscillations, with node 1 grounded, is

$$f_o = \frac{1}{2\pi}\left[\omega_{11}\{\omega_{12}+(1-\beta)B_2\} +(\alpha-\beta)B_1\omega_{12}+\alpha(1-\beta)B_1B_2\right]^{\frac{1}{2}} \qquad (7.16)$$

Thus, this circuit of Nandi also does not have facility for independent control of frequency. The circuit of Pyara and Jamuar [4] is the same as the circuit of Figure 7.1 except for the introduction of a potential divider between the output of A_2 and the inverting input terminal of A_1. Hence, the transfer function for the circuit of Pyara and Jamuar [4] is the same as

equation (7.4) with α replaced by $\alpha\delta$, where δ represents the additional attenuation.

Equation (7.2) (with a negative sign in the numerator) can be written as

$$T(s) = \frac{-d/(s+f)}{1 + \frac{-d}{s+f}\left[-\frac{c-e(a-b-e)}{d(s+e)} - \frac{a}{d} + \frac{b+e+f}{d}\right]} \qquad (7.17)$$

The second and third terms in the denominator of equation (7.17), together represent the summation of a non-inverting LP function and a constant term. The circuit realisation corresponding to equation (7.17) is by Drake and Michell [5]. This circuit is the same as the inverting BPF circuit of Figure 3.3 (Chapter III). This circuit, reproduced in Figure 7.4, has the transfer function.

$$T(s) = \frac{(1-\gamma)B_1/(s+\omega_{11})}{1 + \frac{B_1}{s+\omega_{11}}\left[\frac{\alpha(1-\beta)B_2}{s+\omega_{12}} + \gamma-\beta\right]}$$

$$= \frac{-(1-\gamma)B_1(s+\omega_{12})}{s^2+[\omega_{11}+\omega_{12}+(\gamma-\beta)B_1]s+\omega_{11}\omega_{12}+(\gamma-\beta)B_1\omega_{12}+\alpha(1-\beta)B_1B_2} \qquad (7.18)$$

where

$$\alpha = \frac{R_a}{R_a+R_b}\ ,\ \beta = \frac{R_c}{R_c+R_d}\ ,\ \gamma = \frac{R_e}{R_e+R_f}$$

The condition for oscillation is

$$\beta \geq \frac{\omega_{11}+\omega_{12}+\gamma B_1}{B_1} \qquad (7.19)$$

The frequency of oscillations, with node 1 grounded, is

$$f_o = \frac{1}{2\pi} [\omega_{11}\omega_{12}+(\gamma-\beta)B_1\omega_{12}+\alpha(1-\beta)B_1B_2]^{\frac{1}{2}} \qquad (7.20)$$

Thus, independent control of frequency, through α, is possible.

7.3 Comparison of oscillator circuits :

The circuits of Pyara and Jamuar [4], Drake and Michell [5] and the new oscillator circuit of Figure 7.1 have the facility for independent frequency control without upsetting the condition for oscillations. However, the circuit of Pyara and Jamuar [4] uses two additional resistors. The circuits of Ahmed and Siddiqui [2] and Nandi [3] have only four resistors. But their circuits do not have independent frequency control facility. The circuit of Bhattacharyya and Natarajan [1] uses three OAs, as compared to two in other circuits. Single pole model analysis of their circuit shows [6] absense of oscillations. The oscillation condition and frequency of oscillations can be obtained by a two pole model analysis [6].

7.4 Voltage controlled oscillator :

The frequency determining grounded resistance, R_a, in Figure 7.1 can be replaced by the drain-source resistance of a JFET. Then voltage control of frequency can be obtained by varying the gate-source dc voltage. Then the circuit becomes a voltage controlled oscillator (VCO).

7.4.1 FET as variable resistor :

The field effect transistor has an important property, viz., behaviour as an ohmic resistor. Operated under suitable conditions [7], the FET can exhibit the properties of an ohmic resistor, so far as the circuit between source and drain terminals is considered. The value of the resistance is electrically controlled by the potential difference between the source and gate terminals. For the FET to behave like a ohmic resistor the following two conditions must be fulfilled [8]. These are :

i) the potential difference between the gate region and the conducting channel must be such that no significant gate current flows and

ii) the depletion region of the reverse biased gate to channel p-n junction must at no point along the axis of the channel extend so far as to close or 'pinch-off' the channel.

With these two conditions fulfilled the source to drain channel shows ohmic properties. However, there will be departure from a linear voltage current relationship as pinch-off condition is approached. The drain characteristics of a FET, near the origin, are shown in Figure 7.5. For drain-source voltage values close to zero, the characteristics are linear. The value of the resistance measured between drain and source depends upon the gate-source voltage. As the reverse bias voltage applied to the gate junction is increased, the drain-

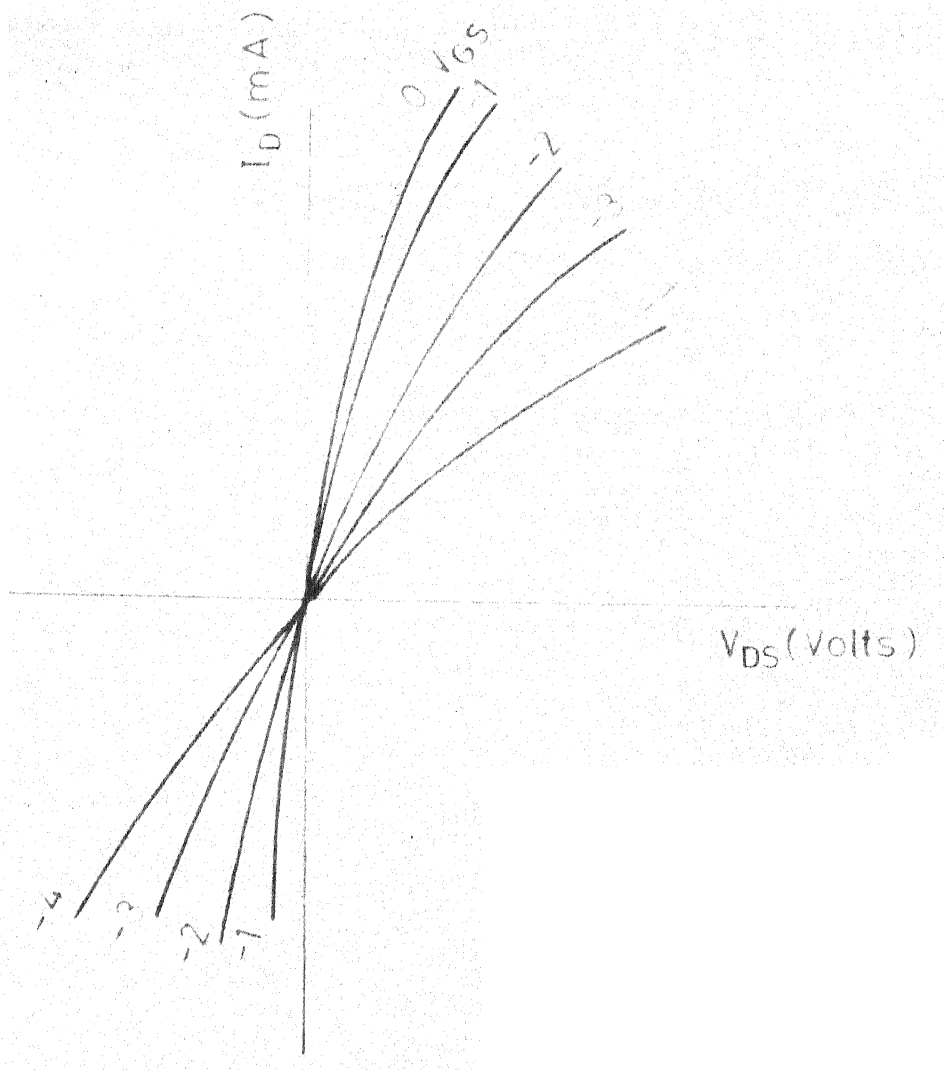

FIG. 7.5 FET DRAIN CHARACTERISTICS CLOSE TO ORIGIN

source resistance increases exponentially. The exact law relating the drain-source resistance (r_{DS}) to the gate-source voltage depends critically on the structural details of the FET.

7.4.2 VCO realisation :

A voltage controlled oscillator was obtained from the circuit of Figure 7.1 by replacing the frequency determining grounded resistor R_a, by an n channel JFET as shown in Figure 7.6. Here, variation of the dc gate-source voltage, V_{GS}, varies the drain source resistance. Hence, α (which is now equal to $(\frac{r_{DS}}{R_b+r_{DS}})$ is varied. Thus frequency is varied by voltage variation.

7.5 Sensitivity analysis :

The angular frequency of oscillations, ω_o, for the circuit of Figure 7.1 is

$$\omega_o = [\omega_{11}B_\beta - \gamma B_1\omega_{12} + (\alpha-\beta\gamma)B_1B_2]^{\frac{1}{2}} \qquad (7.21)$$

The sensitivities of ω_o with respect to all passive and active parameters are given in Table 7.1. Since, only resistor ratios appear in the expression for ω_o, the algebraic sum of ω_o sensitivities with respect to the six resistors is zero. The algebraic sum of the ω_o sensitivities with respect to the OA parameters (ω_{1i} and B_i) is equal to unity. All the sensitivites are less than 0.5.

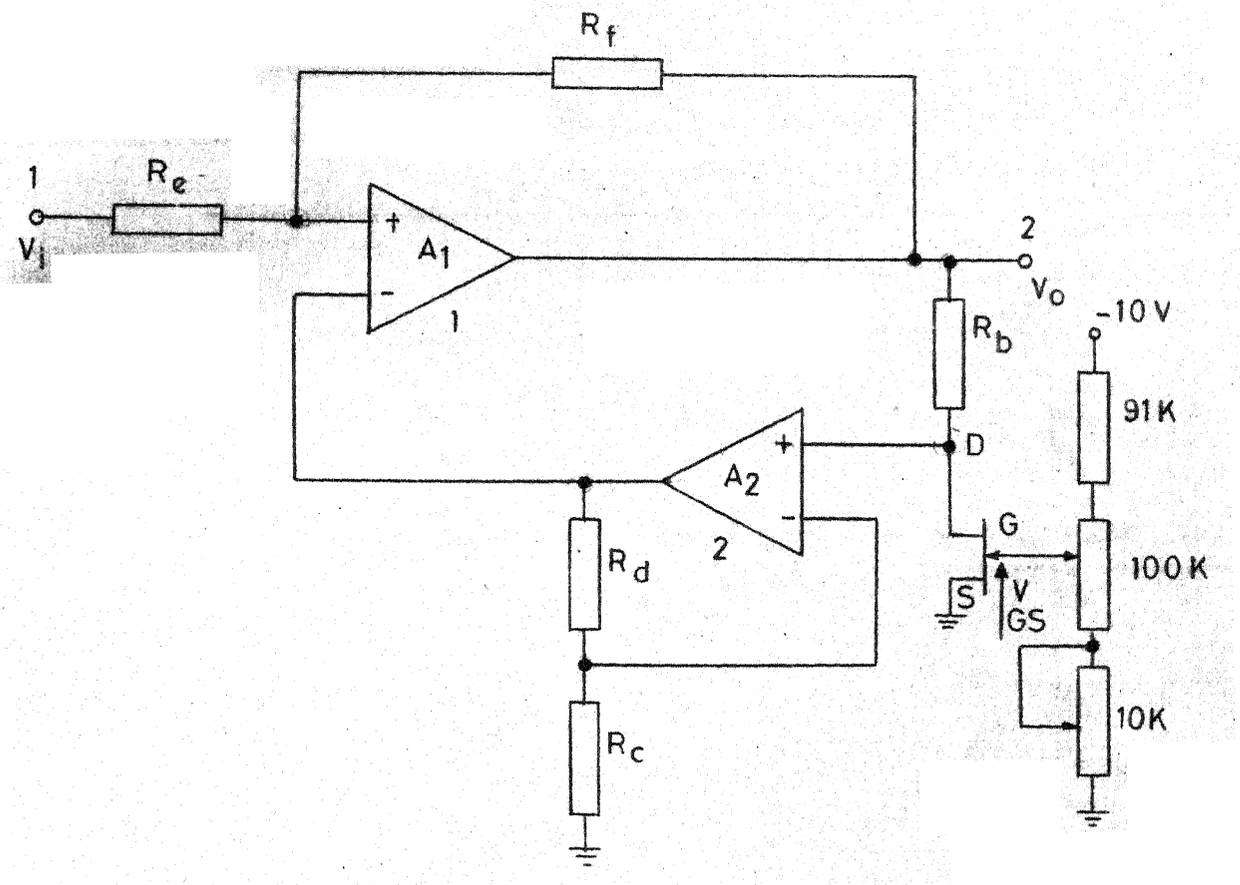

FIG. 7.6 VOLTAGE CONTROLLED OSCILLATOR CIRCUIT

TABLE 7.1

ω_o sensitivities for oscillator

Variable (x)	$S_x^{\omega_o}$
R_a	$\frac{\alpha(1-\alpha)B_1B_2}{2\omega_o^2}$
R_b	$-S_{R_a}^{\omega_o}$
R_c	$\frac{\beta(1-\beta)B_2(\omega_{11}-\gamma B_1)}{2\omega_o^2}$
R_d	$-S_{R_c}^{\omega_o}$
R_e	$-\frac{\gamma(1-\gamma)B_1B_\beta}{2\omega_o^2}$
R_f	$-S_{R_e}^{\omega_o}$
ω_{11}	$\frac{\omega_{11}B_\beta}{2\omega_o^2}$
ω_{12}	$\frac{\omega_{12}(\omega_{11}-\gamma B_1)}{2\omega_o^2}$
B_1	$\frac{(\alpha B_2-\gamma B_\beta)B_1}{2\omega_o^2}$
B_2	$\frac{[\beta\omega_{11}+(\alpha-\beta\gamma)B_1]B_2}{2\omega_o^2}$

7.6 Effect of OA second pole on oscillator performance :

For the oscillator circuit of Bhattacharyya and Natarajan [1], it has been shown by Venkateswaran and Venkataramani [6] that the effect of the OA second pole causes the conjugate poles to be shifted to the right half plane. At high frequencies, the shift will be more and consequently distortion increases.

For the circuit of Figure 7.1, pole-zero model analysis leads to the following transfer function

$$T(s) = \frac{(1-\gamma)B_1(\omega_{21}-s)[(\omega_{22}-\beta B_2)s+\omega_{22}B_\beta]}{D} \qquad (7.22)$$

where

$$D = [\omega_{21}\omega_{22}-\beta B_2\omega_{21}+\gamma B_1\omega_{22}+(\alpha-\beta\gamma)B_1B_2]s^2$$

$$+ [\omega_{21}\omega_{22}(\omega_{11}+\omega_{12}+\beta B_2-\gamma B_1)$$

$$- \beta B_2\omega_{11}\omega_{21}+\gamma B_1\omega_{12}\omega_{22}-(\alpha-\beta\gamma)B_1B_2(\omega_{21}+\omega_{22})]s$$

$$+ \omega_{21}\omega_{22}[\omega_{11}\omega_{12}+\beta B_2\omega_{11}-\gamma B_1\omega_{12}+(\alpha-\beta\gamma)B_1B_2]$$

If the oscillation condition, based on single pole model (given by equation (7.8)) is applied in equation (7.22) the denominator 's' coefficient becomes negative indicating shifting of poles to right half plane.

7.7 Experimental results :

The resistance controlled oscillator of Figure 7.1 and the voltage controlled oscillator of Figure 7.6 were built using two BEL 741C OAs, 0.1 percent metal film resistors and miniature multiturn potentiometers. The relevant parameters of the two OAs are given in Table 7.2.

TABLE 7.2

OA 741 parameters

OA	Parameter		
	$\frac{\omega_{1i}}{2\pi}$ (Hz)	$\frac{\omega_{2i}}{2\pi}$ (MHz)	A_{oi}
OA 1	8.5	1.6	1.46×10^5
OA 2	9.0	1.4	1.32×10^5

$V_{CC} = \pm 15V$, Temp. = $27^{\circ}C$

7.7.1 Resistance controlled oscillator :

The component values for the circuit of Figure 7.1 (in kilo ohms) were : $R_b = 7.9$, $R_c = 1.18$, $R_d = 8.35$, $R_e = 1.19$, $R_f = 8.82$. With R_a varied from 118 ohms to 434 ohms constant amplitude, low distortion sinusoidal oscillations, in the

range 4.63 KHz to 233 KHz, were obtained. The amplitude was 0.5V RMS. Below 4.63 KHz, even a very small reduction in R_a causes the oscillations to die down. Above 250 KHz, the waveform becomes nearly triangular due to the slew rate limitations of the OAs. Within the range 4.63 KHz to 233 KHz distortion was less than 1.5 percent. Variation of harmonic distortion with frequency is shown in Figure 7.7. Variation of frequency with R_a is shown in Figure 7.8.

7.7.2 Voltage controlled oscillator :

The voltage controlled oscillator of Figure 7.6 was set up using an N channel JFET BFW 10. Value of R_b was 24 KΩ . The other component values and OAs were the same as used for the resistance controlled oscillator. The drain-source resistance variation with gate-source voltage, for the FET, was obtained using the circuit of Figure 7.9(a). Corresponding to variation of V_{GS} from -1.24 V to -3.75V, r_{DS} varied from 359 ohms to 1.36 kilo ohms. The variation is shown in Figure 7.9(b). Corresponding to this, the frequency of oscillations varied from 4.8 KHz to 238 KHz. Over this frequency range, constant amplitude (0.51 V RMS) low distortion (< 1.52 percent) oscillations were obtained. Variation of oscillation frequency with V_{GS} is shown in Figure 7.10. Above 250 KHz waveform becomes nearly triangular as in the case of resistance controlled oscillator.

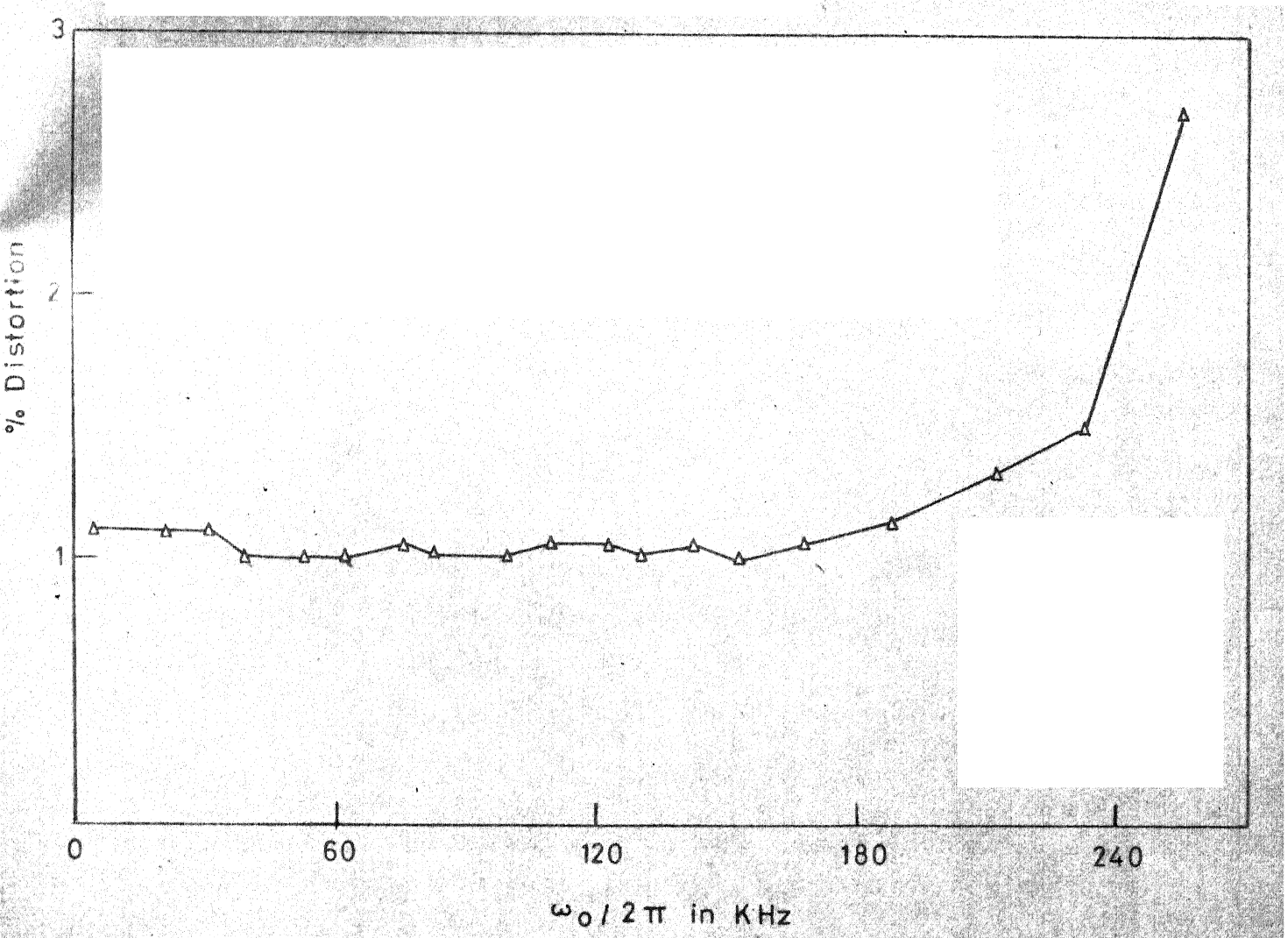

FIG. 7.7 RESISTANCE CONTROLLED OSCILLATOR: VARIATION OF HARMONIC DISTORTION WITH FREQUENCY

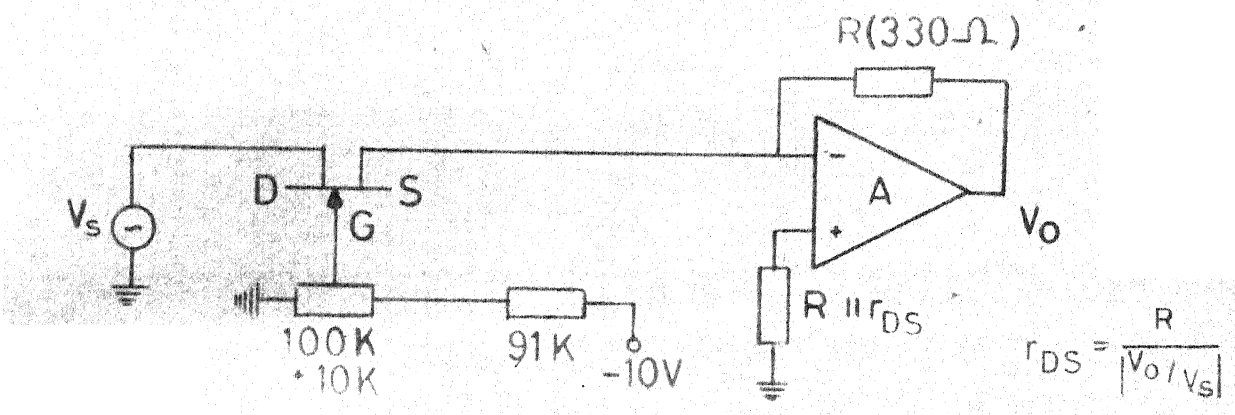

MEASUREMENT CIRCUIT

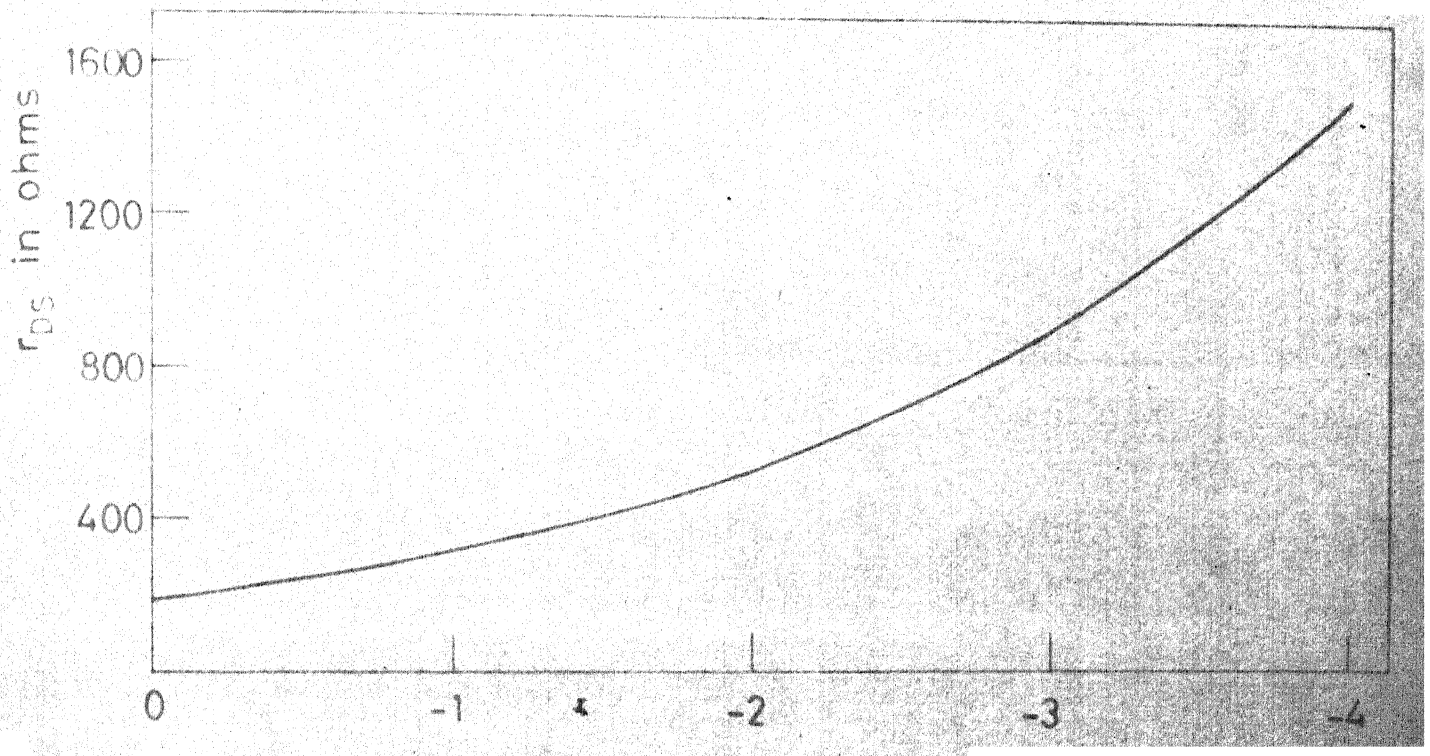

FIG. 7.9 (b) r_{DS} VARIATION WITH V_{GS}

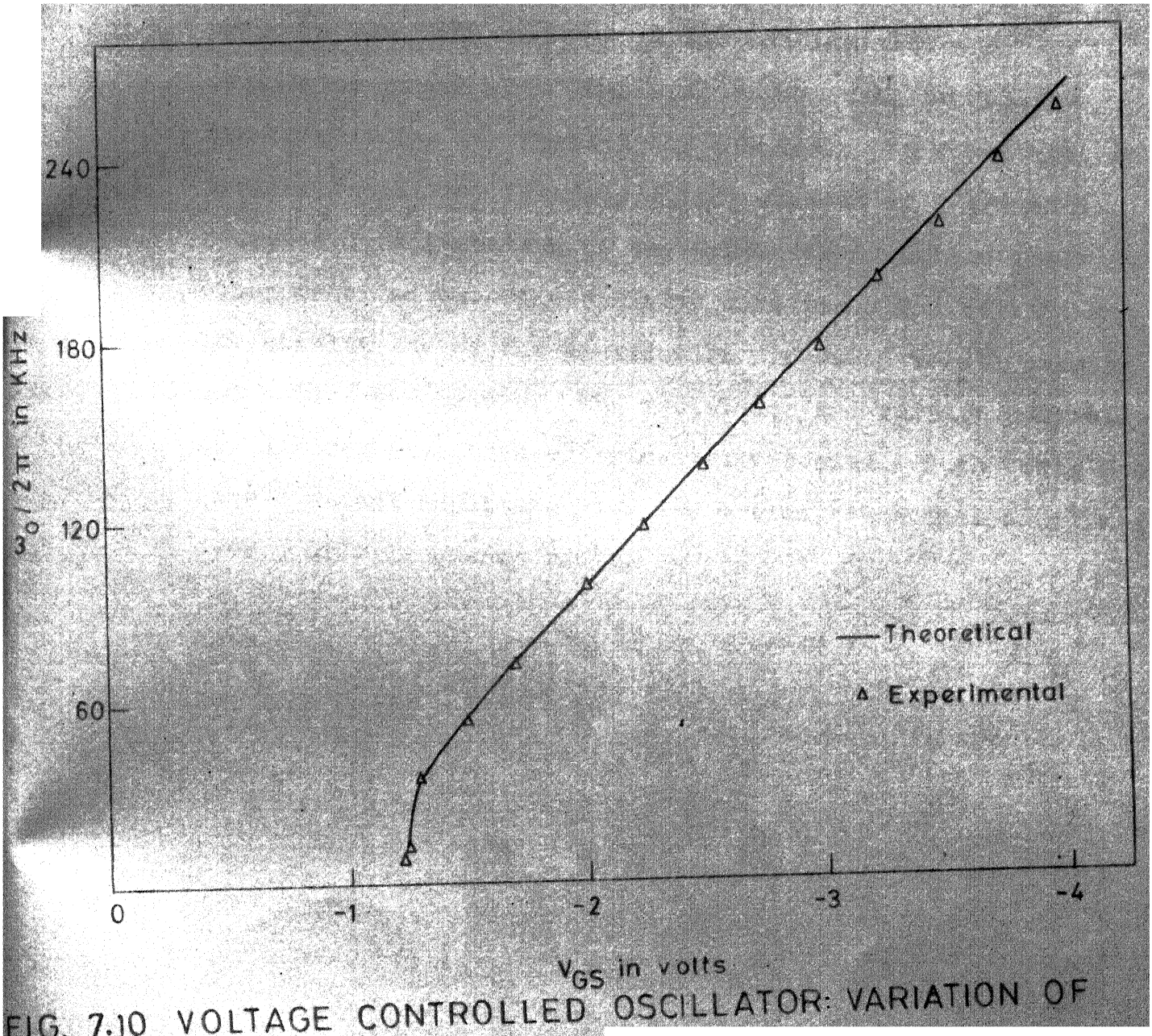

FIG. 7.10 VOLTAGE CONTROLLED OSCILLATOR: VARIATION OF FREQUENCY WITH V_{GS}

7.8 Conclusions :

A synthesis technique for active R oscillators has been proposed in this chapter. A new continuously tunable oscillator circuit has been realised by this technique. The circuit has the facility of conversion to a voltage controlled oscillator by using a JFET instead of a grounded resistor. Modification of the synthesis technique leads to other reported two OA oscillator circuits. The circuit has low sensitivity of the oscillation frequency to all passive and active parameters. The resistance and voltage controlled oscillators have been experimentally tested. Both oscillators give constant amplitude, low distortion, sinusoidal oscillations over a wide frequency range.

References

1. Bhattacharyya, B.B., and Natarajan, S., 'A new continuously tunable sinusoidal oscillator without external capacitors', Proc. IEEE, Vol. 65, no.12, pp 1726-1727, December, 1977.

2. Ahmed, M.T. and Siddiqui, M.A., 'A low component oscillator with operational amplifiers and resistors', Proc. 12th Asilomar Conf. on Ckts. Sys. and Comp. (Calif.) (U.S.A.), November, 1978.

3. Nandi, R., 'Active R realisation of bilinear RL impedances and their application is high Q parallel resonator and external capacitorless oscillator', Proc. IEEE, Vol. 66, no.12, pp 1666-1668, December, 1978.

4. Pyara, V.P. and Jamuar, S.S., 'Single element controlled oscillator without external capacitors', Eln. Lett., Vol.16, no.15, pp 607-608, July, 1980.

5. Drake, J.M. and Michell, J.A., 'Continuously tunable sinusoidal R oscillators with a minimum number of elements', Int. J. Electron., Vol. 50, no.2, pp 141-147, February,1981.

6. Venkateswaran, S. and Venkataramani, Y., 'Comments on a new continuously tunable sinusoidal oscillator without external capacitors', Proc. IEEE, Vol. 67, no.10, pp 1452-1453, October, 1979.

7. Morgan, A.N., 'The FET as an electronically variable resistor', Proc. IEEE, Vol. 54, no.5, pp 892-893, May, 1966.

8. Gosling, W., Townsend, W.G. and Watson, J., 'Field-effect electronics', Butterworths Publishers, London, 1971, pp 215-218.

CHAPTER VIII

SYNTHESIS OF DELAY NETWORKS

The output of an ideal delay network with a pulse input, is an exact replica of the input except for a time delay. Such delay networks are widely used in radar and other communication systems. A number of active RC and passive delay networks have been reported in literature. All the reported realisations are based on Pade's all pass approximation functions or on low pass non-minimum phase approximation functions. Morril [1] has reported a second order active RC delay network and has indicated the possibility of obtaining sixth order delay network by cascading a fourth order Pade approximation delay network with a second order delay equaliser. Deliyannis and Ream [2] have obtained an active RC biquartic circuit to realise the fourth order Pade approximation all pass function. Deliyannis [3] has proposed active RC circuits to realise six new delay functions, each with three right half plane zeros and four left half plane poles. Till now no active R delay networks have been reported. In this chapter a technique for realising active R delay networks corresponding to Pade approximation all pass delay functions is presented.

8.1 Concept of delay :

Transient response of a system is important, particularly in pulse communication systems. In these systems, rise time and overshoot are important since they indicate the extent of distortion in the output pulse. Rise time and overshoot are time domain quantities. The corresponding frequency domain quantity, that indicates the quality of a system's transient response, is delay. If a system is such that the output pulse is an exact replica of the input pulse, except for a time delay, then the system has an ideal transient response. This is illustrated in Figure 8.1 where T represents the delay. The transfer function for the ideal system of Figure 8.1 can be determined from the fact that

$$v_2(t) = v_1(t-T) \tag{8.1}$$

From equation (8.1) it follows that

$$V_2(s) = e^{-sT} V_1(s) \tag{8.2}$$

where $V_1(s)$ and $V_2(s)$ represent the Laplace transforms of $v_1(t)$ and $v_2(t)$ respectively.

Equation (8.2) implies that

$$T(s) = \frac{V_2(s)}{V_1(s)} = e^{-sT} \tag{8.3}$$

From equation (8.3) it is seen that if the output pulse is a

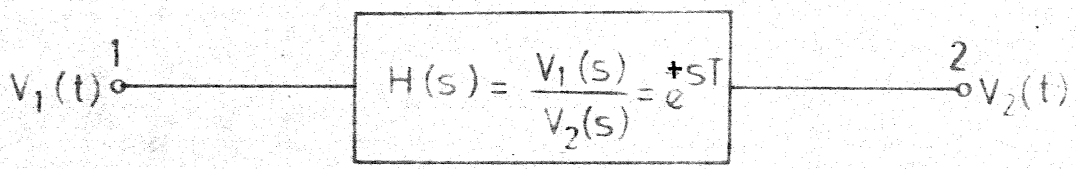

(b)

FIG. 8.1 CONCEPT OF DELAY : (a) INPUT PULSE (b) IDEAL DELAY SYSTEM (c) OUTPUT PULSE.

a time delayed replica of the input pulse then

$$\arg\ T(j\omega) = -\ \omega T \qquad (8.4)$$

Based on equation (8.4), the delay $D(\omega)$ of a system with a transfer function given by equation (8.3), can be defined as

$$D(\omega) = -\ \frac{d}{d\omega} \arg\ T(j\omega) \qquad (8.5)$$

The delay as defined here is also referred to as envelop delay or group delay to differentiate it from phase delay which is equal to $[\arg H(j\omega)]/\omega$.

8.2 Pade approximation :

To realise delay networks all pass transfer functions are commonly employed. This is because all pass functions provide a constant amplitude response independent of frequency. The phase response varies with frequency in a prescribed manner depending upon order of the function and the pole locations. To simulate the ideal delay transfer function, e^{-sT}, it is necessary to approximate it by a ratio of polynomials. The Pade approximation can be used for this purpose.

A Pade approximation is a rational fraction $P_m(x)/Q_n(x)$, where $P_m(x)$ and $Q_n(x)$ are polynomials of degree m and n, respectively. This rational fraction, denoted F(m,n), is said to be a Pade approximation of a function, $F_1(x)$, if and only if,

the power series expansion of F(m,n) is identical with that of $F_1(x)$, upto and including terms of order x^{m+n}. Thus, if

$$F_1(x) = \sum_{i=0}^{\infty} a_i x^i \tag{8.6}$$

then F(m,n) is the Pade approximation of $F_1(x)$, if and only if

$$F(m,n) = \frac{P_m(x)}{Q_n(x)} = \sum_{i=0}^{m+n} a_i x^i + \sum_{i=m+n+1}^{\infty} b_i x^i \tag{8.7}$$

For $F_1(s) = e^{-sT}$, the unique solution for F(m,n) is given by

$$P_m(-sT) = \left[1 - \left(\frac{m}{m+n}\right)\frac{sT}{1!} + \frac{m(m-1)}{(m+n)(m+n-1)}\frac{s^2T^2}{2!} - \cdots \right.$$
$$\left. \cdots + \frac{(-1)^m\, m(m-1)\cdots 2\cdot 1}{(m+n)\cdots(n+1)} \cdot \frac{s^m T^m}{m!}\right] \tag{8.8}$$

and

$$Q_n(-sT) = \left[1 + \left(\frac{n}{m+n}\right)\frac{sT}{1!} + \frac{n(n-1)}{(m+n)(m+n-1)}\frac{s^2T^2}{2!} + \cdots \right.$$
$$\left. \cdots + \frac{n(n-1)\cdots 2\cdot 1}{(m+n)\cdots(m+1)}\frac{s^n T^n}{n!}\right] \tag{8.9}$$

The Pade approximations of first to fourth order, for m = n, are given in Table 8.1.

From Table 8.1 it is seen that the Pade function, F(n,n) is realised by an AP transfer function. Higher the order of the approximation closer will be the realised response to that of

e^{-sT}. Active R all pass networks can be realised only with an attenuation constant, K. Hence, it is possible only to approximate the function Ke^{-sT}, where K is less than one. Thus the output pulse will be a delayed and attenuated replica of the input.

TABLE 8.1

Pade approximation [F(n,n)] for e^{-sT}

Order	F(n,n)
1	$\frac{-(sT-2)}{sT+2}$
2	$\frac{s^2T^2-6sT+12}{s^2T^2+6sT+12}$
3	$\frac{-(s^3T^3-12s^2T^2+60sT-120)}{s^3T^3+12s^2T^2+60sT+120}$
4	$\frac{s^4T^4-20s^3T^3+180s^2T^2-840sT+1680}{s^4T^4+20s^3T^3+180s^2T^2+840sT+1680}$

8.3 Synthesis :

In order to achieve good approximations to the ideal delay function (e^{-sT}) higher order functions must be used.

Thus the fourth order function in Table 8.1 will give a better approximation or better response as compared to the first three order functions. The first and third order functions in Table 8.1 are of the inverting type. However, only non-inverting active R APFs can be realised in practice. Hence active R APFs of first and third order can approximate $-e^{-sT}$ and not e^{-sT}. The first and second order Pade functions can be realised by the circuits of Figures 4.4(a) and 4.7(a) respectively. The third order Pade function can be realised by the circuits of Figure 4.7(b) or 5.5. In this section synthesis of the fourth order Pade all pass function, F(4,4), is described.

The fourth order Pade all pass function, F(4,4) (to approximate e^{-sT}) is,

$$F(4,4) = \frac{s^4T^4-20s^3T^3+180s^2T^2-840sT+1680}{s^4T^4+20s^3T^3+180s^2T^2+840sT+1680} \qquad (8.10)$$

This function can be split into a product of two biquadratic functions, as shown by Deliyannis and Ream [2]. The function now becomes

$$F(4,4) = \frac{(s^2-a_1s+a_2)(s^2-b_1s+b_2)}{(s^2+a_1s+a_2)(s^2+b_1s+b_2)} \qquad (8.11)$$

where

$$a_1 = \frac{11.5848}{T}\ ,\ a_2 = \frac{36.5605}{T^2}\ ,\ b_1 = \frac{8.4152}{T},\ b_2 = \frac{45.9512}{T^2}$$

Equation (8.11) can be expressed in terms of partial fractions, as

$$F(4,4) = [1 + \frac{K_1 s+K_2}{s^2+a_1 s+a_2} + \frac{K_3 s+K_4}{s^2+b_1 s+b_2}] \qquad (8.12)$$

Comparison of equations (8.11) and (8.12) gives the values of K_1, K_2, K_3 and K_4 as

$$K_1 = \frac{2a_1[(a_1+b_1)(a_2b_1-a_1b_2) - (a_2-b_2)^2]}{D} \qquad (8.13)$$

$$K_2 = \frac{-4a_1a_2b_1(b_2-a_2)}{D} \qquad (8.14)$$

$$K_3 = \frac{-2b_1[(a_1+b_1)(a_2b_1-a_1b_2)+(a_2-b_2)^2]}{D} \qquad (8.15)$$

and

$$K_4 = \frac{4a_1b_1b_2(b_2-a_2)}{D} \qquad (8.16)$$

where

$$D = (b_1-a_1)(a_2b_1-a_1b_2)+(b_2-a_2)^2$$

Substituting the values of a_1, a_2, b_1 and b_2 given under equation (8.11), K_1 to K_4 values are

$$K_1 = -\frac{132.64}{T}, \quad K_2 = -\frac{167.29}{T^2}, \quad K_3 = \frac{92.64}{T}, \quad K_4 = \frac{210.26}{T^2} \qquad (8.17)$$

Thus, from equations (8.12) and (8.17) it is seen that the second term in equation (8.12) is the summation of inverting second order BP and LP functions. The third term is the

summation of non-inverting second order BP and LP functions. All these functions have complex conjugate poles. The corresponding circuit realisation is shown in Figure 8.2. The circuit uses four OAs and sixteen resistors. This is a typical parallel realisation circuit. The transfer function of this circuit is

$$T(s) = \frac{V_o}{V_i} = \frac{R}{R_1}\left[1 + \frac{-\frac{R_x}{R_A}\cdot\frac{R_1}{R_2}B_1(s+\omega_{12}) - \alpha\frac{R_x}{R_A}\frac{R_1}{R_3}B_1B_2}{D_1} + \frac{\frac{R_1}{R_4}B_4(s+\omega_{13}+\beta B_3)}{D_2}\right] \qquad (8.18)$$

where

$$R = R_1||R_2||R_3||R_4||R_L,\quad R_x = R_A||R_B||R_C$$

$$\alpha = \frac{R_a}{R_a+R_b},\quad \beta = \frac{R_c}{R_c+R_d},\quad \gamma = \frac{R_e}{R_e+R_f},\quad \delta = \frac{R_g}{R_g+R_h}$$

$$D_1 = s^2+(\omega_{11}+\omega_{12}+\frac{R_x}{R_B}B_1)s + (\omega_{11}+\frac{R_x}{R_B}B_1)\omega_{12}+\alpha\frac{R_x}{R_c}B_1B_2$$

$$D_2 = s^2+(\omega_{13}+\omega_{14}+\beta B_3+\gamma B_4)s+(\omega_{13}+\beta B_3)(\omega_{14}+\gamma B_4)+\delta(1-\gamma)B_3B_4$$

Comparison of equations (8.12) (with attenuation constant K, included) and (8.18) gives the following design equations.

$$\frac{R}{R_1} = K \qquad (8.19)$$

$$\omega_{11}+\omega_{12}+\frac{R_x}{R_B}B_1 = a_1, \qquad (8.20)$$

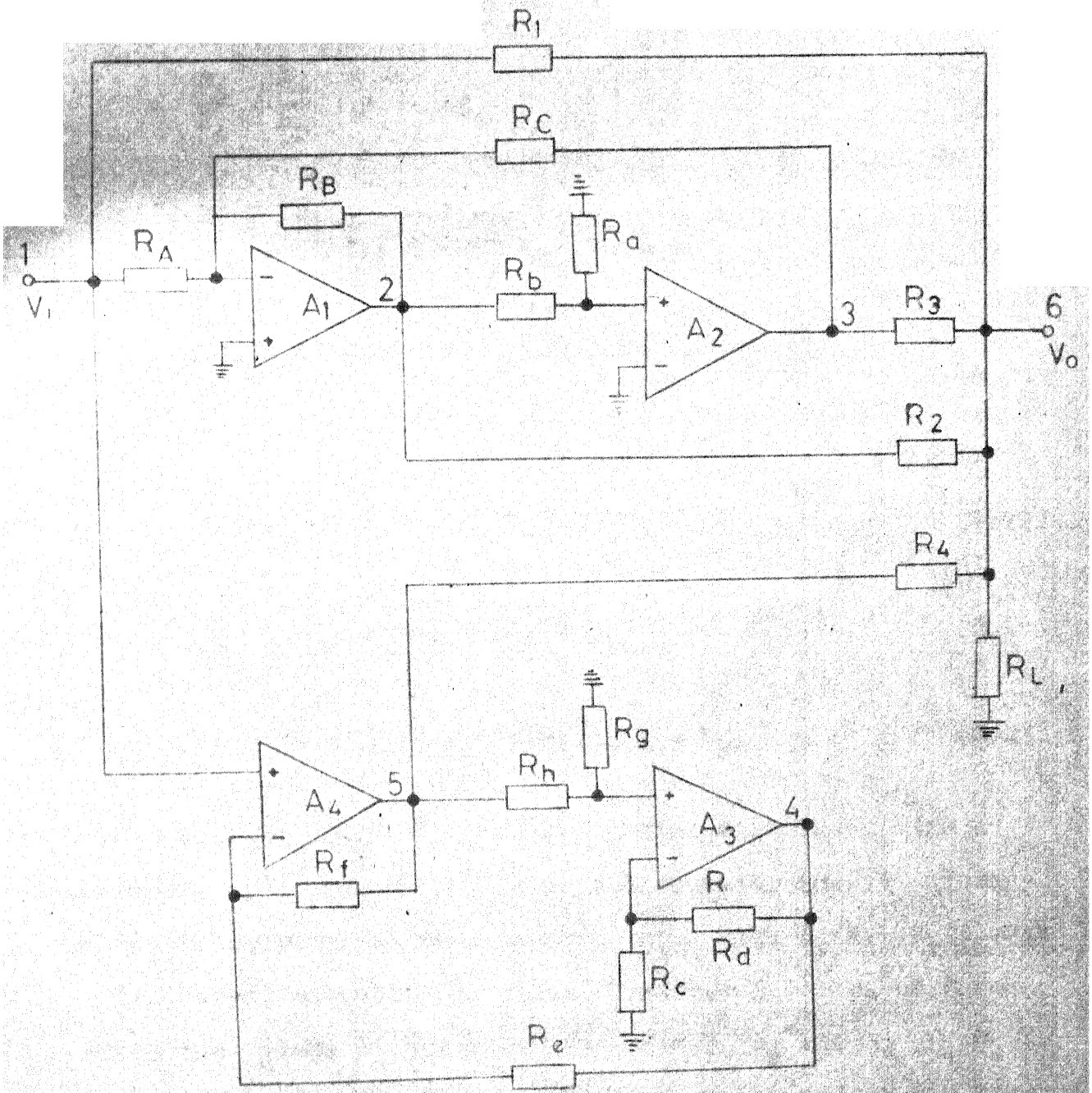

FIG. 8.2 CIRCUIT TO REALISE FOURTH ORDER PADE DELAY FUNCTION

$$(\omega_{11} + \frac{R_x}{R_B} B_1)\, \omega_{12} + \alpha \frac{R_x}{R_C} B_1 B_2 = a_2 \tag{8.21}$$

$$\frac{R_x}{R_A} \cdot \frac{R_1}{R_2} \cdot B_1 = -K_1 \tag{8.22}$$

$$\frac{R_x}{R_A} B_1 (\frac{R_1}{R_2} \omega_{12} + \alpha \frac{R_1}{R_3} B_2) = -K_2 \tag{8.23}$$

$$\frac{R_1}{R_4} B_4 = K_3 \tag{8.24}$$

$$\frac{R_1}{R_4} B_4 (\omega_{13} + \beta B_3) = K_4 \tag{8.25}$$

$$\omega_{13} + \omega_{14} + \beta B_3 + \gamma B_4 = b_1 \tag{8.26}$$

$$(\omega_{13} + \beta B_3)(\omega_{14} + \gamma B_4) + \delta(1-\gamma) B_3 B_4 = b_2 \tag{8.27}$$

From equation (8.20) R_x/R_B can be obtained. Then, with α assumed, R_x/R_C can be obtained from equation (8.21). Then R_x/R_A is known since $\frac{R_x}{R_A} = 1 - \frac{R_x}{R_B} - \frac{R_x}{R_C}$. With R_x/R_A, R_x/R_B and R_x/R_C known, choosing the value of either R_A or R_B or R_C fixes the values of the other two with R_x/R_A known. R_1/R_2 and R_1/R_3 are obtained from equations (8.22) and (8.23) respectively. R_1/R_4 is obtained from equation (8.24). Then β can be obtained from equation (8.25).. With β determined, γ and δ can be obtained from equations (8.26) and (8.27)

respectively. With R_1/R_2, R_1/R_3 and R_1/R_4 values determined, R_2,R_3 and R_4 can be obtained by choosing R_1 value. Thus with one parameter (α) assumed, all the other parameters are obtained in terms of the Pade coefficients and the parameters of the four OAs.

8.4 Experimental results :

The active R delay network of Figure 8.2 was designed on the basis of design equations (8.19) to (8.27) for a delay of 30 microseconds. The circuit was tested using a National Semiconductor LM 324 quad OA chip. The relevant parameters of the four OAs in this chip are given in Table 4.2 (Chapter IV). The resistor values for the circuit, in kilo ohms, were :

$R_a = R_c = 0.2$, $R_b = 1.8$, $R_d = 12$, $R_e = 0.12$, $R_f = 2.6$, $R_g = 0.15$, $R_h = 88$, $R_A = 1.0$, $R_B = 11$, $R_C = 47$, $R_1 = 1.1$, $R_2 = 1.0$, $R_3 = 9.0$, $R_4 = 1.6$, $R_L = 10$.

The magnitude and phase response for the circuit are shown in Figure 8.3. The magnitude response shows the effect of OA second pole at high frequencies. The phase response is practically unaffected by the OA second pole effects.

Responses of the delay network to triangular wave and pulse inputs are shown in Figure 8.4. With a triangular wave input a delay of 29.2 μs was obtained as shown in Figure 8.4(a). The input and output waveforms for a pulse input are shown in

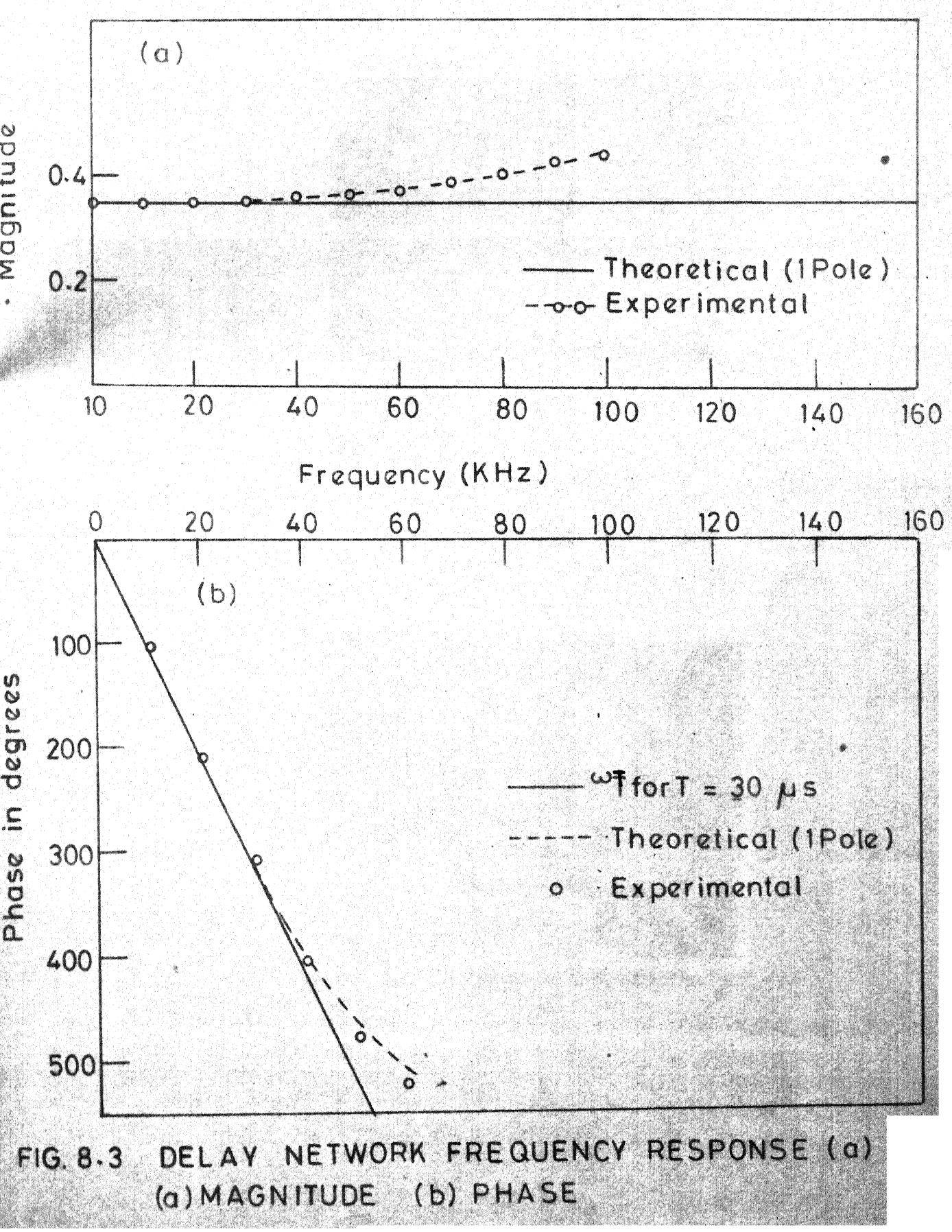

FIG. 8.3 DELAY NETWORK FREQUENCY RESPONSE (a) (a) MAGNITUDE (b) PHASE

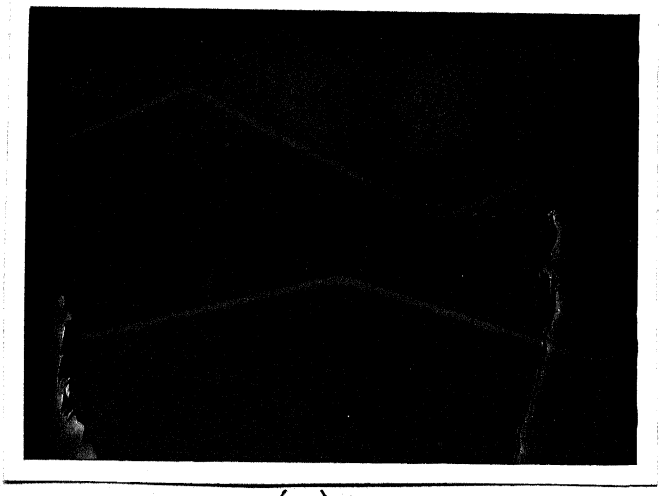

(a)

Upper trace (input) : Vertical scale 0.1 V/div.
Horizontal scale 20 μs/div.

Lower trace (output): Vertical scale 0.05 V/div.
Horizontal scale 20 μs/div.

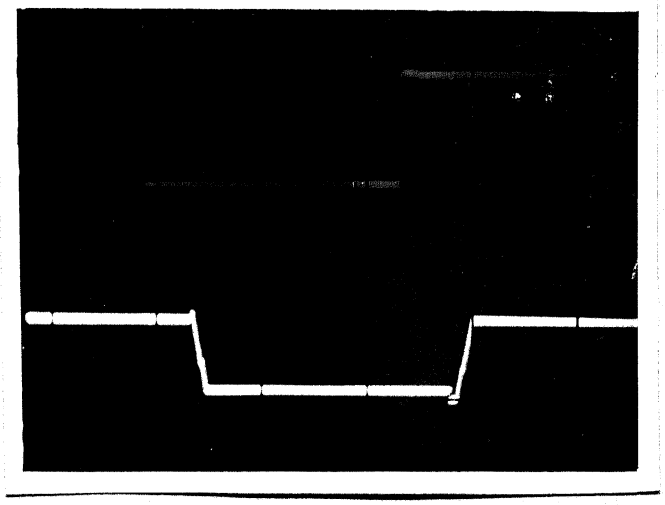

(b)

Upper trace (input) : Vertical scale 0.1 V/div.
Horizontal scale 50 μs/div.

Lower trace (output): Vertical scale 0.05 V/div.
Horizontal scale 50 μs/div.

Fig. 8.4 Delay network response (a) triangular wave input (b) pulse input

Figure 8.4(b). The observed delay was 28.6 μs. The leading and trailing edges of the output pulse indicate some amount of distortion.

8.5 Conclusions :

An active R delay network to realise the Pade fourth order all pass approximation for e^{-sT} has been synthesised by the parallel realisation technique. Due to resistive summation realisation is possible only with an attenuation constant. The magnitude response of the circuit shows the effect of OA second pole. The phase response deviates from true delay response beyond 35 KHz. The responses of the circuit to triangular wave and pulse inputs show the effectiveness of the circuit as a delay network.

References

1. Morril, C.D., 'A sub audio time delay circuit', IRE Trans. Eln. Compt., Vol. EC-3, no.2, pp 45-49, June, 1954.

2. Deliyannis, T. and Ream, N., 'An active RC synthesis of a biquartic function with complex poles', Int.J.Electron., Vol.23, no.5, pp 413-415, May, 1967.

3. Deliyannis, T., 'Six new delay functions and their realisation using active RC networks', Radio and Electron., Engineer, Vol. 39, no.3, pp 139-144, March, 1970.

4. Stover, J.E., 'Passive network synthesis', McGraw-Hill, 1965, pp 272-276.

CHAPTER IX

CONCLUSIONS

Active R networks of three different categories, viz., filters, oscillators and delay networks have been synthesised. A number of new circuits have been realised. Many of these circuits have been experimentally tested. A new pole-zero model for the operational amplifier has been proposed to simplify analysis for OA second pole effects.

The proposed synthesis techniques are general. Hence, they can realise a number of alternate configurations. The techniques can also be adapted for active RC synthesis of filters, oscillators and delay networks.

Characteristics of the realised active R networks are dependent on OA parameters and resistor ratios and not on individual resistor values. Thus, these circuits are well suited for fabrication by monolithic IC technology, where resistor ratios track.

A band pass filter, with multifunction capability has been synthesised. The circuit realises inverting and non-inverting BP, non-inverting LP, oscillator, AP and notch functions. If the band pass filter is designed for high ω_o and Q values, it becomes oscillatory due to the effect of

OA second pole. To overcome this effect, the circuit has been designed on the basis of pole-zero model and tested for high ω_o and Q values.

Two new synthesis techniques for all pass filters have been developed. These techniques lead to a large number of new circuits. It has been theoretically shown and experimentally verified that OA second pole causes APF magnitude response to increase with frequency while the phase response remains practically unaffected. An APF has designed on the basis of pole-zero model so as to get a flat magnitude response over a wider frequency range. Techniques similar to those for all pass filters realise high pass and notch filters. Instability problems in active R notch filter, with high notch frequency, due to OA second pole effect, can be avoided by pole-zero model design for the circuit. This has been experimentally demonstrated.

Active RC all pass, high pass and notch filters can be realised with unity gain or gains greater than unity. Active R all pass, high pass and notch filter functions are realised resistive summation points and hence realisations are possible only with an attenuation constant. This is because a true active R summer circuit has not been realised till now.

An active R oscillator circuit has been synthesised. It can be continuously tuned over a wide frequency range,

without upsetting the condition for oscillations. Both, condition for oscillations and frequency of oscillations are controlled by grounded resistors. Replacement of the frequency deciding resistor by a JFET has given rise to a voltage controlled oscillator. Experiments on both resistance and voltage controlled oscillators indicates the availability of constant amplitude, low distortion, sinusoidal oscillations over a wide frequency range.

For the first time an active R delay network has been synthesised. The circuit realises the fourth order Pade approximation of e^{-sT}, where T is the delay. The circuit can realise delays upto tens of microseconds. For larger delays, the required resistor ratios become too large to be practicable.

In active R networks all the network characteristics are strongly dependent on the parameters of the OAs, particularly gain-bandwidth product. Gain-band width product of an OA is highly sensitive to bias voltage and temperature variations. Hence, for satisfactory performance, highly regulated power supplies and OAs with temperature stabilised gain-bandwidth products must be used. Such OAs are commercially available.

The effect of OA second pole on active R networks can be overcome by designing them on the basis of two pole model or pole-zero model for the OAs. However, this leads to the

dependence of network characteristics on the OA second pole frequency also. The OA second pole frequency is also sensitive to temperature variations. There is at present no known method for temperature stabilisation of the second pole frequency.

Further investigations in active R networks could be in the following areas :

1) Development of OAs specifically meant for active R applications. These must have a very low first pole frequency, very large gain-bandwidth product, very high second pole frequency and high slew rate. Both gain-bandwidth product and second pole frequency must be temperature stabilised.

2) Development of stabilisation arrangements for presently available OAs to stabilise OA parameters against temperature variations.

3) Realisation of a compensated active R summer circuit so that all pass, high pass and notch responses can be obtained without attenuation.